



Università degli Studi di Ferrara

DOTTORATO DI RICERCA IN
"SCIENZE DELLA TERRA"

CICLO XXV

COORDINATORE

Prof. Luigi Beccaluva

**EARTH SCIENCE AND MODERN - CONTEMPORARY ART: FINGER-
PRINTS FOR THE SAFEGUARD OF ARTWORKS IN VIEW OF
FINE ARTS TRANSPORTATION**

Settore Scientifico Disciplinare GEO/09

Dottorando

Dott. Volpe Lisa

Tutore

Prof. Vaccaro Carmela

Cotutore

Prof. Maino Giuseppe

Dott. Bruni Stefania

Anni 2010/2012

... è noto che l'olio di lino cotto ha costituito per molti secoli la materia prima della nostra arte. E' questa un'arte antica e perciò nobile [...]. Ma è anche un'arte sottilmente frodolenta, come quella che mira ad occultare il substrato conferendogli il colore e l'apparenza di ciò che non è...

*(Primo Levi,
da Il sistema periodico, capitolo Cromo)*

"...it is known that linseed oil painting has been primary matter of our art for a lot of centuries. An ancient art and therefore noble [...]. But it is also a subtly fraudulent art, like that which aims at concealing the substratum by conferring on it the color and appearance of what it is not..."

*(Primo Levi,
in "The Periodic TABLE", chapter Chromium)*

"Il y a des circonstances où je vois clairement l'alliance possible et désirable de la Science et de l'Art, et où le chimiste et le physicien peuvent prendre place auprès de vous et vous éclairer."

*(Louis Pasteur,
fragment du discours qu'il prononce à l'École des Beaux-Arts à Paris en 1865)*

"There are situations in which I clearly see the possible and desirable collaboration between Science and Art and where chemist and physician can sit down with you and brighten up."

*(Louis Pasteur,
snatch of an address delivered at Fine Art School of Paris in 1865)*

CONTENTS

Contents.....	3
1.Introduction	5
2. Fine Art transportation and counterfeit Artworks	10
2.1 Transportation of artworks: risk and insurance policy.....	10
2.2 How to safeguard from forgery	11
2.2.1 Anti-counterfeiting-proof mark: “Invisible” by Elettra Synchrotron and EUV tag by ENEA	12
2.2.2 New proposed solution: Art-Fingerprints and Art-Fingerprints database.....	14
3. Art works: easel painting.....	15
4. Multi-analytical approach	24
4.1 Surface investigation at macroscopic level	27
4.1.1 Multispectral Imaging and X ray radiography	27
4.1.2 Image processing.....	30
4.2 Surface investigation at microscopic level.....	35
4.2.1 Optical microscopy	36
4.2.2 Electron microscopy.....	38
4.3 Pigment analysis.....	40
4.3.1 Energy Dispersive X-ray Fluorescence (EDXRF)	41
4.3.2 Proton Induced X-ray Emission (PIXE).....	42
4.3.3 Raman Spectroscopy (RS)	45
4.3.4 X-ray Diffraction (XRD).....	46
4.4 Art-fingerprints database.....	48
4.4.1 Traditional database	48
4.4.2 Interactive Image database: AIAD (Art Image and Analysis Database)	50
5. Results and Discussion.....	51

5.1 "Caffè orientale sulla Riva degli Schiavoni" by J.S. Sargent	53
5.2 "Cubist figure" by Pablo Picasso	72
5.3 "Scolaro con libro illustrato" by Amedeo Modigliani	88
5.3 "Dama che legge con signore", Giovanni Boldini	97
5.4 "Flowers", Filippo De Pisis	124
5.6 "Flowers in glass vase", Filippo De Pisis.....	155
6. Conclusion.....	179
Appendix I.....	186
Appendix II	187
References	189
Web references	202
Table.....	204
Acknowledgements	206

1.INTRODUCTION

The study and the conservation of artworks and monuments is “*one of the most exciting new frontiers of the XXI century, where scientific progress can pit itself against the creativity and technical knowledge of the past*”(Arbizzani *et al.*, 2004).

In Cultural Heritage domain, since years it has known that an artwork, further to be studied by the historical-artistic and stylistic point of view, could be examined taking advantage from scientific support of different disciplines.

Among the different search fields, various disciplines of Earth Science also offer a valid contribution in the sector of the Cultural Heritage: for instance, geological researches can support archaeological studies (Ambraseys N.N., 2006; Battarbee R.W., 1988; Kooistra M.J. *et al.*, 2003; Homburg J.A., 2005; Macphall R.I., 2008), material analysis give useful information not only for artworks formed by rocks or gemstones, etc. (Calligaro T. *et al.*, 2000; Querré G. *et al.*, 1996; Re A. *et al.*, 2011) but also for paintings, that are an essential component of Cultural Heritage. If we consider, in fact, that, among pigments used to painting, there are inorganic pigments obtained by grinding natural stone (i.e. Natural Ultramarine Blue by *Lapis lazuli*) and earth (Green earth, Ochre, etc.) or produced by artificial process of some mineralogical phases (i.e. White titanium dioxide), it is easy to understand that also Earth Science could contribute to the identification of pigments and, when it is possible, to deepen the research with the identification of mineralogical phases. Therefore, through the study and the identification of materials and executive techniques, science allows to obtain fundamental information for the optimal maintenance and restoration actions on Cultural Heritage and, sometimes, to support research of artworks’ dating and study of authentication (Appoloni C.R. *et al.*, 2007; Taylor R.P. *et al.*, 2007).

These last two aspects are particularly interesting if we consider that, in the Art-commerce, the presence of non-original and original paintings is a very important problem difficult to solve. The discrimination and characterization of these paintings is usually based on historical-artistic criteria and on stylistic-aesthetic information obtained by *Catalogues Raisonnés*¹ or art critics’ experiences; but, these data are not enough to accurately differentiate the originality of artworks (Vila A. *et al.*, 2007). For this reason, in addition to the classical humanistic approach, the identification of materials and artistic techniques give more useful information in support to this kind of studies.

¹ *Catalogues Raisonnés* is a monograph, that shows an exhaustive catalogue of artworks made by an artist, describing the work in a way that it may be reliably identified by other people.

Furthermore, considering that the introduction of fakes on Art-market could happen principally in two ways (sale of non- original artworks and/or replacing original with counterfeit artwork), artworks' handling for art-exhibitions around the world can increase the problems linked to this aspect. Nowadays, indeed, among news stories, it is ever more easy to read about traditional Art-heists in museum, etc. [1, 2] or new sly Art-thefts, i.e. replacing painting with the perfect copy that not making suspicious the owners [3, 4] and so “*there are sometimes suspicious when a stolen painting is returned to its owner. People are not always convinced that they have been given the genuine article* (Wei B.)” [5].

However, it is well known that a painting or a mobile artwork increase its value also in correlation to the number of art-exhibition, and so this kind of risks could increase, binding proprietors to be very careful (Marinelli N. *et al.*, 2011). Otherwise, the force of Art-commerce is absolutely linked to the uniqueness of the artwork. Even if, nowadays, this problem is very present, assurance agency requires to owner's artworks documentations that are not very detailed: insurance documents, in fact, demand only some general information (owner, economic value, title, artist, etc.) and also condition report does not request details on materials, etc.

If we consider also this aspect, scientific examination acquires more value and, in some case, a detailed report could be very important.

During the last years, historical-artistic-stylistic studies, designed for false artworks' identification, are increasingly followed by chemical and spectrographic analyzes that allow material characterization of support and painting, underlining the important role of pigments considered "dating pigment ". These concepts are very often applied for the recognition of false or remakes of ancient artworks, but they are not very reliable when artworks was made near the periods of production and/or commercial introduction of some of these pigments, which are currently used in restoration.

For this reason, the knowledge of some characteristics of these artworks, not reproducible and punctual peaceable is very important to establish the authenticity and uniqueness of artwork.

The current study focuses its attention to the identification of these microscopic characteristics - *ArtFingerprints* - (not only pigments but also pictorial peculiarities of artistic technique, trace of restoration acts, structural and material characteristics, etc.), that, in addition to support historical-artistic studies (dating, artistic techniques, etc.), could be useful also for the safeguard of painting in view of fine arts transportation.

In fact, the creation of a database in which all the *ArtFingerprints* are recorded, taking note of their spatial coordinates on the paintings during the analysis, allows to obtain a “painting's iden-

tity card” that could follow the artworks during its transportation. In this way, the exact correspondence between point analysis and ArtFingerprints could define if the artworks analyzed today are the same as the one that it was originally studied yesterday (i.e. before fine art transportation) and so if there could be a painting’s replacement. Further benefit of this methodological procedure is that, knowing the exact position of point in previous analysis, it is possible to examine, with major precision, the same point analysis by different non-invasive and complementary scientific techniques. This allows to better understand analytical data and to carry out analysis after time, particularly useful to control conservative condition and originality of artworks.

Afterwards, the research of detailed characteristic features of studied painting is carried out developing four different aspects:

- elaboration and representation of data obtained by imaging analysis, in order to support more chemical-mineralogical-physical analysis too;
- study of pictorial layer in color (pigments) and shape (superficial morphology, artistic technique);
- characterization of inorganic pigments (i.e. artificial post-queam pigments) through chemical-mineralogical approach;
- creation of an interactive database both in traditional and on image format.

The result of this investigation is a map that is completely unique and linked to the object that it is cataloguing.

To achieve these goals, methodologies (i.e. microscopy, XRF analysis, XRD analysis, PIXE analysis, μ -Raman, etc.) and software (Image processing SW), used a lot in Earth Science disciplines, are applied.

The contribution of these analytical techniques is very useful especially on the choice of point analysis, on the consequent interpretation of data and on the characterization of some particular artificial pigments. Even if the research is carried out on a great number of artificial pigments found in the analyzed painting, particular attention is paid onto a color which is probably the most important in art, used for preparatory layer, to create tone or brightness/volume and to otherwise dull and uniform backgrounds: white color.

As concern, for example, the new white pigments, the contribution of Earth Science could be particularly interesting in the study of White titanium dioxide: chemical-physical analysis, that are usually carried out to recognize it, could be implemented by chemical-mineralogical information about two of the three mineral phases of this pigment (anatase and rutile), whose presence can deepen the studies, avoiding dating errors on modern and contemporary paintings.

The complete analytical suite, suggested in this study, allows to obtain a better scientific data interpretation and an exhaustive database: more ArtFingerprints are collected and more the ArtFingerprints database is detailed; in this way, the crossed comparison of the artwork - before and then fine arts transportation - is more efficient. However, even if it is not always possible to apply the whole analytical suite, ArtFingerprints database can work also with information obtained by some analysis, adapting itself to request and economic possibilities of the paintings' owner and offering better control in assurance field.

Finally, the choice to test this analytical procedure to Modern and Contemporary Art is tied up to the fact that, for this kind of fine arts objects, the traditional stylistic-artistic and scientific approach encounters more difficulties for the following reasons:

- according to Art historians, the correct evaluation of modern and contemporary objects is more difficult rather than ancient artworks because, belonging to the context-fashion time in which the art objects has been created, it is quite demanding to have the right philological distance;
- the quite diffuse non-conventional artistic techniques increase the complexity of investigated subject linked to artists' desire to experiment new material and new artistic techniques;
- pigments, that are usually considered dating pigments for ancient artworks, in Modern and Contemporary paintings could be the main matter of pictorial layers, given that to Modern and Contemporary Art consists also of fine arts objects dated from XIX century. In this case, as concern some artificial pigments, the identification of some mineralogical phase could help to deep dating studies.

This study was performed on artworks and on samples taken from paintings of important national and international artist. Dating and attribution studies of these artworks are currently in progress. The research aimed to the detection of ArtFingerprints could be useful in support to these studies, in addition to bring important data for the safeguard of artworks during fine art transportation.

In conclusion, even if this research can be applied also to ancient paintings and to all kind of artworks, the preference to test it on Modern and Contemporary paintings allows to show what could be the scientific contribution of Earth Science also in this field and not only in archaeological domain, pointing out how this solution could prove particularly useful in a sector in which stylistic-philological-scientific traditional approach can find some difficulties.

A briefly introduction about the main risk linked to transportation, followed by proposed analytical procedure for the identification of ArtFingerprints, introduce the study carried out on artwork (or on samples) organized by single Artwork Plate.

2. FINE ART TRANSPORTATION AND COUNTERFEIT ARTWORKS

2.1 Transportation of artworks: risk and insurance policy

The risks that can happen during fine arts transportation are mainly the following:

- artworks' damages due to bad transport, packaging, accident, etc.;
- art-heists with artworks' replacement or not.

In insurance field and in fine arts transportation sector, the damages in artworks link to transport, etc. are always verified using the *condition report*², a document that accompanies the artworks during the phase of loan. The compilation of the condition report is an important operation although, sometimes, it is underestimated: this document becomes fundamental when there are some disagreement between owner and borrower of the artistic objects and, if it is well filled out, it is very useful for restorer and art exhibition curator, giving information about conservative condition of artworks. Immediately after openings and before closing of the packing boxes, register takes note of all the damages on artwork, paying also attention to the instance of a possible or apparent damage. Even if it is advised a detailed and well-done condition report, the majority of them are meager documents not so useful in case of accident, ensuing from a quickly and handwritten compiling.

In recent years, more restorer, register, conservator, etc. expressed the longing and proposed a more detailed condition report, especially for contemporary art, according to artworks analyzed (Preatoni F. *et al.*, 2008), but, however, the contribution of scientific analysis on material is not well described in this new proposal.

Even if condition report could be useful in assurance field, it is not required to contract an insurance policy. One of the most common policy for the coverage of artworks in view of art exhibition or simple transport is “nail to nail” fine art insurance, used to assure painting during the passage between departure place and arrival site, or better “the cover insures fine art in transport from one hanging to another, and [...] everything in between” [8]. For this kind of policy, the company usually requires only some general information about the painting (size, date, artist, title and economic value), but, in case of accident, the owner or the curator should provide the condition report or a photograph took immediately before the departure. In the event that insured desires to receive a coverage with “accepted assessment”³ and that the artworks does not come from well-known collections, insurance company can require a deepen study of assured artwork, appointing specialist and the appraisal will be paid by insured. Otherwise, if the artworks come

² App. A: example format of Condition Report.

³ In assurance fields, “accepted assessment” stands for a value that assurance company could not challenge in case of incident.

from well-known collections, the insurance company often accepts the art-object value specified by the owner, unless to carry out evaluations by its specialist; in this case, all the costs will be covered by insurance company. For all these investigation, the assurance agency, usually, applies to specialized societies that offer this kind of service (Maggio M., [9]).

Afterwards, even if most of “nail to nail” policies or policies for Fine Arts have often “all risks” insurance system, that covers also deftly theft [10-15], scientific and specific analysis are not required but they could be very useful especially to control replacement of original artwork with counterfeit work.

2.2 How to safeguard from forgery

Nowadays, except probably art thefts for commission, thieves could encounter more and more difficulties to sell stolen artworks to few people who could afford to pay it or onto the black market. Among main advices given by national (Comando Carabinieri TPC⁴, [16-17]) and international police (i.e. FBI [18-19]), in fact, three are the suggested basic things to require during an art purchase: certificate of authenticity, provenance and some proof of legal ownership.

Therefore, stolen masterpieces could usually follow different paths:

- it could be bought for less than the true market value or for the real economic value but, in this case, it is very easy that the buyer is an undercover agent;
- it could be used as commodity, requiring a reward for helping return artwork, even if, since 2001, in some countries, like Great Britain, it is passed a law for which “no reward could be paid for the return of a stolen artwork without it also including an arrest” [20];
- it could be hidden by thieves until it will be verified one of the previous event or the thieves get arrested for some other crime.

However, when a stolen masterpieces artwork end up back in the hands of authorities, the owner could be not sure that the returned artworks is actually which was taken; in fact, “there are sometimes suspicions when a stolen painting is returned to its owner. People are not always convinced that they have been given the genuine article (B. Wei, 5)”. In this way, some problems regarding authentication could arise.

In the last years, lots of scientists have tried to propose new solution for the safeguard of artworks taking advantage by important scientific equipment (i.e. Elettra- Synchrotron light source) and offering new technology (e.g. Elettra- Synchrotron lightsource, ENEA Research Centre).

⁴ *Arma dei Carabinieri* is one of the four Italian military police. *Comando dei Carabinieri Tutela Patrimonio Culturale* (or TPC) is the Arma dei Carabinieri Division for the Protection of Cultural Heritage.

2.2.1 Anti-counterfeiting-proof mark: “Invisible” by Elettra Synchrotron and EUV tag by ENEA

During the recent years, many anti-counterfeiting techniques have been developed exploiting new high-tech labels, characterized by thermo-chromic or fluorescent inks (currently used, e.g., in banknotes), holograms, radiofrequency identifiers, particular foils, etc. The lifetime of these techniques is quite limited both for materials characteristics and for the ability of counterfeiters to replicate them. For this reason, Research in this sector is involved in development and survey new innovative technologies difficult to replicate and useful in anti-counterfeiting (Bollanti S. *et al.*, 2012).

Elettra – Synchrotron lightsource facility (Trieste, Italy) is an international laboratory specialized in synchrotron light and its applications in materials science. In latest years, it has developed a new anti-counterfeiting technology, object of numerous patents between 2007 and 2009: “Invisible”. This new system consists of applying, directly or indirectly to the artworks, an anti-counterfeiting-proof mark, without affecting them in any way. The mark is invisible to the naked eye and it is seeing only when it is illuminated by an appropriate light beam with the correct wavelength. The positioning of the invisible mark directly on artworks or on a special support that is subsequently applied to masterpieces allows to consider it removable or not [21].

“Invisible” technology is based on optical properties of microscopic fluorescent particles that are activated taking advantage from a focused synchrotron light source or a beam of particles. The creation of CC (Color Centre) in alkali halide crystals using ionizing radiation is a phenomenon, well-known before 1950. In a crystalline structure, CC is a defect in which a vacancy is filled by one or more electrons and it can be generated by ionizing radiation, for example as Synchrotron Radiation. In the case that the CC is lit by a correct radiation (Blue/UltraViolet radiation), it fluoresces emitting light with wavelength belonging to visible region of electromagnetic spectrum. Depending on ionizing radiation, the CC has characteristic spectrum not reproducible by other activation methods and so it will be recognizable if synchrotron lightsource is used. Lithium fluoride is used to produce “Invisible”: after activation process using synchrotron radiation, this chemical compound becomes an invisible pigment and the powder of small crystals could be applied on the surface in several ways, such as:

- evaporation: particles, evaporated on surface, form thin layer (few tens nanometers thick), allowing the creation of the mark using a narrow beam;
- printing: inks or paints, applied on artworks surface, contain activated particles;

- mixing: glue, used to fix tags on artwork, includes activated particles. In this case, the fluorescence of glue could be considered a tag's mark [22].

“Invisible” has already been successfully experimented on a variety of items (historical documents, jewels, paintings, etc.). FIG.1 shows an example of “Invisible” use to mark ancient coins.

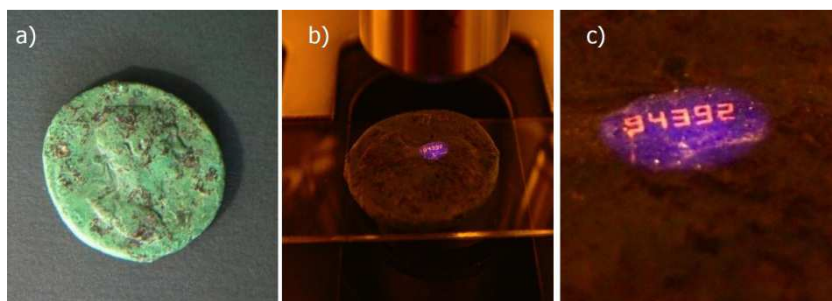


FIG. 1 Ancient coin marked with “Invisible”: a) natural light; b) under ultraviolet source; c) detail of the surface of the coin, showing the mark, under UV light. Image taken from [22].

Even if “Invisible”, for these characteristics, could be an effective anti-counterfeiting and cataloguing system, this technology is linked to Elettra – Synchrotron lightsource facility in Trieste and only few people (the person who applied the mark) knows the exact position, allowing control operations and its identification [21]. In this way, it is possible to think that “Invisible” could not become a common use solution because, maybe, not all museums, collectors, etc. could afford to pay and to use it to mark their masterpieces.

Exploiting the same basic physical phenomenon and optical properties of alkali halide, the researches of ENEA⁵ have developed and patented new tracking tags, based on lithography on luminescent materials using Extreme Ultraviolet radiation source (EUV). Until now, this apparatus has been applied to tag containers of radioactive wastes, credit card, etc. but recent studies have used it for the protection of artworks against forgeries (Bollanti S. *et al.*, 2012). In this case, EUV irradiation allows to transfer an arbitrary and invisible pattern on thin labels that contain lithium fluoride film.

Also this mark can be detected by a specific reading system, appropriate to detect luminescent material but the comparison, between patterns obtained by fluorescent-ink writing and by LiF layer illuminated with EUV source, highlights that they have different spectral response to UV light illumination, easy to detect by differential spectral reading system: in ink jet, the CC absorb rather than LiF-EUV patterns. Moreover, in contrast with fluorescent-ink writing, this technology allows to trace the tag with a better spatial resolution; this label are resistant to normal use

⁵ ENEA (Italian National Agency for New Technologies, Energy and Sustainable Economic Development), is an Italian public company mainly specialized in research, energy-environment and innovation technology in support of sustainable progress.

condition and a thermoplastic film protect it when it is exposed to severe conditions (abrasions, heavy scratching, etc.).

Then, it is easy to control every tampering attempt because if the label is detached from the original item and paste onto another object, the LiF-EUV pattern become visible at ambient light illumination (FIG. 2d) (Bollanti S. *et al.*, 2012).

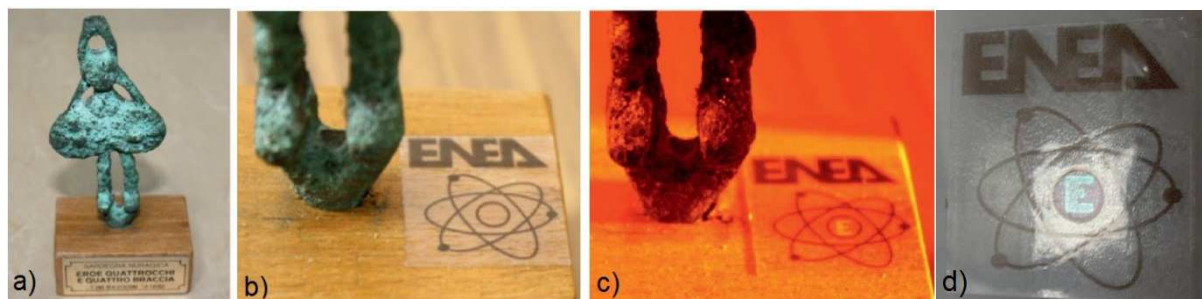


FIG. 2 LiF-EUV tested on a copy of an archaeological bronze statue, known as “Hero four-eyes and four-arms”: a) object with wooden base; b) adhesive tag under normal illumination; c) letter “E” patterned with EUV source appears in the centre of label using specific reading technique; d) LiF-EUV letter “E” is visible under normal light after attempt to remove it from an original item and to replace onto another (Bollanti S. *et al.*, 2012).

However, even if this proposed tag could be an useful anti-counterfeiting tool, it is not so advised to apply a label on the surface of artworks.

2.2.2 New proposed solution: Art-Fingerprints and Art-Fingerprints database

In addition to technology that suggest to mark the surface or to apply something like tags, barcode or radio-frequency identification object (RFID system), considering that this procedure is not always allowed for all artworks, it is interesting to propose other possible solution in order to prevent forgery and unpleasant replacement.

Thinking about that artworks are unique and consequently also the surface of this masterpieces is unique, search of microscopic characteristic features, that are difficult to reproduce and gathered together through a database, could be very useful. As briefly described in Chapter 1, among art-fingerprints studied and analysed in this research, more interesting are those characterized thanks to contribution of Earth Science: identification of some mineralogical phases, presence or absence of impurity on inorganic pigment, particle morphology, etc.

All of these characteristics could make Art-fingerprint and related database a possible anti-counterfeiting system, proving their contributions also to control the originality of a masterpieces or its replacement with a copy.

Analytical procedure and main art-fingerprints found in studied artworks will be showed in next chapter.

3. ART WORKS: EASEL PAINTING

To better understand where the most interesting art-fingerprints could be on paintings, the knowledge of likely materials and artistic techniques employed by the artist is very important.

This allows also to explain the choose of the analytical methods applied in this study. Considering that the research deals with artworks, in particular modern and contemporary paintings, this chapter will describe artistic techniques used to create these masterpieces, underlining the main differences between ancient and modern-contemporary easel paintings.

3.1 Material and techniques in ancient and modern painting

“A painting is the result of a complex of cognitive and intuitive choices made by the artist who is inspired from his visual perception (from the external world) and his emotional perception (from inside)” (Leonardi R., 2005).

The traditional technical definition of a painting is artwork made by pigments mixed in a medium and applied to a support. The term “easel painting” identifies a painting with small or average size, easy to transport. Since XVIII century, the use of this expression has become more frequent, even if this kind of artworks were also in previous century (Paolini C. *et al.*, 2000). Depending on material used, the artistic techniques changes but a typical easel painting has at least four layers: support, ground, paint and varnish [23].

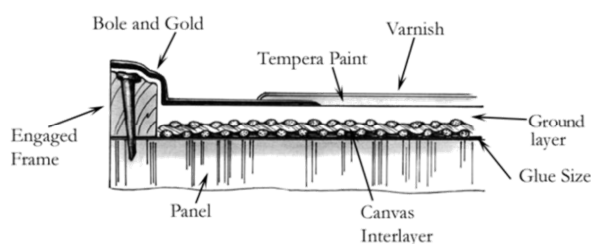


FIG. 3 Model of traditional tempera painting on wood panel [23].

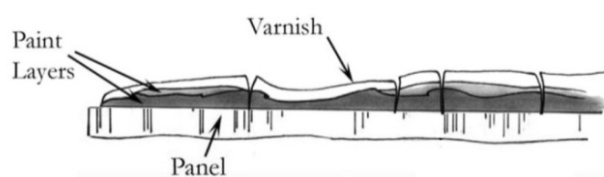


FIG. 4 Model of contemporary painting on wood panel.

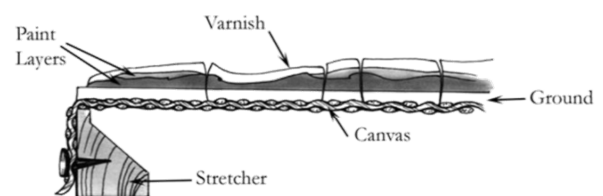


FIG. 5 Model of traditional oil painting on canvas [23].

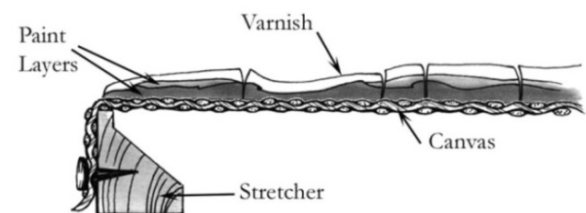


FIG. 6 Model of contemporary painting on pre-primed canvas.

In modern and contemporary artworks, instead, it is quite often easy to find not all the four basic layers: the introduction, in fact, of new materials such as artificial pigment and pre-stretched and pre-primed available canvases from manufacturers, allows artist to create artworks without any kind of materials' preparation and to experiment new artistic techniques.

Painting 1st layer: support

Among the main support used for paintings, canvas and wood are the most common. Since Medieval times through Renaissance, wood was very used until trade and society changed the role played by art: people required more and more large paintings and, in this way, the flexibility and portability of the canvas support was preferred to wood panel. In Italy, canvas became widely used as support for oil painting since 15th/16th century, even if its use as painting support was known to ancients; until then, wood panels had been used, mostly for tempera technique. This aspect is considered also by art-historian as one of the element to discriminate fake artworks: if a painting, in fact, is made on canvas and it is dated before 15th century, it could be a counterfeit. Material for canvas could be different: linen is usually preferred for its superior strength but also cotton, hemp, jute are used. In contemporary paintings, it is possible also to find polyester canvas, made by synthetic fibers, probably more durable than linen or cotton support and more resistant to acid attack [24]. When canvas is used for painting, to stretch it over time the support, a stretcher is designed to expand thank wedges which can be hammered in it.

Wood panels, instead, for ancient Flemish and German paintings are traditionally in oak wood or in poplar for Italian artworks [23]. In contrast to the use of well-seasoned wood panels, especially in contemporary art, it is possible that artist chose a support made by multiple panels glued together tongue-in-groove with fibres crossed in opposite directions, that is more resistant to bow than a wood board. Among other wooden support, artist can use also plywood (thin layers of wood are glued together a wooden core), block wood (narrow parallel softwood or hardwood strips glued edge to edge), chipboard (“chips” of wood compressed into a rigid panels and glued thanks to synthetic resins), etc. [24].

Painting 2nd layer: ground (imprimitura)

According to support and artistic technique, the ground, usually namely “imprimitura” or “preparatory layer”, could be made by different materials. In “tempera” technique, wood panel for painting was usually prepared with a mixture of organic glue and calcium sulfate (gypsum), primarily in Southern Europe, or calcium carbonate in North of Europe. To obtain a better artistic

effect and to improve ground properties for gilding, a film made by Bole, a mixture of natural red clay and glue, was usually spread onto gypsum/carbonate-glue ground. Meanwhile, with the coming of canvas, the ground layer had undergone a change: the brittleness of gypsum/carbonate-glue ground made it unusable for ground layer of a flexible support like canvas. In this way a ground, based on a compound made by oil medium and pigment, was preferred [23]. Artists choose the pigment according to the effect that they would give to artworks: traditionally, the preparatory layer is white and, in the past, it was made by oil and Lead White, even if there are some masterpiece with a colored preparatory layer (green, brown/red) for using colored pigment, such as Veronese's masterpieces (Penny N. et al., 1995) or Van Dycks' artworks (Roi A., 1999). In addition, important artist and writer, as Cennino Cennini, recommended the use of Green Earth for underpainting flesh tones and particularly for the pallor of human bodies (Eastaugh N. et al., 2008). The *imprimitura* was useful both to flatten support surface and to limit oil absorption, improving the aptitude to paint [24].

Since 18th century, with the advent of new technique (i.e. en plain air technique) and of new art materials, artists have more and more preferred to use pre-primed canvas already available: this support is usually treat with artificial organic binders (acrylic resins, glue, etc.) and pigments, among that White titanium dioxide is the most common. So, in modern and contemporary artworks, the pictorial layer is usually spread directly on support, without any kind of *imprimitura*, and the preparatory drawing (*usually charcoal drawing*), if it is present, is designed onto the support.

Painting 3rd layer: pictorial layer

The pictorial layer is a film made by binder mixed together with colored particle (pigment); in a painting there can be different overlapping pictorial layers. Concerning the artistic technique, the medium can be egg or casein (tempera technique), oil (mainly linseed oil) or acrylic compounds (oil painting technique). The choice of the painting medium and the method of application, used by the artist to achieve the desired effects, have affected the conservative condition, determining the longevity of the artworks. As concern, instead, pigments, they can be mainly classified in organic (i.e. cochineal, indigo, Indian yellow, saffron, etc.) or inorganic (ochre, malachite, ultramarine, etc.). Until 19th and 20th centuries, artist had usually used natural pigment, occurring from nature (grounding earth, drying of organic material, etc.), and made by himself or by his apprentices. However, at the end of 18th century, the introduction on commerce of new colored artificial pigments that can have, sometime, the same color of natural but a lower cost (i.e. Artificial Ul-

tramarine Blue vs Natural Ultramarine Blue), pandered artists to experiment new material, creating new colored composition.

Painting 4th layer: varnish and coatings

Before 20th century, for a better aesthetic presentation, in most paintings, pictorial layer was covered by a final coat which brings all the previous layers together and it protects the artworks from dirt and abrasion. The composition of this kind of surface coating changes according to the artistic technique:

- in tempera paintings of 13th-15th centuries, it was usually made by glair, a mixture of water and albumen, that protected but it did not necessarily cause a change of the paints' optical qualities;
- in oil paintings, varnish was principally made by natural resin (dammar or mastic, shellac, amber, etc.) suspended in turpentine, although there are many variants, to saturate the colors, giving more depth and unifying surface gloss. Today, there are few of the original resin coatings onto the artworks because, for the chemical and mechanical transformations causing yellowing, etc., they have been removed by previous restoration actions.

As concern, instead, modern and especially contemporary paintings, being not precise guidelines, varnish coat could be applied or not onto artworks: sometimes, the varnish, made by acrylic resin or other artificial polymers, is spread onto the pictorial layer or also directly onto the support. Finally, if artworks have not been processed to good cleaning before new covering, it could have several layers of dirt deposit, trapped between varnish layers.

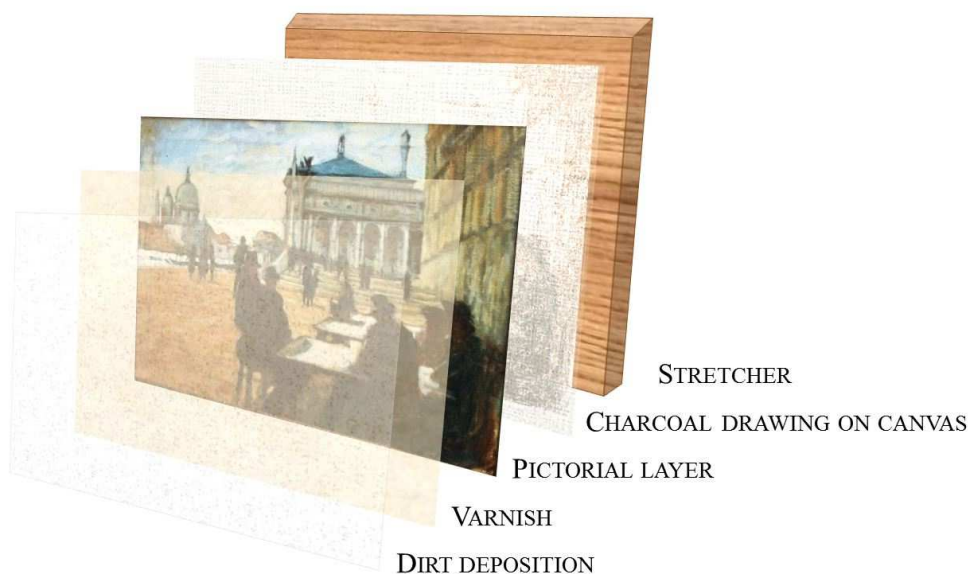


FIG. 7 Proposal model of “Caffè orientale sulla Riva degli Schiavoni a Venezia”, made by J.S. Sargent (artwork plate I): physical layers of different materials composing the painting.

3.2 Pigment

Pigments are the coloring materials employed to create pictorial film. Pigment is a compound made by fine colored particles that, thanks to a selective absorption of characteristic wavelengths, allow to change the color of reflected or transmitted light. Considering that, in nature, the material that can selectively absorb certain wavelengths of light are numerous, for coloring purpose, it has chosen and developed for use as pigments such materials that shown particular properties making them ideal for coloring other materials: the most employed pigment are usually in solid phase at environmental temperature and they are very stable, especially if we consider in artistic field.

There are different way to classify pigments according to their origin (organic or inorganic origin), color (red, blue, etc.), chemically compounds (Cu based pigments, etc.). Other distinction is usually made describing their soluble proprieties: insoluble pigment in the vehicle (resulting in a suspension), dye (aliquid) or soluble in its vehicle (resulting in a solution).

Considering that, in this study, particular attention was paid to artificial pigments, especially on White titanium dioxide, I briefly describe this pigment and its use in art field. As concern, instead, pigments detected on studied specimens, the main component and characteristic are show in TABLE 2.

White Titanium Dioxide

With the general term White Titanium dioxide, it is considered a class of pigments constituted by titanium dioxide, notably the two mineralogical phases of rutile and anatase. This pigment was preferred to numerous other white pigments, especially to White Lead, being more white, with low cost and not toxic.

The pigment were products only in the 20th century, even if colors made by grounding mineral rutile was tested before. Considering, in fact, that this products was white/yellow-red for the presence of iron, the success of this new pigment is linked to the artificial one and so to the technology of 20th century. The synthetic form of White Titanium dioxide, in fact, was obtained or as a pure titanium dioxide or as a composite made by barium or calcium sulfate particles on which a coating of titanium dioxide has been precipitate. The use of rutile phase for the production of art-pigment was limited because it was difficult to grounding. Even if, in 1821 Rose H. tested an intermediate products (hydrous titanic oxide), the difficult to obtain a pure white color passed only in the 20th century. After numerous attempt during the year, the earliest commercially successful titanium dioxide was made by a compound of anatase, prepared by calcination od synthesized ti-

tanic acid, but this product not had a great application in artistic field for its poor technical properties. In 1916 in Norway, the Titanium Pigment Company was founded and, after being purchased by the National Lead company, the production of this pigment developed, The initial process involved the reaction of ilmentite with sulfuric acid and the pigment obtained was made by 25%of anatase and 75% of barium sulfate. The first “pure” white pigment based on anatase phase was produced in 1923. Initially only anatase phase were available but, considered that paints based on anatase tended to chalk if exposed to environmental condition. Research to obtaine titanium dioxide pigment rutile form continued until 1939, when rutile pigments was introduced on commerce by Czechoslovakia. Unfortunately, the advent of the WWII prevented its development in Europe. In United States, instead, the research continued and in the 1940 rutile pigments were marketed. Studies on this pigment brought to obtain a titanium pigment of high quality in 1957 in United States, taking advantage by the new production, born in 1948 and based on chloride process (Lewis P.A., 1987; West Fitzhugh E., 1997; Brachert T., 1988; West Fitzhugh E., 1997).

The history of the use of Titanium White Pigment for artistic materials followed the history of its production. Several research summarized as below the main important date linked to this pigment and when it came in use (Table).

TABLE 1 History of use of Titanium White pigment in art field (McCrone W., 1990; Leonardi R., 2005).

1791	The element titanium discovered
1821	Titanium dioxide (TiO ₂) studies
1900	TiO ₂ as yellow enamel opacifier
1913	Norwegian iO ₂ pigment patent
1919	Production of anatase/BaSO ₄ pigment
1919	House paint (cream color)
1923	Anatase artist s paint (TiO ₂ /BaSO ₄)
1925	Anatase artist s paint (TiO ₂ /CaSO ₄)
1926	First white anatase pigment
1930	Gradual acceptance by artists
1934	Suggested for watercolors and tempera
1939	Production of rutile TiO ₂ /BaSO ₄ pigments
1941	Production of rutile TiO ₂ /CaSo ₄ pigments
1942	Suggested for oil-base paints
1957	Production of high quality (pure rutile pigment)

TABLE 2 Summary of the main pigments identified in samples belonging to studied paintings: Modern and Contemporary Art, 1882-1956 (Eastaugh N. et al., 2004B; Eastaugh N. et al., 2008).

COLOR	COMMERCIAL NAME	CHEMICAL FORMULA	MINERALOGICAL PHASE	NOTES
<i>Blue</i>	Ultramarine Blue	$\text{Na}_7\text{Al}_6\text{Si}_6\text{O}_{24}\text{S}_3$	Lazurite	<i>Ultramarine Blue</i> is the synthetic analogue of the mineral lazurite. Use: since 1827
<i>Green</i>	Opaque Chromium Green	Cr_2O_3	Eskolaite (chromium oxide)	<i>Opaque Chromium Green</i> is the synthetic analogue of eskolaite (rare mineral). Use: since 1809
<i>Green</i>	Chrome Transparent Green (Viridian)	$\text{Cr}_2\text{O}_3 \cdot 2\text{H}_2\text{O}$		<i>Viridian</i> particles appear typically blue-green and translucent. Use: since 1797
<i>Green</i>	Green Earth	complex	Glauconite Celadonite Chlorite Calcite Feldspar Quartz, etc.	The term <i>Green Earth</i> includes numerous geological deposits that contains a mixture of several minerals, among that, the main colouring agents are glauconite and celadonite. Use: ancient
<i>Red</i>	Cadmium Red	$\text{Cd}(\text{Se},\text{S})$ CdSe	Greenockite (similar) (Cadmium selenide sulfide Cadmium selenide)	In <i>Cadmium sulfide</i> (synthetic analogue of the mineral greenockite), the substitution of selenium for sulfur produces a range of colours (from yellow to red-orange). However, some feature characteristics of greenockite crystal can persist (i.e., structure, refractive index and birefringence, etc.). Use: since 1830, 1910
<i>Red</i>	Chrome Red	$\text{PbCrO}_4 \cdot \text{PbO}$	Lead chromate oxide	Synthesis pigment: 1809; it probably came into use in the early part of the 19 th century.
<i>Red</i>	Minium	Pb_3O_4	Minium	<i>Use: ancient</i>

<i>Red-violet</i>	Ultramarine Red	$\text{Na}_7\text{Al}_6\text{Si}_6\text{O}_{24}\text{S}_3$		<i>Ultramarine red</i> is a synthetic pigment obtained by calcination of Blue Ultramarine silicates. Use: since 1828
<i>Red</i>	Vermilion	HgS	Cinnabar (mercury sulfide, dry-process type)	<i>Vermilion</i> is the synthetic analogue of the mineral cinnabar. Use: since 1916, 1923 in pigment for art
<i>White</i>	White titanium dioxide	TiO ₂	Anatase (Titanium Oxide) Rutile (Titanium Oxide)	Use: 1939 in pigment for art
<i>White</i>	White Barium Sulfate	BaSO ₄	Baryte	<i>White Barium Sulfate</i> is the synthetic analogue of the mineral baryte.
<i>White</i>	Lead Carbonate (Italian: Biacca)	PbCO ₃	Cerussite	<i>Lead carbonate</i> is the synthetic analogue of the mineral cerussite. Use: ancient-1912c. recognized its toxicity
<i>White</i>	White Zinc Oxide	ZnO		Use: since 1746
<i>White</i>	Calcium carbonate	CaCO ₃	Calcite	Use: ancient
<i>White</i>	Calcium sulfate	CaSO ₄	Gypsum	Use: ancient
<i>Yellow</i>	Chrome Yellow	PbCrO ₄	Crocoite (Lead Chromate)	Use: since 1797, 1809
<i>Yellow</i>	Chrome Yellow	Pb ₂ O(CrO ₄)	Phoenicochroite (Lead Chromate Oxide)	
<i>Yellow</i>	Strontium Yellow	CrO ₄ Sr		Use: 19 th century
<i>Yellow</i>	Massicot	PbO	Massicot (Lead Oxyde)	<i>Lead(II) oxide</i> is the synthetic analogue of the mineral litharge and it is obtained by <i>Lead Carbonate</i> oxidation at 400°C. Use: ancient

Litharge

PbO

Litharge
(Lead Oxide)

Lead(II) oxide is the synthetic analogue of the mineral litharge and it is obtained by *Massicot* oxidation at 400°C.
Use: ancient

4. MULTI-ANALYTICAL APPROACH

As previously introduced, one of the principal aims of this study is to define scientific analytical protocols that allow to identify unrepeatable features at microscopic level that could be used as “chemical-mineralogical and physical-morphological fingerprints for artworks” during their movement for art exhibition and so particularly important in insurance procedures.

Many techniques are used to study artworks and the possibilities to apply each of them depend on the possibility to take samples from cultural heritage items and to destroy or modify the nature of sample. For this reason, techniques used in Cultural Heritage field could be divided in two categories: non-invasive and non-destructive methods (Calligaro T. *et al.*, 2004).

Non-invasive techniques are all those techniques that allow to provide some kind of artworks examination without extraction of sample and material consumption; considering that it is very important to safeguard Cultural Heritage items, non-invasive approach is usually preferred. According to beam energy, to particle, to physical process detected or to kind of artworks material, some of these techniques could only probe the outer surface of the items and, if the object presents complex structure or inner material different from the surface, it is possible to be misled in the interpretation of the true composition of the objects. Sometimes, although the technique itself is non-invasive, to study the object it is necessary to move it from its location especially if it must be analyzed by special instruments; this aspect could create some risk of damage during transport and manipulation of item and so, to avoid this risk, it is suggested using portable techniques developed to acquire information in situ like portable XRF, XRD, Raman, etc. but being careful to geometry limitations and surface contamination give false data or only qualitative (Artioli G., 2010).

In other cases, sampling could solve in part these problems even if it is an invasive action not often allowed. In fact, the physical actions of extracting a part of material from artworks (sampling) is in contradiction with the philosophical concept of conservation (Pallot-Frossard *et al.*, 2007): in cultural heritage domain, it must be avoided any unnecessary damage. However, thanks to the high sensitivity of modern analytical instruments, micro-sampling will be a possible compromise especially when there are not the possibilities to move both instrument and the artworks. In this way, after a preliminary study of object using non-invasive technique, the most representative area, in which it is possible to sample, are chosen attending to collect appropriate samples to avoid that the results will be meaningless although the technique is very sophisticated and the analytical protocol is optimized (Artioli G., 2010).

TABLE 1 lists some non-invasive and non-destructive techniques used for chemical-physical analysis of mobile artworks together with their acronym, the nature of incident beam and type of radiation or particle detected (Artioli G., 2010).

TABLE 3. Some of the most employed non-invasive and non-destructive analytical techniques used for Cultural Heritage studies are explained. The techniques used in this research are highlighted in bold type.

Incident probe	Analytical techniques		Detected signal	
light	Multispectral Imaging	VIS	Visible (normal, grazing light)	visible
		UV	Ultraviolet Fluorescence	visible
		IRR	Infrared Reflectography	infrared
	OM	Optical Microscopy	visible	
	RS	Raman Spectroscopy	infrared	
	FT-IR	Fourier Transform Infrared Spectroscopy	infrared	
X-ray	XRF	X-ray Fluorescence	X-rays	
	XRD	X-ray Diffraction	X-rays	
	X-Ray Exam	X-Ray Radiography	X-rays	
electrons	SEM-EDX	Scanning Electron Microscopy – Energy Dispersive Spectrometry	secondary electron - X-rays	
protons	PIGE	Proton Induced Gamma Emission	γ -rays	
	PIXE	Proton Induced X-rays fluorescence	X-rays	

Most of techniques in the previous list are particularly useful for the analysis of inorganic material. As concern the study of organic component that it is always present in paintings (binder, protective varnish, etc.), it is often necessary carrying out analysis on specimen that it will be modified (FT-IR, etc.) or destroyed (GC-MS, DT-MS, TG, etc.) (Artioli G., 2010; Kellner *et al.*, 2003).

Considering that artworks object of this work have high artistic and historical value of artworks, the analysis on surface of artworks and on samples studied are carried out with a multi- non-destructive approach in order to not damage artworks and to preserve samples for further and deepen analysis and researches.

The techniques used in this research are highlighted in bold type (TABLE 1) and the methodological approach differs in the possibility to study the entire painting or only the samples. On painting artworks, after Multispectral Imaging survey, most interesting area for each analysis and tested-sample point were chosen under microscope and after Image processing. Tests on samples, instead, were carried out trying to preserve material using system that allow also non-

invasive scientific approach; in this way, it was possible verify if this kind of methodological approach is possible also to apply to future whole artworks or if it will better sampling.

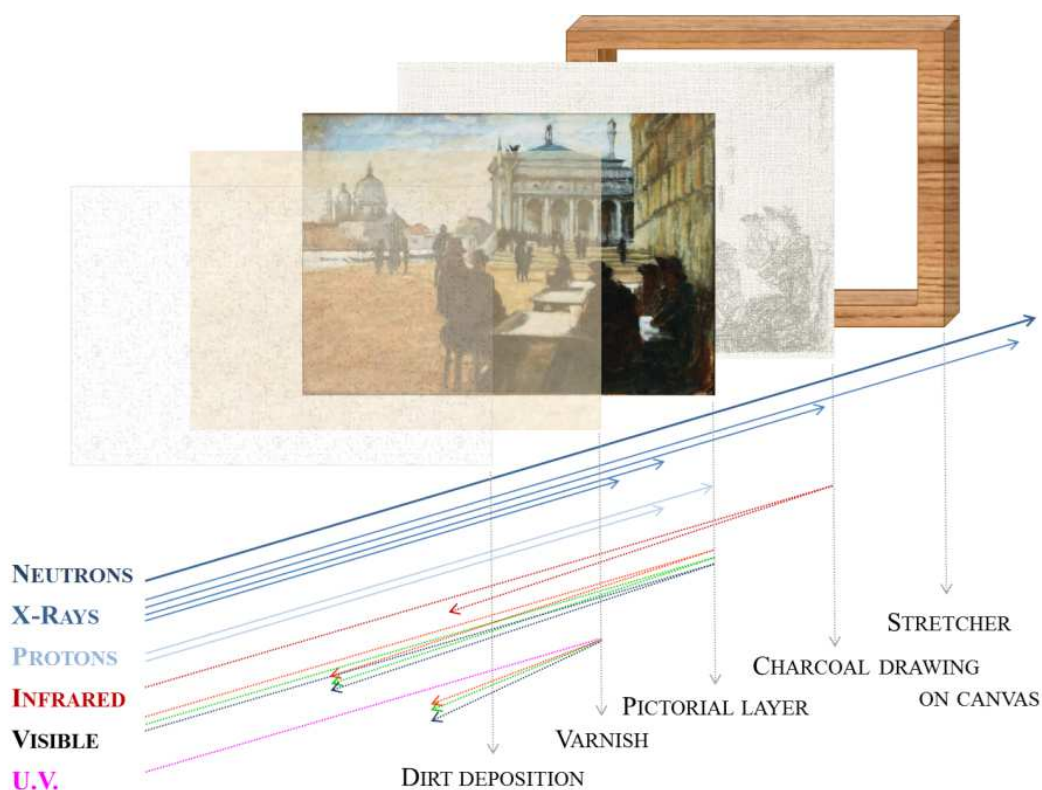


FIG. 8 Schematic representation of the different penetration depth and layers probed by various analytical techniques that employ diverse radiation and particle source⁶.

The chemical composition of pigments is studied using EXDRF, PIXE and SEM/EDS analysis. The results obtained are integrated by μ -Raman spectra carried out on the same samples and XRD analysis carried out on specimens-stub: unfortunately, the impossibility to investigate samples before other techniques (SEM/EDS) did not allowed to apply it on for all the analyzed artworks.

Analytical methodologies, used in this study, will briefly described in the following paragraphs, adverting to principal concepts of techniques and employed experimental equipment. In each schedule of analyzed artworks, experimental set up is described according to analysis carried out. The described techniques are grouped according to the three main approaches in the research of ArtFingerprints: investigation of surface at macroscopic level, at microscopic level and pigment analysis.

⁶ The image is a reworked version of picture in Leonardi R., 2005.

4.1 Surface investigation at macroscopic level

4.1.1 Multispectral Imaging and X ray radiography

The procedure used to observe an object, selecting different wavelengths' ranges in the electromagnetic spectrum is called "Multispectral Imaging".

The visible images, collected by digital cameras in high-resolution digital color files, are used as referential images to create a multispectral model of the analyzed painting. Overlapping these images to those obtained by UV fluorescence investigation, Infrared Reflectography, X-ray radiography it is possible to have a complete painting's vision at different energy range, considering that each spectral range interacts with a different layer of the painting.

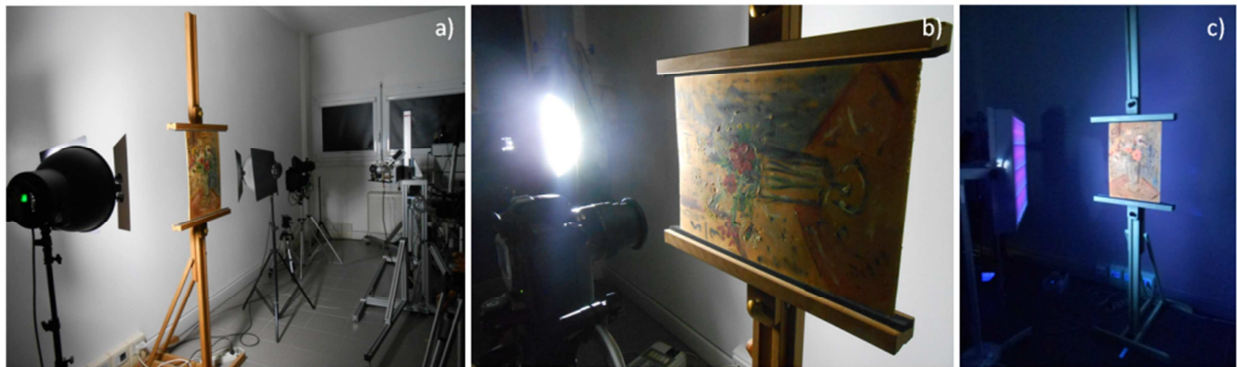
Dividing the light spectrum into a number of frequency bands, digital camera can take many pictures of the same scene at different wavelength that, gathered together, give rise to a multispectral image.

The capability to acquire multispectral images of painting surface allows to investigate whole artworks using non-invasive methods, giving interesting information about conservative condition, *preparatory drawing*, *pentimento*, materials, etc.; this kind of data are very useful not only to choice better area that will be further investigate by other analysis but also to a correct interpretation of obtained data.



FIG. 9 Multispectral imaging applied in this research: studied artwork "Reader woman on bed and old man" (artwork plate IV).

Multispectral Imaging on whole painting were carried out at Laboratory of Archeometry (Department of Physics and Earth Science, Ferrara University – Italy) meanwhile X-ray radiography were performed at Larix Laboratory (Department of Physics and Earth Science, Ferrara University – Italy)⁷.



Multispectral Imaging on “Flowers in glass vase”, artwork VI (Physics and Earth Science Department, Ferrara University, Italy): a) b) VIS-GL survey; c) UV-VIS investigation.

Visible Light exams: VIS, GL and transmitted light

The first visual examination of artworks usually begins with the inspection of painting in the visible spectrum (780-400 nm) and, according to light set up, it is possible to get different kinds of images: plain photographic picture (VIS), raking light image (GL) and transmitted image (trans-illumination).

In fact, different illumination of object allows to investigate painting surface at different shallow angles, creating what is commonly known as *raking light* or *grazing light*. Increasing the depth of brushstrokes and highlighting the difference of thickness, this kind of survey usually reveals interesting details such as *craquelures*⁸, defects, support’s distortions, etc. The study of stroke patterns (manner, directions, viscosity of brushstrokes) renders a lots of information about the artist’s technique, very useful to compare, for instance, artworks which authentication process is still in course.

⁷ Gratefully acknowledge to Prof. Ferruccio Carlo Petrucci and all his staff (Department of Physics and Earth Science, Ferrara University – Italy) for their kind collaboration in performing Multispectral Imaging and X-ray radiography measurements.

⁸ *Craquelure* (French term, or *cretatura* in Italian) refers to the fine pattern of dense “cracking” formed on the pictorial surface due to chemical and physical that caused mechanic tractions in the artwork’s matter (Paolini C. *et al.*, 2000). It is possible to distinguish two main kind of *craquelures*: *craquelure prèmatuurès* and *craquelure d’age*. *Craquelures prèmatuurès* are caused by internal chemical transformation that originate break in pictorial and varnish layer and they are frequent when the artist does not employs convenient materials and technique. The latter, instead, is mainly linked to medium that, during drying process in the course of time, causes mechanic tractions in the inner part of layer causing thin but deep breaking lines (Jagut P., 1988).

If lights are set up behind the paintings (“*transmitted light*”), it is possible to deep the investigation of conservative condition (loss of materials, depth of *craquelures*, etc.), of signatures and overpaints, alterations, etc. [25] (Cucci C. *et al.*, 2012).

Ultraviolet Fluorescence (UV)

Ultraviolet Fluorescence is an imaging methodology that takes advantage of the interactions between a UV radiation (400-360 nm) and superficial layer of painting: when an artwork is exposed to this kind of radiation, pictorial layer adsorbs and reflects it. Thanks to fluorescence phenomenon, a part of adsorbed energy is then emitted in the form of radiation in the visible spectrum range and it can be shot.

Considering that pictorial layers are usually covered by varnish or coating layer and that resins contained in them show high and uniform fluorescence that change according to age and composition, UVF allows to investigate superficial layer detecting the presence of possible removal, retouchings on the top of ancient varnish, etc. (Cetica M. *et al.*, 2007).

Infrared Reflectography (IRR)

Infrared Reflectography is an optical non-invasive diagnostic techniques for the analysis of painted surface that allows to investigate underdrawing under pictorial layer. Radiation in the range of Infrared usually passes through pictorial layer and it is reflected and scattered by underlying layer, in which preparatory drawing is sketched. Detecting reflected radiations from artwork, it is possible to obtain infrared reflectogram, in which the main interesting details is underdrawing (preparatory drawing, usually made by charcoal). Its visibility depends on employed technique and material and it is more visible if artist used material that adsorb IR radiation (i.e. charcoal, lead pencil, metal tip, etc.). Infrared reflectogram can also reveal different pictorial layer hidden by additional superficial films linked to artist’s choice, namely *pentimenti*⁹, or to subsequent restoration actions; sometimes, it is also possible to find artist’s fingerprints, if they are highlighted by carbon powder (Cetica M. *et al.*, 2007).

X-Ray Radiography (RX)

In the X-Ray radiography diagnostic technique, a painting is shot at X-ray exposures and the dose of electromagnetic radiation does not alter painting materials. The radiographic image is

⁹ *Pentimento* (pl. *pentimenti*): changed adjustments of artwork according to subsequent thought. The final result is different from the original draw or artistic idea, which traces remain in the inner part of the painting. In an artwork, Finding *pentimenti* is often considered a proof of its authenticity, because an imitator does not usually change his composition, if it is a copy from an original work (Cetica M. *et al.*, 2007) .

due to the x-ray absorption of pigments and support, to the thickness of layer and their concentration. So, chemical composition of pigments is very important: pigment that contains chemical elements with a high atomic number or metals in its formulae, absorbs x-rays better than pigment with low atomic number element and it is easy to recognize in grey scale radiography. Among the pigments, those made by lead, $Z=82$ (e.g. Lead White, Minium, etc.), for example, well block x-rays instead the worst absorbers are the organic pigments mainly based on carbon, $Z=6$ (i.e. carbon black, organic lake, etc.).

Generally, radiographic techniques allow to evaluate conservative condition of artworks, to detect *pentimenti*, to investigate possible restoration acts and technique of achievement (Castellano A. et al., 2007).

In addition to the continuous improvement of experimental set up and scientific technologies, the development of statistic algorithms and data analysis offers the possibilities to understand better acquired images, deepening on features not always immediately recognizable (Cetica M. et al., 2007). Application of Principal Component Analysis (PCA) to multispectral examination of artwork or to chemical spectra, for example, allow to describe the presence of defects and different material, improving the precision and the reliability of diagnostic exams (Bonifazzi C. et al., 2003^A; Bonifazzi C. et al., 2003^B). Furthermore, new interesting applications of image analysis methods allowed to obtain important results for Cultural Heritage investigation, especially for authenticity research: for instance, the application of multifractal analysis of digitized paintings, measuring features that characterize painting texture, allow to assist art-historical studies and art investigations on attribution decision (Abry P. et al., 2013; Taylor R.P. et al., 2007).

4.1.2 Image processing

The possibility to view different images simultaneously is very important, especially if we considering that images obtained from Imaging Analysis are, usually, compared together to draw conclusions about conservative condition, point/area for not-invasive analysis and for sampling, support for maintenance and restoration works. Restorers and researchers usually use printed image on transparent acetate sheets or, recently, they use image software like CorelDraw, Gimp, etc. in which the different layer could be overlapped.

But, if the images have different dimension, resolution, etc. according to different system acquisition and videotape geometry, it happens that the comparison between this image could be difficult even if it pays attention to resize images with the same dimensions.

For this reason, in this research, for the elaboration of images obtained by multispectral imaging survey and x-ray radiography, it was tested a software, usually used in Geography and Geology, that allows to connect different images through a control of sectioned point: ENVI 4.3 suite.

ENVI (acronym for “ENvironment for Visualizing Images”) is a software application mostly used in remote sensing field for analyzing and processing geospatial image [27]. It is principally used in Geographical and Geological sector (Jusuf S.K. *et al.*, 2007) to process satellite images and also applied in Archaeology to uncover important and unique data unobtainable using traditional archaeological methods such as excavation, etc. (Giardino M.J., 2011; Malinverni E.S. *et al.*, 2009).

This suite analyses images obtained by remote sensing systems but if it considers the main basic concepts of them, it is possible to verify that it is not so distance from multispectral imaging on painting, previously illustrated.

In fact, according to Kumar “remote sensing is the science and art of obtaining information about an object, area or phenomena, through that analysis of data, acquired by a device, that is not in contact with the object, area or phenomena under investigation” (Kumar Dr. S., 2005). Other important concept in remote sensing is that it is necessary a physical carrier to travel the information from the objects to sensors and in this field it is normally used electromagnetic radiation (Kumar Dr. S., 2005). Considering this concepts, we could try to apply remote sensing techniques also to investigate cultural heritage objects using image taken from Multispectral Imaging and X-Rays image; in this case, the application will deal with modern and contemporary paintings.

In TABLE 4 the principle elements of remote sensing are correlated to a possible application in painting’s fields.

TABLE 4. Comparison between remote sensing principles and its application on Cultural Heritage domain.

Elements required in remote sensing process¹⁰	Description of phenomena	Possible application in paintings
Energy Source or Illumination	Energy source which provides electromagnetic energy to the target	Lamp (Tungstene, Wood, etc.)
Radiation and atmosphere	Travel energy comes in contact and interact with atmosphere when it passes through	Multispectral Imaging and X-Rays image are carried out in environmental condition

¹⁰ Kumar Dr. S., 2005

Elements required in remote sensing process¹¹	Description of phenomena	Possible application in paintings
Interaction with the target	Energy, that ATTRAVERATO atmosphere, interacts with target according to their properties.	Interaction phenomena due to physical-chemical characteristics of paintings and energy radiation.
Recording of Energy by the Sensor	Sensor (remote sensor: not in contact with the target) collects and records electromagnetic radiation scattered or emitted by the target.	Detector and sensor used for Multispectral Imaging and X-Rays image (i.e. IR-camera, Digital camera, etc.).
Transmission, reception and processing	Receiving station processes data into an digital image.	VIS-image, UV-VIS-image, IR-image and X-rays image.
Interpretation and Analysis	Processed analysis is interpreted in different way (visually, digitally or electronically) to obtain information about target.	Elaboration and interpretation of acquired imagery to better define main characteristics of painting.
Application	Extracted information from imagery about target helps to better understand it, revealing news information or assisting to solve some particular problems.	Interpretation of acquired data gives information about conservative state, materials, repainting-area etc. of studied paintings. It is very useful to select point area to deepen with other scientific analysis.

As it is possible notice, principle elements of remote sensing procedure are also respected during a common non-invasive diagnostic on paintings.

In this way, ENVI 4.3 suite was tested onto the image obtained by multispectral imaging of studied artworks, that have all different dimension and resolution. This image processing was carried out at UTSISM Unit of ENEA Research Centre (Bologna, Italy), where there are workspace equipped by PC with ENVI 4.3 SW license¹².

After download the different paintings' pictures and used a filter to correct the true color of images, the identification of the possible well recognizable point of connection started.

Using the tool "Select GPs image to image", a "warp" file was create for each image (VIS, RK, TRASINLL, UV, IR, XR) that will be uploaded, connecting referent points well recognizable in each of them (i.e. border of alarm clock, point of female foot's fingers, etc.). To improve the correspondence of images, it was chosen more point as possible.

¹¹ Kumar Dr. S., 2005

¹² Gratefully acknowledge to Prof. Francesco Immordino and Arch. Elena Candigliota (ENEA UTSISM, Centre Research Bologna – Italy) for their support in Image processing.

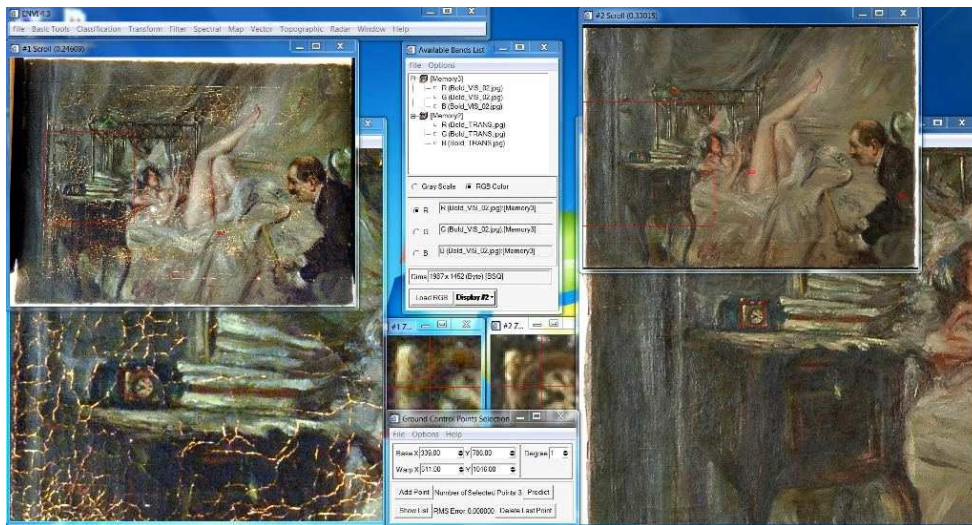


FIG. 10 Image Processing on “Reader woman on bed and old man” (artwork plate IV): Warp file creation VIS-TRANSILL images.

Once create this “warp” files, it is possible to download and to visualize them in different displays; after that, linking each other using the tools “Link display”, the operator could visualize and investigate all the downloaded images two by two or more, if it is necessary (FIG.11). This application is very useful for the choice of point area, that will be deepened through other scientific techniques: unlike the traditional comparing methods and SW based on visualizing image at different time, this allows to study different images just clicking on the interested point to visualize an interactive overlapping images, without moving mouse pointer.

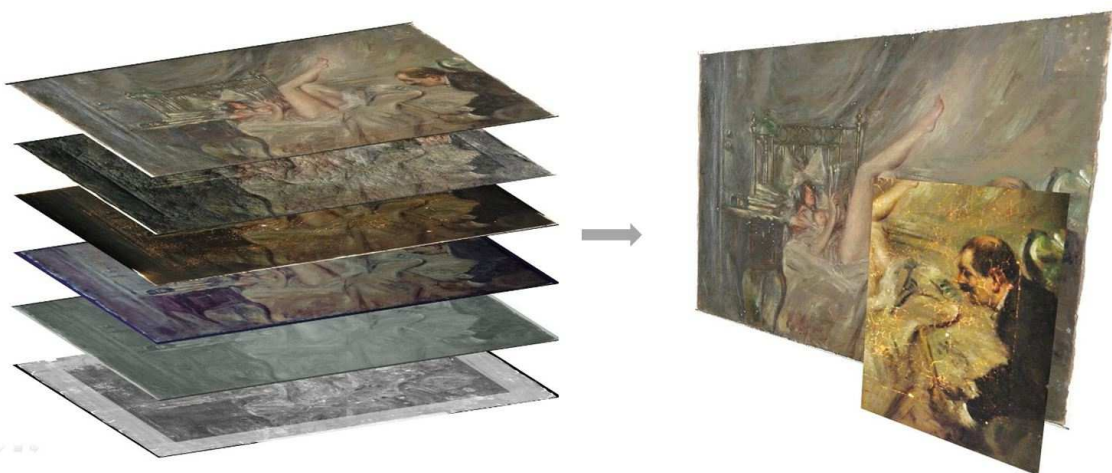


FIG. 11 Model: image Processing on “Reader woman on bed and old man” (artwork plate IV), results from “Warp file creation”.



FIG. 12 Results from “Warp file creation”, clicking it is possible to pass from image to other linked: a) transillumination image onto visible photograph; b) X-ray image onto visible photograph.

Therefore, considering also that ENVI suite is usually used to classify images according to elements with the same selected characteristic, the software was applied to obtain model distribution of chosen features according to analyzed picture: for instance, color class on VIS image, *craquelures* class on transillumination picture, etc.

The procedure is the same for each ROIs (Region Of Interest) and for each image. For example, it was tested onto VIS image to quickly visualize macroscopic color classes (ROIs) that are used for characterization in pigment analysis (blue, green, red, white, black, brown, yellow) and color obtained mixing different color pigment like pink (red and white). When the color mixture creates an effect that is difficult to classify with less than two different color, it was create two ROI background according their major color tone (blue, violet or green-brown-yellow tone): for the complexity of this color composition it is not suggest carrying analysis here to define pigments used by the artist.

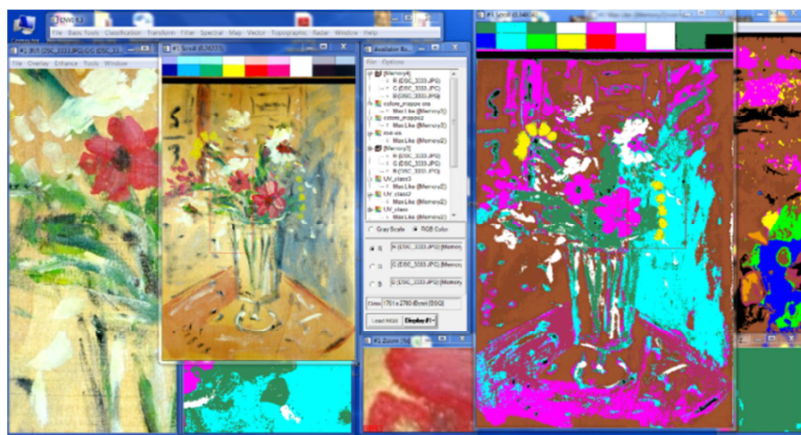


FIG. 13 Image Processing on “*Flowers in glass vase*” (artwork plate VI): images’ group on left show the original photograph; images’ group on right show ROIs’ color class on the painting.

After ROIs selection, to create the “color model distribution” it was applied to image the maximum likelihood (ML) registration method: this kind of classification calculates the probability that a pixel belongs to a specific class (in this case: choose color), assuming that the statistics values are distributed for each selected class in each of the three band (R,G,B). Not selecting a particular probability threshold, each pixel was assigned to that class that had the highest probability, and so maximum likelihood (Richards J.A. *et al.*, 1999).



FIG. 14 “Flowers” (artwork plate V): VIS photograph.



FIG. 15 “Flowers” (artwork plate V): ROIs’ color class through Image Processing.

4.2 Surface investigation at microscopic level

After a detailed macroscopic investigation of painting (multispectral imaging and image processing), the artworks is observed at microscopic levels, through optical microscopy, both to study the morphology of pictorial layers, to examination of *craquelures* and to choose the most interesting area that can be analysed with a number of instruments and where it is possible a next sampling.

In fact, considering that microscopy can reveal a lots of information about painting’s structure, brushstrokes and artistic technique, conservative condition (i.e. wide *craquelures prèmatuurès* or very thin *craquelure d’age*), this kind of survey, that is usually used on samples, was also exploited onto whole paintings to catch also all these features, that can be considered as art-fingerprints.

According to investigate artworks’ surface or samples, it was used different optical microscopes (visible radiation): stereomicroscope, polarized light microscope (PLM) and 3D digital microscope.

As concern, instead, morphological characteristics of pigment, a deepen study on samples was carried out with electron microscope (SEM/EDS analysis), in order to investigate the materials feature with a very high magnification and with chemical microanalysis.

4.2.1 Optical microscopy

Stereomicroscope

The stereomicroscope, a kind of optical microscope, allowed a 3D vision of examined painting surface or specimens. Taking advantage from two separate optical paths with two different objectives and two eyepieces, in fact, it provided little diverse angular views for the left and the right eye, producing, in this way the 3D visualization. The use of incident reflected rather than transmitted illumination permitted, in this way, to examine materials that could be too opaque or thick for a normal investigation under optical microscope.

For the investigation of studied paintings and specimens and for the sampling, it was used a stereomicroscope Optika SZ6745TR (total magnification x 90) equipped with webcam MOTICAM 2005 5.0 Mp and software Moticam Image Plus 2.0. Thanks to mechanical arm, it was also possible analyzed painting of great dimension (i.e. “Flowers” by F. De Pisis, 70 cm * 50 cm), both vertically and horizontally; moreover, the analysis were carried out using perpendicular LED light or with different tilt angle in order to obtain grazing effect at microscopic level.



FIG. 16 Stereomicroscope OPTIKA SZ6745TR (Physics and Earth Science Department, Ferrara University, Italy): a) horizontal working set up; b) vertical working set up; c) sampling on artwork “Reader woman on bed and old man” (artwork plate IV) under stereomicroscope.

Polarized light microscope (PLM)

The investigation of studied μ -specimens was carried out by Optika Polarized light microscope (total magnification x 100) equipped with webcam MOTICAM 2005 5.0 Mp and software Moticam Image Plus 2.0 (Physics and Earth Science Department, Ferrara University, Italy).

The possibilities to use both reflected and transmitted light allowed to detect the dimension and size of the pigment grains, to examine artistic technique, pictorial layer and also some canvas fibers extract from two samples of studied painting on canvas support. This survey was very useful to understand better the nature of pigment in order to focus further analysis and to correct interpret analytical data. Furthermore, exploiting polarized light, PLM revealed interesting results about structure of fibers permitting the identification of biological species used to create canvas support.

3D digital microscope

In order to a better exam of samples' surface, at *Centre de Recherche et de Restauration des Musées de France* (Carrousel Laboratory, CNRS-LC2RMF UMR 171, Palais du Louvre, Paris – France), a further analysis was carried out through Hirox KH-7700 3D Digital Microscope System, using MXG-2500REZ lens with magnifications from 140 X to 500 X and spatial resolution around 1µm.

This technology provides a precise observation and analysis by gathering together the different slices-image of samples thanks to automatic Z-axis control and focusing system. After the acquisition of great number of image captured at different heights, the system achieves all the image reconstructing a 3D model of samples that allows also surface profile measurements ([Van Den Berg K.J. et al., 2008](#)).

A deep 3D profilometric characterization of surface is useful for conservative studies: for example, to the study depth of *craquelures*, facilitating the identification and the possible cause (*craquelures prèmatùres* or *d'age*); but the application of this technique could give interesting results also for the art-fingerprints database. In fact, considering that also the surface roughness is unique for each sample/artworks/etc., its measurement, carried out in several areas and taking note of the exact position, allowed to consider it like an art-fingerprints. Moreover, the non-invasive approach permits to apply it also to whole artworks (without necessary sampling), if the it is possible to place it onto the microscope's stage and under the microscope.

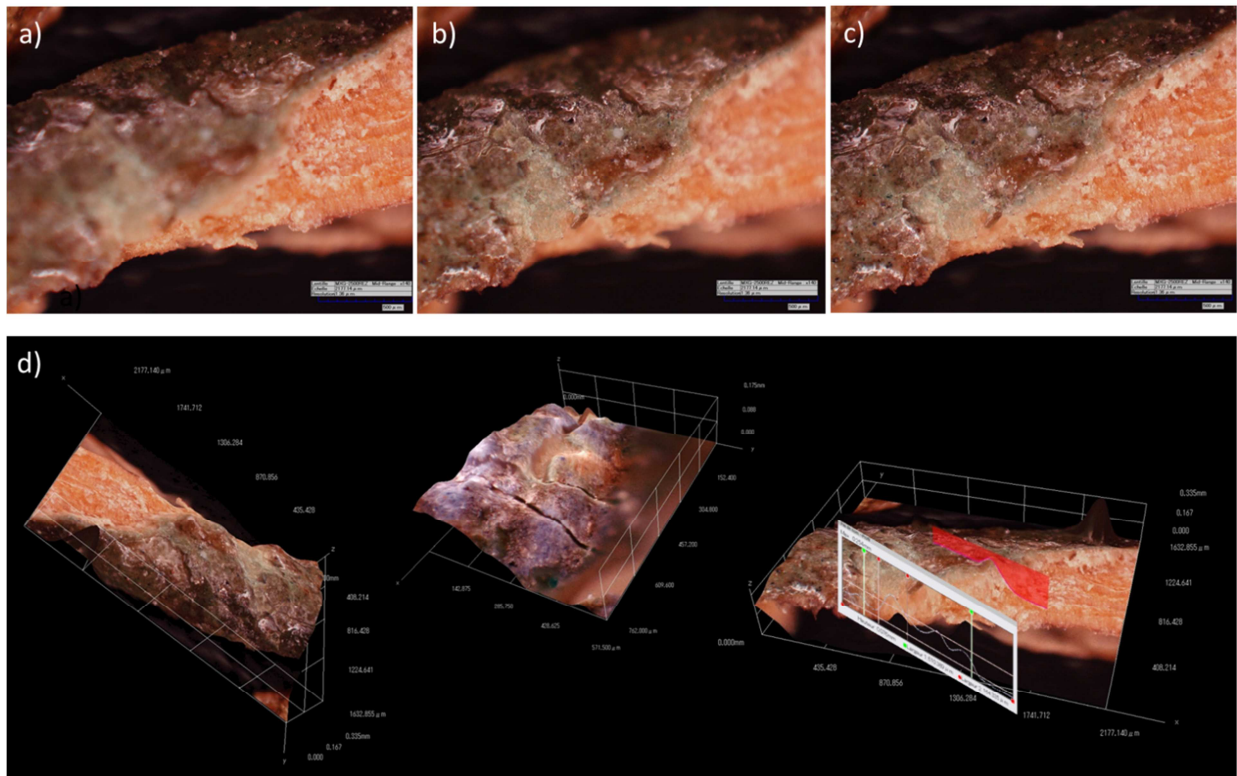


FIG. 17 3D Digital Microscope System Hirox KH-7700 (CNRS-LC2RMF UMR 171, Palais du Louvre - Paris, France): a) microphotograph of sample, focused on wood support (magnification 140 X); b) microphotograph of studied sample, focused on pictorial layer (magnification 140 X); c) microphotograph of studied sample, obtained by multi-focus system; d) 3D model of sample in the previous image and surface profile measurements.

4.2.2 Electron microscopy

Scanning Electron Microscope with Energy Dispersive X-ray spectroscopy (SEM/EDS)

Using electron beams accelerated in the range of 10^2 - 10^4 eV, scanning electron microscope allows to obtain images of the surface with a magnification over 100000 times (unlike OM, maximum 1000 X). The signal resulting from the interaction of electron beam with the near surface or atoms of the sample (secondary electrons, X-rays, backscattered electrons, etc.) is collected by specific and synchronized specialized detector in order to obtain:

- an image in which the contrast depends on the number of detected secondary electrons (through low energy secondary electrons);
- an image in which the contrast is linked to different chemical composition of the surface (through backscattered electrons);
- chemical composition of a selected point of interest and, if it is possible, a map of elemental distribution, in which, intensity of the characteristic X-Ray line of a specific elements is recorded for each raster point (EDS analysis) (Kellner R. *et al.*, 1998).

All these information are very useful in the examination of pigment grains, studying both their morphology (energy secondary electrons image) and their chemical composition, also interpreting the element distribution onto pictorial surface (Artioli G., 2010).

The paint samples were mounted onto sample holder (aluminum, diameter 1 cm) with conductive double-sided carbon tape and they are analyzed in variable pressure; in this way, it was not necessary any kind of pre-treatment of the sample (metal or carbon coating), allowing to preserve samples for further analysis. Secondary electron images were taken at various magnification and the condition used for imaging and microchemical analysis changed, according to the following employed different instruments:

- SEM FEI Inspect S Quanta 200 LV equipped by EDAX SW for EDS chemical microanalysis (Electron Microscopy Laboratory, ENEA-UTSISM, Research Centre Bologna, Italy). Working set up: electron source tungsten filament, accelerating voltage 30 kV, working distance around 10 mm (10 mm for EDS); same set up for EDS microanalysis. Detected signal: secondary electron, EDS microanalysis for area of interest;
- SEM ZEISS EVO MA15-HR equipped by software OXFORD Smatmap EDS INCA Energy 250 X-Act for EDS chemical microanalysis (Electron Microscopy Laboratory, Scientific and Technologic Centre, University of Ferrara, Italy). Working set up: electron source LaB₆ cathode, accelerating voltage 20-22 kV, working distance from 8 to 9.5 mm (20 kV and 8.5 mm for EDS). Detected signal: secondary electron, backscattered electron, EDS microanalysis for point/area of interest and map acquisition system;
- SEM ZEISS EVO 40 supplied by OXFORD INCA 300 SW for EDS chemical microanalysis (Electron Microscopy Laboratory, Chemical and Biomedical Centre, University of Ferrara, Italy); Working set up: electron source tungsten filament, accelerating voltage 10 kV, working distance from 8 mm to 10 mm (10 mm for EDS). Detected signal: secondary electron, EDS microanalysis for point/area of interest and map acquisition system.

For the identification of pigment compounds, reference manuals are used (Eastaugh N. et al., 2004; Eastaugh N. et al., 2008; Montagna G., 1999; Seccaroni C. et al., 2002).

4.3 Pigment analysis

In addition to obtain results that can be collected as art-fingerprints, a deepen pigment analysis can give a lots of information in support of dating and authentication studies.

A pigment analysis determines what type of pigments were used, that are different according to painter, technique and times. Many studies were carried out in order to classify pigments in chronological tables showing when they first came into use (e.g. thanks to patent date) and when and if they stopped being used (Eastaugh N. *et al.*, 2008; Feller R.L., 1985; Roi A., 1986; West Fitzhugh E.,1997). In fact, certain pigments were used after a certain date, namely *post quem* pigment, while other disappear before a certain date, known as *ante quem* pigments. For this reason pigments, especially the artificial pigments, are an important tool in support to dating and authentication studies, not providing proof of authenticity or an exact data when the artwork was painted, but, considering when this type of pigment first became available. It means that a pigment analysis can provide cut-off dates and tell before what date a painting could not have been painted.

Moreover, considering that the most common “dating pigment” are the artificial pigment, produced with the advent of new technology of 18th century, for modern and contemporary art a pigments’ analysis focused only to the simple identification of pigment (i.e. White titanium dioxide) can be not always adequate; in this case, it is preferred a deep pigments’ analysis, that allow to recognize pigment mineralogical phase, trace of production methods, etc. in order to compare data with detailed chronological table and results obtained in other artworks considered datum-point (e.g. White titanium dioxide pigment in West Fitzhugh E.,1997).

For this reason, Earth Science can supply an important contribution in this research.

In this research, pigments’ analysis were carried out through:

- μ EDXRF, SEM/EDS, μ PIXE analysis in order to obtain chemical composition of pigments and eventually trace elements that are characteristic of a particular production process;
- SEM/EDS analysis to study the morphology of pigment grains linking morphology and corresponding chemical analysis;
- μ Raman and XRD analysis for the identification of mineralogical phase of analyzed pigments found in studied artworks.

4.3.1 Energy Dispersive X-ray Fluorescence (EDXRF)

Energy dispersive x-ray fluorescence (EDXRF) demonstrated to be particularly useful for the noninvasive and nondestructive multielemental analysis of pictorial layer and its technology allowed to perform analysis on the whole object (sample or painting) without any kind of surface preparation. The interactions of material surface, when it is exposed to a primary high energy X-rays beam, causes the expulsion of core electrons of the atoms; to fill the vacancy due to move of these electrons (belonging to inner atomic orbitals), a series of electron jumps, from external to lower atomic orbital, allow the unstable ionized atom to return to ground state. The electrons' jump causes the emission of fluorescence photons in the X-rays region (secondary X-rays), corresponding to the quantum structure of the atom. Secondary X-rays allow to obtain the characteristic fluorescence emission spectrum of the atom, detectable by XRF analysis (Artioli G., 2010); thanks to deepened X-ray Data Booklet it is possible to interpret all measured spectra, in which X-ray emission line is calculated for all the elements in the periodic table (Thompson A. *et al.*, 2009).

Preliminary measures were carried out on the whole paintings to understand possible pigments' composition and in order to aid the choice of most relevant colored area to sampling those pigments that could be more useful for dating studies presently in course. Considering the complex nature, artistic technique and consequently mixture of pigment and color, a deep μ EDXRF analysis was performed onto sample to obtain chemical information more precise as possible linked to a specific color.

Even if its portability, the measurements were carried out with portable Bruker ARTAX 200 μ EDXRF spectrometer at Larix Laboratory (Department of Physics and Earth Science, Ferrara University – Italy) equipped by Mo X-ray tube and by a Peltier cooled Si(Li) detector, that allows high energy resolution. Thanks to a color CCD camera (500 x 582 pixels, magnification 20 X), X-ray beam was focused onto paintings and samples, through a laser spot and using a collimator with diameter from 200 μ m to 650 μ m; the possibility to position the measuring head, in different way, allowed to investigate paintings in vertical or horizontal plan. Considering that the range of elements that can efficiently be detected changes according to the energy of primary X-rays, to a better detection of light and heavy element, on the same spot, the analysis were carried out using helium purging system and with voltage from 15 kV to 50 kV and current from 700 μ A to 1500 μ A (Live time: 60s, 120 s). The escape correction of peaks' spectra were performed by ARTAXControl 7.2 software, that permitted also to better investigate summing spectra (i.e. spectra 15 kV, 30 kV and 50 kV) or subtracting spectra (e.g. background spectra, carried out on

each carbon-tape/stub where samples are placed). The software is not able to remove the lines produced by the scattering of the characteristic X-ray tube (Mo) on the sample: in each spectra, therefore, the Rayleigh and Compton lines of Mo-K_α and Mo-K_β, which intensity depends on the density of the samples, are enclosed in a grey rectangle.

Even if EDXRF elemental analysis (spectra and tables) in Chapter 5 shows the complete data obtained by EDXRF carried out, for a more reliable qualitative identification of pigment, it was considered mainly those elements having a net area of the XRF peak greater than one standard deviations. Several reference manuals are used to recognize the pigment compounds (Eastaugh N. et al., 2004; Eastaugh N. et al., 2008; Montagna G., 1999; Seccaroni C. et al., 2002).

Finally, considering however that the signals came from overlapping layers of painting and that EDXRF does not allow to obtain quantitative results, further chemical analysis (SEM/EDS, Cap. 4.2.2 and PIXE) were performed for a more detailed composition of pigments.



FIG. 18 μEDXRF Bruker ARTAX 200 (Larix Laboratory, Department of Physics and Earth Science, Ferrara University – Italy): EDXRF analysis on “Flowers in glass vase” (artwork plate VI).

4.3.2 Proton Induced X-ray Emission (PIXE)

Among IBA analysis¹³, Proton Induced X-ray Emission (or Particle Induced X-ray Emission) is one of the most effective technique used for the physical and chemical analysis at the level of atomic components and, since its introduction, it has brought a lots of benefits to the study of cultural heritage (Calligaro T. et al., 2004; Gordon B.M. et al., 1972).

PIXE analysis were performed at AGLAE facility of the Centre de Recherche et de Restauration des Musées de France (Carrousel Laboratory, CNRS-LC2RMF UMR 171, Palais du Louvre,

¹³ Ion Beam Analysis (IBA), suite analytical techniques that probes chemical-physical nature and state of atoms constituent the material, exploiting the interaction between accelerated charged particle beam and material, detect different signals such as X-rays, γ-rays, visible photon, etc. (Artioli G., 2010; Breese M. et al., 1996; Hellborg R., 2005; Jeynes C. et al., 2012). For in-depth information: App. II.

Paris – France)¹⁴, where it is also possible to carry out simultaneous PIXE, PIGE and RBS analysis (Beck L. *et al.*, 2011; Calligaro T. *et al.*, 2000; Pichon L. *et al.*, 2010).

When a material is hit by a beam of charged and accelerated particles (protons, α -particles, etc.) with energy in the range 200keV-4MeV, the atomic interactions, that occur, cause the emission of photons in the X-ray range, neutrons and charged particles. In the case that protons' beam interacts with the sample, the stimulated emission of X-rays by protons is detected through PIXE analysis; meanwhile, γ -rays, emitted by nuclear process during the proton's interaction with sample are detected, by PIGE technique and the backscattered protons, pursuant to elastic collisions, by RBS. The possibility to select energy beam and preset dose value allow to PIXE to be non-invasive technique, permitting also the investigation of different layer (depth profiling) in according to the beam's penetration, that depends both on the composition of the samples and on the beam energy. For this reason, in the analysis of heterogeneous materials, such as painting layers, it is considered as a bulk analysis, providing a signal that is an average of the multilayers structure (Artioli G., 2010; Kellner R. *et al.*, 1998).

However, its high sensitivity to detect also trace elements contained in the material suggested to apply it in support of this research both for the art-fingerprints and in support of dating studies.

In fact, pigments' analysis of artificial compound, especially if it is employed in support of dating and authentication studies for modern and contemporary paintings, requires a very deepened and detailed study for the use of these pigments to create the artwork.

Considering, then, that “these synthetic inorganic pigments continue to evolve today, the identification of their composition, and sometimes their recipes for fabrication, may bring clues for dating and authenticating paintings” (Leonardi R., 2005), it is very interesting to deep the research of that material's feature: products, in fact, used at the time, if macroscopically or through traditional noninvasive techniques (multi-spectral techniques, etc.), are difficult to diversify from recent materials, they are identifiable on a microscopic scale for a particular morphology, for the presence of trace elements that are characteristic of a specific production process, etc.

Given that all these characteristic chemical compositions can be considered among the “not reproducible characteristics' artworks” belonging to studied paintings and so, artfingerprints, PIXE analysis were performed onto samples in order to confirm chemical composition obtained with previous chemical analysis, recognizing also light elements not detectable with EDXRF system

¹⁴ Thanks to financial support by the Transnational Access to Research Infrastructures activity in the 7th Framework Programme of the EU (CHARISMA Grant Agreement n. 228330). Gratefully acknowledge to Prof. Claire Pacheco and all her staff (AGLAE facility, CNRS-LC2RMF, Paris – France) for their kind collaboration in performing measurements.

and supplying quantitative analysis, and to catch elements that are on trace concentration and probably linked to a particular production process.

At Centre de Recherche et de Restauration des Musées de France, AGLAE facility (Accélérateur Grand Louvre d'Analyse Élémentaire) is based on 2MV tandem accelerator and a 3 MeV proton extracted beam was focused on samples placed on stub or onto a filter (made by cellulose fibers) in handmade vacuum system (for free μ specimens). In order to not damage samples, the maps were acquired by scanning the area at different times, according to analyzed samples, and thanks to dose monitor, it was possible to control the charge deposited at each position. X-ray spectra were recorded by two Si(Li) detectors oriented at 45° to the beam: one detector is devoted to detection of low energy X-rays (0.1-15 keV), meanwhile the other for higher energy X-rays (4-40 keV); moreover, considering the matrix of analyzed specimens, a Mylar filter (100 μ m) was used to reduce pileup by attenuating intense X-rays and the analysis were performed under a continuous flow of He, used to expel air between the specimen and the detectors. Elemental maps¹⁵ of specimens were obtained thanks to a motorized sample holder and to the new mapping acquisition system (Pichon L. *et al.*, 2010), that stores all the spectra for each detector in EDF format. This allowed to use PyMCA¹⁶ program suite, in order to select region of interest (ROI), through ROI_Imaging_tool, and to verify the overlapping of some chemical element, using RGB_correlator.

Finally, elemental concentration was obtained by using TRAUPIXE_EDF (Traitement AUtomatique des spectre PIXE) and GUPIXWIN V2.1¹⁷ engine, that, processing in sequence high and low energy spectra for each pixel map and using the “pivot element” method, allow to extract peak intensities, converting them into concentrations; the final result is a table of quantitative element composition, related to the previous selected ROI (Calligaro T. *et al.*, 2011; Pichon L. *et al.*, 2010).

¹⁵ Map size: from 640 μ m x 640 μ m to 640 μ m x 1280 μ m, according to the samples.

¹⁶ PyMCA, free software developed by the BLISS (Beam Line Instrumentation Software Support of ESRF), that is used for the analysis and visualization of Energy-Dispersive X-Ray Fluorescence data (Pichon L. *et al.*, 2010; Solé V.A. *et al.*, 2007).

¹⁷ GUPIXWIN V2.1, upgrade version of GUPIX engine, used to process each pixel in order to extract elemental concentration from PIXE maps. For in-depth information: (IAEA, 2003; Pichon L. *et al.*, 2010).



FIG. 19 AGLAE facility (Centre de Recherche et de Restauration des Musées de France, Palais du Louvre, Paris – France): a) AGLAE, external microbeam used to perform PIXE analysis; b) PIXE analysis on samples placed on stub (specimens taken from studied Modigliani’s artwork); c) PIXE analysis on free samples placed on filter in hand-made vacuum system (specimens taken from “Flowers” by F. De Pisis).

4.3.3 Raman Spectroscopy (RS)

Considering that previous techniques (EDXRF, SEM/EDS, PIXE) do not allow to tell how the elements are combined together to form molecules and crystal, other techniques were performed to obtain complementary information for a better pigments’ analysis (μ RS, XRD).

Taking advantage from the inelastic exchange of energy (Raman scattering) between a vibrating atomic group and an incident beam, Raman spectroscopy provides to be an efficient technique to probe the vibrational and rotational states of the molecules. When a material is exposed to monochromatic light (single λ), usually light from a laser in the near IR, visible or near UV range, it emits radiation with increased λ (lower energy) for the adsorption energy linked to vibrational states of molecules. Depending on nature of atoms, inter-atomic chemical bonds and dynamism, each atomic group or molecule has, in fact, a specific vibrational proprieties that, if detected, allow to identify molecules and atomic bounds. Therefore, Raman spectroscopy detects backscattered energy from functional groups after adsorption (Artioli G., 2010).

For a more precise analysis on pigments, μ Raman technology, obtained coupling Raman spectrometer with optical microscope, was performed onto samples.

μ -Raman measurements were carried out at Department of Physics and Earth Science of Ferrara University (Ferrara, Italy) using HORIBA Jobin Yvon LabRam HR800 spectrometer coupled to Olympus BXFM optical microscope, geared with 10x, 50x and 100x objectives. The spectrometer, with a focal length of 80 mm, is equipped with two 600 and 1800 groove/mm gratings and with an air-cooled CCD detector at -70°C (1024×256 pixels); the instrument operates with He-Ne laser source with excitation wavelength at 632.81 nm and laser beam diameter is about 1 mm.

The system was calibrated and checked with silicon standard at 520 cm^{-1} . Raman spectra were acquired with an irradiating laser power kept at 2 mW. The spectral resolution was about 2 cm^{-1} and the investigated spectral range mainly spanned from about 200 to 1600 cm^{-1} , where the main diagnostic signals of inorganic materials (pigments and minerals) fall. The 50x and 100 x magnification objectives were employed to focus the laser beam onto the samples placed on the X-Y motorized sample holder. Considering that the microscope stage allows to measure up to 10 cm from painting's border, this techniques was previously tested onto whole paintings, to avoid sampling, but the emitted fluorescence of the varnish layer was so intense to hide the Raman lines.

Finally, Raman spectra were recorded and elaborated using LabSpec 5 software and each

spectrum was acquired with exposure time that varied between 10 and 15 seconds with 5 accumulations. For the identification of pigments' compound, acquired spectra are compared both with several reference database and research for pigments [28, 29], or specific for mineralogical phases [30] and LabSpec 5 Raman Spectroscopy Library. In the Raman interpretation the following letter indicate kinds of Raman bands and they stand for weak (w), very (v), strong (s), medium (m), shoulder (sh), broad (br).

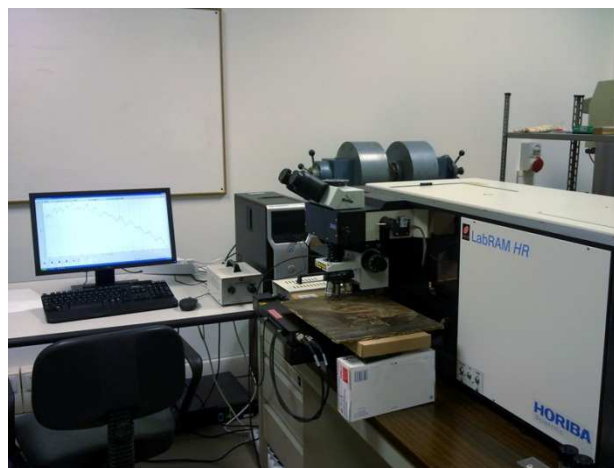


FIG. 20 μ Raman Spectroscopy (Department of Physics and Earth Science, Ferrara University, Italy): investigation on studied painting “Reader woman on bed and old man” (G. Boldini).

4.3.4 X-ray Diffraction (XRD)

In order to obtain a more precise and reliable pigment analysis, X-ray diffraction was carried out on samples in order to validate the presence of inorganic pigments previously detected by μ Raman spectroscopy.

XRD analysis, in fact, is a fundamental technique for the identification of crystalline compounds and, if working in optimal condition, it allows also to carry out quantitative analysis, physical analysis of crystalline aggregates (texture, crystallite size distribution, etc.), etc.

It founds on the interaction between an incident beam of X-rays and a target material: in materials with some regular structure (i.e., crystalline structure), the emitted X-rays are scattered in a certain directions and, measuring the angular relationships between the incident and diffracted x-rays and applying Bragg's Law ($N\lambda=2d \sin\theta$, where N , λ , θ are known for analytical set up and measure)¹⁸, it is possible to identify d , distance between lattice planes, that it is characteristics of each crystal structure. The data collected in a X-ray diffraction pattern are generally the intensity profiles of the diffracted X-rays in function to scattering angle (Artioli G., 2010).

Unfortunately, as for the other analyses, unfavorable circumstances did not allow to perform XRD analysis before SEM/EDS and due to frailty of samples it was not possible to remove them from double-sided carbon tape without damaging the specimens. Moreover, the complex mixture of painting samples in which pigment particles are embedded into the organic medium does not make XRD from single crystals as a suitable technique. In spite of the above difficulties, considering information about mineralogical phases useful for the current study, powder XRD analysis was tested onto the whole stubs containing pictorial samples, carbon tape and aluminum sample-holder stub. For these purpose, a specifically designed plexiglas stub-holder was used in order to best align the stub on the XRD goniometer. Due to the natural divergence of the incident beam from the conventional Cu X-ray tube source, sample-displacement errors arising from parts of the specimen lying above and below the focusing plane could not be avoided altogether. These errors were modeled and taken in to account when performing the phase search-match. XRD patterns were collected at XRD Laboratory (Department of Physics and Earth Science of Ferrara University, Ferrara – Italy)¹⁹ with a Bruker D8 ADVANCE X-ray diffractometer based on a Bragg-Brentano θ/θ geometry and equipped with a Si(Li) solid-state detector set to detect the $\text{CuK}\alpha$ radiation. Measurements were carried out on samples/stub, in the range from 5° up to 75° 2θ with a step size of 0.02° 2θ and exposure time of 15 s. Search-match for phase recognition was performed after subtraction of background from plexiglas holder and carbon tape. Besides the few strong diffraction peaks from the aluminum stub, the complex diffraction pattern coming from the mixture of crystalline pigments was of enough quality to allow a clear-cut identification of many phases with reference to the Powder Diffraction File (PDF-2) database.

¹⁸ In Bragg's Law: θ is half of the diffraction angle between the incident beam and diffracted beams; λ , is the wavelength of the incoming radiation; N is number of reflection's order.

¹⁹ Gratefully acknowledge to Prof. Giuseppe Cruciani (Department of Physics and Earth Science, Ferrara University – Italy) for his collaboration in performing measurements and for the support of interpretation XRD spectra.

4.4 Art-fingerprints database

All the information obtained by non invasive investigation on artworks (both macroscopically and microscopically), chemical-mineralogical pigment analysis, studies under microscope of samples and data elaboration from image processing define, in their complexity, all features and artwork characteristics that are difficult to reproduce, especially, to reproduce in the same position.

For this reason, each points of analysis was measured considering coordinate (0;0) the origin on bottom-left of painting stretcher; in this way each information are referred to an internal coordinate system. Considering that the traditional approach to archive data is to collect information in a database, all the art-fingerprints were gathered together proposing two kind of database: traditional database and an interactive database based on image.

4.4.1 Traditional database

Art-fingerprints can collected and catalogued using common commercial software to record data, i.e. Microsoft Access 2010 or open-source software. The basic components of this database should be tables for each analysis that we are interested to insert.

First of all, it is necessary to appoint to both X-Y coordinates the value of “key-words”: in this way each information, inserted in the database, can be univocally identified through its coordinates. After that it is possible to choose the tables that will belong to the database, according own use.

The database created was tested for example on the following six table, but the number can increase according to the number of categories of art-fingerprints to catalogue: Craquelures, Fluorescence area, XRF analysis, PIXE analysis, Raman analysis. TABLES such as “Craquelures” or “Fluorescence area” could have field that could be ticked Yes/No or they can contain the possibility to describe the art-fingerprints, specifying for example if there are *craquelure d’âgé* or *craquelures premature* or describing the color of fluorescence. XRF and PIXE tables could be organized in two different way: they could contain or a list with all chemical elements found in the entire painting (each element box could be ticked Yes/No) or character line in which it is possible write found elements. Paying attention to connect the different tables in a correct way, with an appropriate use of relationship among tables, database can be personalized concerning the use, the analysis, etc.

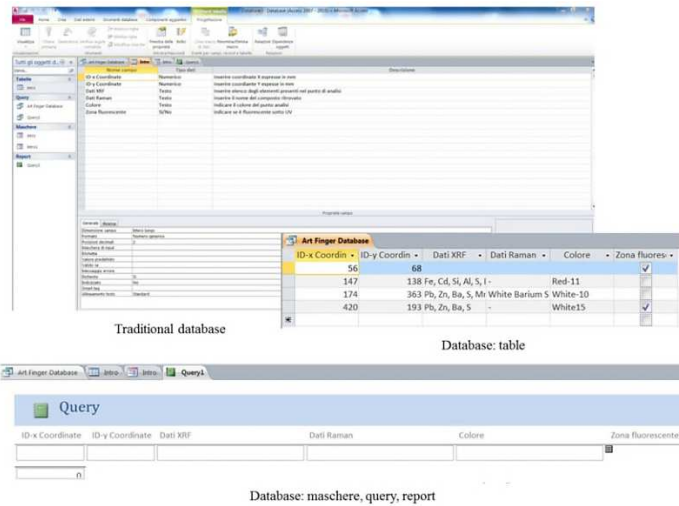


FIG. 21 Example of Art-fingerprints dataset: traditional approach.

4.4.2 Interactive Image database: AIAD (Art Image and Analysis Database)

Considering the great number of images that are used for painting investigation, it is possible to propose an “art-image database” in which, each analytical information, is referred to a single point with known coordinates. This will allow to examine the image and obtain all the information required. Attributing art-fingerprints to cartesian coordinates, it will be more easy and exact to find previous analysis position, permitting in this way to better compare different analysis on the same area, even after time. The application could be used also to control conservative condition if the little movements of referent points, in the same direction, are due to environment (possible slack of canvas) and not to a substitution.

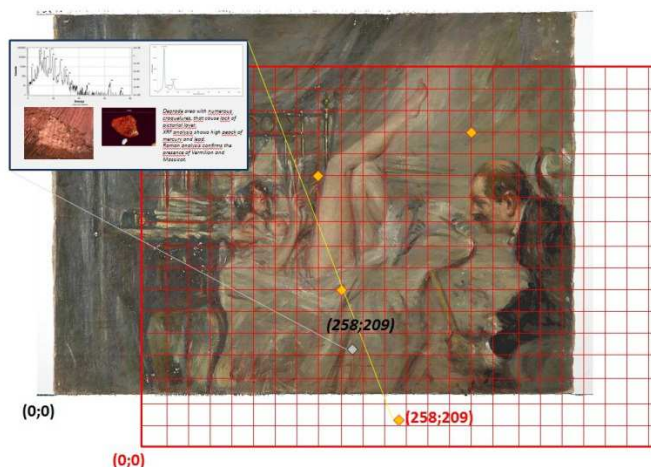


FIG. 22 Schema: proposal “Art Image and Analysis Database” on “Reader woman on bed and old man” (artwork plate IV).

This procedure is possible using design software like AutoCAD or free software that allow the relationship between point analysis and external objects. In this study, for the creation of AIAD

(Art Image and Analysis Database) it was used AutoCAD 2010 and the procedure is briefly shown below.

After gathered together all the art-fingerprints in a folder, the achievement of the database started with the insertion of mill metric references, in order to create X and Y axis with the dimension of the image that it will be used as background image (i.e. VIS image of the painting). The exact dimension of the painting was linked to each respective axis and the reference image was downloaded.

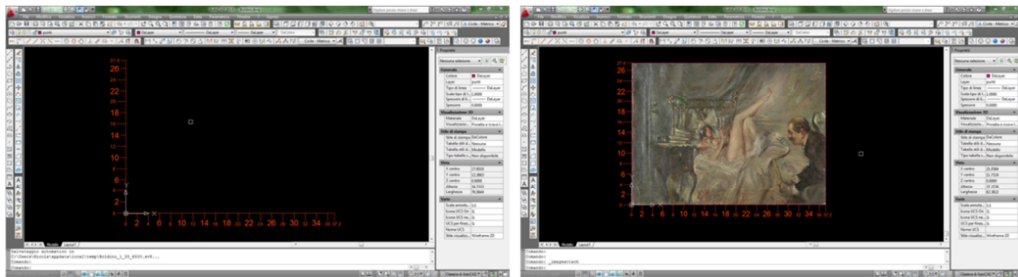


FIG. 23 Art Image and Analysis Database: creation of internal reference coordinate system.

For this test it was used single point (dimension 0.5 unit), but the object to which create the external link could be a line, etc.. To insert the point in the exact coordinates, it is possible to write its coordinate in the command bar and, using the command “insert external link”, the external file was linked with the selected art-fingerprints corresponding to that point. In this proposal AI-AD two possible objects were created: “*.pdf” file with a short report about interested art-fingerprints and a image plate in which the data were exposed in graphic format.

Therefore, the selection of reference points onto the image in correspondence of art-fingerprints coordinates allowed to link the art-fingerprints to the image reference points; in this way, it is possible to click on the interested point and the connected art-fingerprint plate will be displayed.

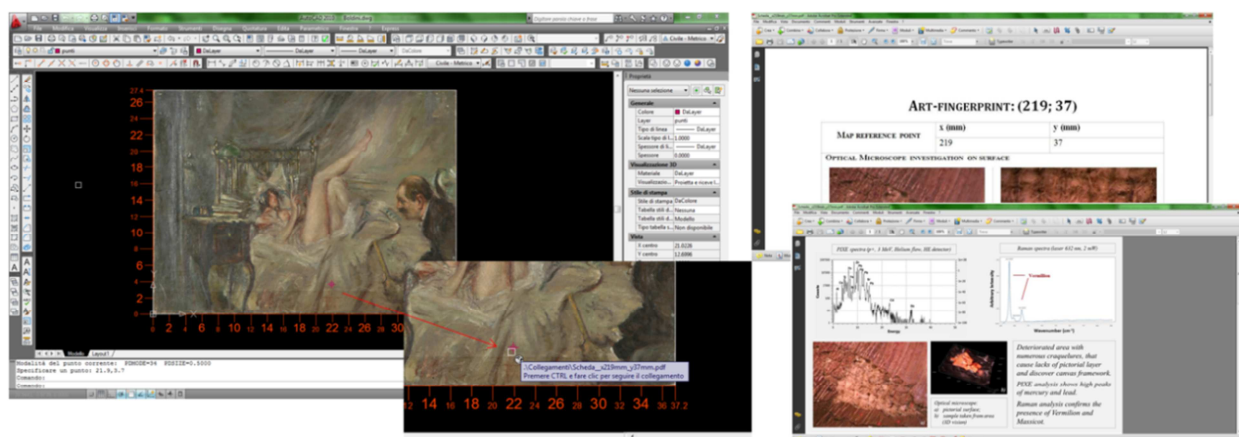


FIG. 24 Art Image and Analysis Database: interaction between point analysis and external associated file containing ArtFingerprints.

III. RESULTS AND DISCUSSION

In order to best explain results and highlight research's hypothesis, I will describe, one by one, the researches on the six artworks studied, dealing with short introduction about artist and his artistic production or studied artworks.

The studies on each artworks will be introduced by an *Artwork Plate* and the paintings are displayed in chronological order (suggested by owner).

When it was possible, entire analytical suite of methodologies was carried out on artworks; on the other hand, received samples taken from paintings were analyzed using techniques in order to not modify or damage specimens.

In this work, examined ArtFingerprints can be gathered according to two main categories:

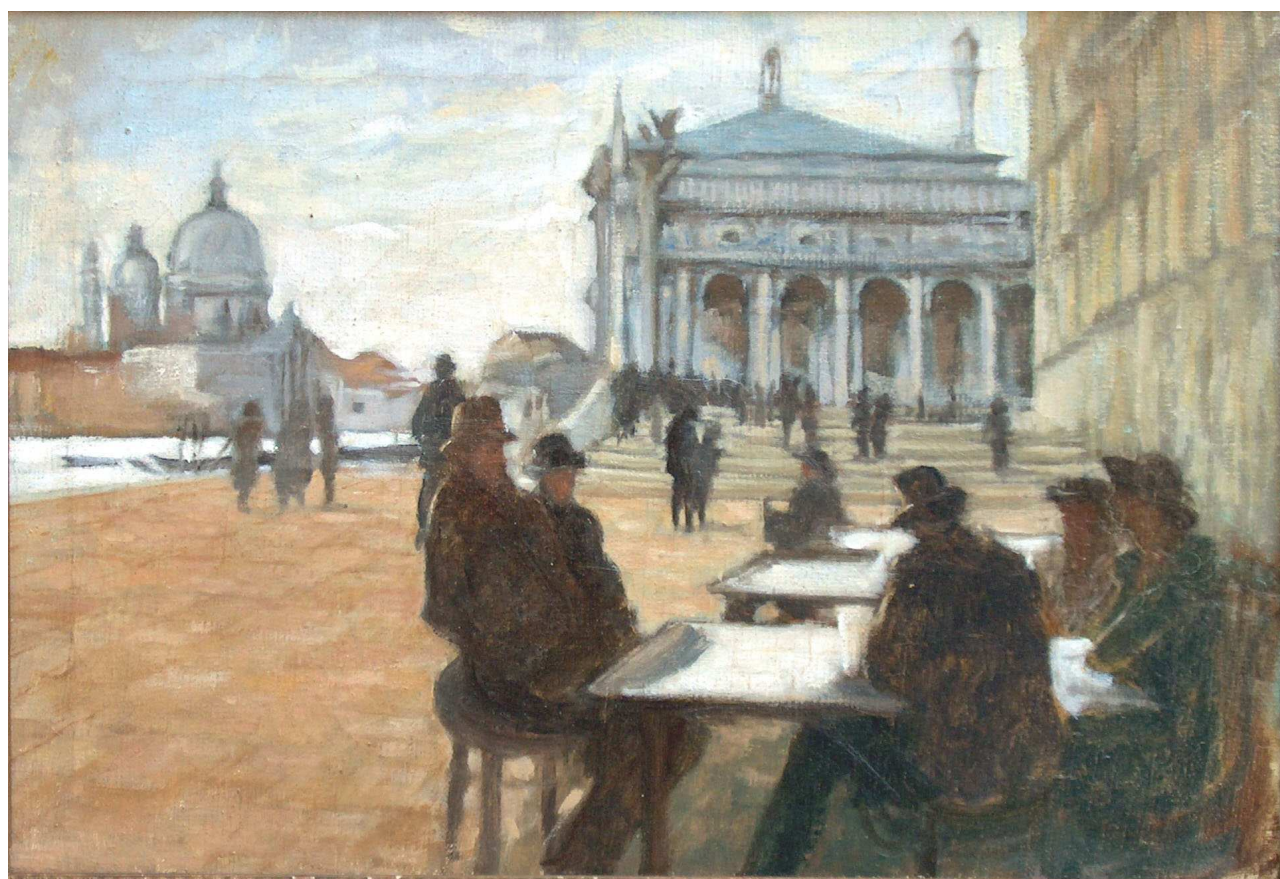
- Superficial features: pictorial layer morphology, artistic techniques, film thickness, etc.;
- Chemical-mineralogical composition of inorganic materials: study of pigment.

As concern the study on samples, the attention was focused on the identification of pigments used by artist in order to give chemical-mineralogical art-fingerprints; in addition to restoration project, these information are useful also to support dating studies on analyzed paintings.

Regarding, instead, overall paintings, art-fingerprints were identified not only among chemical-mineralogical features of pigments but also in peculiarity of artistic techniques at microscopic level, that will support some of the studies of authentication presently in progress.

The precise spatial coordinates of all point analysis collected for the analyzed artwork are kept thanks to informatics database (Chapter 4.4); nevertheless they are not inserted in this manuscript for previous agreement with owners about these confidential data. Database models is shown in Chapter 4.4.

ARTWORK PLATE I



Author: *John Singer Sargent (American artist, 1856-1925)*

Title: *Caffè orientale sulla Riva degli Schiavoni a Venezia*

Object: *Painting (oil on canvas)*

Date: *post 1880/1882 ?*

Overall: *55,5 cm (height) * 38,0 cm (width)*

Location: *Private Collection*

Note: *study of dating in progress*

5.1 “Caffè Orientale sulla Riva degli Schiavoni a Venezia” by John Singer Sargent (oil on canvas, c. 1880/1882?)

Size: 55,5 cm (h) x 38 cm (w)

The research of art-fingerprints was performed on the specimens taken from this artwork. In-depth study was focused on pigment analysis, in particular on mineralogical phases that can be useful for a more precise dating studies, currently in progress.

5.1.1 The artist

John Singer Sargent (January 12th, 1856 – April 14th, 1925) was one of the most famous and successful painter of his generation (Kilmurray E. *et al.*, 1998).

Born in Florence in 1856 to expatriate American parents, Sargent spent his childhood touring Europe, mainly in France (Paris), Italy (Rome, Florence, Venice, etc.), England (London), etc. (Ratcliff C., 2001). In 1868, he received his first formal art instruction at Rome and then sporadically attended the Accademia delle Belle Arti in Florence between 1870 and 1873 [35].

He was introduced to watercolor world thanks to one of his first teaching, Carl Welsh, (Warren A., 2006) and he began his art studies in Carolus Duran’s atelier, where the traditional academic approach (careful drawing and under-painting) was replaced with a new method of painting: loaded brush were spread directly on the canvas like Velázquez manner (named “alla prima” method), permitting also spontaneous flourishes of color not linked to an under-drawing. Sargent, in fact, loved to say “I am an American, born in Italy, educated in France, that speaks English; I look like German and I paint like a Spaniard” [36].

During his career, Sargent made a lot of paintings and watercolors: after brilliant and insightful portraits of genteel society using the grand manner of portraiture, he turned his artistic skill to the execution of landscape paintings made with Impressionism style (*en plain air*), especially in later part of his life in which he captured common life scene and characteristic foreshortening, in particular way place like Venetian “calli²⁰” (Ayres L.,1986; Blaugrund A.,1986; Kilmurray E. *et al.*, 1999; Ormond R., 2007; Romanelli G., 2007).

5.1.2 The painting: subject and artistic technique

“Venice has been described so indelibly in words and images that she has become like a palimpsest with different impressions overlaid one on another, a place that can be visited and

²⁰ Calle: pl. “calli”. *Calle* is a typical Venetian street, built between two continuous queue of buildings. The width of *calle* is changeable from around 60 cm for narrow calle (alias “calleséle” or “callètte”) to 5/6 m or more for wide streets.

experienced in the imagination” (Warren A., 2006).

Considering Sargent’s artistic Venetian artworks (Ayres L.,1986; Blaugrund A.,1986; Warren A., 2007), it is possible to assure that Sargent had a double language capacity: Sargent “portraitist of aristocratic Venetian world” and solitary Sargent “landscape painter”, that had roamed through tiny Venetian street to capture on paint architectural features that change aspects according to different daylight and color (De Rossi L., 2009).

In this artwork, Sargent painted one of Venetian characteristic foreshortening: Riva degli Schiavoni²¹, a monumental historical quay in Sestriere di Castello that widens, towards Bacino di San Marco, in the stretch of road between Ponte della Paglia on Rio di Palazzo, in front of Palazzo Ducale, and Rio di Ca’ Dio. As well described by Kilmurray and Ormond, “Riva degli Schiavoni in Venice is the paved quay which extends eastwards on the northern side of the Canale di San Marco, from the Molo” of San Marco square, “in front of the Palazzo Ducale, curving gently down towards the Giardini Pubblici. It is a favourite promenade and meeting place and some very famous names have inhabited the houses and hotels punctuating its length including Henry James. [...] The scene is the celebrated Café Orientale” (nowadays replaced by a part of luxurious Hotel Danieli) “with the Ponte della Paglia and the façade of the Palazzo Ducale in the middle distance, Sansovino’s Libreria and the two pillars in the piazzetta in the background and the commanding domes of Santa Maria della Salute rising to the left” (Kilmurray E. et al., 1999).



FIG. 25 Caffè Orientale in Riva degli Schiavoni (Venice): ancient photo Naya (De Rossi L., 2009).



FIG. 26 Riva degli Schiavoni (Venice): nowadays (2011).

²¹ The origin of the name *Riva degli Schiavoni* is due by a group of merchant, which, in the period of Serenissima Repubblica di Venezia (c. 742-1797), came from Dalmatia (also named Slavonia or Schiavonia) and that, in this quay, landed with their merchant ships and they had their commercial activities. The quay, in fact, belonged to Venice commercial seaport and it was very important for its proximity to Piazza San Marco and the centre of politic Venetian power (Tassini G., 1964).

This composition depicts informal scenes of contemporary life and the witty disposition of the figures, that are sitting on café chairs and that are looking at Ponte della Paglia, picks out a “confidential Sargent”, poet of artistic beauty of this lagoon city and its particular life (Kilmurray E. et al., 1999; De Rossi L., 2009). In fact, differently from other Venetian artworks, Sargent’s curiosity was riveted by common people meeting-place and not by aristocratic Venetian drawing room: in this case, he took no notice of human portrait and psychological value of his subject but he suggested only human element with monochromatic use of color that highlights silhouette profile, giving them, anyway, a specific role thanks to generous use of matter and color.

According to De Rossi, this artwork could be refer to Impressionism and Post-Impressionism French period: the matter of figure and the not respected elementary prospective rule of the café table remembers the dense painting of Cézanne and the room painted by Degas, respectively (De Rossi L., 2009).

The silence, the particular troubled atmosphere, the immobility captured in this artwork could well explain how Venetian paintings made by Sargent are considered as a break towards genre painting of the period (De Rossi L., 2009; Mamoli Zorzi R., 2007). Further, the comparison between this artwork on canvas with the homonymous watercolour with the same subject, “Café on the Riva degli Schiavoni” (J.S. Sargent, watercolour on paper, c.1880-1882, *Private Collection*) supports this concepts: the watercolour appears more conventional thanks to spatial distribution where symmetry and proportion rule give more credibility to holy and profane buildings in background over Ponte della Paglia (FIG. 27-28).



FIG. 27 J.S. Sargent, *Café on the Riva degli Schiavoni*, c.1880/1882, watercolour on paper, Private Collection Courtesy of Adelson Galleries, New York (Kilmurray E. et al., 1999).



FIG. 28 J.S. Sargent, *Caffè orientale sulla Riva degli Schiavoni a Venezia*, 1880/1882?, oil on canvas, Private Collection (De Rossi L., 2009).

Limited color scale use, original composition, the choice to well fill the right part of the oil painting (FIG. 27) leaving, in the distance, only Redentore Church's shape on the left could be considered elements break with romantic traditional description of Venice, a charming city but, in the meantime, mysterious with no-time dimensional unreality. In this painting, it is possible notice that the façade of Palazzo delle Prigioni and the "palladiana"²² Basilica in Fondamenta della Giudecca (Redentore Church) are quickly painted, whereas Sargent paid more attention to draw Libreria Sansovino with detailed representation of loggia arches, columns and relief frame. In this way, with shadows and illuminate areas, the artist succeeded to give sculptural aspect to composition in spite of the bi-dimensionality of painting surface; therefore, the two dominant elements in the composition are the National Library Marciana²³ and the human shape sat at café. During Infrared Reflectography examination, oil painting showed a detailed underdrawing and also a *pentimento* concerning a chair near the two person that sat down at the first table: this chair, that survives in the watercolour, is painted out by the artist but its trace are visible on Infrared reflectogram (De Rossi L., 2009).



FIG. 29 J.S. Sargent, *Caffè orientale sulla Riva degli Schiavoni*, oil on canvas: a) VIS detail; b) Infrared reflectogram detail (De Rossi L., 2009).



FIG. 30 J.S. Sargent, *Caffè orientale sulla Riva degli Schiavoni*, oil on canvas: a) VIS detail missed chair; b) Infrared reflectogram detail missed chair (De Rossi L., 2009).

This secrets, hidden by the final painting, are not so unusual in Sargent artworks: in *Madame X* (oil on Canvas, 1916), for example, Infrared Reflectography showed a detail of proper right arm revealing jeweled shoulder strap painted out by the artist (Mahon D. *et al.*, 2005).

²² "Palladiana": based on architectural project by famous Italian architect Andrea Palladio (1508-1580).

²³ National library Marciana, also known as Biblioteca Marciana, Biblioteca di San Marco, Libreria Sansoviniana, etc. It is one of the most important Italian library. The original nucleus dates at 1468, when the cardinal Giovanni Bessarione donated ancient Greek and Roman codices and manuscripts to Republic of Venice "ad communem hominum utilitatem" (for common good of human being) [37].



FIG. 31 J.S. Sargent, *Madame X* (Madame Pierre Gautreau), 1883-84. Oil on canvas. The Metropolitan Museum of Art, Arthur Hoppock Hearn Fund (Mahon D. et al. 2005): a) photograph in visible light; b) Photograph of Sargent's *Madame X* as it was exhibited at the Salon of 1884 before repainting of shoulder strap and background. The Metropolitan Museum of Art, Gift of Mrs. Francis Ormond, 1950 (Mahon D. et al. 2005).

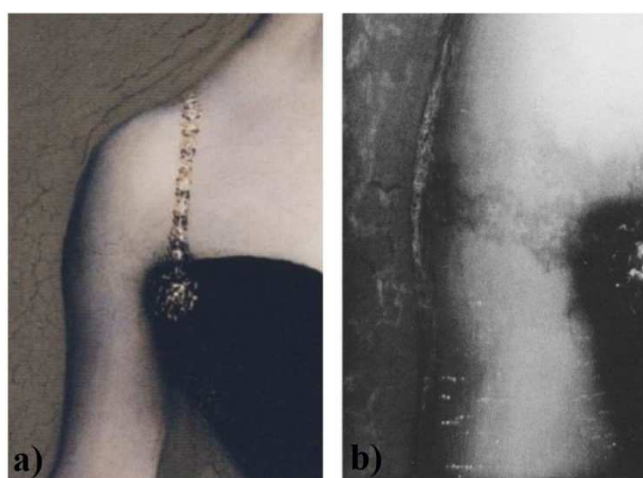


FIG. 32 J.S. Sargent, *Madame X* (Madame Pierre Gautreau), 1883-84. Oil on canvas, detail: a) right arm with the correct shoulder strap (photograph in visible light); b) infrared reflectogram of proper right arm revealing jeweled shoulder strap painted out by the artist (Mahon D. et al. 2005).

Considering, therefore, that this artwork was previously ascribed to Sargent, the artistic difference between the oil painting and the watercolor and the results of Infrared Reflectography lead to the conclusion that the two artworks are strictly linked and that it could be possible that the oil painting is subsequent toward the homonymous watercolor (De Rossi L., 2009).

For this reason, in-depth pigment analysis for art-fingerprints can be useful also to provide information that could be interesting in order to better identify data of painting's achievement.

5.1.3 Experimental methods

Micro-specimens amount of painted materials (maximum size: 2,5 mm²) were taken from convenient areas²⁴. Thinking about what color could help the identification of post-quem pigments used in this period, sampling was chosen in correspondence of enlightened (white) and shadow zone (dark brown). FIG. 33-34 show points of sampling on studied artwork.

²⁴ According to who provide the samples, the specimens were taken from original and not re-painted zone, without damaging further the picture.



FIG. 33 Caffè orientale sulla Riva degli Schiavoni: sampling mapping.



FIG. 34 Detailed of sampling areas: a) sampling area 1 (white and dark brown); b) sampling area 2 (white); c) sampling area 3 (white).

At first, samples were observed under stereomicroscope to study artistic technique and to select best samples for each kind of chemical analysis. Observation under microscope allowed to study some prints on pictorial layer probably due to fibers of the canvas support and SEM/EDS analysis were carried out, without any treatment of samples, to study the morphology and chemical elemental composition. XRF were performed at different Energy range (15 KeV, 30 KeV, 50 KeV) and spectra of pigments were compared with spectra of support (stub and double-sided tape black disk) to best characterize pigments. PIXE were performed for a better chemical identification focused on the research of chemical element difficult to detect with the previous analysis. Meanwhile, thanks to Raman spectroscopy, it was possible to deepen and to identify some mineralogical phase present in the white pigment, that were then confirmed by XRD analysis.

5.1.4 Results and discussion

5.1.4.1 Pigment analysis

Under optical microscope, specimens show that white pigment was used both for white area and under dark-brown pigment (FIG. 35a, b), that is less thick than the white one. However, lack of other colored samples, stratigraphy and failing other information obtained from imagery diagnostic techniques, does not allow to assure if there is a white preparatory layer under painting material and if it has the same chemical and mineralogical composition of analyzed white color. On dark-brown samples, it is possible to observe that the surface is covered by shiny layer, probably organic protective varnish (FIG. 35c, d), and that the dark-brown area show dark-red and black-brown particles surrounded by the brown of surface (FIG. 35d) not found, instead, in white area (FIG. 35b).

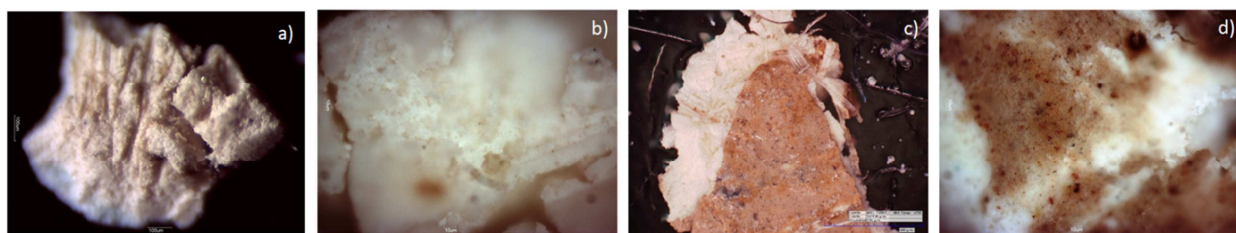


FIG. 35 Micro-photograph of white and white/brown samples: a) b) white sample backside (magnification 80x, 100x); white/brown sample (magnification 60x, 100x).

As concern the micro-features of the material, SEM micro-photographs, obtained from sample (FIG. 36), show that the morphological appearance of the pigment is characterized by rounded and small particles:

- in white pigment, the rounded grains are smaller than dark-brown one and their dimension are less than $1\ \mu\text{m}$, suggesting the artificial origin of this pigment (Montagna G., 1999; Eastaugh N. et al., 2008);
- in the dark-brown sample, instead, there are agglomerated particles and particles with changeable size from $4/5\ \mu\text{m}$ to $10\ \mu\text{m}$. The morphology of the pigment is characterized by rounded and rough grains, that can be found generally in Burnt Green Earth pigment (Montagna G., 1999).

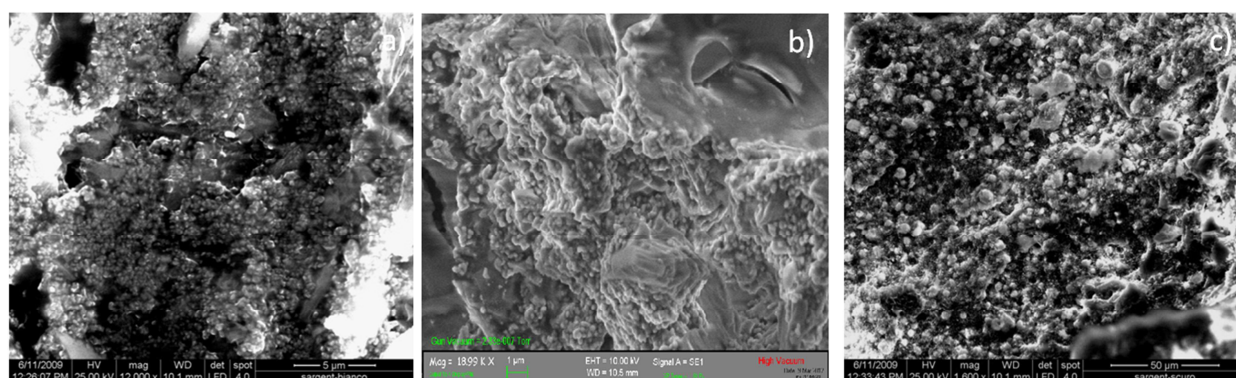


FIG. 36 SEM micro-photographs of analyzed samples: a) white pigment particles (magnification 12 kx); b) white pigment particles (magnification 18.99 kx); c) white/brown pigment (magnification 1.6 kx).

These samples were further examined by EDS where, in the white color, titanium, barium, magnesium and calcium peak intensities were significantly higher than dark brown pigment area. The presence of high value of carbon and oxygen are probably due to organic binder, while the little increase of iron, silicon, aluminum concentration in dark/brown samples are presumably linked to dark-brown pigment (TABLE n. 3; FIG. 37-38).

Therefore, SEM/EDS analysis suggest the use of White titanium dioxide mixed with Barium sulfate, calcium sulfate or calcium/magnesium carbonate and the presence of brown earth for the dark/brown pigment.

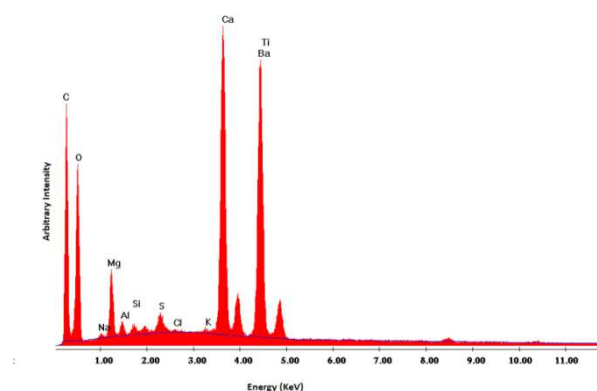


FIG. 37 EDS spectra of white pigment.

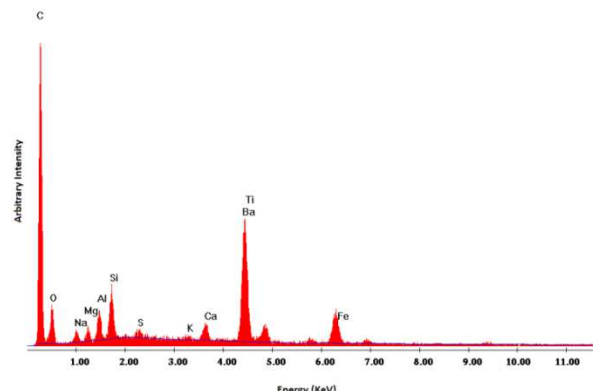


FIG. 38 EDS spectra of dark-brown pigment.

TABLE 5. SEM-EDS analytical data of pigment: results of average of measure carried out in different point on white pigment and on dark-brown specimens (σ from 1.2 to 1.9).

	C	O	Na	Mg	Al	Si	S	K	Ca	Ba	Ti	Fe
White	39.02	17.14	2.14	0.57	0.47	0.68	2.52	0.05	15.95	9.25	12.75	-
Dark-Brown	68.28	13.02	0.52	0.64	0.86	1.19	0.19	0.09	0.28	4.05	9.12	1.77

Excluding the background chemical contribution, EDXRF examination of white samples, carried out at different energy beam (15 KeV, 30 KeV, 50KeV), reveals the presence of titanium, barium, calcium and sulfur (FIG. 39) and strontium in minor concentration, confirming the previous hypothesizes about white color. Moreover, the detection of zinc in the white area suggest also the presence of Zinc Oxide.

As concern, instead, the dark-brown pigment (FIG.40), analysis show chemical composition of white color component, maybe due to size of thin dark-brown layer, and peaks of manganese and iron, probably linked to dark-brown component. In this case, in fact, iron and manganese concentration is more than on background or on white color, supporting the hypothesize that the dark-brown pigment could be made by Burnt Green Earth or burnt earth (FIG. 39-40; TABLE 4).

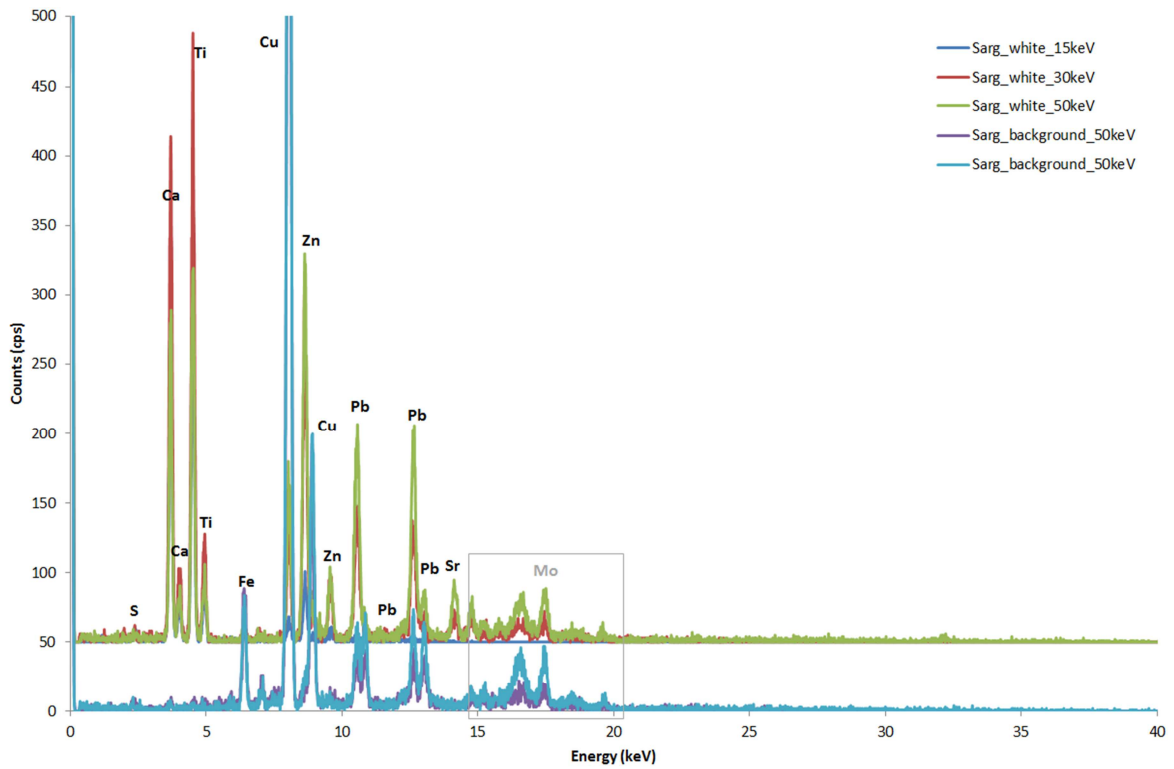


FIG. 39 XRF spectra on White pigment: total spectra from different set-up, not subtracting background. Experimental set up: voltage 50 KeV and current 700 μ A, voltage 30 KeV and current 1300 μ A, 15 KeV and 1500 μ A current. Live time: 120 s, no filter, Anode Molybdenum, collimator 0.650.

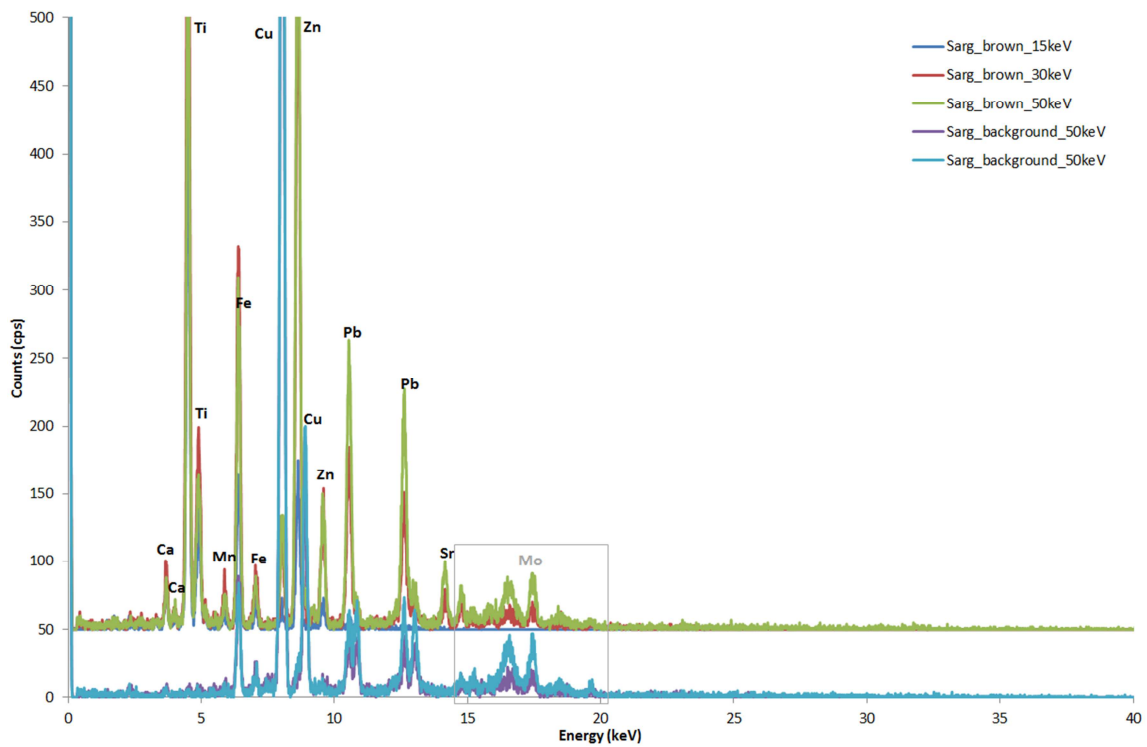


FIG. 40 XRF spectra on Dark-Brown pigment: total spectra from different set-up, not subtracting background. Experimental set up: voltage 50 KeV and current 700 μ A, voltage 30 KeV and current 1300 μ A, 15 KeV and 1500 μ A current. Live time: 120 s, no filter, Anode Molybdenum, collimator 0.650.

TABLE 6 XRF data of pigments: results of average measure carried out in different point on white pigment and on dark-brown specimens.

	Si	S	Ca	Ti	Mn	Fe	Zn	Pb	Sr	Ba
White	-	64	2439	2935	-	131	3832	2492	664	256
Dark-Brown	30	36	325	524	234	2985	903	1243	85	99
Background	3	-	57	-	-	972	321	928	8	34

Similar results are obtained also by PIXE analysis. As it is possible to observe in Fig 41 , titanium, barium, calcium, sulfur are confirmed in white pigment, meanwhile characteristic chemical elements of dark-brown pigment are iron, manganese. PIXE analysis reveals also the presence of other chemical elements such as cobalt: this element could be due not to pigments compound but maybe to industrial process, being often used for its catalytic activity and as drier promoter for alkyd paints (Tanese S. *et al.*, 2004).

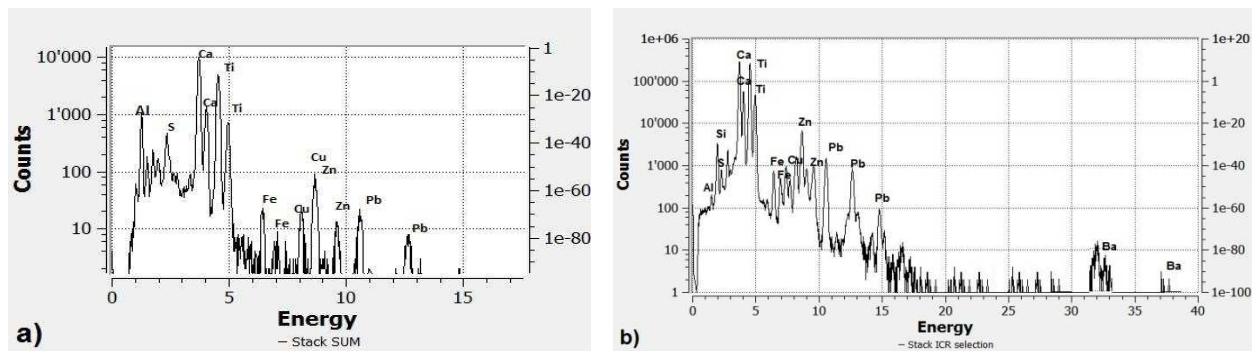


FIG. 41 PIXE spectra of white pigment: a) low energy detector; b) high energy detector. Experimental set up: particle/energy 3 MeV, current p+, Dose/s 200, Helium flow.

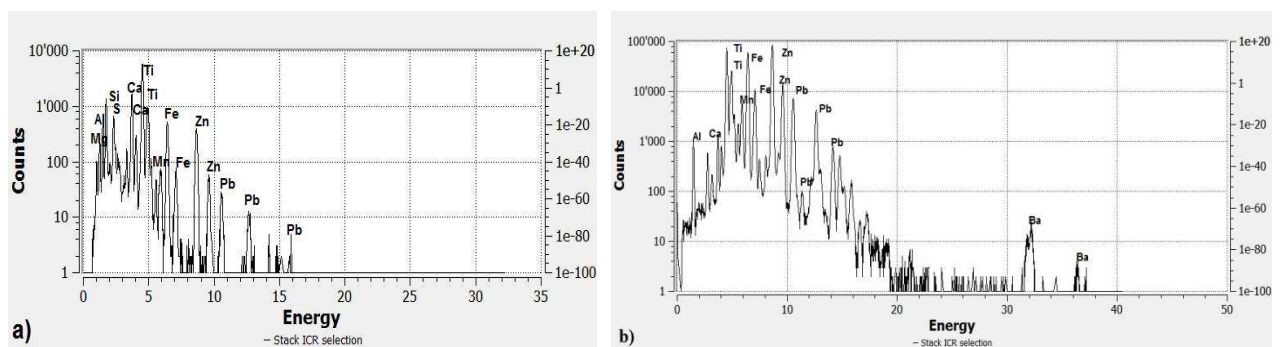


FIG. 42 PIXE spectra of Sarg_3 (white and dark-brown pigment): a) low energy detector; b) high energy detector. Experimental set up: particle/energy 3 MeV, current p+, Dose/s 200, Helium flow.

TABLE 7 PIXE analysis on Sargent sample: data are referred to area that cover white zone (sarg_1 e sarg_2) and dark-brown/white zone pigment (sarg_3). Average value: region of interest were extracted using PyMCA software, data expressed in counts. Experimental set up: particle/energy 3 MeV, current p+, Dose/s 200, Helium flow.

Low Energy												
	Na	Mg	Al	Si	P	S	Cl	K	Ca	Ti	Cr	Mn
Sarg_1	0	73145	8831	8282	2204	14312	2215	1455	206406	248676	372	-
Sarg_2	758	74842	8330	8268	2209	13124	2152	1458	206138	248290	93	517
Sarg_3	124	50177	24254	33716	2333	12224	2288	2385	135725	224525	331	2484
High Energy												
Sarg_1	-	-	-	-	-	0	-	665482	21128548	3203233	676	1025
Sarg_2	-	-	-	-	-	3.37E+08	-	19913	353508	360053	212	407
Sarg_3	-	-	-	-	-	0	-	21518	141498	265844	103	3732

Low Energy											
	Fe	Co	Ni	Cu	Zn	Ba # K	Zn # L α	Ba # L α	Pb # L α	Pb # M α	Sr
Sarg_1	4751	729	158	3666	25869	0	32241	0	20846	18024	-
Sarg_2	4040	830	39	4026	25700	0	22527	0	25376	21346	-
Sarg_3	27118	517	182	393	44432	0	29543	0	23721	20478	-
High Energy								Ba # L β	Pb # L α	Pb # M1	
Sarg_1	7837	918	219	3646	25869	5799	-	95587	16843	22709088	983
Sarg_2	4381	649	131	3204	25700	23949	-	28342	21274	7173073	1476
Sarg_3	33783	386	187	306	44432	31854	-	67185	21530	5555200	2309

Thanks to new mapping acquisition system for PIXE analysis used at Paris AGLAE facility (Pichon L., 2010), it was possible notice that sulfur is linked with barium and not with calcium: this confirms the presence of Barium Sulfate and not Calcium Sulfate.

In FIG. 44 are shown the results obtained by the elaboration of PIXE maps analysis with PyMCA software: in a) and b), area with high concentration of sulfur are highlight in green and in red color calcium and barium respectively; in c) violet tone is due to region that have both calcium and barium. In this way, the calcium is probably linked to carbon to form a calcium carbonate.



FIG. 43 Sample of white pigment (magn. x 90).

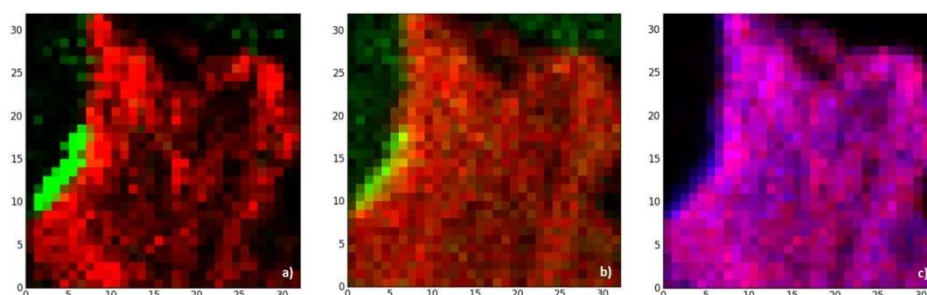


FIG. 44 PyMCA elaboration of PIXE maps: a) sulfur in green color and calcium in red one; b) sulfur in green color and barium in red one; c) calcium in red color and barium in blue one.

Finally, results from Raman spectroscopy, on white particles, confirm the use of White titanium dioxide, detecting characteristic Raman bands of Rutile phase at 446 cm^{-1} (s) and at 609 cm^{-1} (s) (Burgio L. *et al.*, 2001; Chen G. *et al.*, 2012; Ropret P. *et al.*, 2008) (FIG. 45).

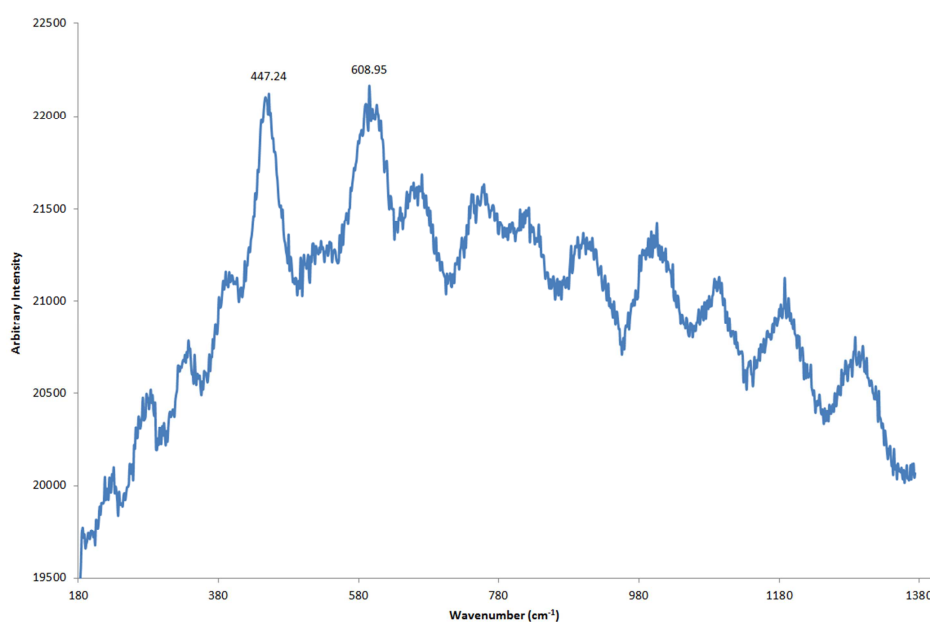


FIG. 45 Raman spectra on white samples (632,81 nm excitation, 50 x magnification): Rutile phase.

As concern the dark-brown pigment, μ -Raman investigation carried out on red particles in the brown/white samples revealed the presence of hematite, which characteristic Raman bands are at 224 cm^{-1} (s), at 290 cm^{-1} (s) and 408 cm^{-1} (m). FIG. 46 shows Raman bands of hematite and characteristic Raman bands of Rutile phase at 446 cm^{-1} (s) and at 609 cm^{-1} (s) (Burgio L. *et al.*, 2001; Chen G. *et al.*, 2012; Ropret P. *et al.*, 2008).

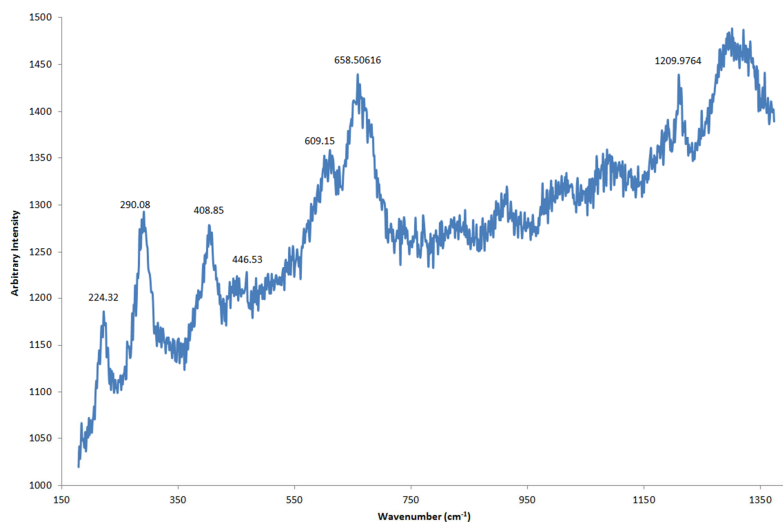


FIG. 46 Raman spectra on white-brown samples (632,81 nm excitation, 100 x magnification): Hematite and Rutile.

Raman spectra on black/dark brown grains show Raman bands of Black Lamp pigment (carbon) at 1372 cm^{-1} and 1583 cm^{-1} [28, LabSpec 5 Raman Spectroscopy Library].

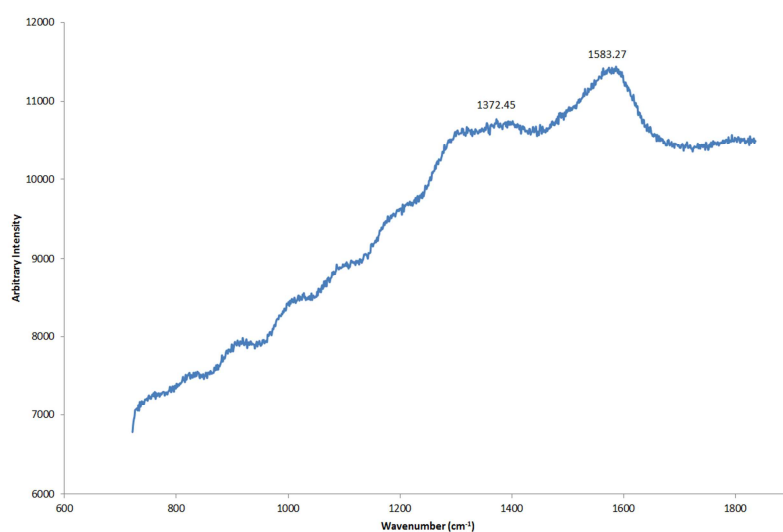


FIG. 47 Raman spectra on dark-brown particles (632,81 nm excitation, 50 x magnification): carbon (Black lamp pigment).

Moreover, further analysis on brown/white samples allowed to identify the presence of Burnt Green Earth, that is characterized by the following Raman bands at: 1532 cm^{-1} (w), 1033 cm^{-1} (w), 1275 cm^{-1} (w), 1207 cm^{-1} (w), 1083 cm^{-1} (w), 813 cm^{-1} (w), 771 cm^{-1} (w), 734 cm^{-1} (m), 505 cm^{-1} (w) [28; 29; 31; LabSpec 5 Raman Spectroscopy Library].

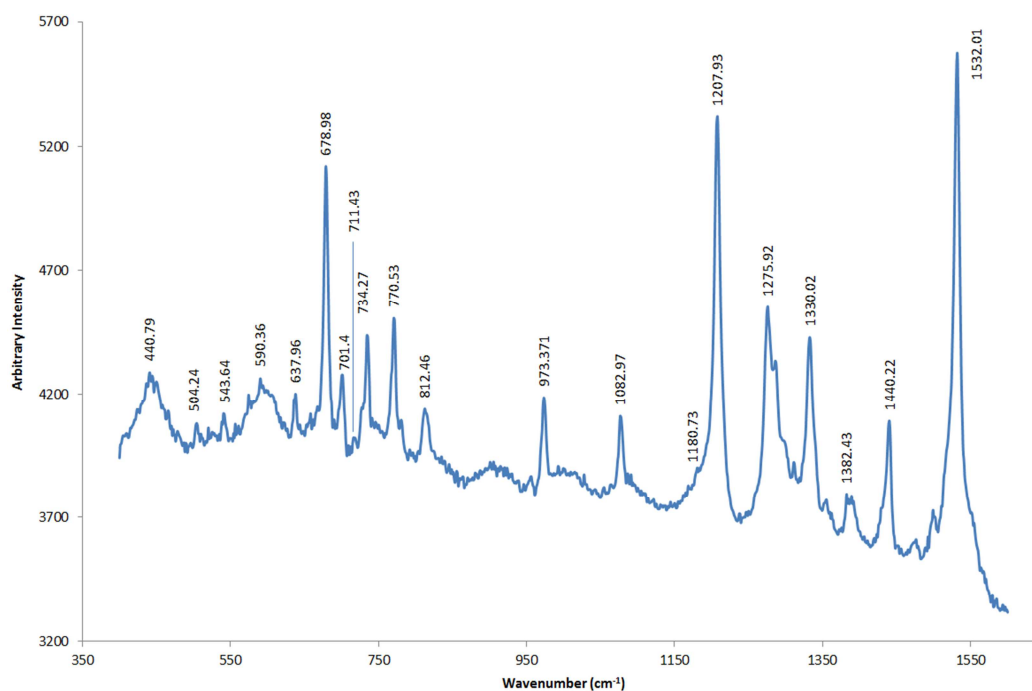


FIG. 48 Raman spectra on dark-brown particles (632,81 nm excitation, 50 x magnification): Burnt Green Earth.

Considering that the pigment Burnt Green Earth (shade of Green Earth) indicates compound characterized by different minerals, the mineralogical composition can be different for one Burnt Green Earth pigment and another, according to the manufacture that produced it (Eastaugh N. et al., 2008). For these reasons, the identification of the pigment's mineralogical composition could be interesting as further art-fingerprints. In the Raman spectra of Green Earth pigment, the following minerals were identified through a research among their Raman peaks:

- Celadonite : 544 cm^{-1} , 701 cm^{-1} , 1085 cm^{-1} (Aliatis I. et al., 2009; 28; 30);
- Calcite: 711 cm^{-1} , 1083 cm^{-1} (Aliatis I. et al., 2009; Jehlička J. et al., 2009 ; Lécuyer C. et al., 2012 ; Park K.,1967; Vagenas N.V. et al., 2003);
- Chlorite: 678 cm^{-1} , 544 cm^{-1} (Wang Y.Y. et al., 2013 ; 28; 30);
- Graphite: 1330 cm^{-1} , 1532 cm^{-1} (Smith G.D. et al., 2004; Van der Weerd J. et al., 2004; 28; 30).

Finally, XRD analysis revealed mineralogical phases of rutile, hematite and both calcite (calcium carbonate) and dolomite (magnesium-calcium carbonate), confirming results and hypothesis suggested by previous analysis. The detection of peaks attributable to barite, lazurite and rhodocrosite could be compatible with the performed chemical analysis, suggesting the use of White barium sulfate for the white color and the other minerals contained in the dark/brown area (FIG. 49).

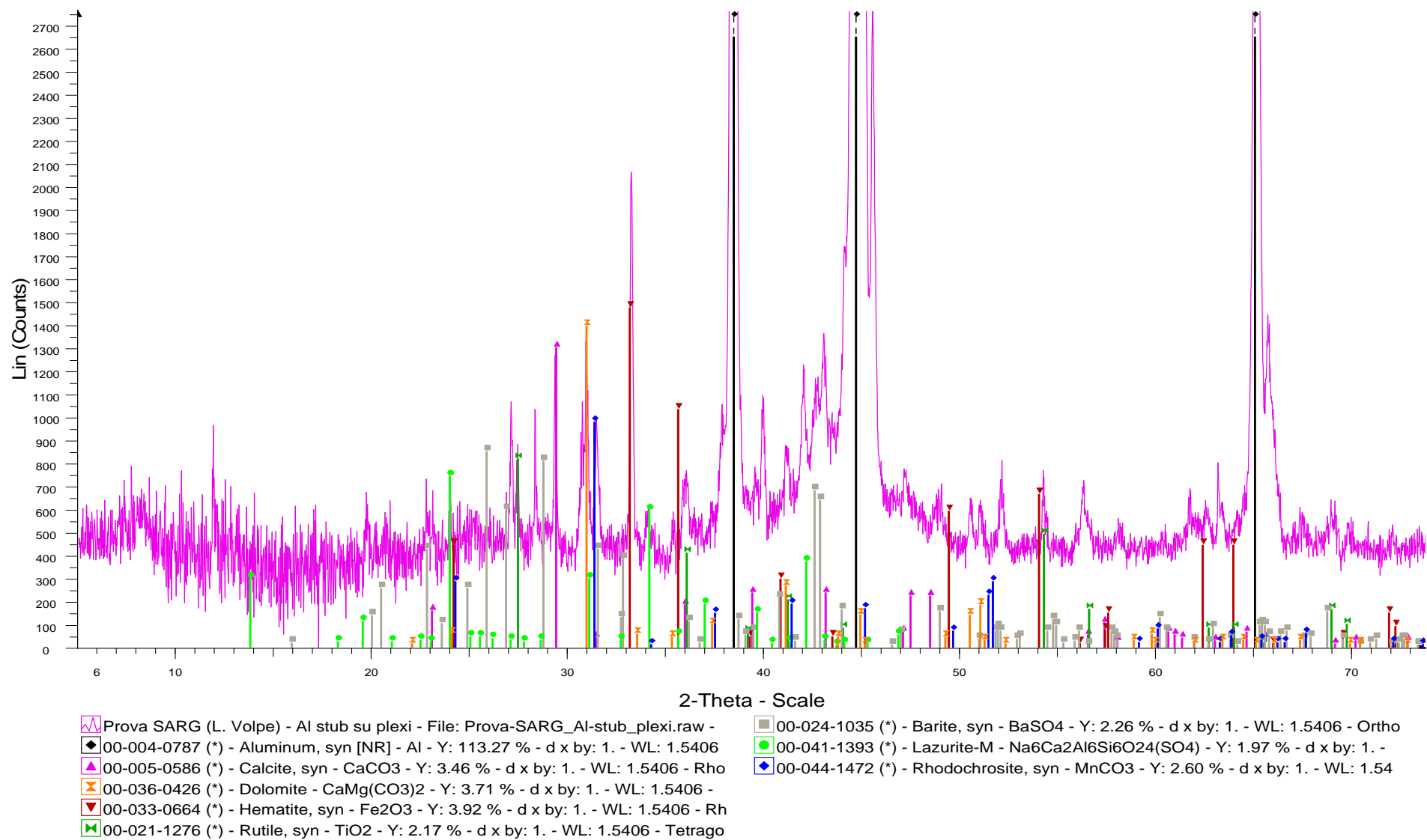


FIG. 49 XRD spectra obtained on stub containing white, brown and white/brown samples.

5.1.4.2 Fibers and print on back side of sample

Observing the back side of samples, it was possible notice the presence of some support's fibers and some print probably made by the canvas on pictorial layer.

The analysis suggest that the canvas is constituted by fibers of *Linum usitatissimum* (Reis D., 2006; Scicolone G.C., 2004), which diameter is between 12.5 μm and 20 μm .

3D model of sample surface, obtained by 3D microscope Hirox KH770, revealed the correspondence between the print and the fibers size, supporting the hypothesis that there was not a preparatory layer and so that the artist used a pre-treated available support (FIG. 50d).

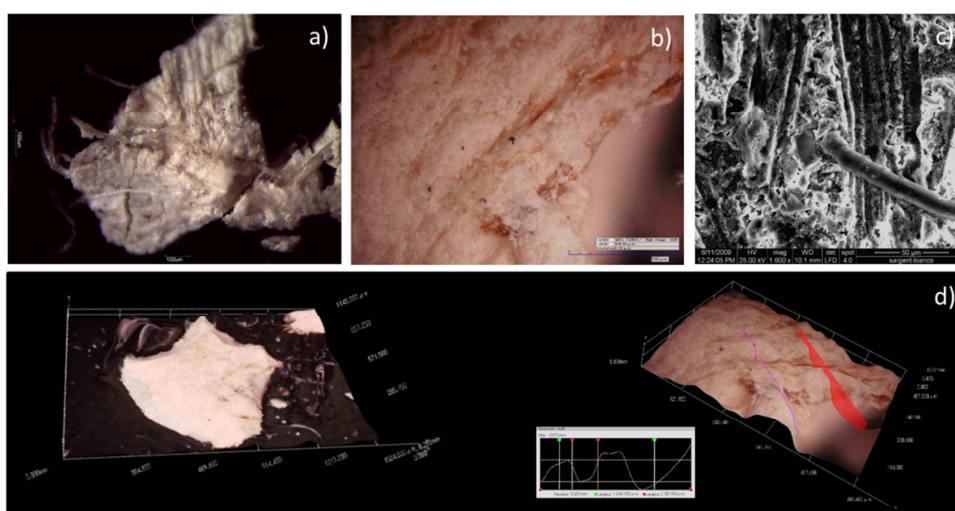


FIG. 50 Micro-photograph of white sample's backside with fibers: a) b) OM image; c) SEM image of pictorial layer and fibers (magnification x 1.6 kx); d) 3D model and image of pictorial layer and fibers' print.

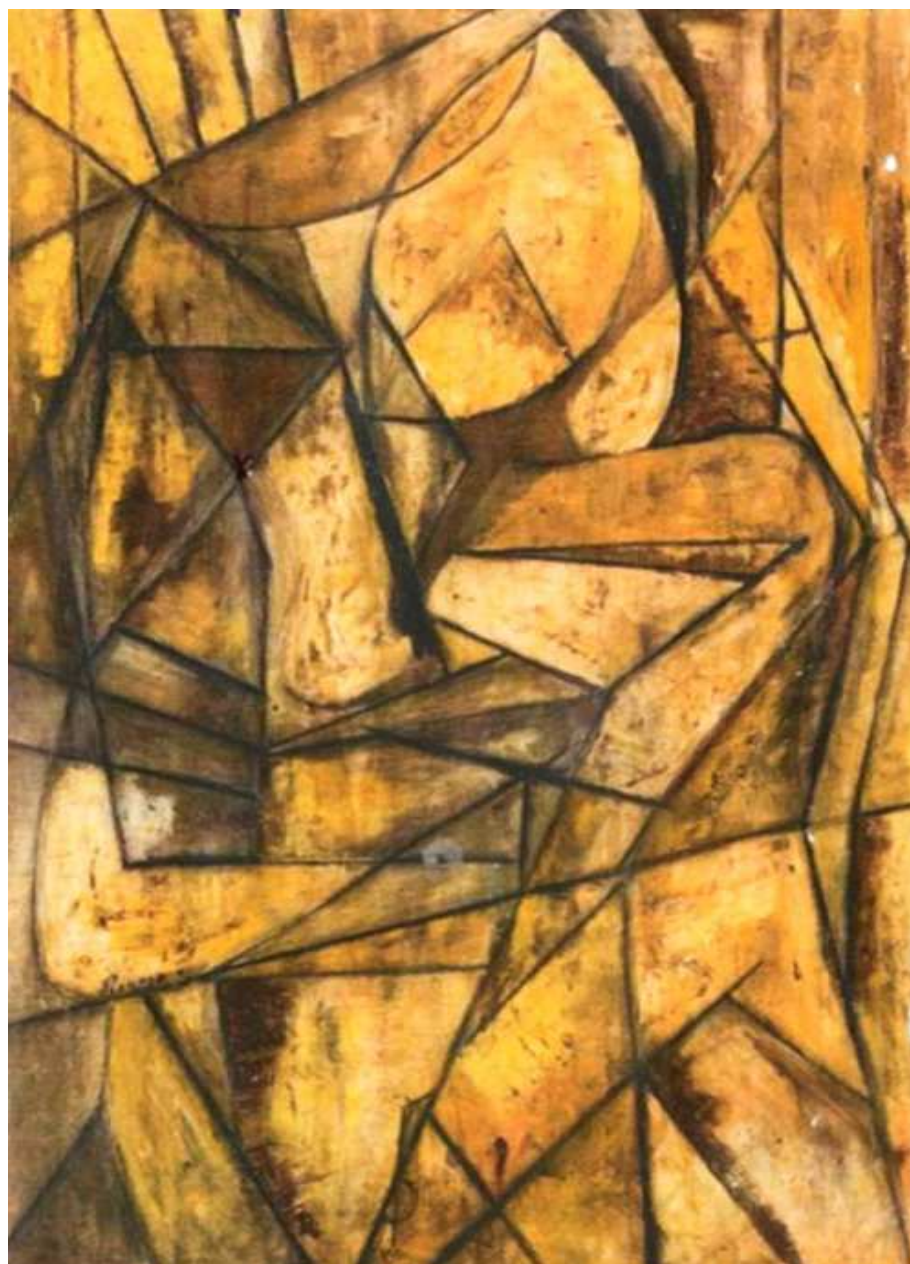
5.1.5 Conclusion

Pigment analysis carried out on white and white/brown samples suggest the use of mixture mainly constituted by White titanium dioxide (Rutile phase), Barium Sulfate and Calcium carbonate (calcite) and calcium-magnesium carbonate (dolomite) for the white colors. As concern, instead, the dark-brown pigment, chemical-mineralogical composition and particle morphologies suggest the use of Burnt Green Earth, in which the main coloring minerals are chlorite, celadonite, hematite and probably rhodocrosite.

In addition to art-fingerprints' identification, chemical-mineralogical analysis provide interesting data that can be useful in support to dating studies in progress. In particular, the detection of rutile phase (White titanium dioxide), which commercial entry dated around 1937/1939, could support the hypothesis for that the artwork could be painted after 1880/1882 (De Rossi L., 2009). For these reason, it is important to examine further in-depth the whole artwork, the artistic tech-

niques, its material and their history in order to better support the historical-artistic investigation for dating purpose.

ARTWORK PLATE II



Author: *Pablo Picasso (Spanish artist, 1881-1973)*

Title: *Cubist figure*

Object: *Painting (oil on canvas)*

Date: *1909 c.*

Overall: *unknown*

Location: *Private Collection*

5.2 “Cubist Figure” by Pablo Picasso (oil on canvas, 1909?)

Size: unknown

Samples collected from the painting “Cubist Figure” by Pablo Picasso (1909?, private collection) were analyzed to better characterize white pigment, in support to dating studies. The presence, however, of other colored particle allowed to give information also to red-orange and blue color pigment.

For this artwork, the research of art-fingerprints were obtained by pigment analysis, in particular through in-depth study concerning the chemical-mineralogical composition of analyzed pigments.

5.2.1 The artist

Pablo Diego José Francisco de Paula Juan Nepomuceno María de los Remedios Crispiniano de la Santísima Trinidad Ruiz y Picasso (October 25th, 1881 – April 8th, 1973), better known as Pablo Picasso [32], was one of the most famous Spanish painter, sculptor, printmaker and ceramicist of 20th century.

Born in Málaga (Andalusia, Spain) in 1856 to Don José Ruiz y Blasco, important professor at School of Fine Arts and curator of a local museum, and María Picasso y López (Hamilton G.H., 1976), Picasso showed artistic talent since he was a child. Belonging to middle-class family, when he was seven years old, his father taught him traditional and academic concepts of drawing and oil painting: disciplined copying of the masters’ artworks and drawing the human body from plaster and living models (Richardson J., 1991; Walter I.F.,1990).

During the years, Picasso had increased his artistic skills and, after travel to A Coruña (Spain) and to Barcelona for his father’s work, he entered at Royal Academy of San Fernando in Madrid, the most important art school in Spain. Disliking formal instruction, he preferred to visit Madrid attractions like the Padro, that housed painting by El Greco, Velázquez and Goya (Richardson J., 1991; Walter I.F.,1990).

In 1900, he moved in Paris, where he became friend of a lot of important poet and artist like Max Jacob, Breton, Apollinaire, but, new poor life constrained him to come back to Madrid until 1905, when his works were very appreciated by The Steins, an American art collectors family, and they were exposed in Paris (Claire J. et al.,1998).

Picasso, in the early 20th century, divided his life between Paris and Barcelona and, apart the several anti-war paintings that he made, he remained neutral both during the Spanish civil war

(1936-1939) and also World War I and World War II: being Spaniard that lived in France, he was not obligated to fight against German invaders (Walter I.F., 1991).

Finally, the experiment continuously of different techniques, theories, ideas and “*his revolutionary artistic accomplishments brought him universal renown and immense fortune, making him one of the best-known figures in 20th century Art*” [33].

5.2.2 The painting: subject and artistic technique

“Ma i raffinati, i ricchi, gl'indolenti, distillatori di quintessenza, cercano il nuovo, l'insolito, l'originale, lo stravagante, lo scioccante. Ed io, a partire dal cubismo e dopo, io ho soddisfatto questi gentlemen e questi critici con tutte le bizzarrie che mi passavano per la testa, e quanto meno le capivano, tanto più ammiravano. Divertendomi con questi giochi, acrobazie, rompicapo, indovinelli ed arabeschi, sono diventato famoso in fretta. E la celebrità per un pittore significa incremento nelle vendite, soldi, ricchezza. Oggi, come è risaputo, sono famoso e molto ricco. Ma quando sono solo con me stesso, non ho il coraggio di considerarmi un artista nel senso grandioso e antico del termine.[...] Io sono soltanto un entertainer pubblico che ha capito il suo tempo. Questa mia è un'amara confessione, assai più penosa di quanto appaia, ma ha il pregio di essere sincera (Pablo Picasso)”. (Papini G., 1951).

“The 'refined', the 'rich', the 'professional do nothing', the 'distiller of quintessence' desire only the peculiar, and sensational, the eccentric, the scandalous in today's art. And I myself, since the advent of cubism, have fed these fellows what they wanted and satisfied these critics with all the ridiculous ideas that have passed through my head. The less they understood, the more they have admired me! [...] Today, as you know, I am celebrated, I am rich. But when I am alone, I do not have the effrontery to consider myself an artist at all, not in the grand meaning of the word. ...I am only a public clown, a mountebank. I have understood my time and exploited the imbecility, the vanity, the greed of my contemporaries. It is a bitter confession, this confession of mine, more painful than it may seem. But, at least, and at last, it does have the merit of being honest. (Pablo Picasso)” [34].

It is possible to categorize Picasso's artworks into different periods, named:

- Blue Period (1901-1904), in which Picasso's style is characterized mostly for somber blue and blue-green shadows (Moravia A. et al., 1979);

- Rose Period (1905-1907), that consists of paintings in which Picasso, using orange and pink colors, created a cheerful artworks painting mainly circus people and acrobats (Moravia A. *et al.*, 1979).
- African-influenced period (1908-1909), that begins with “Le Demoiselles d’Avignon” inspired by African artifacts and that influenced Picasso for the following Cubism period;
- Cubism period that it is separated into Analytic Cubism (1909-1912) and Synthetic Cubism (1912-1919).

Analyzed artwork, being dated around 1909, for the presence of “9” near the word “Picasso”, could be enter in Analytic Cubism period, in which, in effect, Picasso used monochrome brownish and neutral colors and he did not use the collage technique, typical of synthetic period (Hilton T., 1988).

5.2.3 Experimental methods

Considering the dimension of the micro-samples (maximum size: 1/1.5 mm²), specimens were placed on SEM’s stub without carrying out any kind of treatment: in this way, it was possible to deepen the research using other analytical techniques. In FIG. 51 point of sampling on the painting are showed²⁵.

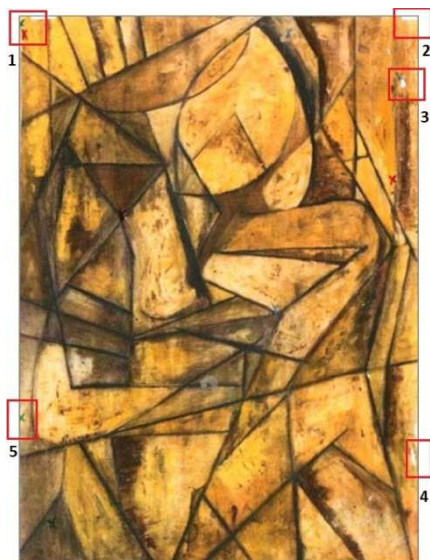


FIG. 51 Cubist figure: sampling mapping.



FIG. 52 Detailed of sampling areas: a) sampling area 1; b) sampling area 4; c) sampling area 5.

²⁵ According to who provide the samples, the specimens were taken from original and not re-painted zone, without damaging further the picture

In addition to required SEM/EDS analysis, EDXRF, PIXE and μ -Raman were carried out for a better pigments' analysis and correct data interpretation. Moreover, investigation under microscope revealed the presence of white particles mixed with different colors grains (red-orange and blue); even if, the analysis was focused on White color, the research deepened also the identification of other used pigment. Finally, XRD analysis were performed onto the whole stub for a more precise identification of mineralogical phases contained in the studied samples.

5.2.4 Results and discussion

5.2.4.1 Pigment analysis

As previous just mentioned, white specimens contain inside other colored particles, in particular red-orange (FIG.53b, d) and blue (FIG.53c, e) ones. In FIG. 35a it is possible observe that white color was spread directly on canvas and that, probably, there is not a preparatory layer; average measure carried out through acquisition photo software (Motic Image Plus) shows that white layer is around 70 μm thick.

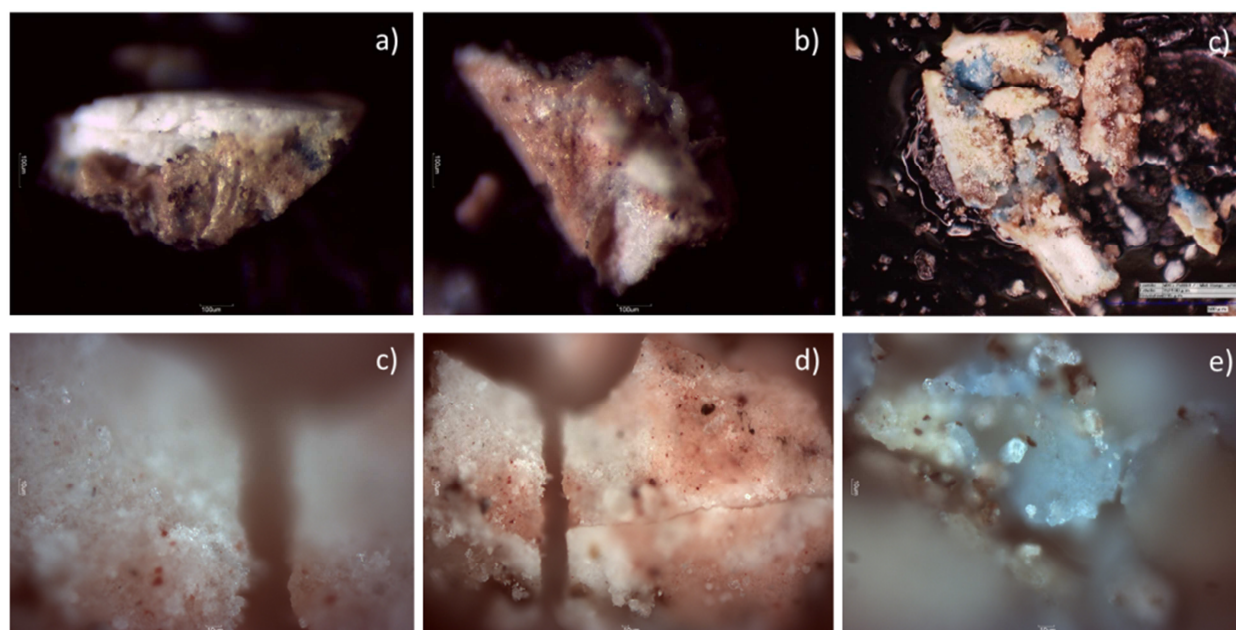


FIG. 53 OM photomicrograph of samples: a) c) white sample (magnification 60x, 100x); b) d) red/white sample (magnification 65x, 90x); c) e) blue/white samples (magnification 65x, 100x).

SEM/EDS analysis revealed aggregate of particles with different size and shape. The compound, in fact, shows pigment particles with rounded shape and which dimension are around 1 μm (or less), mixed together to other pigment particles, characterized by angular shape grains with average particle size less than 2 μm . Rounded shape and small particle size suggest the artificial origin of the employed pigment, meanwhile the coarse grained particles and the uneven particle

distribution support the hypothesis that some detected pigment were produced by crushing (Eastaugh N. et al., 2008; Montagna G., 1999).

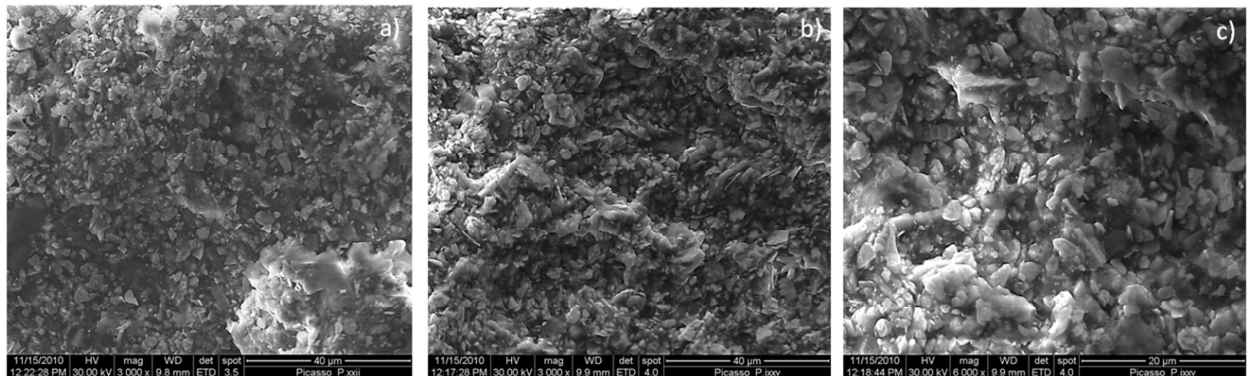


FIG. 54 SEM microphotograph of analyzed white samples at different magnification: a) b) magnification 3 KX; c) magnification 6 KX.

The chemical analysis confirms that pigment particles of white color are mainly constituted by titanium and meanwhile calcium, barium and sulfur peaks are probably due to calcium sulfate and barium sulfate that is usually contained in pigments based on White titanium dioxide (FIG.). Considering that, it is possible to suggest the use of mixture of artificial pigments White titanium dioxide (Eastaugh N. et al., 2008; Montagna G., 1999).

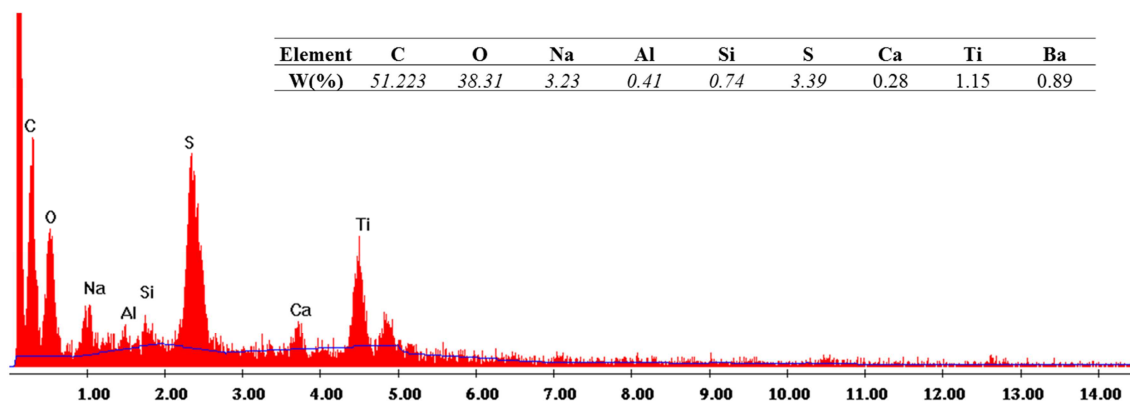


FIG. 55 EDS spectra and analytical data of pigment: results of average measure carried out in different point on white samples. In italic, average value greater than σ .

These samples were further examined by EDXRF analysis, carried out at different energy, to verify especially the presence of barium mixed with white titanium dioxide. Analysis detect barium, sulfur and lead peaks, suggesting the use of White titanium dioxide mixed with barium sulfate and white lead. The comparison between XRF spectra obtained by white/colored specimens confirms the previous hypotheses about the composition of white color but it does not allow to suggest pigments for red pigment and blue color. In fact, the main chemical elements, used usually to characterize red and blue pigment (iron, copper, etc.), were revealed also for the background and without great differences in detected signals.

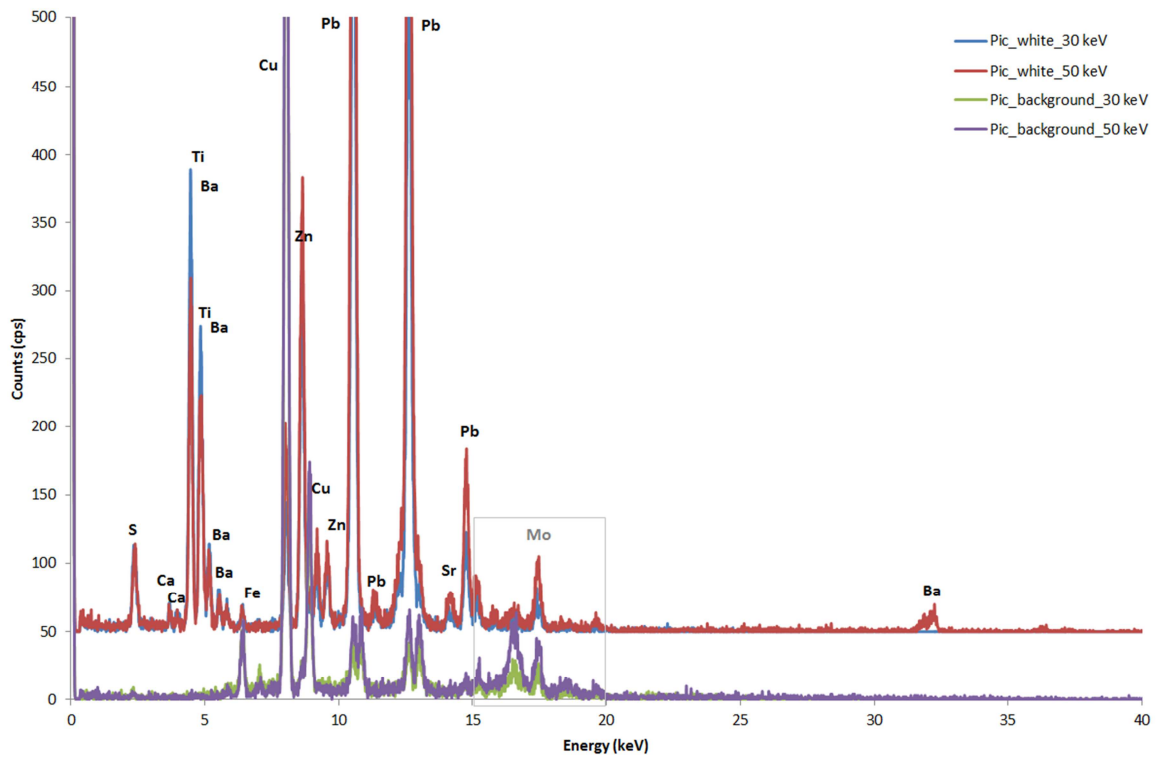


FIG. 56 XRF spectra on white pigment: total spectra from different set-up, not subtracting background. Experimental set up: voltage 50 KeV and current 700 μ A, voltage 30 KeV and current 1300 μ A. Live time: 60 s, no filter, Helium flow, Anode Molybdenum, collimator 0.200

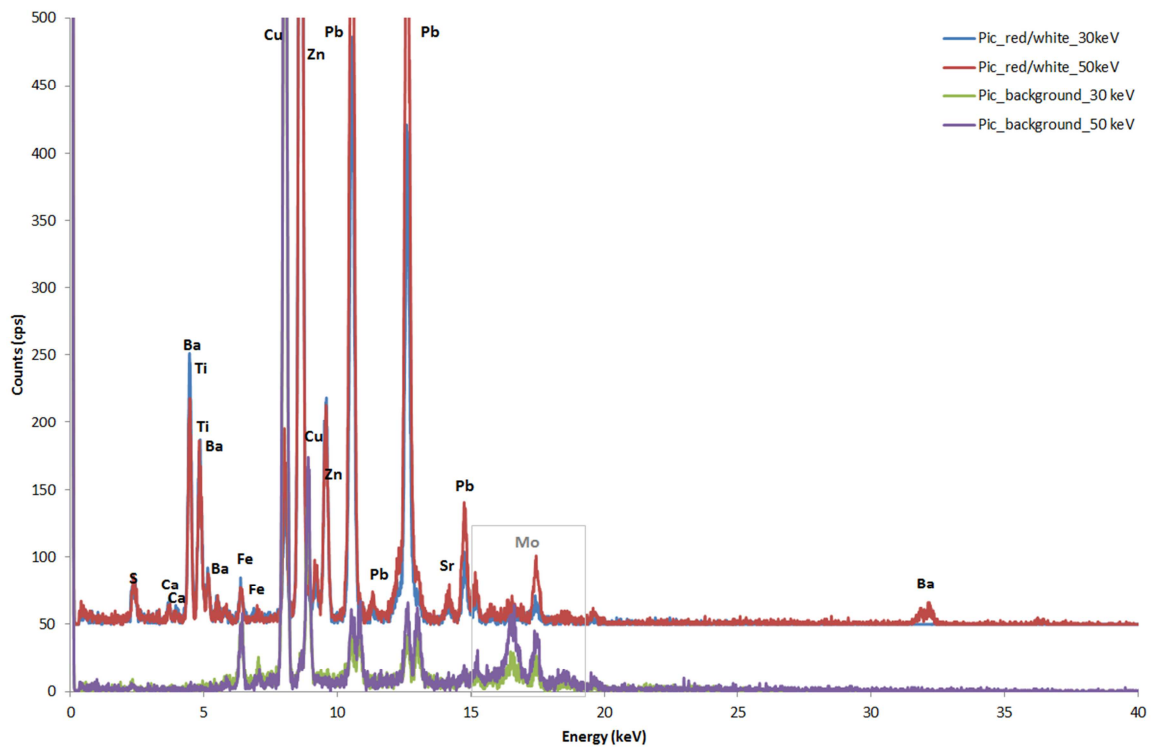


FIG. 57 XRF spectra on red/white pigment: total spectra from different set-up, not subtracting background. Experimental set up: voltage 50 KeV and current 700 μ A, voltage 30 KeV and current 1300 μ A. Live time: 60 s, no filter, Helium flow, Anode Molybdenum, collimator 0.200

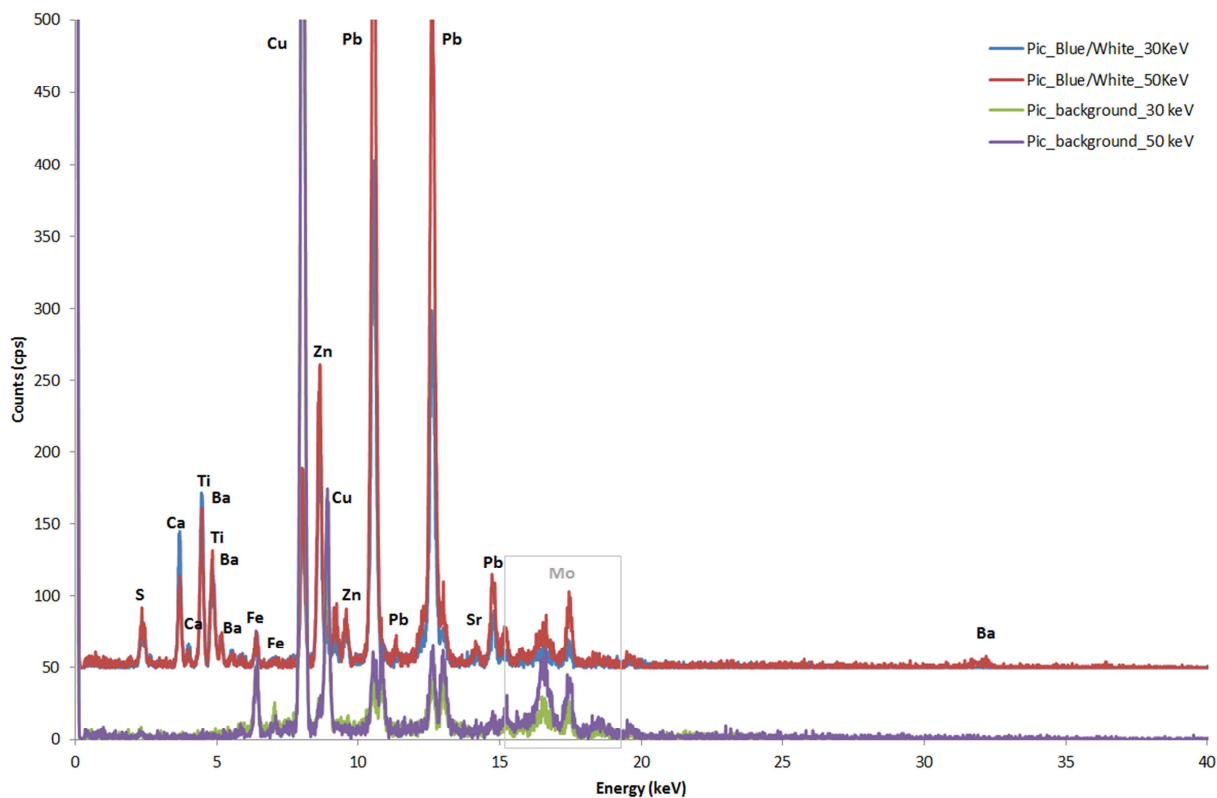


FIG. 58 XRF spectra on blue/white pigment: total spectra from different set-up, not subtracting background. Experimental set up: voltage 50 KeV and current 700 μ A, voltage 30 KeV and current 1300 μ A. Live time: 60 s, no filter, Helium flow, Anode Molybdenum, collimator 0.200

PIXE analysis, detecting titanium, barium and lead, confirms the presence of the mixture based on White titanium dioxide. The detection of element such as zinc, calcium and sulfur allowed to suppose further white pigment likely White calcium carbonate or calcium sulfate and White zinc oxide. Further chemical elements, such as sodium, aluminum, manganese, etc. could be attributable to other colored pigment or to a characteristic chemical formula linked to pigment's production process, becoming in this way art-fingerprints of the entire system pictorial layer-support.

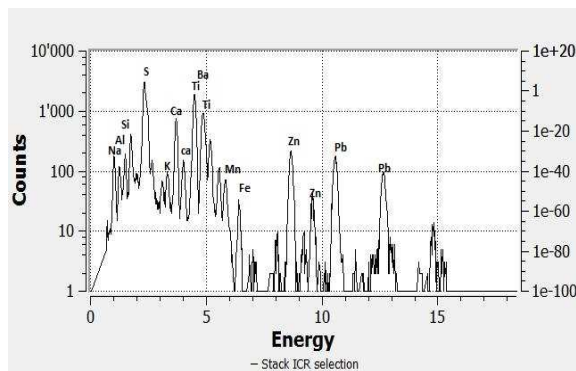


FIG. 59 PIXE spectra of white pigment, low energy detector. Experimental set up: particle/energy 3 MeV, current p+, Dose/s 200 50 KeV, Helium flow.

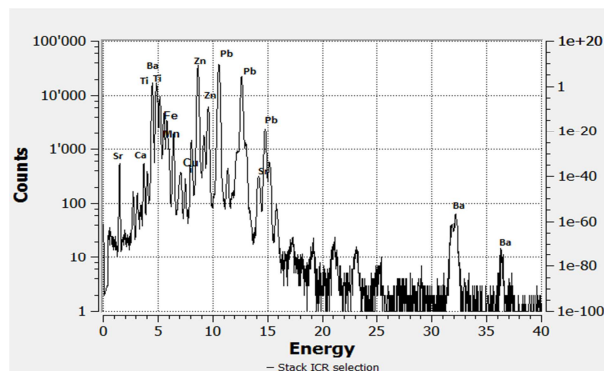


FIG. 60 PIXE spectra of white pigment, high energy detector. Experimental set up: particle/energy 3 MeV, current p+, Dose/s 200 50 KeV, Helium flow.

Exploiting PyMCA software to elaborate PIXE maps, it is possible to suppose that, in the white pigment, sulfur is linked to barium (White Barium Sulfate) and not to calcium (gypsum) (FIG. 62). In this way the white color could be mainly composed by White titanium dioxide, White Barium sulfate, White zinc oxide and calcium carbonate.

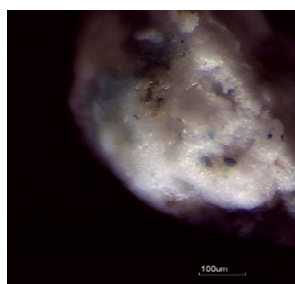


FIG. 61 Sample of white pigment (magn. x 90).

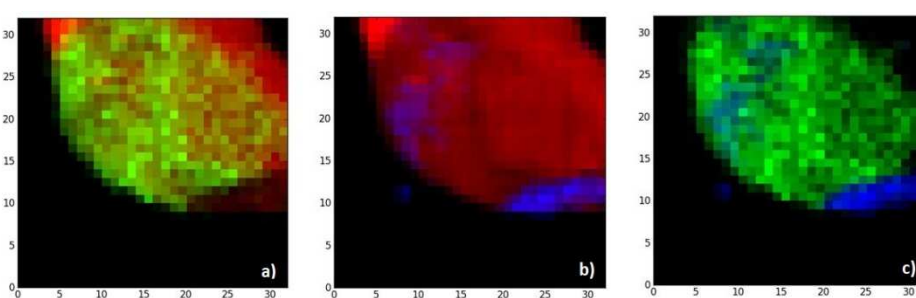


FIG. 62 PyMCA elaboration of PIXE maps: a) sulfur in red color and calcium in blue one; b) sulfur in red color and barium in green one; c) calcium in blue color and barium in green one.

Thanks to micro-beam and to new acquisition mapping system (Calligaro T. *et al.*, 2011; Pichon L. *et al.*, 2010), PIXE analysis allowed to reveal iron peaks in the red/white sample and copper peaks in the blue/white specimen. Therefore, from chemical point of view, the red pigment can be constituted by a compound enrich in iron, likely ochre, meanwhile the blue color is linked to a blue pigment, mainly characterized by copper.

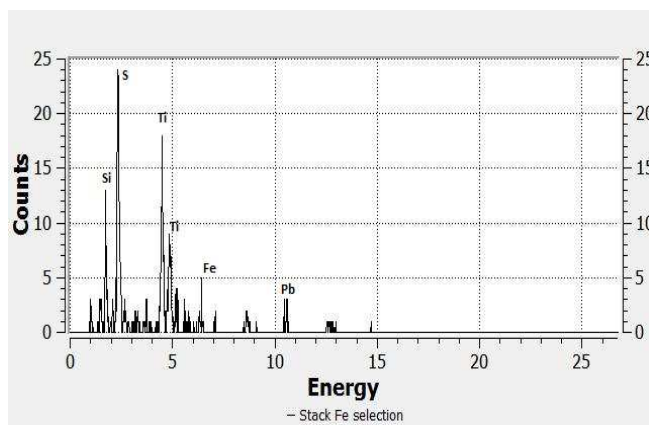


FIG. 63 PIXE spectra of red-white pigment, low energy detector. Experimental set up: particle/energy 3 MeV, current p+, Dose/s 200 50 KeV, Helium flow.

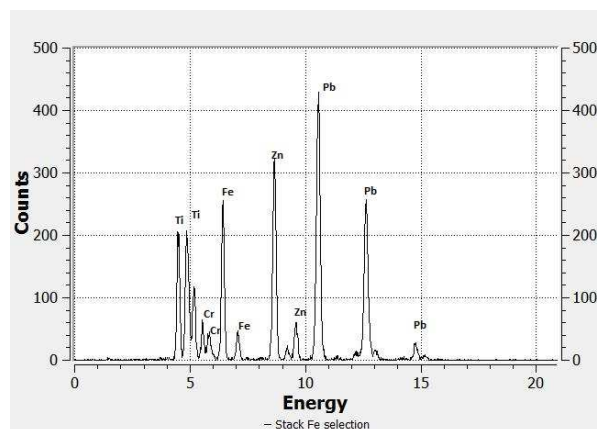


FIG. 64 PIXE spectra of red-white pigment, high energy detector. Experimental set up: particle/energy 3 MeV, current p+, Dose/s 200 50 KeV, Helium flow.

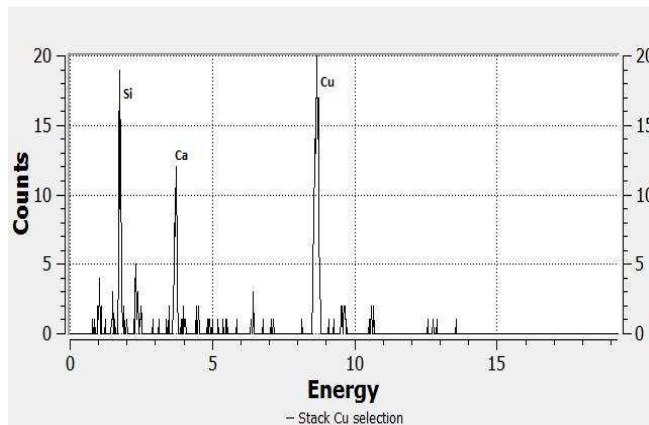


FIG. 65 PIXE spectra of blue-white pigment, low energy detector. Experimental set up: particle/energy 3 MeV, current p+, Dose/s 200 50 KeV, Helium flow.

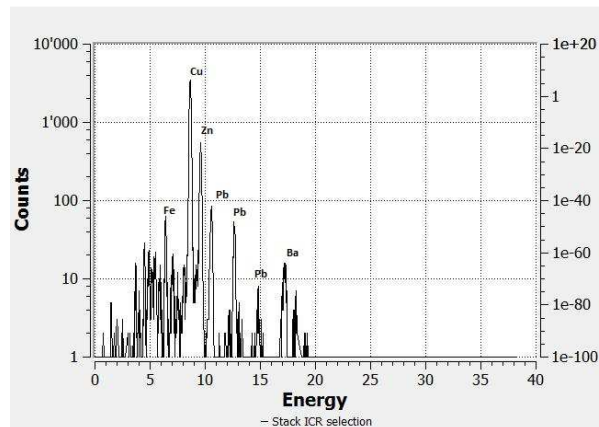


FIG. 66 PIXE spectra of blue-white pigment, high energy detector. Experimental set up: particle/energy 3 MeV, current p+, Dose/s 200 50 KeV, Helium flow.

TABLE 8 PIXE analysis on Picasso samples: data are referred to area with white pigment and red-white, blue-white pigment. Average value: region of interest were extracted using PyMCA software, data expressed in counts. Experimental set up: particle/energy 3 MeV, current p+, Dose/s 200, Helium flow.

Low Energy										
	Na	Mg	Al	Si	P	S	Sr	K	Ca	
White	-	5358	4545	1106	942	72652	-	654	2942	
Red-white	-	2997	9246	26091	592	61768	-	3782	7648	
Blue-white	-	8978	10457	17579	1816	58386	-	4530	36481	
High Energy										
	Na	Mg	Al	Si	P	S	Sr	K	Ca	
White	-	-	-	-	-	1600000000	1301	6176	7999	
Red-white	-	-	-	-	-	570647680	1282	16559	10784	
Blue-white	-	-	-	-	-	680051392	1221	26888	38695	
Low Energy										
	Ti	Fe	Co	Ni	Cu	Zn	Zn # L α	Ba # L α	Pb # L α	Pb # M α
White	32264	72	140	-	428	22348	43912	372833	170327	265243
Red-white	27852	4607	0	-	256	36647	40676	352499	256747	229728
Blue-white	27875	3525	374	-	1071	41886	60687	323860	217575	231547
High Energy										
	Ti	Fe	Co	Ni	Cu	Zn	Zn # L α	Ba # L β	Pb # L α	Pb # M1
White	32264	310	70	128	724	20624	-	353664	135229	-
Red-white	27853	4669	74	143	141	24670	-	313828	137799	-
Blue-white	27876	2386	64	166	1160	30692	-	297972	136502	970793

Considering the great number of possible pigments for red and blue color characterized respectively by iron and copper, Raman analysis demonstrated to be very useful for a in-depth pigment analysis (FIG. 67 - 68).

Raman spectra, in fact, confirm the use of different white pigment, detecting the characteristic Raman bands of:

- Rutile phase (pigment White titanium dioxide) at 446 cm^{-1} (s) and at 609 cm^{-1} (s) (Burgio L. *et al.*, 2001; Chen G. *et al.*, 2012; Ropret P. *et al.*, 2008);
- Barium Sulfate at 453 cm^{-1} (m), 461 cm^{-1} (w-sh), 616 cm^{-1} (w) and 988 cm^{-1} (vs) (Bell I.M. *et al.*, 1997; Halac E.B. *et al.*, 2012);
- Lead white at 1050 cm^{-1} (vs) (Bell I.M. *et al.*, 1997; Frausto-Reyes C., *et al.*, 2007);
- Calcite at 1083 cm^{-1} (w) (Aliatis I. *et al.*, 2009; Jehlička J. *et al.*, 2009 ; Lécuyer C. *et al.*, 2012 ; Park K.,1967; Vagenas N.V. *et al.*, 2003).

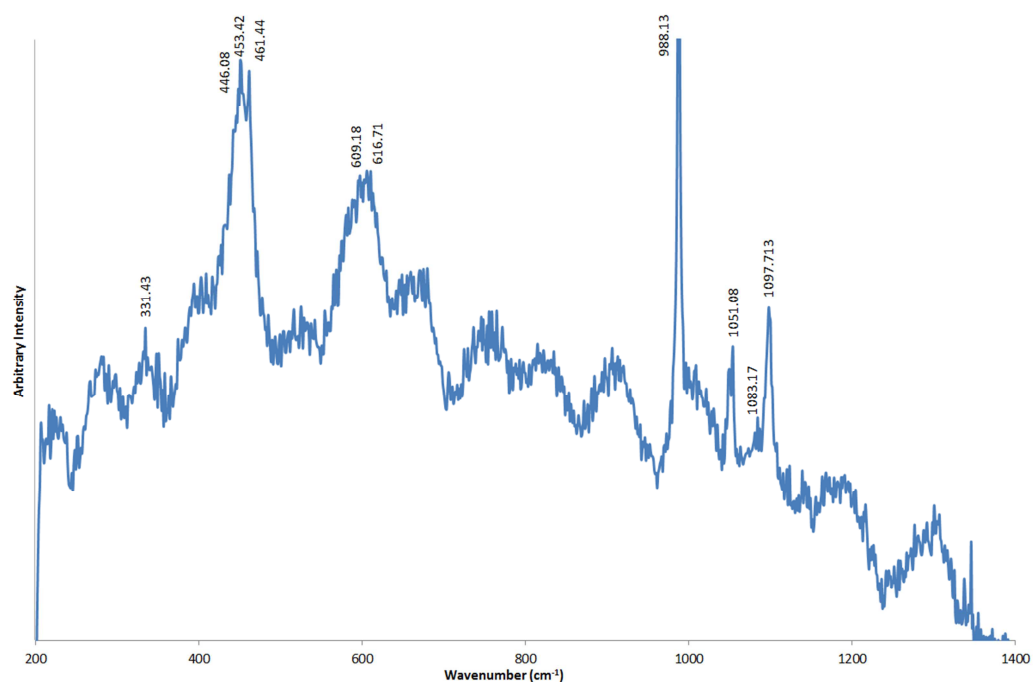


FIG. 67 Raman spectra on white pigment (632,81 nm excitation, 2 mW, 40 s acquisition time): rutile, calcite, barium sulfate, lead oxide.

As concern the red-orange pigment Hematite phase was recognized for its Raman bands at 222 cm^{-1} (s), 295 cm^{-1} (s), 407 cm^{-1} (s), 1306 cm^{-1} (s) (De Faria D.L.A. et al., 2007).

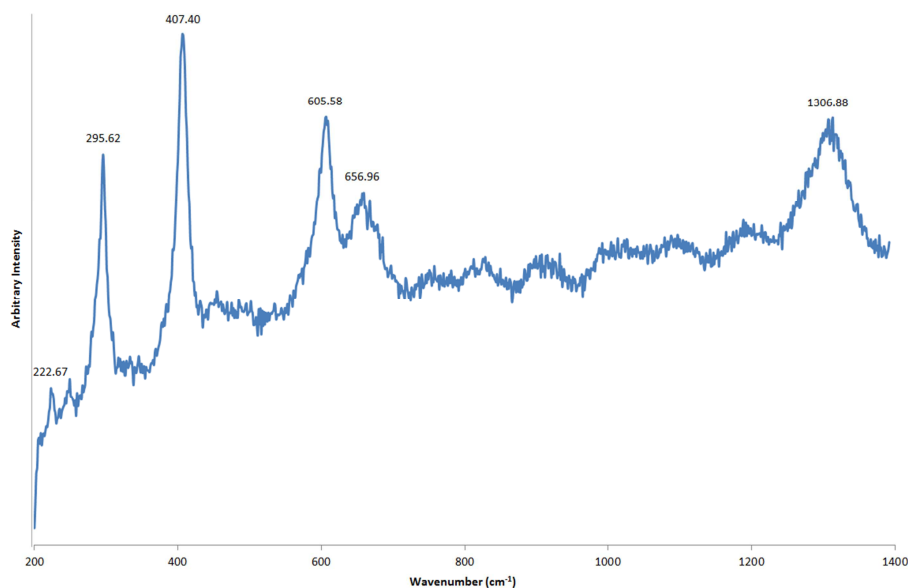


FIG. 68 Raman spectra on red-orange pigment (632,81 nm excitation, 2 mW, 30 s acquisition time): Hematite phase.

Raman spectra obtained by blue particle in white/blue sample reveal numerous peaks that could be attributable to group, in particular Blue Phthalocyanine (Broz'ek-Płuska B. et al., 2005; Nadim C.S. et al., 2009). Considering that PIXE analysis suggested a Blue color based on copper, the pigment employed in this painting could be a Blue Phthalocyanine, in which the coloring agent is copper.

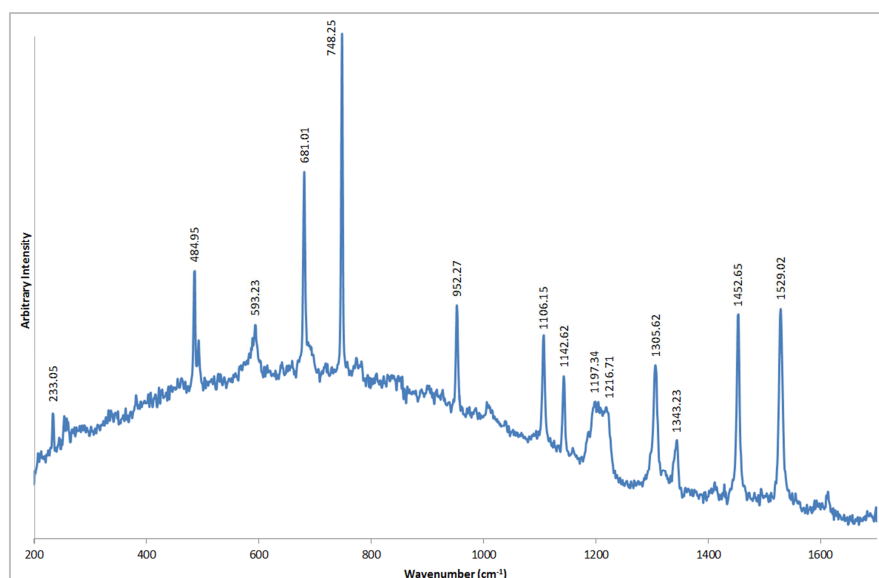


FIG. 69 Raman spectra on Blue particle in white pigment (632,81 nm excitation, 2 mW, 50 s acquisition time): Phthalocyanine Blue.

FIG. 70 shows a comparison between Raman spectra obtained by blue particle in Picasso_blue/white sample and Phthalocyanine Blue extracted by Raman spectra library.

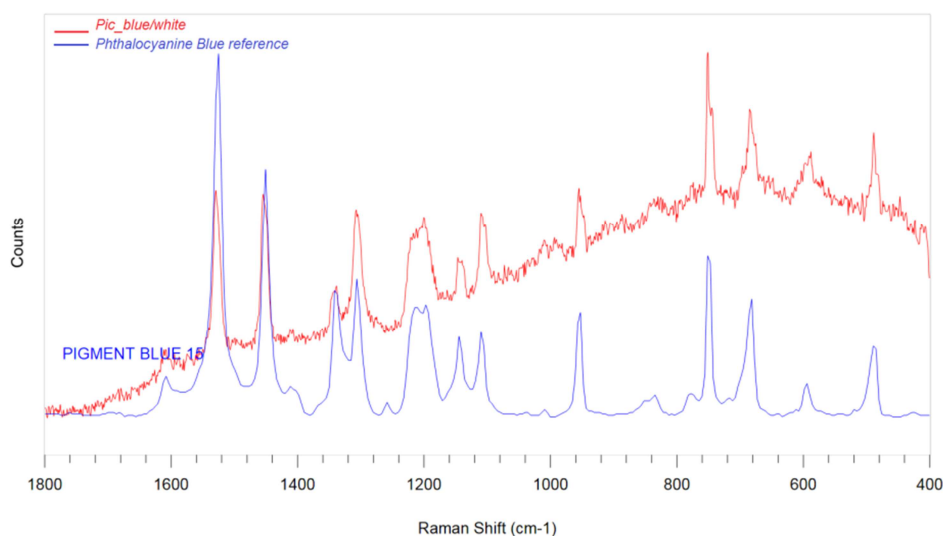
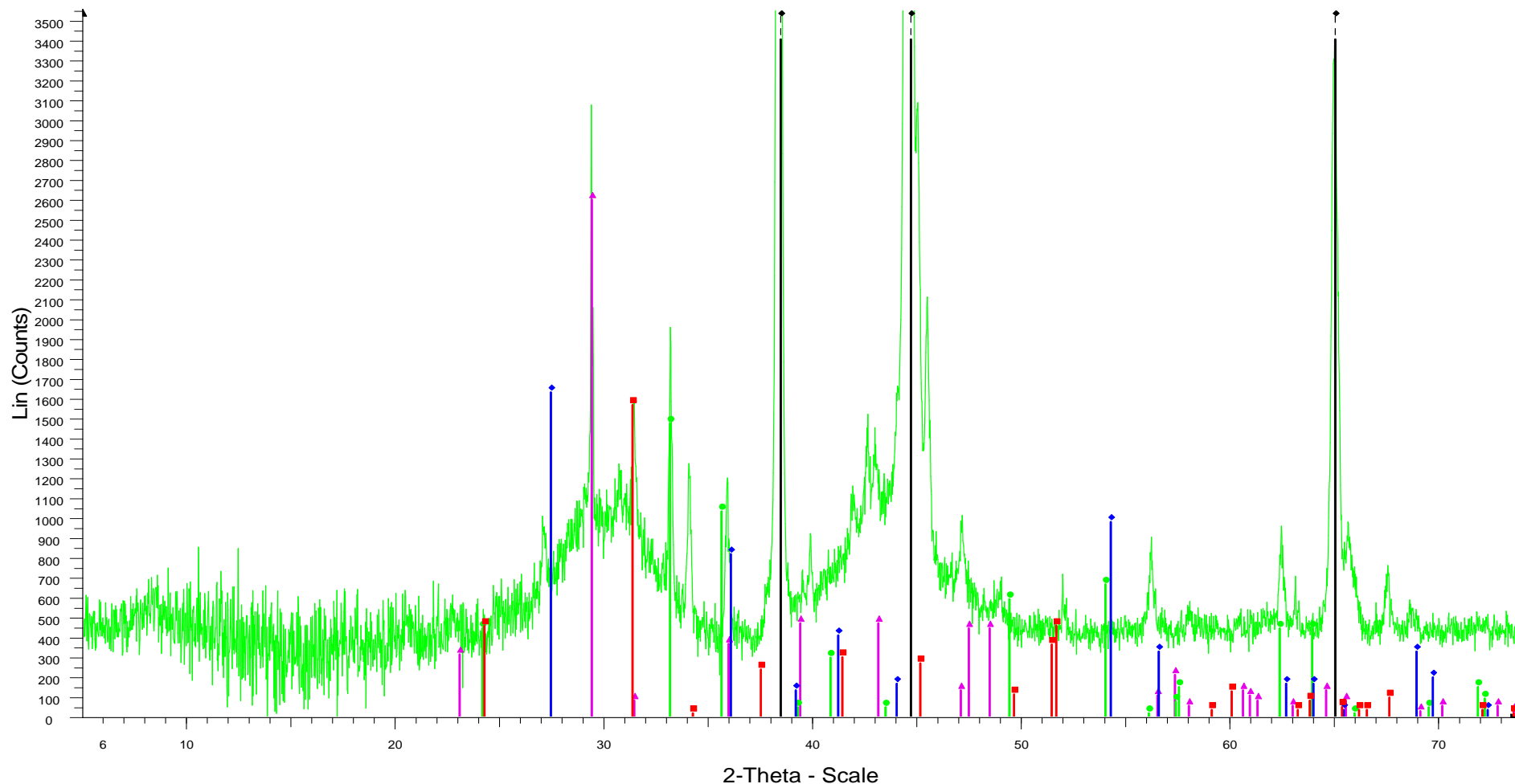


FIG. 70 Comparison Raman spectra obtained on analyzed sample (red) and Phthalocyanine Blue reference spectra.

Finally, for in-depth pigments' identification, XRD analysis were performed on the specimens. XRD spectra revealed the presence of rutile, calcite and hematite phases confirming previous hypotheses. The analysis allowed also to detect Rhodocrosite phase, that can be attributed to a further pigment used for red color (FIG. 71).



- ▲ PIC (L.Volpe) - Al stub - plexi - File: Prova-PIC_Al-stub_plexi.raw - Type: Locked Coupled - Start: 5.000 ° - End: 80.000 ° - Step: 0.020 ° - Step time: 15. s - Temp.: 25 °C (
- ◆ 00-004-0787 (*) - Aluminum, syn [NR] - Al - Y: 113.27 % - d x by: 1. - WL: 1.5406 - Cubic - a 4.04940 - b 4.04940 - c 4.04940 - alpha 90.000 - beta 90.000 - gamma 90.000
- ▲ 00-005-0586 (*) - Calcite, syn - CaCO₃ - Y: 6.92 % - d x by: 1. - WL: 1.5406 - Rhombo.H.axes - a 4.98900 - b 4.98900 - c 17.06200 - alpha 90.000 - beta 90.000 - gamma 90.000
- 00-033-0664 (*) - Hematite, syn - Fe₂O₃ - Y: 3.92 % - d x by: 1. - WL: 1.5406 - Rhombo.H.axes - a 5.03560 - b 5.03560 - c 13.74890 - alpha 90.000 - beta 90.000 - gamma 90.000
- ◆ 00-021-1276 (*) - Rutile, syn - TiO₂ - Y: 4.34 % - d x by: 1. - WL: 1.5406 - Tetragonal - a 4.59330 - b 4.59330 - c 2.95920 - alpha 90.000 - beta 90.000 - gamma 90.000 - P
- 00-044-1472 (*) - Rhodochrosite, syn - MnCO₃ - Y: 4.17 % - d x by: 1. - WL: 1.5406 - Rhombo.H.axes - a 4.79010 - b 4.79010 - c 15.69400 - alpha 90.000 - beta 90.000 - gamma 90.000

FIG. 71 XRD spectra obtained on stub containing white, red/white and white/blue samples.

5.2.5 Conclusion

Pigment analysis, performed onto samples, suggest the use of a white compound based on White titanium dioxide (Rutile phase), Barium sulfate, Calcium carbonate (Calcite phase) and probably mixed with Lead white (basic lead carbonate).

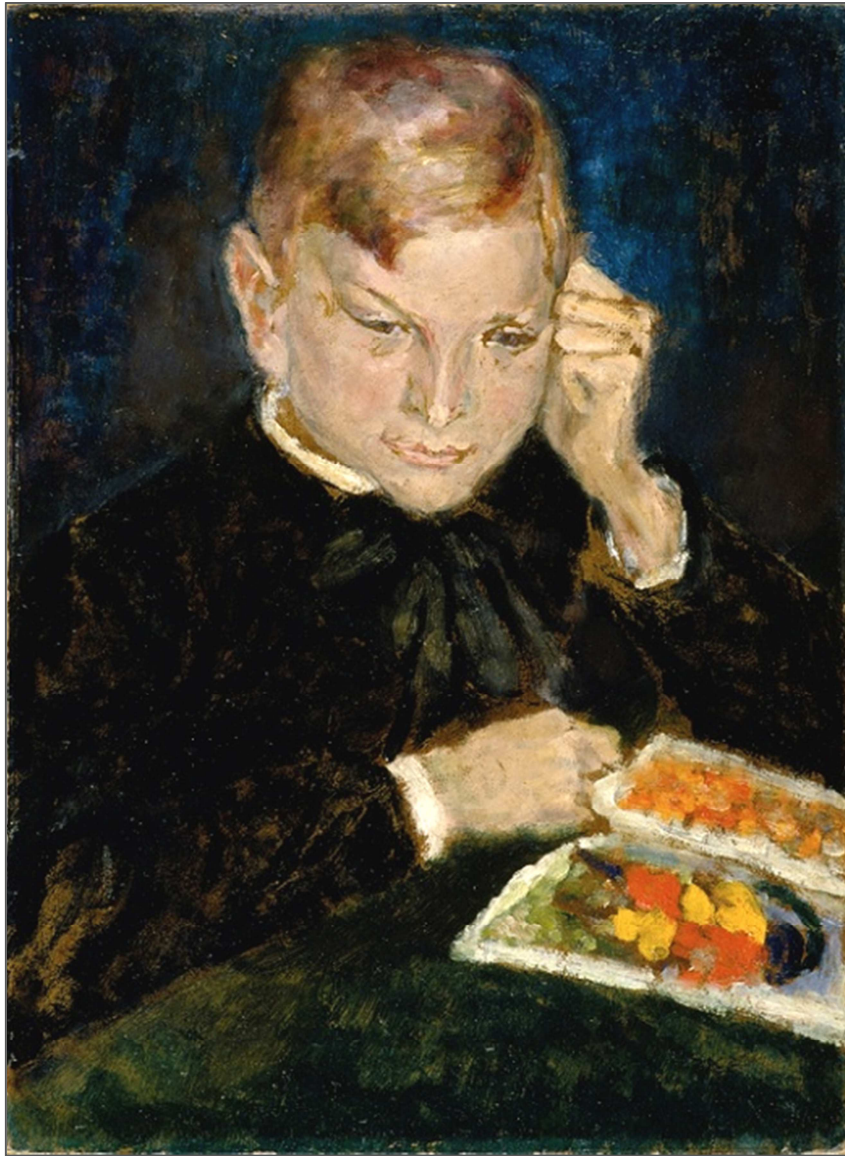
As revealed by microscope survey, specimens show red and blue grains, in addition to white pigment. Chemical-mineralogical analysis carried out on these particles allowed to hypothesize the presence of mineral hematite, used for red color, probably mixed with Rhodochrosite. Results obtained on blue color, instead, suggest the use of Blue Phthalocyanine based on copper.

Therefore, even if it is possible to carry out analysis only on samples, in-depth research of artfingerprints allow to support dating studies, especially if it brings to the identification of mineralogical phases. Considering, in fact, the history of use in artistic field of some identified pigments, it is possible to consider further post-quem data; for example:

- according to numerous studios, the production of rutile $\text{TiO}_2/\text{BaSO}_4$ pigment dated at 1939 (Eastaugh N. *et al.*, 2008; Leonardi R., 2005; Lewis P.A., 1987; McCrone W., 1994; West Fitzhugh E., 1997). The detection of rutile/barium sulfate pigment in this sample suggest an achievement data after 1939;
- phthalocyanine literature describes two early putative synthesis in 1907 and during 1927, when it was create a blue product, probably Cu phthalocyanine (Eastaugh N. *et al.*, 2008); meanwhile the first Pc patent was 1929. Considering that performed analysis identified the pigment as Blue Cu phthalocyanine, the artwork could be made after 1927.

The above mentioned post-quem date are later than 1909 (date proposed for this painting) and before death date of the artist Pablo Picasso (1973). For these reason, it is important to examine further in-depth the whole artwork, the artistic techniques, its material and their history. In this way, a correct pigment analysis can support the historical-artistic investigation for dating purpose.

ARTWORK PLATE III



Author: *Amedeo Modigliani (Italian artist, 1884-1920)*

Title: *Scolaro con libro illustrato (Schoolboy with picture book)*

Object: *Painting (oil on cardboard)*

Date: *1905 c.*

Overall Size: *unknown*

Location: *Private Collection*

5.3.3 “Schoolboy with picture book” by Amedeo Modigliani (oil on plywood, 1905)

Size: unknown

The painting was investigated in order to give information about chemical composition of the pigments for future restoration and maintenance works. Even if it was not possible to investigate the whole artwork, in this study, the methodologies to search *art fingerprints* were tested on samples and they were focused on in-depth pigment analysis, obtaining useful information. Consider that, under microscope, the samples show different colored particles, in addition to white color, the analysis were performed also on these colored grains in order to identify employed pigments.

5.3.3 The artist and the painting

The artist

Amedeo Clemente Modigliani (July 12th, 1884 – January 24th, 1920) was one of the most famous Italian painter who worked mainly in France, becoming known for its paintings and sculptures in a particular modern style: face of his painted subject are with elongated form like a mask.

Born in Livorno in 1884 to Jewish parents, since his childhood, he was in poor health but with a great passion for art. Since 1898 to 1900, he worked in Micheli's Art School, where his earliest formal artistic instruction was characterized by the study of the styles and themes of 19th-century Italian art, that influenced him in his earliest Parisian work. Several travels allowed to Modigliani to discover masterpieces of important artist, such Giovanni Boldini and Domenico Morelli²⁶. When he moved to Paris, in 1906, in spite of he lived with economic difficulties, his passion for art brought him to know painting of Paul Cezanne and other French painter, that influenced him to develop a personal artistic style. Becoming the epitome of the tragic artist (poor, drank, drug addict, etc.) in the last part of his life, he died in Paris in 1920 ([Krystof D., 2000](#); [Lottman H., 2007](#); [Piccioni L. et al., 1981](#); [Werner A., 1990](#)).

The painting

Observing the painting and considering that, being dated 1905, it belongs to pre-Paris period, this painting does not show the particular style that characterized Modigliani “mask”. In fact, main feature of Macchiaoli style are present: the picture is obtained by overlap and juxtaposition of

²⁶ Domenico Morelli was (1826- 1901) was an Italian painter that inspired for "the Macchiaioli"'s group (from *macchia* —"dash of colour", or, more derogatively, "stain").

different colored “macchia” (stain), that creates artwork taking advantage form light and dark shade.

5.3.3 Experimental methods

Micro-specimens amount of painted materials (maximum size: 2-5 mm²) were taken from convenient areas (original and not re-painted zone, without damaging the picture further). Thinking about what color could help the identification of post-quem pigments used in this period, sampling was chosen in correspondence of enlightened (white).

At first, samples are observed under stereomicroscope to study artistic technique and to select best sample for each kind of chemical analysis. After that SEM/EDS analysis are carried out, without any treatment of samples, to study the morphology and chemical elemental composition

XRF were performed at different range of energy (15 KeV, 30 KeV, 50 KeV) to best characterize pigment and PIXE analysis confirmed previous chemical composition identified and it revealed other trace element. Thanks to Raman spectroscopy, it was possible to deepen and to identify other colored particle found on the samples. For in-depth pigment analysis, mineralogical investigation were performed using XRD analysis.

5.3.4 Results and discussion

5.2.4.1 Pigment analysis

Under stereomicroscope, specimens²⁷ show that white samples reveals a lots of different colored particle, such as red, blue, green and yellow, probably due to a contamination of the white zone with other colored area in proximity (FIG. 73 d, e). A thick protective varnish was applied on the entire surface, covering both pictorial layer and support. The layer varnish-pigment is around

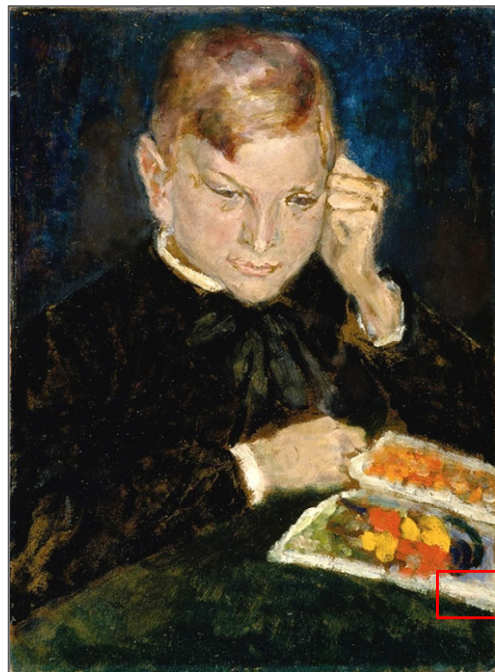


FIG. 72 “Scolaro con libro illustrato”: sampling point.

²⁷ According to who provide the samples, the specimens were taken from original and not re-painted zone, without damaging further the picture

248 μm , which around 80 μm of pictorial blend (FIG. 73 c, f). FIG. 73c shows that the pictorial layer was spread directly on the support and there was not a underpaintig ground.

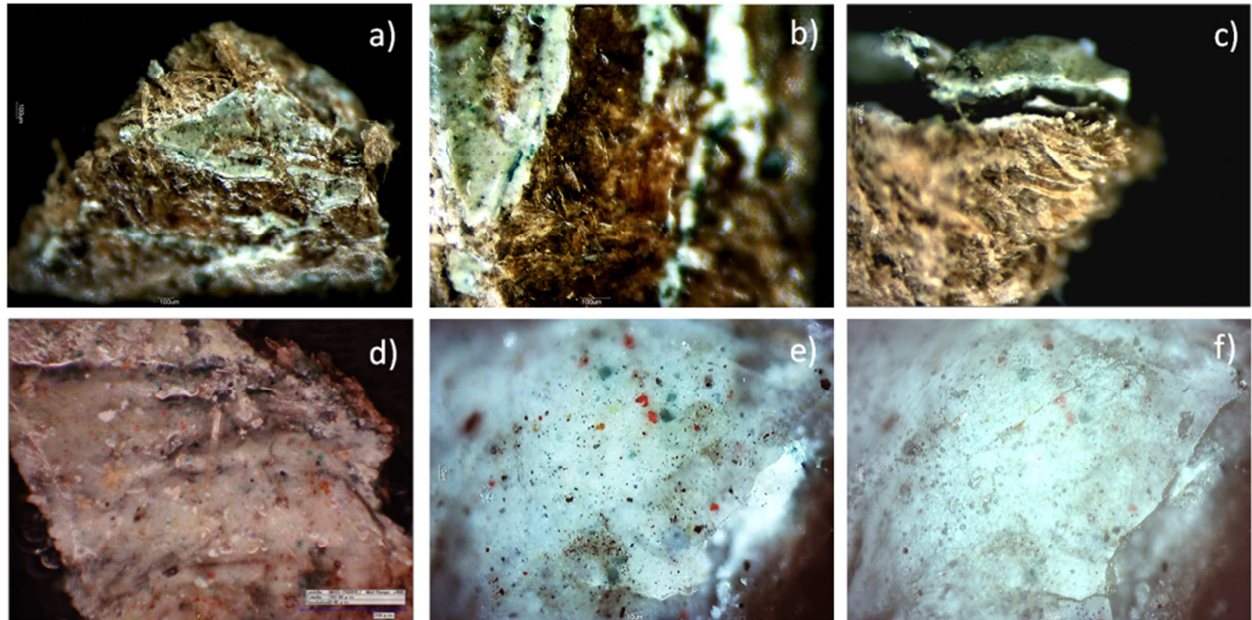


FIG. 73 OM microphotograph of analyzed white samples at different magnification: a) pictorial layer, support and covering varnish (a: magnification 40 x, b: 80x, c: 90x); e) f) colored pigment particles in white layer (normal and GL light, magnification 100 x); d) pictorial layer and varnish (magnification 50x).

As concern the micro-features of the materials, SEM micrographs obtained from samples (FIG. 74) show pigment that is characterized by rounded and very fine particles, that sometimes gathered in aggregates.

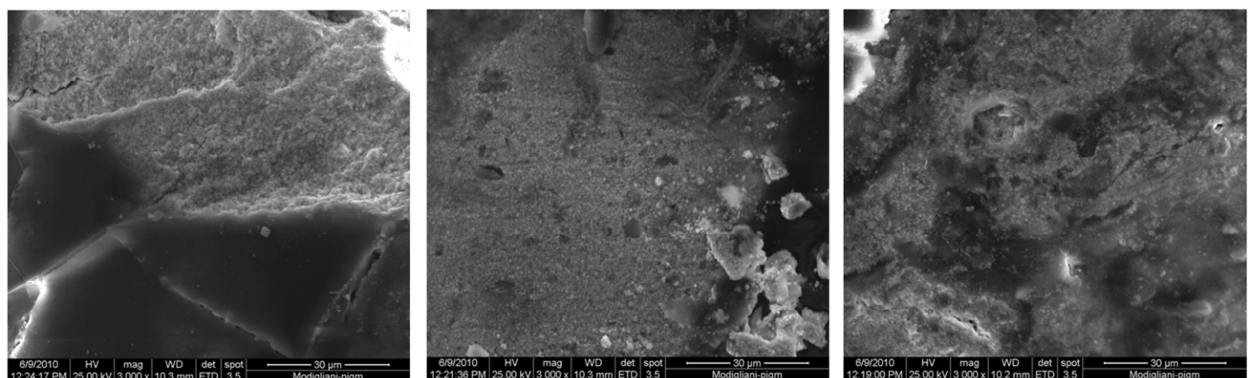


FIG. 74 SEM micrograph of white sample (magnification x 3000).

EDS analysis, performed on the same investigated area, detected high values of lead and sulfur in addition to carbon and oxygen, probably linked to the organic binder. The presence of lead in a white colored compound suggest the use of White Lead for the white color.

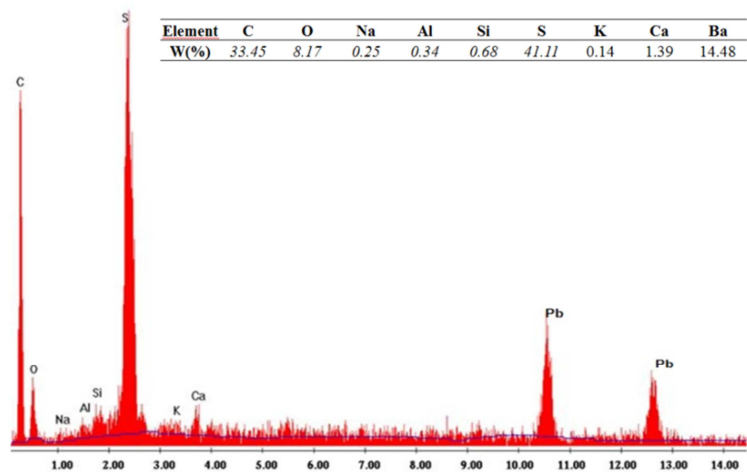


FIG. 75 EDS spectra of white pigment.

EDXRF examination of white area, carried out at different energy beam (15 KeV, 30 KeV, 50KeV), confirms the presence of sulfur and lead and detects Chromium, that was not identified in the background.

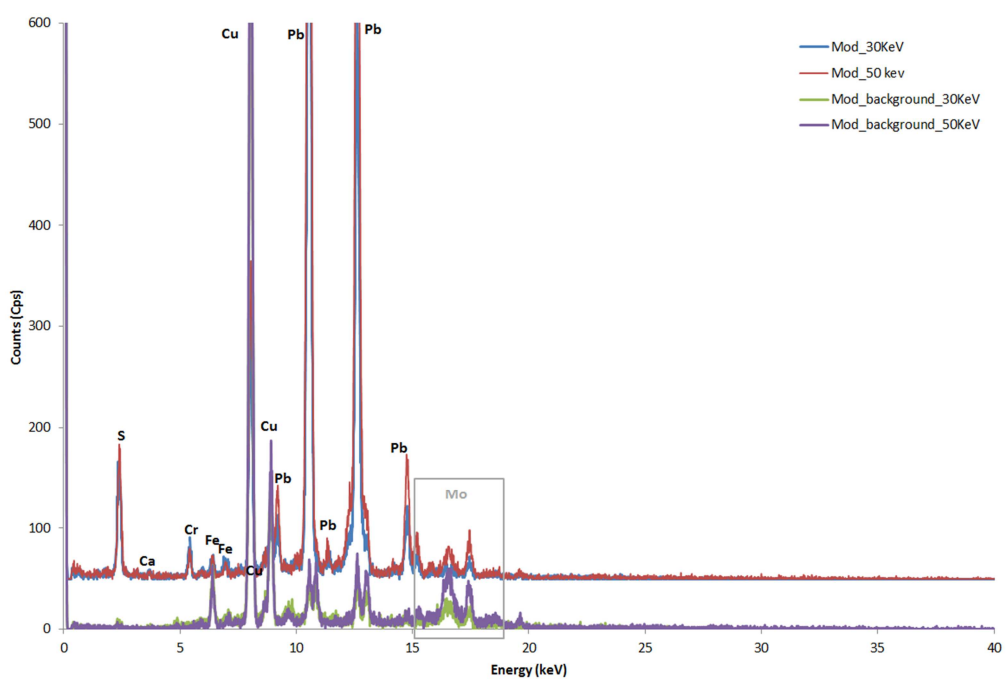


FIG. 76 XRF spectra on White pigment: total spectra from different set-up, not subtracting background. Experimental set up: voltage 50 KeV and current 700 μ A, voltage 30 KeV and current 1300 μ A, Live time: 60 s, no filter, Anode Molybdenum, collimator 0.200.

Similar results were obtained also by PIXE analysis, which data are showed in FIG. 77-78. As it is possible to observe, sulfur and lead are confirmed, but the analysis reveals also other chemical elements such as calcium, copper, iron, zinc, manganese, cadmium and chromium that can be at-

tributable to pigment or to chemical composition of binder and pigment compound. For example, the presence of cadmium and chromium suggest the possible use Yellow-Red cadmium or Chrome Red, respectively.

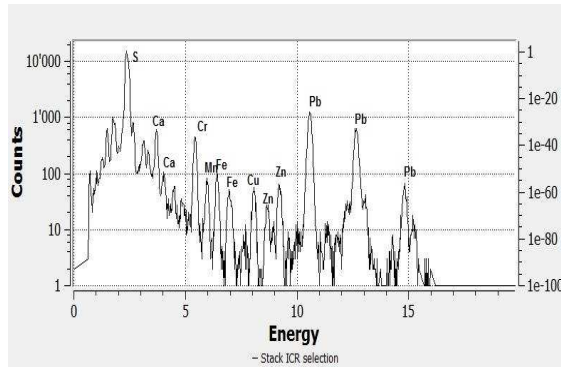


FIG. 77 PIXE spectra of white pigment, low energy detector. Experimental set up: particle/energy 3 MeV, current p+, Dose/s 200 50 KeV, Helium flow.

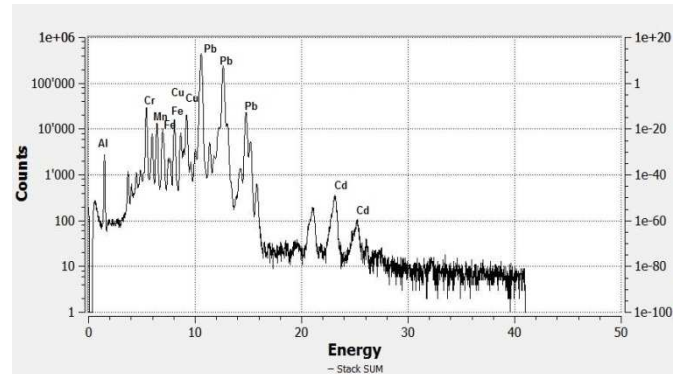


FIG. 78 PIXE spectra of the same sample, high energy detector. Experimental set up: particle/energy 3 MeV, current p+, Dose/s 200 50 KeV, Helium flow.

Raman analysis on white particle did not allow to identify pigment for high value fluorescence of varnish, meanwhile the analysis carried out on red particle show Vermilion peaks (Bell I.M. *et al.*, 1997), with characteristic Raman bands at 250 cm^{-1} (vs), 283 cm^{-1} (w-sh), 343 cm^{-1} (m) (Bell I.M. *et al.*, 1997) [29].

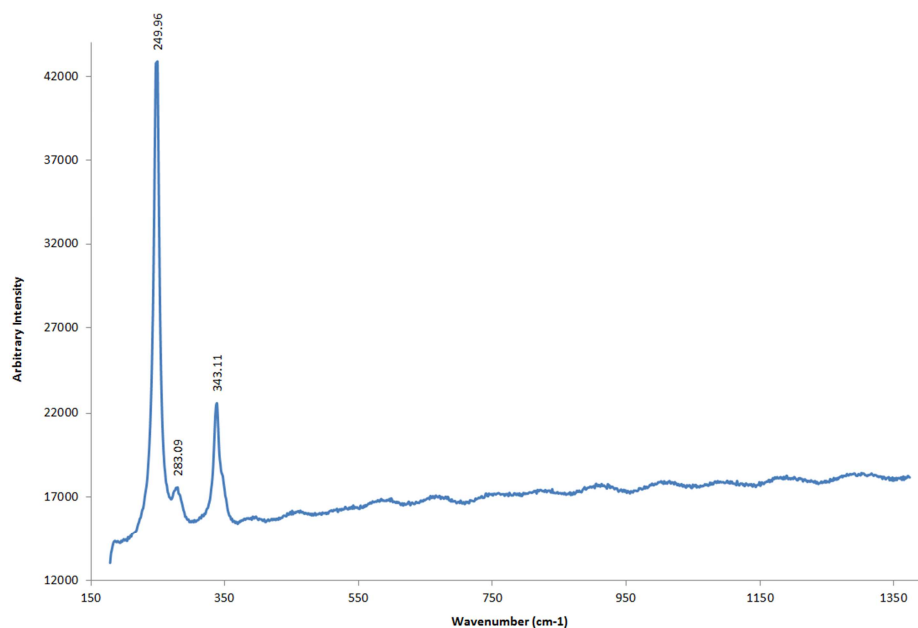


FIG. 79 Raman spectra on red sample (632,81 nm excitation, 2 mW, 50 s acquisition time):Vermilion. Source: Ferrara University.

The survey on blue particles reveals the presence of Artificial Ultramarine Blue, which the characteristics Raman bands of lazurite detected at 258 cm^{-1} (s), 548 cm^{-1} (vs), 581 cm^{-1} (sh), 802 cm^{-1} (v) and 1096 cm^{-1} (w) (Barsan M.M. *et al.*, 2012; Clark R.J.H. *et al.*, 1997; Osticioli I. *et al.*, 2009) [28-30]. Not detecting calcite Raman bands at 283 cm^{-1} (w), 713 cm^{-1} (w) and 1086 cm^{-1} (vs) (Osticioli I. *et al.*, 2009), the analysis suggest the artificial origin of the Ultramarine Blue, that is typically low in impurity such as calcite, pyrite, etc. (Eastaugh N. *et al.*, 2004^B; 28-30).

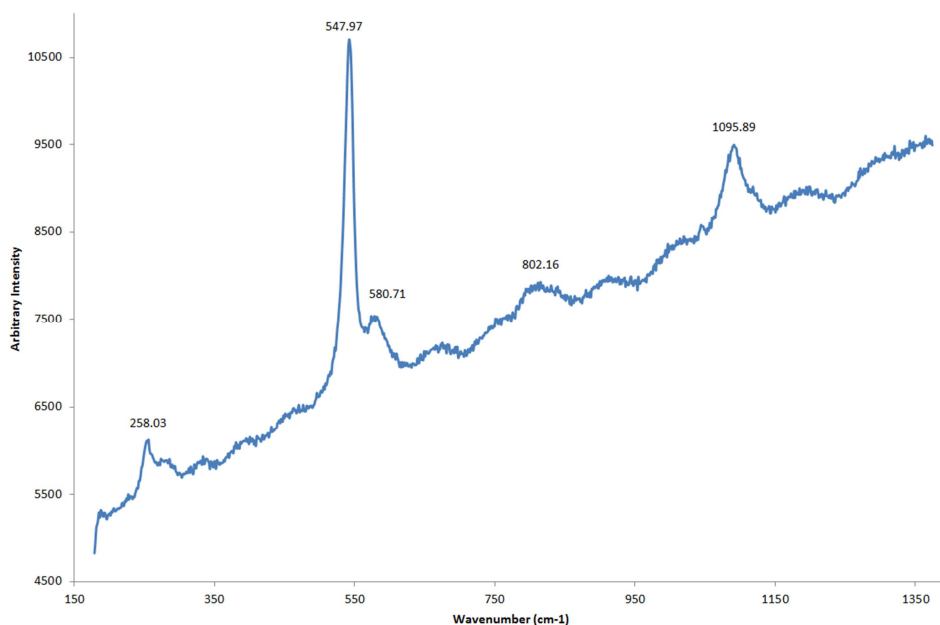
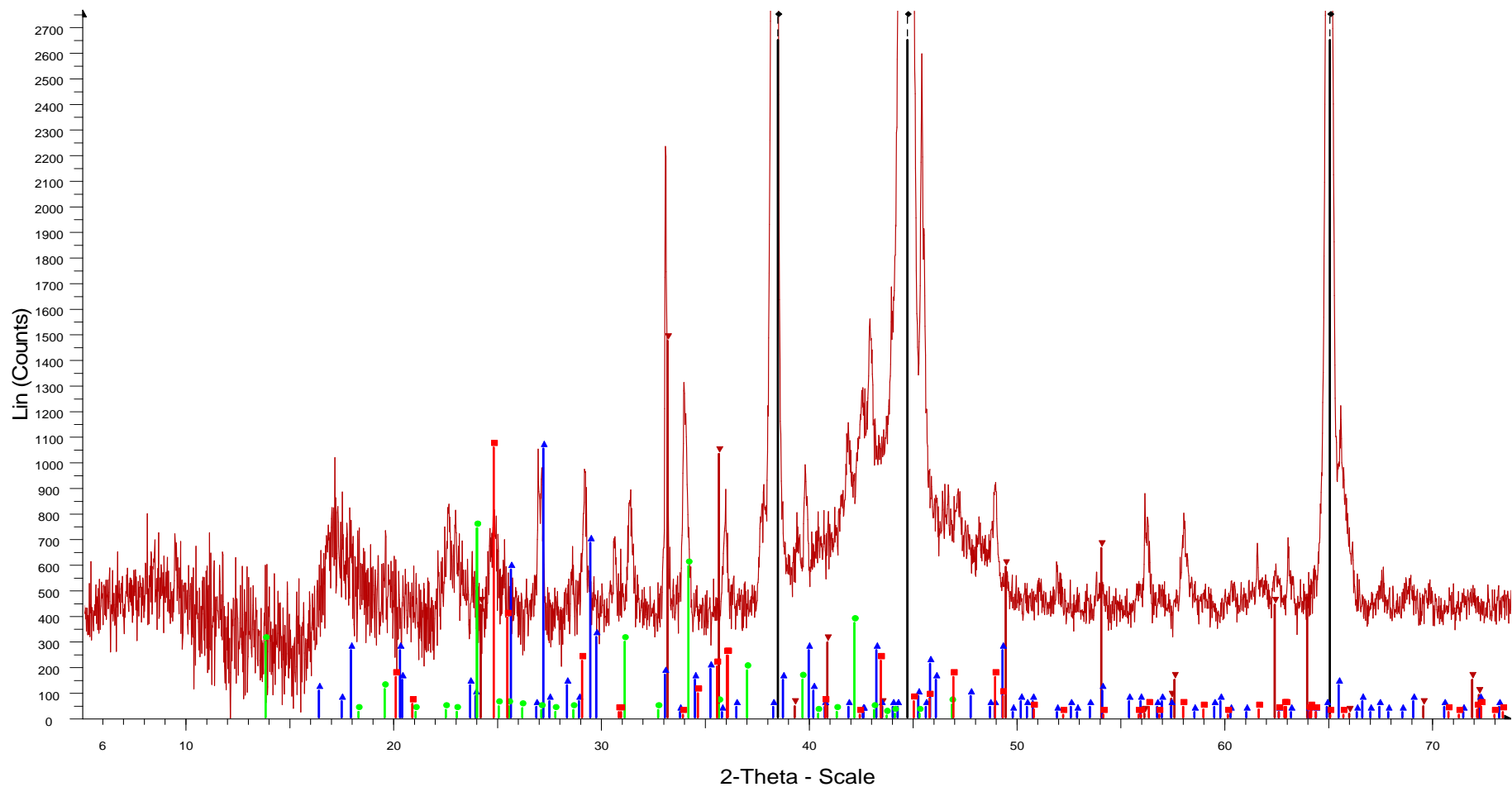


FIG. 80 Raman spectra on blue particles (632,81 nm excitation, 50 x magnification): Artificial Ultramarine Blue.

To confirm the presence of some mineralogical phase hypothesized by previous pigment survey, XRD analysis were performed on the samples.

XRD spectra shows peaks of cerussite, ematite and lazurite phase, confirming, respectively, the presence of White lead (Biacca), Red iron oxide and Blue Ultramarine. Moreover, considering the chemical composition obtained by EDXRF and PIXE analysis, the detection of some peaks could be attributable to crocoite phase (FIG. 81).



- ▲ MOD (L.Volpi) - Al stub - plexi - File: Prova-MOD_Al-stub_plexi.raw - Type: Locked Coupled - Start: 5.000 ° - End: 80.000 ° - Step: 0.020 ° - Step time: 15. s - Temp.: 25 °
- ◆ 00-004-0787 (*) - Aluminum, syn [NR] - Al - Y: 113.27 % - d x by: 1. - WL: 1.5406 - Cubic - a 4.04940 - b 4.04940 - c 4.04940 - alpha 90.000 - beta 90.000 - gamma 90.000
- ▼ 00-033-0664 (*) - Hematite, syn - Fe₂O₃ - Y: 3.92 % - d x by: 1. - WL: 1.5406 - Rhombo.H.axes - a 5.03560 - b 5.03560 - c 13.74890 - alpha 90.000 - beta 90.000 - gamma 90.000
- 00-047-1734 (*) - Cerussite, syn - PbCO₃ - Y: 2.81 % - d x by: 1. - WL: 1.5406 - Orthorhombic - a 5.17800 - b 8.51500 - c 6.14600 - alpha 90.000 - beta 90.000 - gamma 90.000
- ▲ 00-008-0209 (I) - Crocoite, syn - PbCrO₄ - Y: 2.80 % - d x by: 1. - WL: 1.5406 - Monoclinic - a 7.12000 - b 7.44000 - c 6.80000 - alpha 90.000 - beta 102.400 - gamma 90.000
- 00-041-1393 (*) - Lazurite-M - Na₆Ca₂Al₆Si₆O₂₄(SO₄) - Y: 1.97 % - d x by: 1. - WL: 1.5406 - Monoclinic - a 36.36000 - b 51.40000 - c 51.40000 - alpha 90.000 - beta 90.000

FIG. 81 XRD spectra obtained on stub containing white samples with red, yellow and blue particles.

5.3.4.2 Analysis of support: fibers

Through microscope investigation of few fibers taken from analyzed samples, it is possible recognize *Linum usitatissimum* fibers with their characteristics shape: parallel thread linked together in which the growing ring are highlight (FIG. 82) (Reis D. *et al.*, 2006; Scicolone G.C., 2004). The particular birefringence is due to cellulose in cellular lining (about 79/90%).

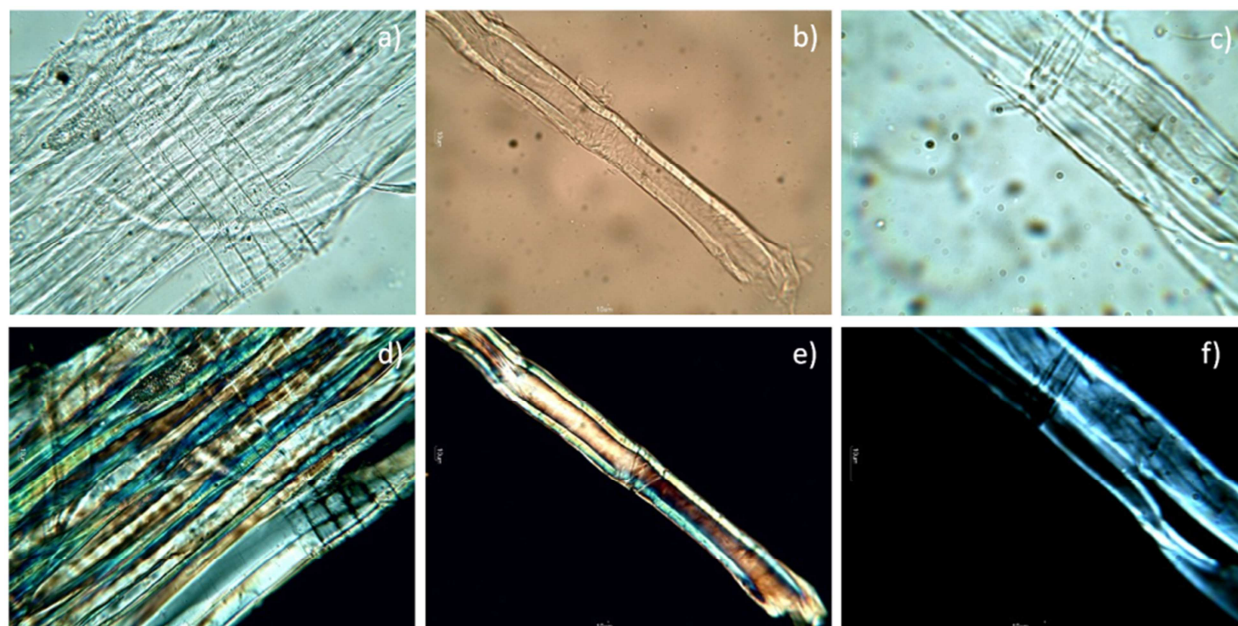


FIG. 82 *Linum usitatissimum* fibers taken from analyzed samples: photomicrograph by optical polarized microscope (normal and polarized transmitted illumination): a) d) magnification 20x; b) e) magnification 40x; c) f) magnification 100x.

5.3.5 Conclusion

The specimens revealed that the pictorial layer was spread directly on an untreated support, that is composed by pressed *Linum usitatissimum* fibers.

Chemical-mineralogical analysis of pigments suggest the use of White Lead for the white color, detecting chemical composition characterized by lead and, through XRD, the mineral cerussite.

As concern other colored particles, PIXE, μ -Raman and XRD demonstrated to be very useful for the characterization. Moreover, the analysis allowed to identify hematite for the red particles and Ultramarine Blue for the blue color.

Finally, considering the history and when these pigments came in use, the results of pigment analysis are compatible with period indicated for this painting.

ARTWORK PLATE IV



Author: *Giovanni Boldini (Italian artist, 1842-1931)*

Title: *Donna in lettura sul letto ed anziano* or *Dama che legge con signore (Reader woman on bed and old man)*

Object: *Painting (oil on canvas)*

Date: *post 1914 (?)*

Overall: *27.20 cm (height) * 37.00 cm (width)*

Location: *Private Collection*

Note: *study of Artist attribution and dating in progress*

5.6 “Reader woman on bed and old man” by Giovanni Boldini (oil on canvas, post 1914)

Size: 27.20 cm (h) * 37.00 cm (w)

The painting “Donna in lettura sul letto con anziano” is a painting (oil on canvas, private collection Italy) signed “Boldini” in left corner of the artwork. For this reason, in addition to evaluate conservative condition and to characterize materials for restoration and maintenance work, the aim of the study was also to verify if pigment used are compatible with the presumed achievement. The opportunity to follow the study of the painting in all its phases allowed to test the “art-fingerprint” procedure to verify if it could be useful for artwork and art assurance field.

5.6.1 The artist

Giovanni Boldini (December 31st, 1842 - July 11th, 1931) was an Italian genre and portrait painter, belonging to the Parisian school. According to a 1933 article in Time magazine, he was known as the "Master of Swish" for his flowing painting style.

Boldini was born in Ferrara, the son of a painter of religious subjects, and went to Florence in 1862 to study painting meeting there the realist painters known as the Macchiaioli (Panconi T., 1998). Their influence is seen in Boldini's landscapes which show his spontaneous response to nature, although it is for his portraits that he became best known. He attained great success in London as a portraitist. From 1872 Boldini lived in Paris, where he became a friend of Edgar Degas, known Gustave Coubert and Edouard Manet, and where he was nominated commissioner of the Italian section of the Paris Exposition in 1889 (Less S., 2009). He also became the most fashionable portrait painter in Paris in the late 19th century, with a dashing style of painting which shows some Impressionist influence but which most closely resembles the work of his contemporaries John Singer Sargent and Paul Helleu. At the beginning of I WW, he moved to London and Nice, but in 1918 he came back to Paris where French government invested him with the *Legion d'Honneur* for this appointment (Doria B., 1998; Lega C., 1963; Lega C. *et al.*, 1994; Torboli M., 2000).

5.6.2 The painting: subject

"Era un artista ultra chic, in suo modo particolare, specialmente quando ritraeva lungiformi signore dell'alta società internazionale che appaiono dipinte come sotto un vetro traslucido. Esperto di quel mondo e della letteratura francese che lo ha rappresentato, interpretava molto

bene la più alta eleganza femminile in un'epoca in cui era anche troppo rivestita dagli artifici dei sarti e delle modiste, figurativamente legata in pose ambigue che stanno tra il salotto e il teatro. Ma quei ritratti hanno un forte potere d'incanto: rivelano spontanee e sicure doti di pittore..." (Berenson B., 1958).

(transl. "He was an ultra-chic artist in its own particular way, especially when depicting elongated international society ladies that appear as painted in a translucent glass. Specialist of that world and French literature that represented him, he played very well the highest feminine elegance at that time, when it was too covered by the artifices of tailors and milliners, figuratively tied in poses that are ambiguous between the living room and the theater. But these portraits have a strong power of charm: they show the spontaneous and secure talent of painter ...", Berenson B., 1958).

Following chronological path among Boldini paintings, it is possible note that the subject of the studied painting was also portrayed in previous artist's artwork:

- similar ancient man is also in "Sunday visit", named also "Old person and two girls in painter's study" (oil on canvas, 1884, 35 h x 27 w cm);
- female figure in "Reading in bed (the romance)" (watercolor on paper, 1914) and in "Woman lies down on bed", known as "Lina reads on bed" (oil on canvas, 1914).



FIG. 83 "Sunday visit" made by G. Boldini (oil on canvas, 1884).

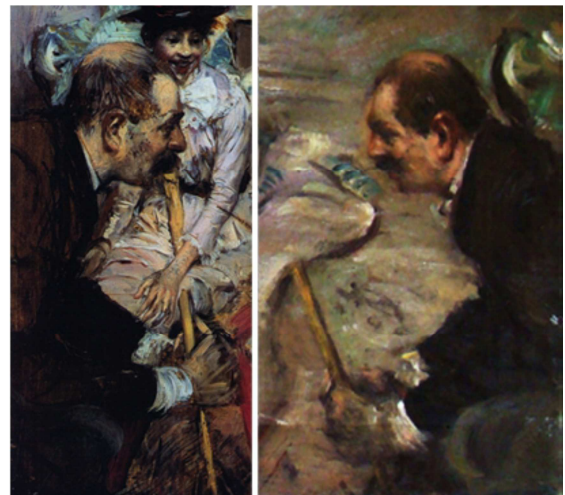


FIG. 84 Comparison between ancient person in a) "Sunday visit" (G. Boldini) and b) "Donna in lettura sul letto con anziano" (G. Boldini?)



FIG. 85 “Reading in bed (the romance)” made by G. Boldini (watercolor on paper, 1914).



FIG. 86 “Lina reads on bed” made by G. Boldini (oil on canvas, 1914).

The studied painting contains elements taken from the previous mentioned artwork: the position of the woman and of the elderly person are the same for both artwork; further, for the female figure, the environment is more similar to watercolour than oil painting, except for the shape of bedside table legs.

Considering that, first depictions of female figure is dated back to 1914, it could be suggest that oil copy could be made after 1914.

As concern the signature, the original paintings (FIG.88-90) do not show the signature of the artist, unlike analysed artwork²⁸. Moreover, even if it considers previous study about the concepts of signature for Boldini²⁹, it is possible to note different shape among “Boldini” signed in original artwork and studied painting (FIG. 87, 88-90)³⁰.

²⁸ Consideration obtained observing images take from book (Camesasca E., 1970; Dini P. et al., 2002). This aspect will be verified observing full image of artworks or directly the original.

²⁹ “Boldini fu assai parco di firme e anche più avaro di date. La firma, appunto, costituiva per lui il contrassegno del lavoro, non solo finito, ma in certo senso “definitivo”: nel quale erano soddisfacentemente confluite (sappiamo che non era di facile accontentatura) le ricerche attraverso disegni e abbozzi dipinti [...]. Da quanto siamo venuti esponendo appare chiaro che per Boldini doveva essere inconcepibile firmare una tavoletta o anche una vasta tela dove avesse studiato un ritratto o qualsiasi altra composizione (in alcuni casi, il paesaggio còlto dal vero in un olio di rispettabili dimensioni ebbe il suo approdo in un acquerello assai più piccolo). Vogliamo giustificare con ciò la nostra perplessità dinanzi ai piccoli dipinti (esclusi alcuni dei primi o del periodo iniziale a Parigi) che esibiscono il suo cognome: contrassegno che, del resto, risulta quasi sempre molto facile da valutare quanto all'autografia” (Camesasca E., 1970).

³⁰ For in depth information: D'avossa E. (2012). “Donna in lettura sul letto ed anziano. Valutazione con metodi non invasivi dello stato di conservazione del dipinto”. Thesis manuscript for triennial degree in “Scienze e tecnologie per l’ambiente, la natura e i beni culturali”- curriculum: Tecnologie per i Beni Culturali (L-43). Tutor: Prof. Carmela Vaccaro, Dr. Lisa Volpe; co-tutor: Dr. Eva Peccenini. University of Ferrara, Ferrara (Italy).



FIG. 87 “Boldini” signature in “Donna in lettura sul letto ed anziano”(oil on canvas, after 1914?).



FIG. 88 “Boldini” signature in "Alaide Banti in bianco" (oil on canvas, 1866).



FIG. 89 “Boldini” signature in "Lina Cavalieri" (oil on canvas, 1901).



FIG. 90 “Boldini” signature in “Madame Michelham” (oil on canvas, 1913).

For this reason, the owner chose to deep the research with a specific characterization of artistic material (pigments), in order to verify the presence of some particular post-quem pigment to better define if this painting could be an ancient or a recent copy.

5.6.3 Experimental methods

Some investigations could be performed directly on the painting through non-invasive techniques: VIS (visible photography), RAK (Raking light), UVF (Ultraviolet Fluorescence), IRR (Infrared Reflectograph), transillumination image and X-ray examination. The information obtained by these methodologies proved to be useful to evaluate conservative condition and to choose area that were following analyzed by EDXRF.

However, considering EDXRF results, the complexity of mixed color of painting and the great possibilities of suggested pigments, sampling of the painting was necessary to better characterize used pigments. Samples were taken onto the vertical side border to study preparatory layer composition and on white area (FIG. ..., point 1) to better characterize white pigment.

The areas that have been examined with EDXRF analysis are marked in FIG. 91, meanwhile sampling area in FIG. 92.



FIG. 91 “Reader woman on bed and old man”: locations for EDXRF point analysis are depicted by numbers.

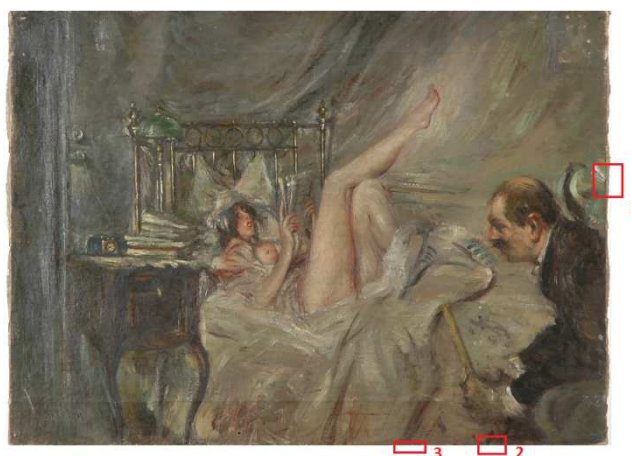


FIG. 92 “Reader woman on bed and old man”: locations of sampling area are depicted by red square and numbers.

Micro-specimens amount of painted materials are observed under microscope to study mainly characteristic and to choose which samples could be most representative for each of the following techniques: SEM/EDS, EDXRF on samples, PIXE and μ Raman analysis.

5.5.4 Results and discussion

5.5.4.1 Artistic technique and conservative conditions

As it is possible to observe in FIG. 93-94, from the comparison between VIS image and GL, trans-illumination image, the painting has not good conservative condition: the attendance, in fact, of a great number of different craquelures (FIG. 94) make the pictorial layer very fragile, that could cause the lack of materials and little holes, as proved in some area of the artwork.

In UVF image (FIG. 96) , the absence of different fluorescence color does not make possible the recognition of retouches; the two figures, so, are made in the same period. The only part of painting that shows some difference is in correspondence of the letter “B” of signature, where the varnish seems to be removed.

IRR image (FIG. 97) does not reveals under-drawing, but it allows to hypothesize the not-organic composition of brushstroke’s signature seeing that it disappears under Infrared investigation.

Finally, the painting, under X-ray examination, does not highlight *pentimenti* but the presence of isolated and random area constituted by quite heavy chemical element. This suggests that maybe a previous preparatory layer was removed by canvas support, that was prepared again with other materials. The presence of red color in the white area X-ray image allows to suppose that this removed layer could be made using red pigment rich in heavy elements, i.e. pigment based on

mercury compounds or iron oxide chemical composition [38]. As concern, instead, conservative condition, X-ray image points out empty xilofagi insects' gallery in the wood stretcher.



FIG. 93 "Reader woman on bed and old man": visible, normal light.



FIG. 94 "Reader woman on bed and old man": visible, grazing light.



FIG. 95 "Reader woman on bed and old man" (trans illumination image): white spots are due to painting's hole.



FIG. 96 "Reader woman on bed and old man": Ultraviolet Fluorescence.



FIG. 97 "Reader woman on bed and old man": Infrared reflectogram.



FIG. 98 "Reader woman on bed and old man": X-Ray radiography.

Under stereomicroscope, it is possible to see how the artistic technique is characterized by brushstroke spread in a quickly way (FIG. 101), that create area with a concentration of materials. The superficial unevenness, due to this brushstroke, facilitated the born of different kind of *craquelures prématurées* and *craquelures d'age* (FIG. 99-104) and, thanks to natural behavior of canvas during time, it caused lack of pictorial layer that allowed to canvas' fibers to spill out from weave. The *craquelures* network interested also signature "Boldini", suggesting that it was made in the same period of the artwork.

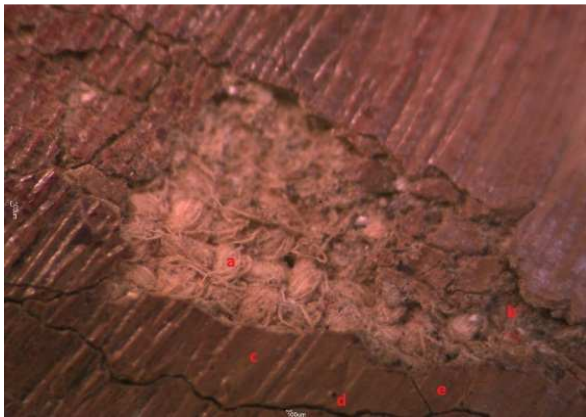


FIG. 99 Photomicrograph of painting layer (visible illumination, original magnification x 20): a) canvas weave, b) ground, c) pictorial layer, d) primary craquelure, e) secondary craquelure. Source: Ferrara University



FIG. 100 Photomicrograph of painting layer (visible illumination, original magnification x 10).



FIG. 101 Photomicrograph of painting layer (visible illumination, original magnification x 10).



FIG. 102 Photomicrograph of painting layer



FIG. 103 Photomicrograph of painting layer (visible illumination, original magnification x 30).

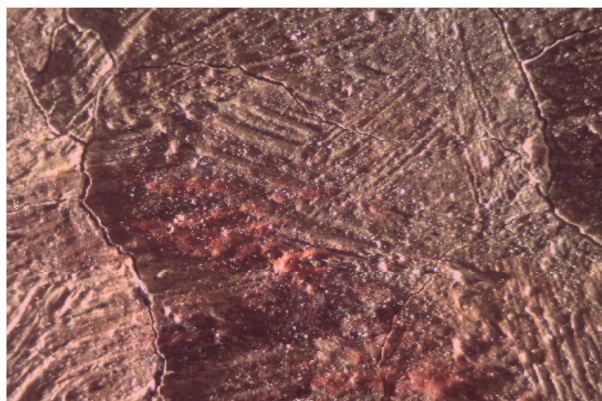


FIG. 104 Photomicrograph of painting layer (GL of FIG. 103).

The investigation under stereomicroscope permitted, also, to capture details difficult to faithfully reproduction that could be useful to employ database of artwork used to control the correspondence with the original painting during his possible movement.

In addition to be considered art-fingerprints, all these features were also useful in support to a good image processing (choice of predominant colors, etc.) and to select the main interesting regions that were subsequently deepened by EDXRF analysis on painting and by analysis on samples.

Initially, Image processing was performed to group different shade and colored brushstrokes into few color pigments, that are usually used for the interpretation of pigment concerning chemical composition, supporting the point analysis and the choice of proposal pigment for data interpretation (FIG. 106).



FIG. 105 "Donna in lettura sul letto ed anziano" (VIS photograph).

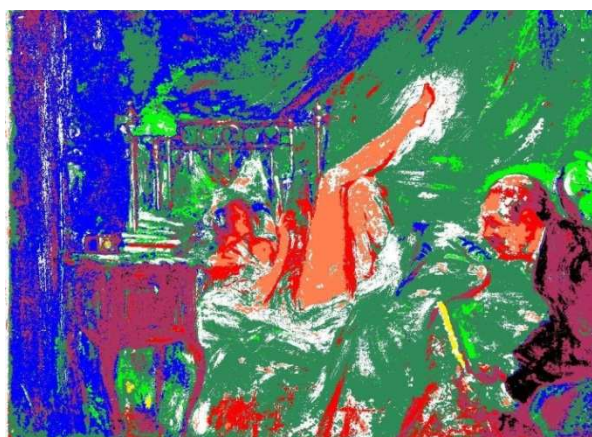


FIG. 106 "Donna in lettura sul letto ed anziano": ROIs' color class through Image Processing.

As concern conservative condition, ENVI was tested to localize the craquelures: it was used transillumination photograph and not RK image because in the first the deepen of craquelure is highlight by different hue of color.

The procedure was tested downloading both greyscale image, that was then stretched to highlight craquelures, and color transillumination image: in the latter better results are obtained.

After numerous tests in which software had con-

fused the pink nuance of painting as pink-orange color characteristics of craquelure, the better solution was to create five ROIs with colors match to conservative danger degree:

- Canvas without great conservative problems: green color;
- Pink color pigment: different nuance of green color;
- Superficial craquelures (craquelures that interest only pictorial layer, i.e. *craquelures prématurées*): yellow color;
- Deepen craquelure (craquelures that arrive up to cloth, i.e. *craquelures d'age*): orange color;
- Lack or hole: red color.

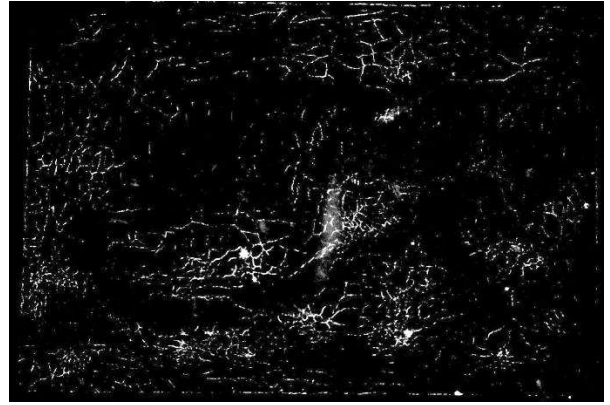


FIG. 107 Detail of “Donna in lettura sul letto ed anziano” (FIG. 95 , greyscale stretched image).



FIG. 108 “Donna in lettura sul letto ed anziano” (transillumination photograph).

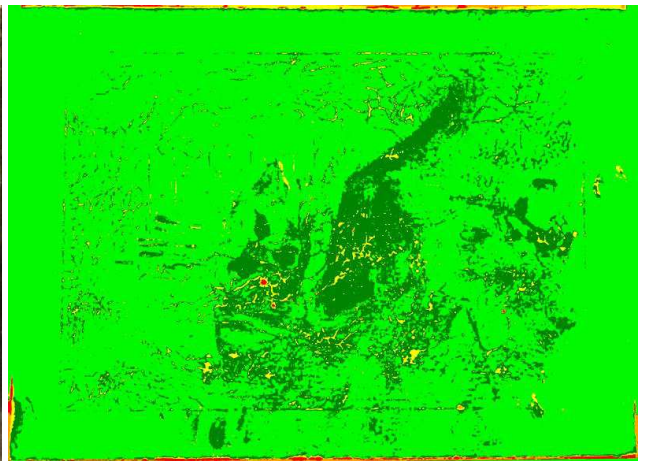


FIG. 109 “Donna in lettura sul letto ed anziano”: ROIs' color class through Image Processing.

Even if the five ROIs have different spectral profile (FIG. 110-114), some regions (i.e. superficial craquelures) are sometimes confused with the pink-orange nuance of the protagonist's skin (FIG.108). For this reason, maybe, an image with more resolution could allow to better identify the different ROIs with major precision.

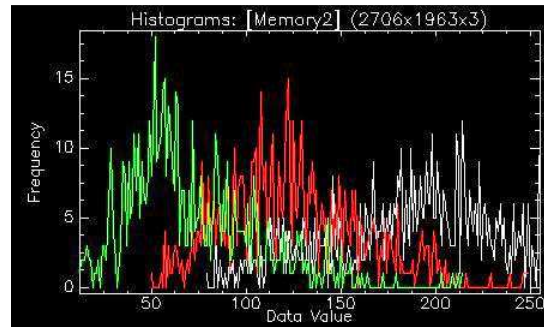


FIG. 110 Spectral profile of ROI "craquelure".

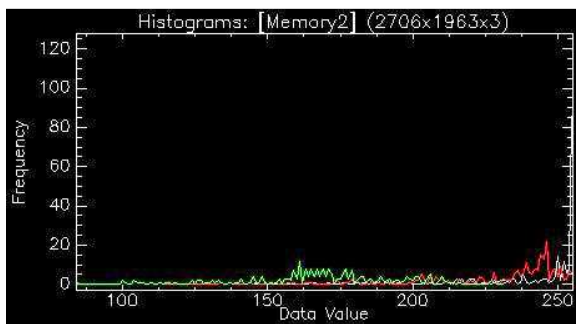


FIG. 111 Spectral profile of ROI "craquelure deep-en".

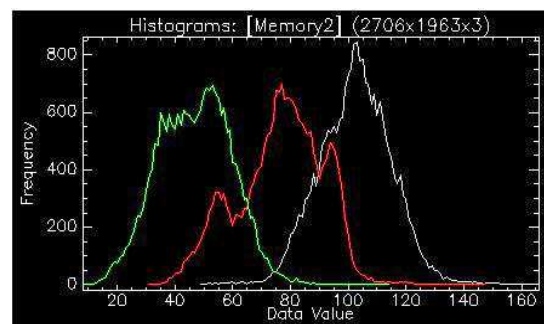


FIG. 112 Spectral profile of ROI "pink on canvas".

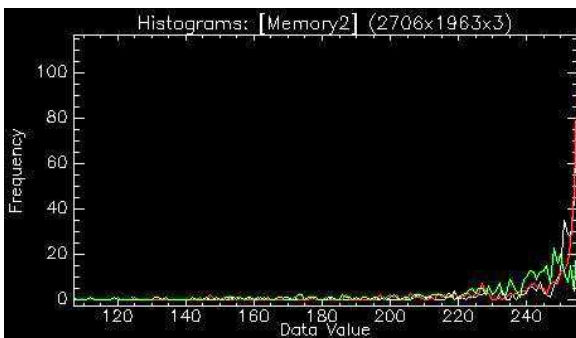


FIG. 113 Spectral profile of ROI "lack".

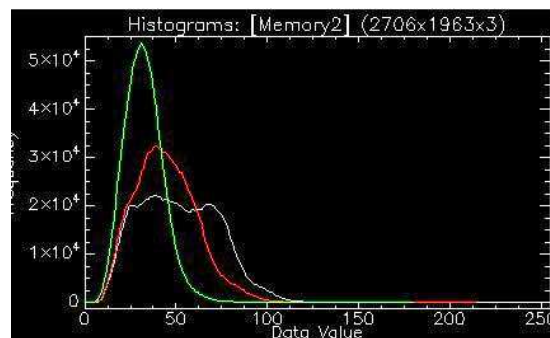


FIG. 114 Spectral profile of ROI "canvas".



FIG. 115 Detail (man): VIS image.



FIG. 116 Detail (man): RK image.



FIG. 117 Detail (man): transillumination image.

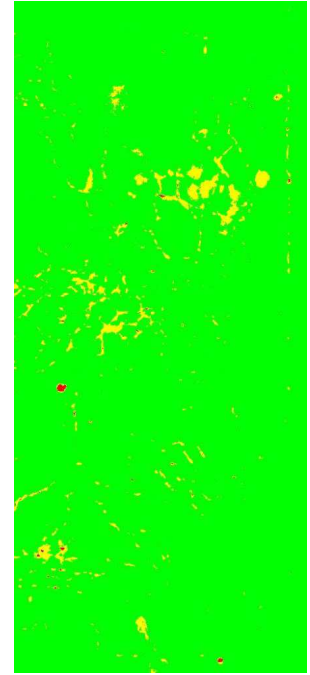


FIG. 118 ROIs' class on FIG. 117: green, not damage; yellow, craquelures; red, lack or hole.

Considering the necessity to compare the images obtained from Imaging Analysis in order to select best point/area for not-invasive analysis and for sampling (i.e., craquelures, etc.), a simultaneous comparison between the different images could support also data interpretation. For this reason ENVI suite was applied also to create the warp file, linking together VIS-transillumination images, VIS-X ray radiography, X ray radiography-transillumination images, VIS-UV, UV-X ray radiography, etc.



FIG. 119 Results from "Warp file creation": transillumination image onto visible photograph.



FIG. 120 Results from "Warp file creation": X-ray image onto visible photograph.

All these information and software elaboration demonstrated to be very useful for a better investigation of the painting, allowing to continue the research more in depth.

5.5.4.2 Pigment analysis

Considering results obtained by multispectral imaging and by image processing, non-invasive EDXRF analysis was carried out on several points of the painting recto both on pictorial layers and on the background, exposed by pictorial matter loss.

As mentioned before, the artistic technique is characterized by pigment mixed together to obtain desired chromatic effect; this aspect makes pigment's identification difficult. The EDXRF analysis, in fact, highlight that all chemical elements belonging to each color are spread in the entire pictorial layer.

TABLE 9 EDXRF analysis on painting "Reader woman on bed and old man": average of Net Area values, gathered for color. Experimental set up: voltage 30 keV, current 1300 μ A, Live time: 120 s, no filter, Helium flow, Anode Molybdenum, collimator 0.650. In italic, average value greater than σ .

	Zn	Pb	Ba	Fe	Ca	Sr	Se	Mn	Cd
White	<i>1085031</i>	<i>41391.67</i>	<i>464.31</i>	<i>25445</i>	<i>11230.56</i>	<i>3932.93</i>	<i>752.43</i>	<i>515.812</i>	<i>1845.25</i>
Brown	<i>112945.5</i>	<i>64970.25</i>	<i>224.5</i>	<i>57972</i>	<i>34844.25</i>	<i>5642</i>	<i>2107.25</i>	<i>1576.25</i>	<i>605.75</i>
Blue	<i>393869.4</i>	<i>48623.4</i>	<i>764.2</i>	<i>40818.6</i>	<i>16287</i>	<i>8157</i>	<i>896.20</i>	<i>803.6</i>	<i>1483</i>
Green	<i>446422.3</i>	<i>57302</i>	<i>689</i>	<i>34927.67</i>	<i>9098.33</i>	<i>5917.33</i>	<i>884.33</i>	<i>828.66</i>	<i>3589.66</i>
Yellow	<i>160288</i>	<i>135811.7</i>	<i>1086.33</i>	<i>29508.67</i>	<i>10654.33</i>	<i>12403.67</i>	<i>1096.33</i>	<i>840.66</i>	<i>4041.66</i>
Pink	<i>1097443</i>	<i>65512.67</i>	<i>415</i>	<i>20905.67</i>	<i>7962.33</i>	<i>3296</i>	<i>9199</i>	<i>621.66</i>	<i>8481</i>
Red	<i>446247.7</i>	<i>43974</i>	<i>466.66</i>	<i>29638.67</i>	<i>12689.33</i>	<i>6466</i>	<i>34371.67</i>	<i>770.33</i>	-
Backgr	<i>151331</i>	<i>133669</i>	<i>175</i>	<i>76683</i>	<i>49089</i>	<i>4108</i>	<i>1863</i>	<i>2568</i>	<i>252</i>

	Cr	Sn	Co	S	Si	Cu	K	Hg
White	<i>2056.67</i>	<i>10.875</i>	<i>60.25</i>	<i>54.8125</i>	<i>1.6875</i>	<i>326.13</i>	<i>29.94</i>	-
Brown	<i>1766.75</i>	-	<i>653.5</i>	<i>203.5</i>	<i>59.75</i>	<i>193.5</i>	-	-
Blue	<i>7149.8</i>	<i>55.8</i>	-	-	-	<i>150</i>	<i>503.8</i>	-
Green	<i>3673</i>	<i>22.33</i>	-	-	-	<i>257.33</i>	-	<i>403</i>
Yellow	<i>13529</i>	<i>167.33</i>	-	-	-	<i>206</i>	-	-
Pink	<i>10320.33</i>	<i>44</i>	-	-	-	<i>782</i>	-	-
Red	<i>2773.67</i>	<i>63</i>	-	<i>488.67</i>	-	-	-	<i>797.67</i>
Backgr	<i>84</i>	-	<i>1278</i>	<i>814</i>	<i>73</i>	-	-	-

The comparison of the different color suggest the followed pigments:

- White: lithopone (Z, Ba, S), White zinc oxide (Zn), White lead (Pb), Gypsum (Ca,S) or Barium Sulfate (Ba, S);
- Brown: Sienna Earth (Fe, Mn), Sienna Earth Burnt (Fe), Burnt Green Earth (Fe, Mn, K, Al), Brown Iron Oxide (Fe), Brown Mars black (Fe), Prussian Blrown (Fe) or Cassel Earth (Fe);
- Blue: Prussian Blue (Fe), Manganese Blue (Ba, Mn) or Ultramarine blue (Na, Al, Si, S);
- Green: Chromium Green Opaque or Viridian (Cr), Lamoriniere Green (Cr), Scheele green (Cu) or Verdigris (Cu);
- Yellow: Barium yellow (Ba, Cr), Chrome yellow (Pb, Cr), Strontium yellow (Sr, Cr), Cadmium yellow (Cd, Zn), Sienna earth (Fe, Mn), yellow ochre (Fe) or lead yellow (massicot or litharge)
- Red: Cadmium Red (Cd, S, Se), Red Ochre (Fe), Chrome red (Pb, Cr), Mars red (Fe), Vermilion (Hg, S) or lead red (minium).

If we consider the results obtained on ground layer, it is possible hypothesize that the preparation could be composed by calcium carbonate and white lead mixed to red ochre; the latter could be refer to the previous layer, that was removed before painting the canvas with this new subject.

White pigment

The analysis on white color were carried out on samples taken from white little brushstroke on the right border of the painting. Under microscope, the sample shows both white pigment and brown shades with colored particles (red and black), around 2.5 μm wide. An organic varnish covers the pictorial film.

Back side white sample reveals that, under white coat, there is a green-brown preparatory layer with yellow and red small particles; but, the impossibility to carry out analysis on the cross section of fragments cannot help to better identify the interlayer relationship.

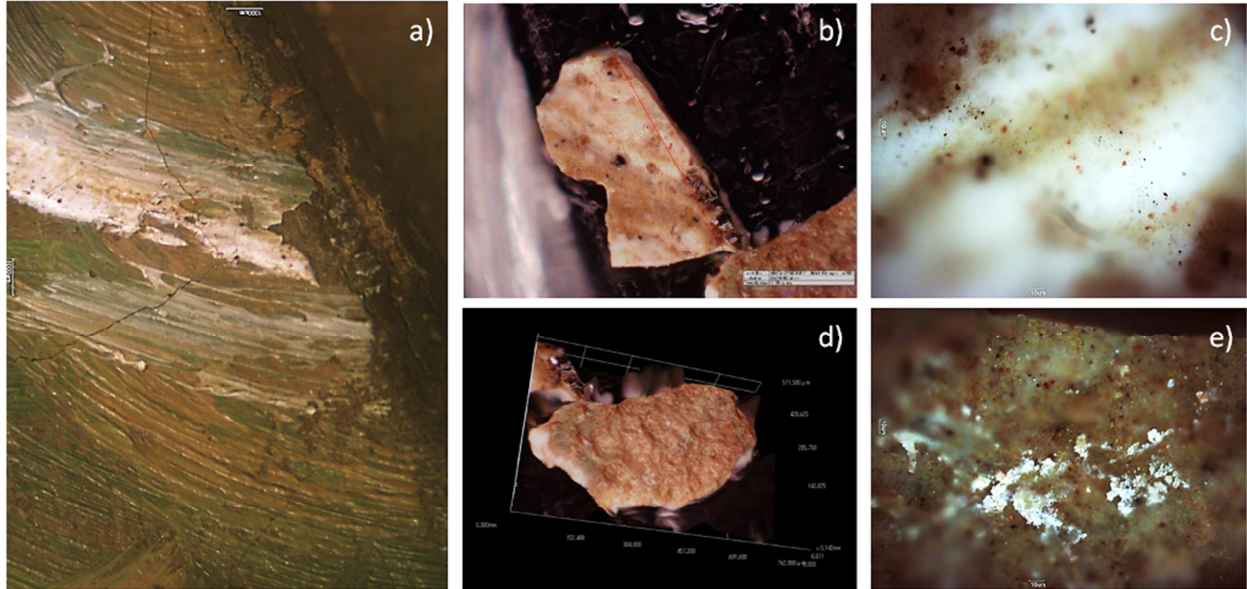


FIG. 121 Investigation under microscope: a) sampling area for white color (magnification 10x). Source: Ferrara University.; b) d) microphotograph of white sample and 3D model of backside (magnification x 20); c) e) microphotograph respectively of white sample and backside (magnification 90x).

Considering the chemical composition of the background (carbon tape – aluminum stub) for a better data interpretation, EDXRF analysis on samples confirms previous hypotheses about white pigment: high signal of zinc, lead, suggest respectively White zinc oxide, Lead white for white color. The detection of calcium and titanium do not permit to exclude calcium carbonate and white titanium dioxide (Montagna G., 1999; Seccaroni C. *et al.*, 2002; Eastaugh N. *et al.*, 2008). The comparison between the recto of white sample and the backside of the same sample confirms the use of white zinc oxide for the white color, probably mixed to white lead and white titanium dioxide (unless lead is not contained in the varnish and medium as accelerator drying process). Under the white color, there is a layer, likely a preparatory layer characterized by calcium carbonate and brown earth (Si, Al, Mn, Fe, etc.) (Montagna G., 1999; Seccaroni C. *et al.*, 2002; Eastaugh N. *et al.*, 2008).

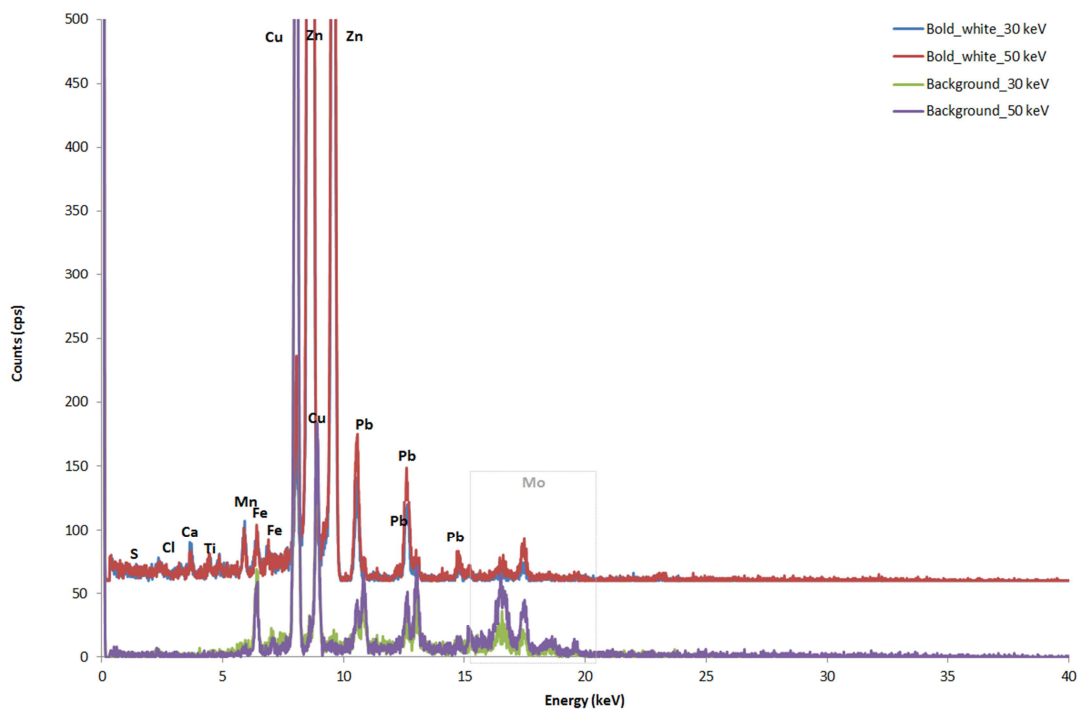


FIG. 122 EDXRF spectra on White pigment: total spectra from different set-up, not subtracting background. Experimental set up: voltage 50 KeV and current 700 μ A, voltage 30 KeV and current 1300 μ A. Live time: 60 s, no filter, Helium flow, Anode Molybdenum, collimator 0.200

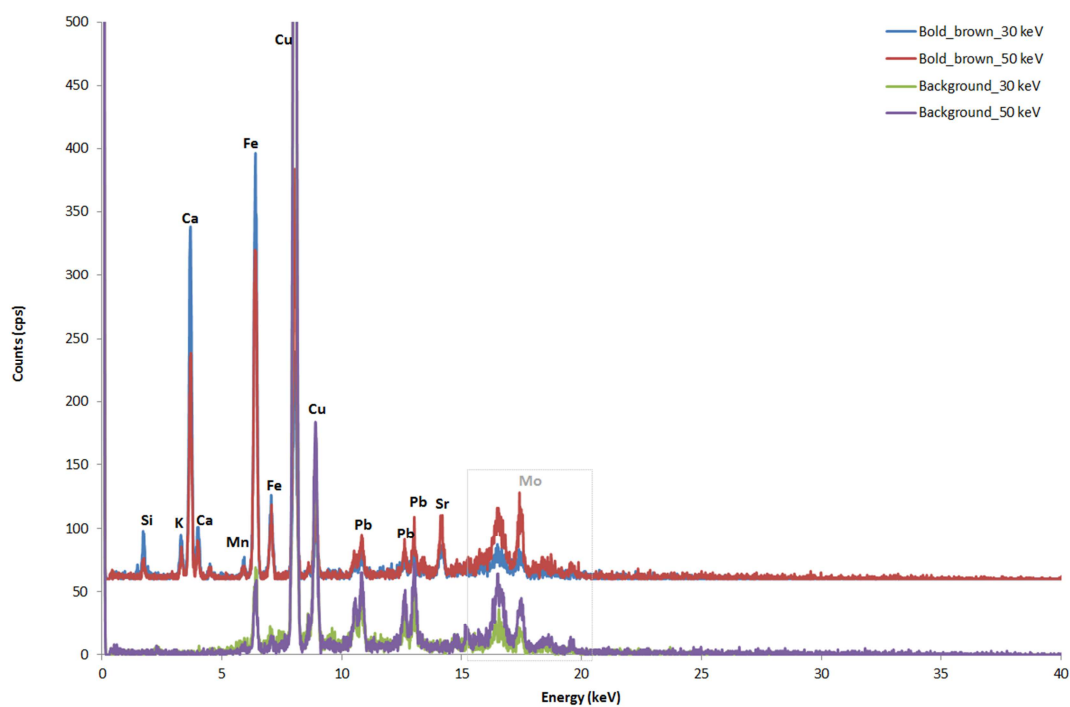


FIG. 123 EDXRF spectra on the backside of White sample: total spectra from different set-up, not subtracting background. Experimental set up: voltage 50 KeV and current 700 μ A, voltage 30 KeV and current 1300 μ A. Live time: 60 s, no filter, Helium flow, Anode Molybdenum, collimator 0.200.

PIXE analysis reinforce the hypothesis about the presence of white zinc oxide mixed with white lead and calcium carbonate or calcium sulfate. Titanium is also detected but it is not one of the main component for the white color. Moreover, other chemical particular element such as strontium, cadmium, chromium and were identified and, they are probably linked to other color particles, well recognizable under microscope. Similar composition was obtained for the backside of sample, but in this case the enhancement of lead and calcium concentration allowed to suppose that the green-brown under-painting layer is mainly composed by calcium carbonate or calcium sulfate and white lead.

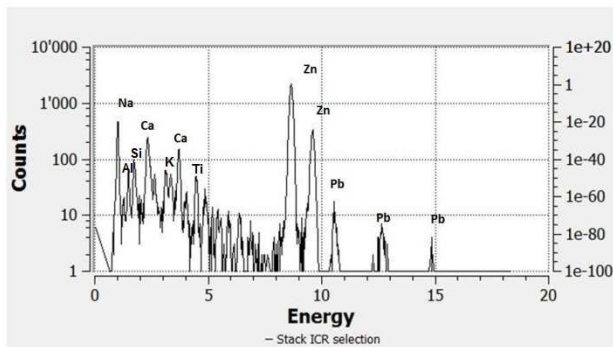


FIG. 124 PIXE spectra of white pigment, low energy detector.

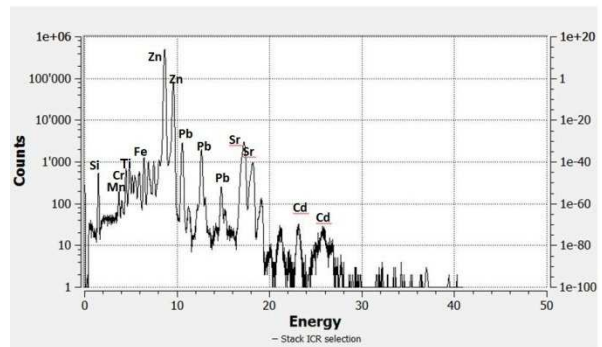


FIG. 125 PIXE spectra of white pigment, high energy detector.

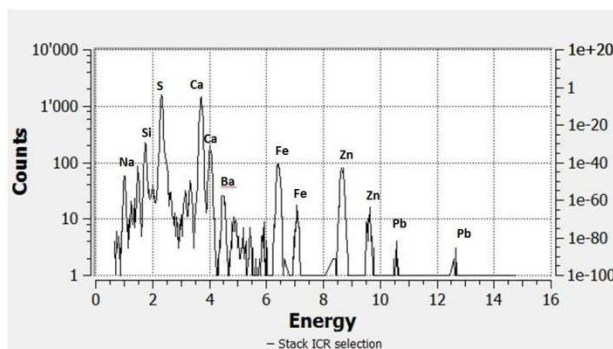


FIG. 126 PIXE spectra of white behind, low energy detector.

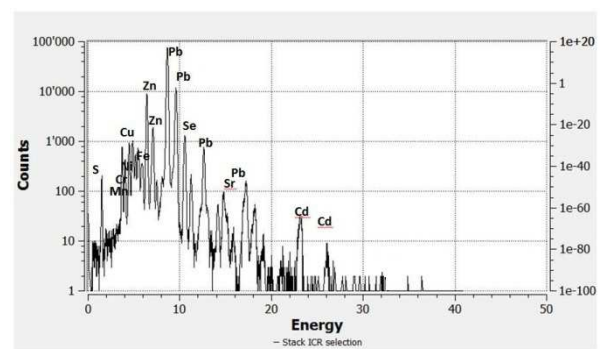


FIG. 127 PIXE spectra of white behind, high energy detector.

TABLE 10 PIXE analysis on Boldini samples. Average value: region of interest were extracted using PyMCA software, data expressed in counts. Experimental set up: particle/energy 3 MeV, current p+, Dose/s 200, Helium flow.

Low Energy										
	Mg	Al	Si	P	S	Cl	K	Ca	Fe	Zn
Red	7312	18270	36840	3768	82335	15439	7324	75095	22127	89571
White	9304	61302	159827	3862	44279	4173	20466	109198	30854	8931
White behind	-	14043	25658	3978	41598	4063	5219	171441	33174	47332

High Energy										
	Mg	Al	Si	P	S	Cl	K	Ca	Fe	Zn
Red	-	-	-	-	<i>1310000000</i>	-	40007	119691	26146	54571
White	-	-	-	-	-	12021984	82705	266177	67853	7431
White behind	-	-	-	-	<i>724406720</i>	-	5982	304833	39145	7332

Low Energy											
	Ba	Hg	Pb	Ti	Cr	Mn	Ni	Cu	Se	Sr	Cd
Red	108821	168663	127880	-	-	-	-	-	-	-	-
White	93546	-	12703	-	-	-	-	-	-	-	-
White behind	34362	<i>28131</i>	21197	-	-	-	-	-	-	-	-

High Energy											
	Ba	Hg	Pb	Ti	Cr	Mn	Ni	Cu	Se	Sr	Cd
Red	129722	146656	102286	10194	888	2180	306	929	-	-	8688
White	124355	-	10488	4345	791	2199	100	542	-	1369	21323
White behind	46299	30023	14709	-	2768	1513	268	226	920	994	13764

SEM/EDS analysis revealed aggregate of fine grained particles of 1 μm or less, with irregular shape; the chemical composition of these fine grains is characterized by zinc, supporting the hypothesis of White zinc pigment (Eastaugh N. et al., 2008; Montagna G., 1999). Moreover, the analysis revealed other chemical element, attributable to different pigment particle, such es. Cadmium red grains or to a white pigment aggregate, such as White Barium sulfate (FIG. 128).

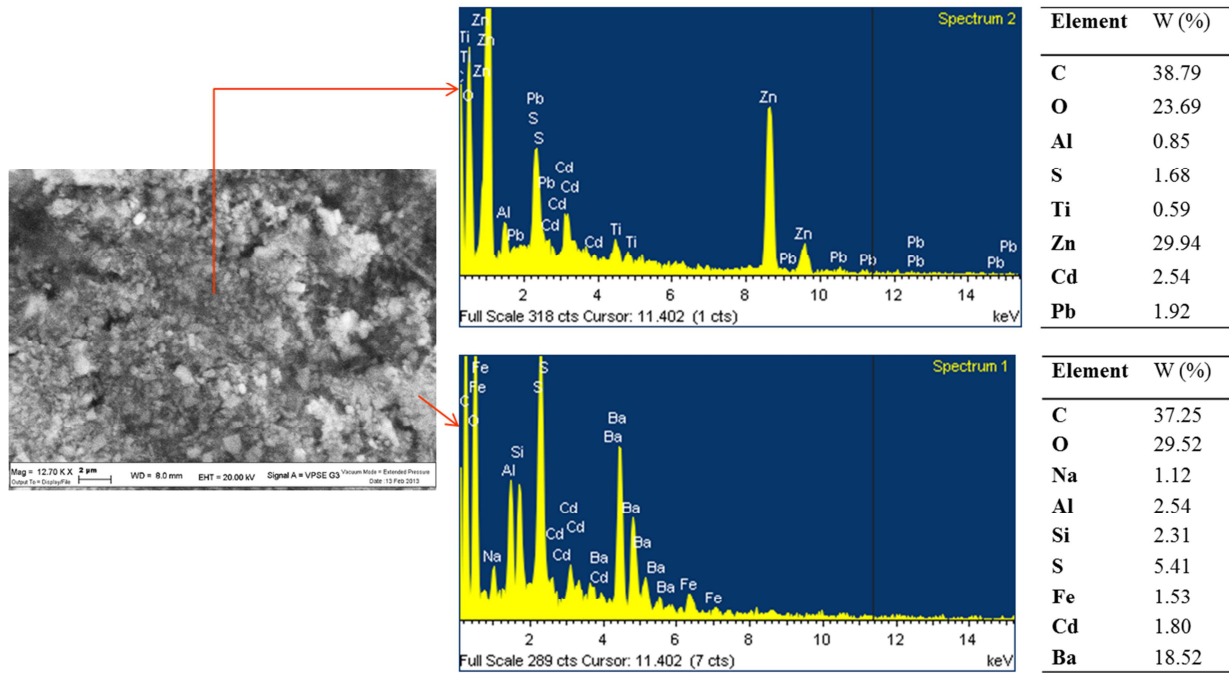


FIG. 128 SEM/EDS analysis on white sample: spectrum 1, aggregate of White Zinc oxide; spectrum 2, aggregate enriched in White Barium sulfate pigment.

Analysis on the backside of white sample detected the presence of calcium carbonate or calcium sulfate, mixed with brown pigment enriched in iron and potassium, confirming the use of this pigment in the preparatory layer (Eastaugh N. et al., 2008; Montagna G., 1999).

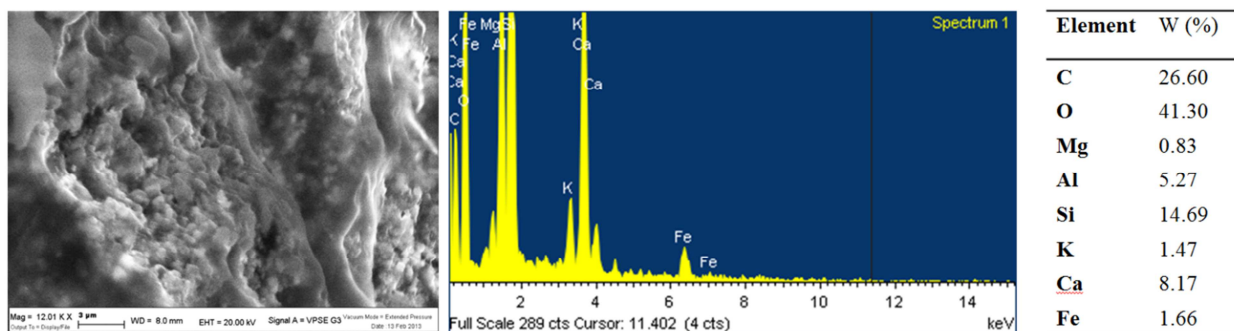


FIG. 129 SEM/EDS analysis on the backside of investigated white sample.

Unfortunately, the Raman analysis, tested both on the painting (white colored area) and on the white sample, do not allowed to better identify the pigment compound.

The high fluorescence of organic varnish or binder hides Raman bands useful for the characterization of pigments, not allowing identification of any pictorial component except Barium Sulphate' s peak at 984 cm^{-1} (vs) (Bell I.M. *et al.*, 1997; Jehlička J. *et al.*, 2009; 28; 30).

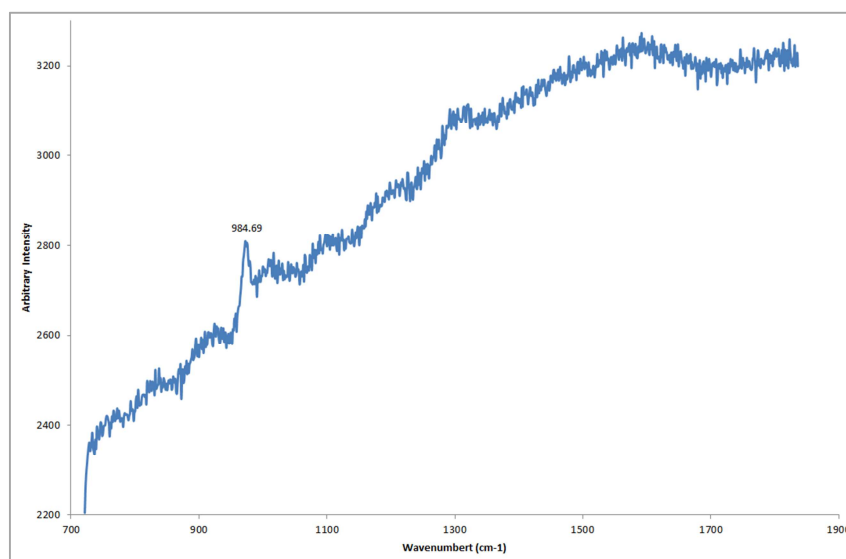


FIG. 130 Raman spectra on white sample (632,81 nm excitation, 2 mW, 50 s acquisition time): High fluorescence, Barium Sulphate peak at 984 cm^{-1} .

In conclusion pigment analysis suggest the use of White zinc oxide for the white color and a compound based on calcium carbonate or calcium sulfate and white lead, mixed with barium sulfate; the green brown pigment, detected on the backside of sample suggest the presence of brown-green earth, used for the layer under the white brushstroke.

Red pigment

X-Ray radiography suggested the possibility that artist used a canvas, in which previous preparatory layer was removed, red samples were collected in correspondence of the border, in the lower part of the painting. Under microscope, it is possible to observe several red grain with different nuance, mixed with some white particles.

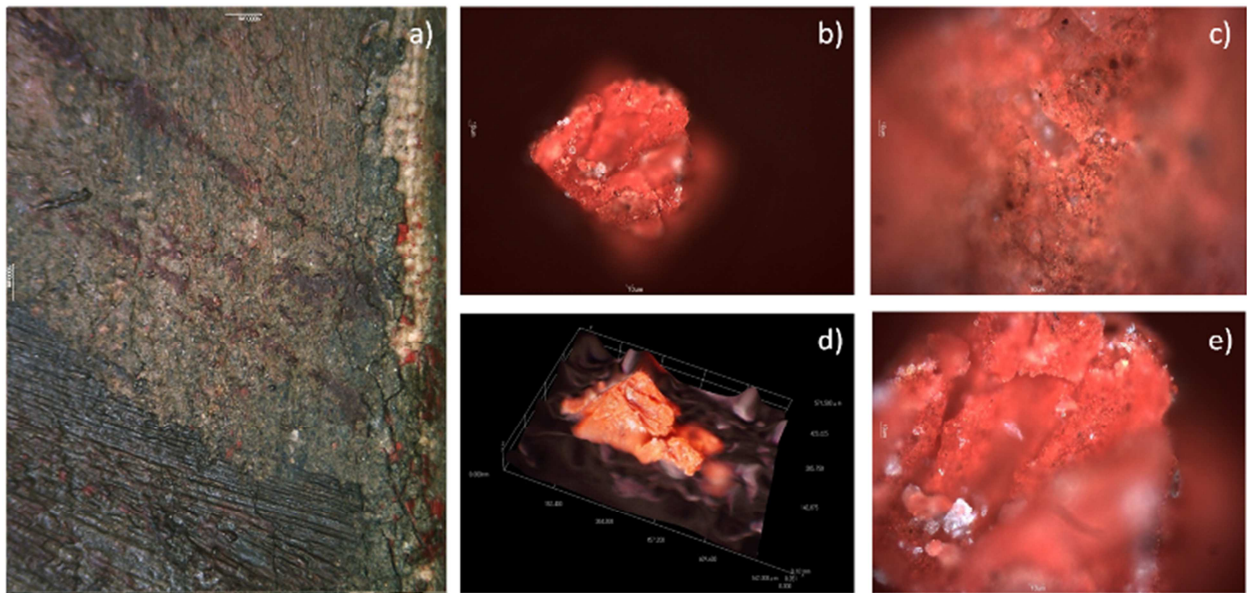


FIG. 131 Investigation under microscope: a) sampling area for red color (magnification 10x); b) microphotograph of red sample (magnification 20x); c) e) microphotograph of red sample (magnification 90x); d) 3D model of red sample (magnification x 20).

EDXRF examination of samples revealed high peaks of Lead and Mercury, suggesting different pigments like Massicot and/or Vermilion (artificial Cinnabar), used in the inner part of painting. Moreover, XRF spectra do not allow to exclude also pigment based on cadmium, chrome and iron, such as Cadmium Red, Red Ochre, Chrome red (Pb, Cr) and Mars red. Barium and titanium peaks are probably linked to white particles, observed also under microscope.

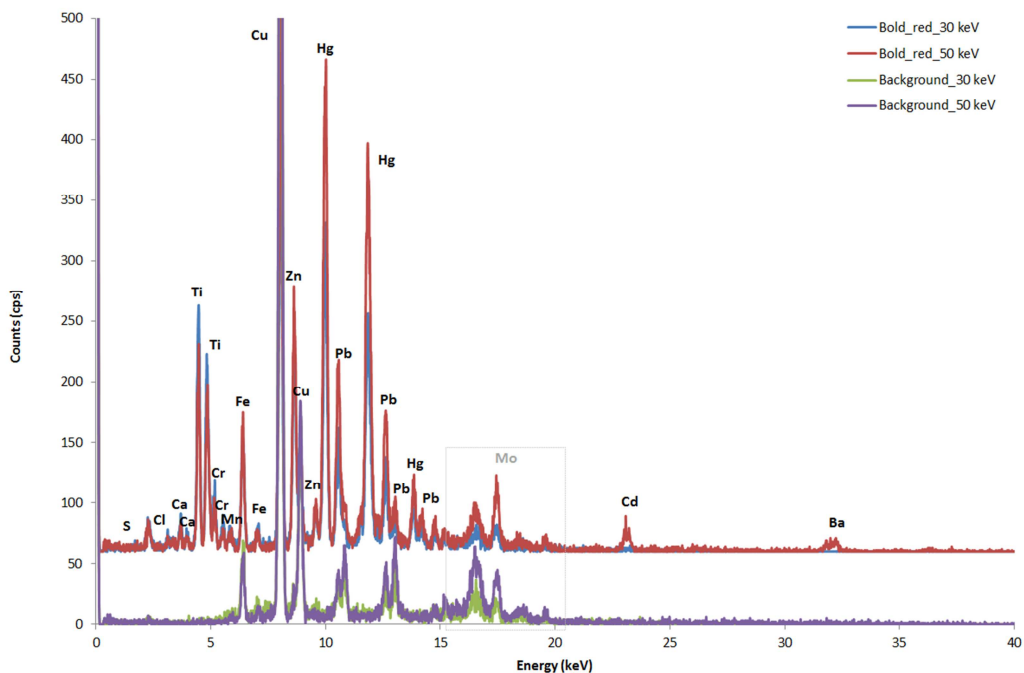


FIG. 132 XRF spectra on red sample: total spectra from different set-up, not subtracting background. Experimental set up: voltage 50 KeV and current 700 μ A, voltage 30 KeV and current 1300 μ A. Live time: 60 s, no filter, Helium flow, Anode Molybdenum, collimator 0.200 μ m.

In addition to confirm the previous composition, PIXE analysis reveals also the presence sodium, aluminum, potassium, probably linked to a contamination by other pigment, environmental pollution or to chemical agents added by manufactories for the production of this pigments (TABLE n.2). The presence of strontium could be attributable to white pigment particles based on calcium.

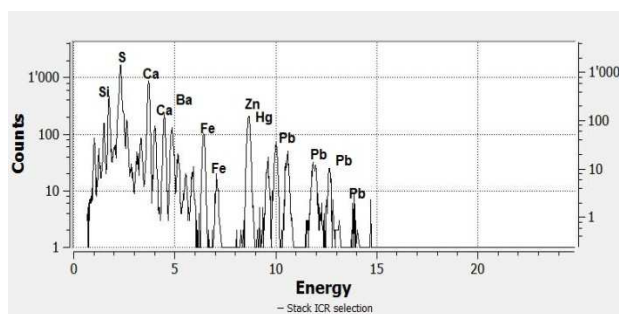


FIG. 133 PIXE spectra of red pigment, high energy detector.

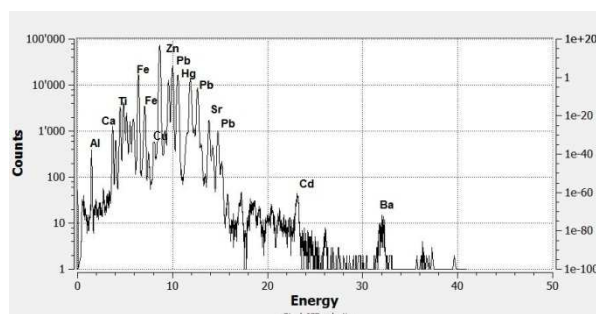


FIG. 134 PIXE spectra of red pigment, high energy detector.

SEM/EDS analysis revealed large aggregate constituted by fine-grained particles with spherical appearance. Particle size is 1 μm or less and with an even distribution; the chemical composition of these fine grains is characterized by sulfur and mercury, supporting the hypothesis of the Vermilion, the synthetic analogue of cinnabar (Eastaugh N. et al., 2004^B; Montagna G., 1999). Other detected chemical elements, such as sulfur, barium and calcium are probably attributable to white colored particles; meanwhile lead peak can refer to red lead pigments (Eastaugh N. et al., 2008).

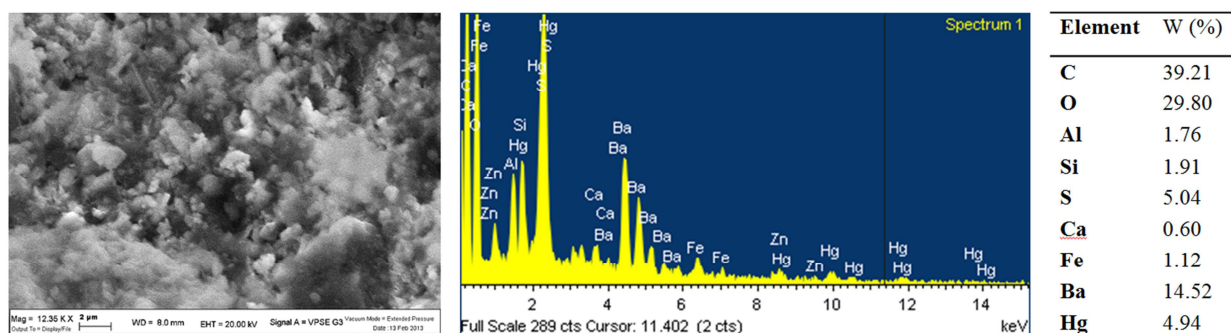


FIG. 135 SEM/EDS analysis on red sample.

Finally, Raman spectra confirms the presence of Litharge, which characteristics Raman bands at 145 cm^{-1} (vs), 258 cm^{-1} (vw), 336 cm^{-1} (w) (Bell I.M. *et al.*, 1997; Smith G.D. *et al.*, 2004; 28; 30), and of Vermilion with peaks at 252 cm^{-1} (vs), 282 cm^{-1} (w-sh), 343 cm^{-1} (m) (Bell I.M. *et al.*, 1997; Edwards H.G.M., 1999; 28; 30).

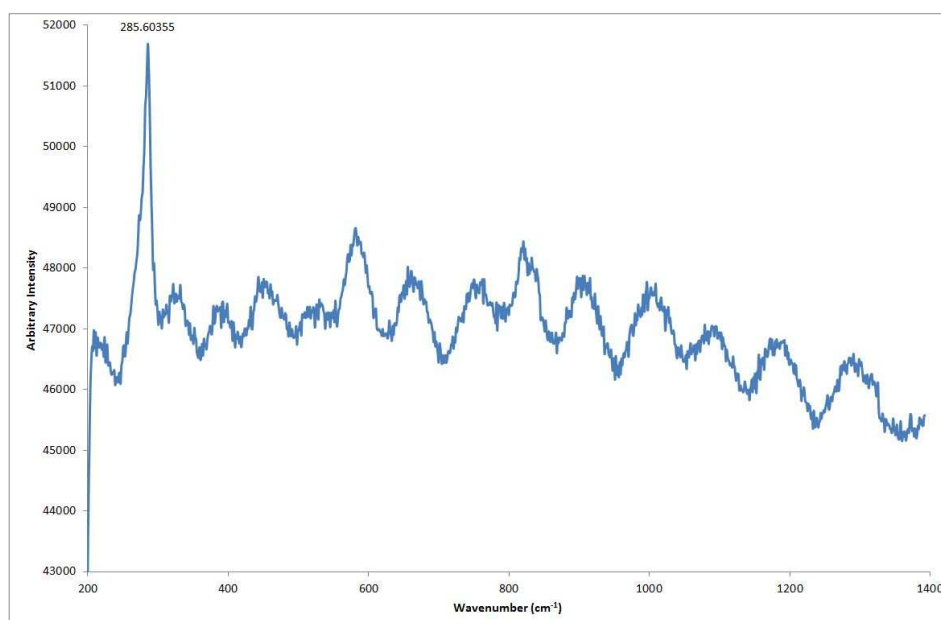


FIG. 136 Raman spectra on red sample (632,81 nm excitation, 2 mW, 50 s acquisition time):Litharge. Source: Ferrara University.

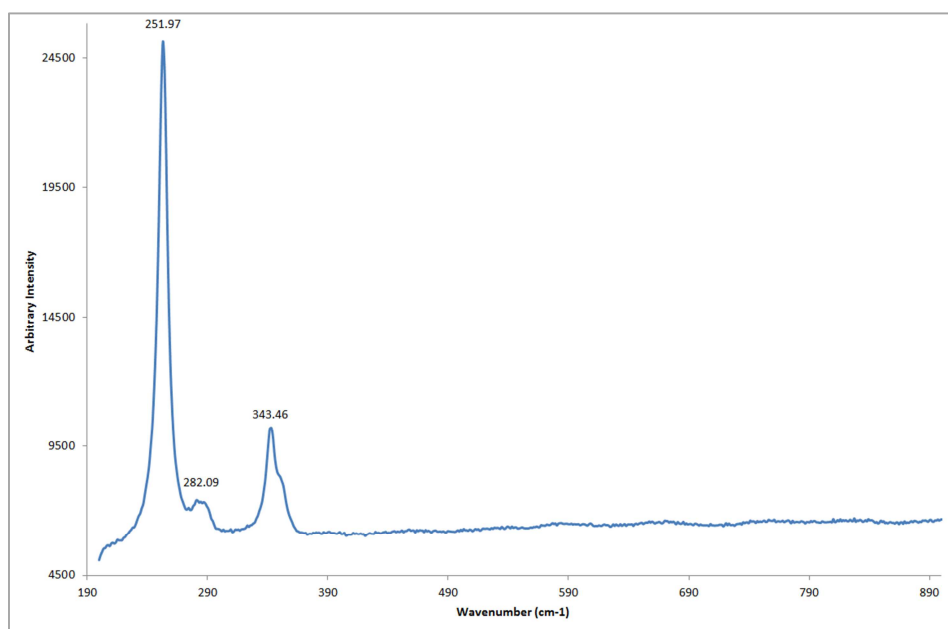


FIG. 137 Raman spectra on other particle in red sample (632,81 nm excitation, 2 mW, 50 s acquisition time): Vermilion. Source: Ferrara University.

5.5.4.2 Support and fibers

Painting stretcher is made by four different wooden plank with different tick between 0.8 and 0.9 cm, linked together through perpendicular wooden joint (FIG. ..). This kind of methods allows to connect wooden boards that have “T” or “L” shape like in this painting. The four joint, then, are fixed using iron nails without head, toed towards wooden board.



FIG. 138 Schema of possible “L” joint in studied painting.

This typology of painting stretcher are easy to construct but they are not extensible (useful characteristic for restoration act)

and, as time goes by, they could bring degradation problems. Studies carried out under microscope, but better X-ray examinations, reveal that the wooden planks have a quite number of internal tunnel made by xilofagi grubs: some of these tunnels, spilling out from wooden surface, indicate a planks’ treatment, like shaving actions very common among restoration, before their use in this painting stretcher.

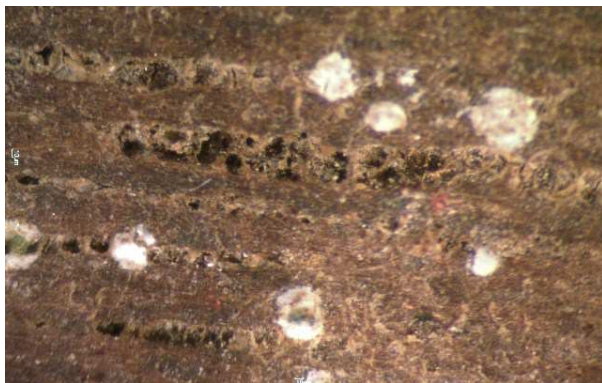


FIG. 139 Photomicrograph of an insect grub on wooden plank (visible illumination, original magnification x 20).



FIG. 140 X ray examination of wooden plank (inverted grey scale color): white for light chemical elements or reduction in the density of material; black for heavy elements.

Canvas was made by two series’ thread, twisted in a perpendicular way. In FIG. .. is well shown the framework, called “*armature a tela*”, in which ratio texture (horizontal threads)/warp (vertical threads) is 1:1 (Perusini G., 2004; Scicolone G.C., 2004).

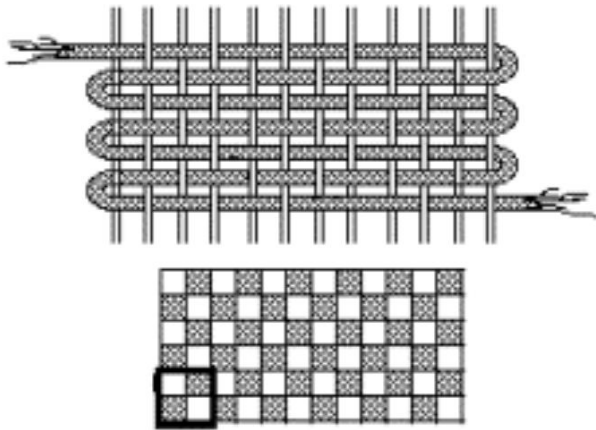


FIG. 141 Schema of “armatura a tela” (canvas framework): texture (horizontal threads) and warp (vertical threads) [39].



FIG. 142 Photomicrograph of canvas framework in studied painting (visible illumination, original magnification x 40).

Observing under microscope, a specimen of canvas taken from a border and degraded side of the painting, it is possible recognize cotton thread with their characteristics shape: flat long thread and irregular spiral twisting (FIG. 143) due to solar exposure (Perusini G., 2004; Scicolone G.C., 2004). The particular birefringence is due to cellulose in cellular lining (about 83-88/93%). The use of cotton in textile is dated back 18th century and so it is compatible with the proposal making period of the analyzed painting.

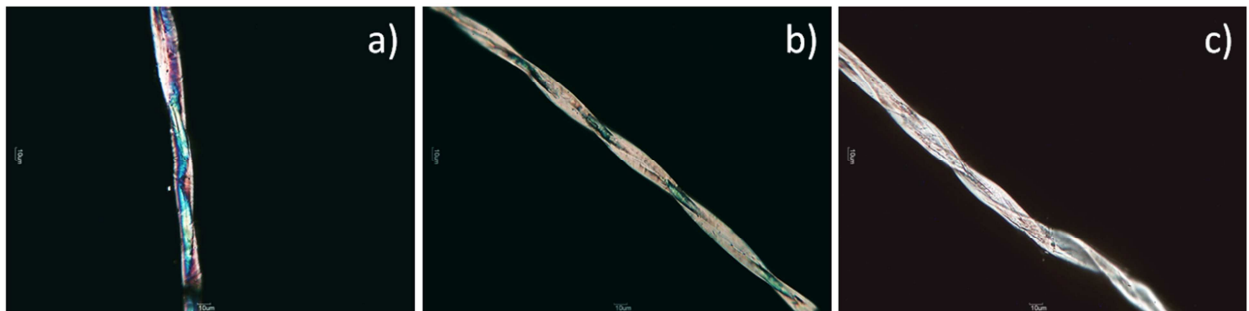


FIG. 143 Cotton fibers taken from analyzed samples: a)b)c) microphotographs by optical polarized microscope (polarized transmitted illumination, magnification 40x).

3.1.5 Conclusion

Even if, in this case, the chemical composition of retrieved pigments do not support authentication and dating of studied painting, it was possible to verify that all the microscopic features and characteristics, that belong to the painting, are useful as “art-fingerprint” and so they could be used in assurance field.

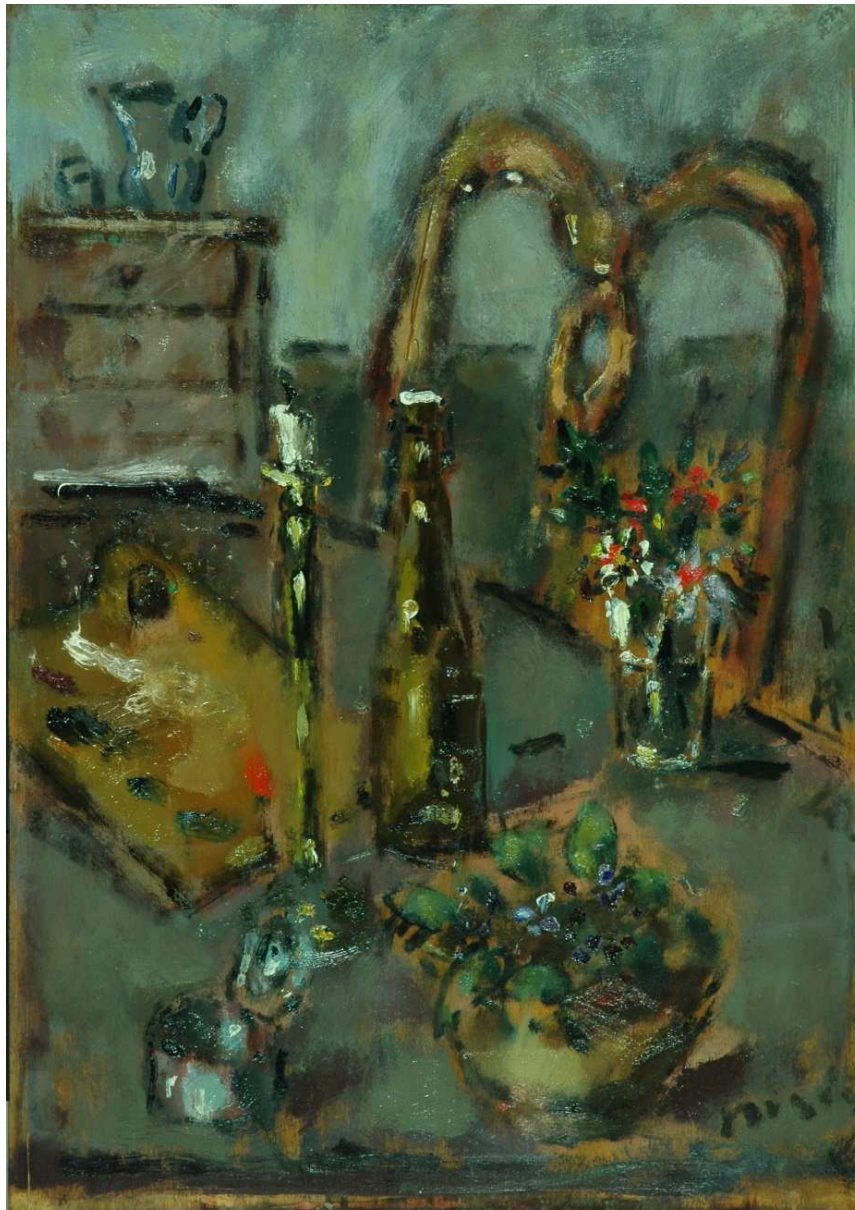
The presence, in fact, of some pigments, like Cadmium Red, being entered in commerce since 1910 and possible lithopone (since 1877), mixture of barium sulfate and zinc oxide pigment,

does not permit to try particular conclusion. In addition, it was not quite strange to find also lead pigments, that were banned in Europe since the first years of 20th century, if we consider that in Italy the law disposition is dated back to second half of 20th century.

However, the characterization of used pigments gives useful information for maintenance and restoration actions: Cadmium and Lead, referred respectively to a probable Red Cadmium and Red/White Lead pigments, suggest to be careful during the cleaning of painting if it will be used some acid like sulfuric (cause Cadmium dissolution) and nitric acid (Lead dissolution).

Finally, the image processing and the proposal could be interesting to improve the interpretation of data obtained by previous analysis, supporting a correct studying of the painting from all the points of view.

ARTWORK PLATE V



Author: *Filippo De Pisis (Italian artist, 1896-1956)*

Title: *Fiori (Flowers)*

Object: *Painting (oil on wood panel)*

Date: *unknown date*

Overall: *70 cm (height) * 50cm (width)*

Location: *Private Collection*

Note: *artwork accompanied by expertise; study of Artist attribution and dating in progress*

5.5 “Flowers” by Filippo De Pisis (oil on wood panel, unknown date)

Size: 70.01 cm (height) * 50.00 cm (width)

The painting named as “Flowers” by its owners belongs to private collection since the end of 20th century, when it was acquired in antique store. Since that date, the painting was not subjected to restoration intervention, except after a little blaze at the end of 20th century/beginnings of 21st century: the restoration act was interested only to remove the thin black layer that covered the entire painting.

This artwork is accompanied by an handwritten expertize with a stamp “GC”³¹: in the backside of a black and white photograph of paintings, the test with the description of the artworks is signed by Giovanni Commisso³² and dated September 13th, 1963; unfortunately there are not information about the achievement’s date of paintings.

The identification of pigments used by artist and in-depth studies about artistic techniques at microscopic level, carried out on this painting, will support the studies of artist authentication and dating presently in progress. The precise spatial coordinates of all point analysis collected for this artwork are kept thanks to informatics database; nevertheless they are not inserted in this manuscript for previous agreement with owners about these confidential data.

5.5.1 The artist

Luigi Filippo Tibertelli, known as Filippo De Pisis, was born in 1896 in Ferrara where, since his childhood, he had shown interest for art and poetry. After the passion for literature, in 1919/1920 he moved to Rome and Venice accepting roles of teacher meanwhile his artworks had been successfully appreciated and art-gallery started to exhibit his creations. Numerous travel to Paris and to Milan allowed him to meet artists and discover new techniques and artistic trends that influenced his personal style. In spite his success, he encountered a lots of difficulties due for his homosexuality (aggression, etc.). In 1943 he moved from Milan to Venice, where he established after that Milan was under bombardment and his artistic production continued to increase and with it his celebrity. After living an extravagant lifestyle, at the end of 1949 his illness obligated him

³¹ G.C. probably refers to Giovanni Commisso.

³² Giovanni Commisso (1895-1969), Italian writer, was friend and art critic of Filippo De Pisis. After being news correspondent of important newspapers, after the 2nd World War, it devoted him to the narrative production. Among his works, it is possible to remember "Mio sodalizio con De Pisis", a book of memories of his important friendship with the painter. For in depth information: Commisso G. 1954.

Even if he was a friend of Filippo De Pisis, some historical reference reports that, in the last part of De Pisis life (when he was at Villa Fiorita, Brugherio – Milan, Italy), Giovanni Commisso was under suspicion to require signature and authentication on artworks of uncertain origin, considering also that De Pisis artworks are among the most counterfeited easel paintings of 20th century (Marsiglia L. *et al.*, 1996).

to remain in several hospital, such as Villa Fiorita (Brugherio, Milan – Italy), where slowly demoralized until his death in Milan in 1956 (Ferrari C.G., 2000; Salvagnini S., 2006).

5.5.2 The painting: subject

Several *Catalogues Raisonnés*, concerning De Pisis' works, show an exhaustive catalogue of artworks in which flowers, vases and bottles were painted, especially for the artistic production between 1940s and 1950s. The technique, reported for these paintings, changed from oil on canvas or paper to oil on panel wood (Brigante G., 1991).

The artist painted different objects placed on a table (flowers pots, bottle, single candleholder with a wax candle burnt down, metallic box and a book); backward it a chair back, a furniture with a water pitcher and a glass have emerged from the light blue background of the wall (FIG.144). On the left bottom, there is the signature “Pisis”.

In the picture scene flowers are predominant. The passion of De Pisis for nature, flowers and plant dated since he was young, when teenager he collected several specimens of plants, flowers, insect, etc. gathering together in a “herbal book” that gave in 1927, after followed humanistic career (Commisso G., 1954).

5.5.3 Experimental methods

Initially, multispectral imaging analysis (VIS, UV, IR), stereomicroscope investigation and image processing were carried out in support to choose regions of interest that, subsequently, were deepened with EDXRF analysis on the whole painting (Fig...). However, considering that artistic technique consists in a very complex mixing of pigments to create particular colored effects, for a more detailed study of the paint materials, fourteen micro-samples amount of painted materials (maximum size: 1,5 mm²) were taken from convenient areas (rich in matter, where needle did not have resistance and so without damaging the picture further) with a sterilized point of needle and under microscope (FIG. 145).



FIG. 144 Flowers: locations sampled for pigment mapping by the XRF technique are depicted by numbers.



FIG. 145 Flowers: sampling point are indicated with “C-numbers”.

To preserve samples for future other analysis, they were not embedded in resin and they are previously observed with optical microscope. For their irregular and particular morphology (FIG. 3e 4) XRF, PIXE and SEM/EDS analysis were carried out on samples to detect chemical composition of pigments and μ Raman spectroscopy were performed for a better identifying pigment analysis.

5.5.4 Results and discussion

5.5.4.1 Artistic technique and conservative conditions

The technique used by the artist is oil on commercially plywood, confirming what is written in the expertize and it seems that there is not a preparatory pictorial layer: the color was spread directly on the surface and there are some part in relief (FIG. 146-147). As well pointed out by GL investigations, the painting reveals brushstrokes enriched in matter and other part of painting in which the pigment was accurate spread onto the wooden panel. Like in other artworks made by De Pisis, also in this painting the words, written by his friend writer Giuseppe Raimondi, are respected: “*si espandono le pennellate a furia, larghe, non grasse di colore, intense nella materia, scorrevoli, asciutte e solo a tratti raggrumate in una sosta più densa, come i nodi in una canna di bambù*” [27] (“*the brushworks are spread in raging way; they are wide, with not so much color, dense in matter, flowing, dry and only in some parte they become lumpy and the lines are clotted in a denser standstill as the knots in a bamboo reed*”).



FIG. 146 GL photograph: detailed of spread and in relief paint.



FIG. 147 Studied painting: detailed of in relief paint.

Even if the stiff wooden support shows arching in the middle horizontal part of the panel, the visual examination of the painting highlights good conservative condition: the pictorial layer does not have lack and the wide *craquelures* network is not widespread on the whole painting but there are only few deep *craquelures* in pictorial part enriched in matter, probably linked to drying medium process.

Comparing FIG. 148 a and FIG.148 c, it is possible to observe that final coating varnish was not spread on the painting: specular reflection survey, in fact, revealed that reflectance is in correspondence of pictorial layer differently from the opaque background due to non-treated wood FIG. 148c.

Moreover, in UVF image (FIG. 148b) , the absence of different color fluorescence does not make possible the recognition of retouches; this allowed to think that the entire composition, included signature, was made in the same period. Finally, IRR image (FIG. 148d) does not reveal under-drawing, but it allows to observe two diagonal sign on the table, maybe used as guide to draw; this two lines could be made with graphite pencil or material with organic composition, seeing that it does not disappear under Infrared investigation.

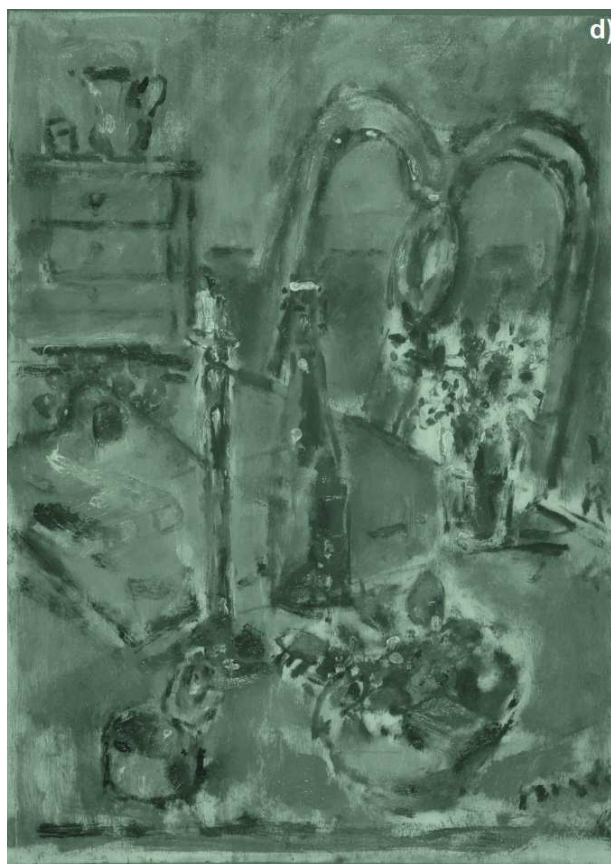
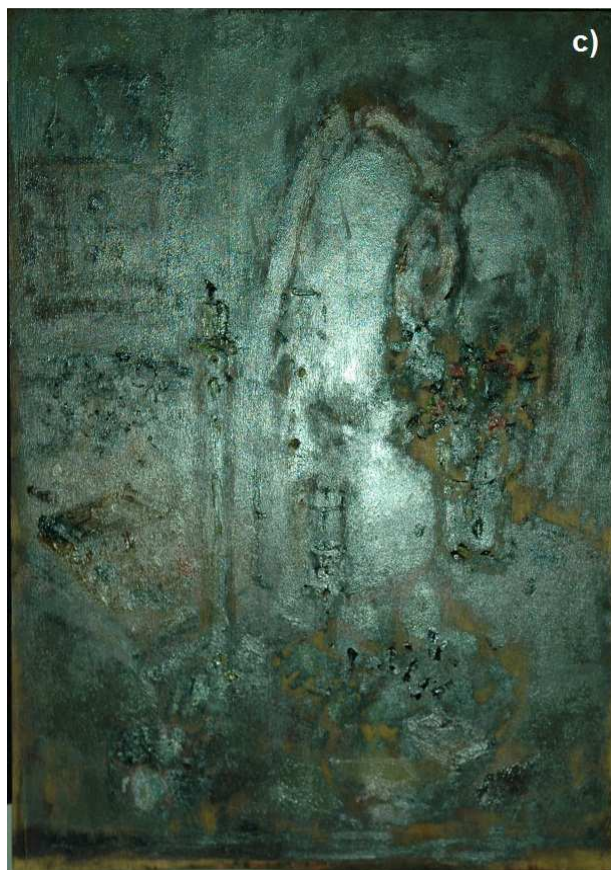


FIG. 148 "Flowers in glass vase": "": a) VIS photograph; b) Specular reflection photograph; c) UV-VIS photograph; d) IR photograph.

In addition to confirms the artistic techniques described in the expertise and previously observed by multispectral imaging, the study of the painting under stereomicroscope revealed a lots of interesting microscopic details, giving more information about employed painting technique, conservative condition, etc.

Several chromatic effects, in fact, were obtained by using different colored blends: the one shade color pigments/medium compound was not mixed with other colored compounds before being spread on the support but the mixing had happened during the artistic achievement. In fact, it is possible to observe that in the painting zones, in which there is a mix of colors, pigment particles are oriented according to one shade color overlapped brushstrokes (FIG. 150).

Moreover, a deepened samples' investigation under microscope confirmed the speed of artistic brushstrokes that caused little empty hole within brushstroke itself (FIG. 149)

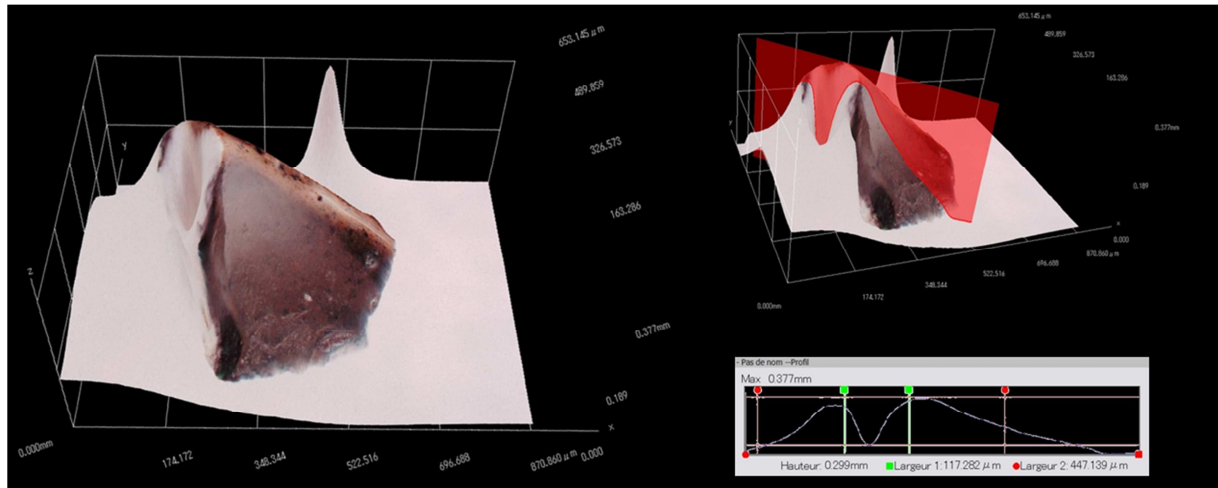


FIG. 149 3D acquisition of a sample taken from “Flowers” by F. De Pisis: empty hole within brushstroke, about 100 μm (h) and 120 μm (w).

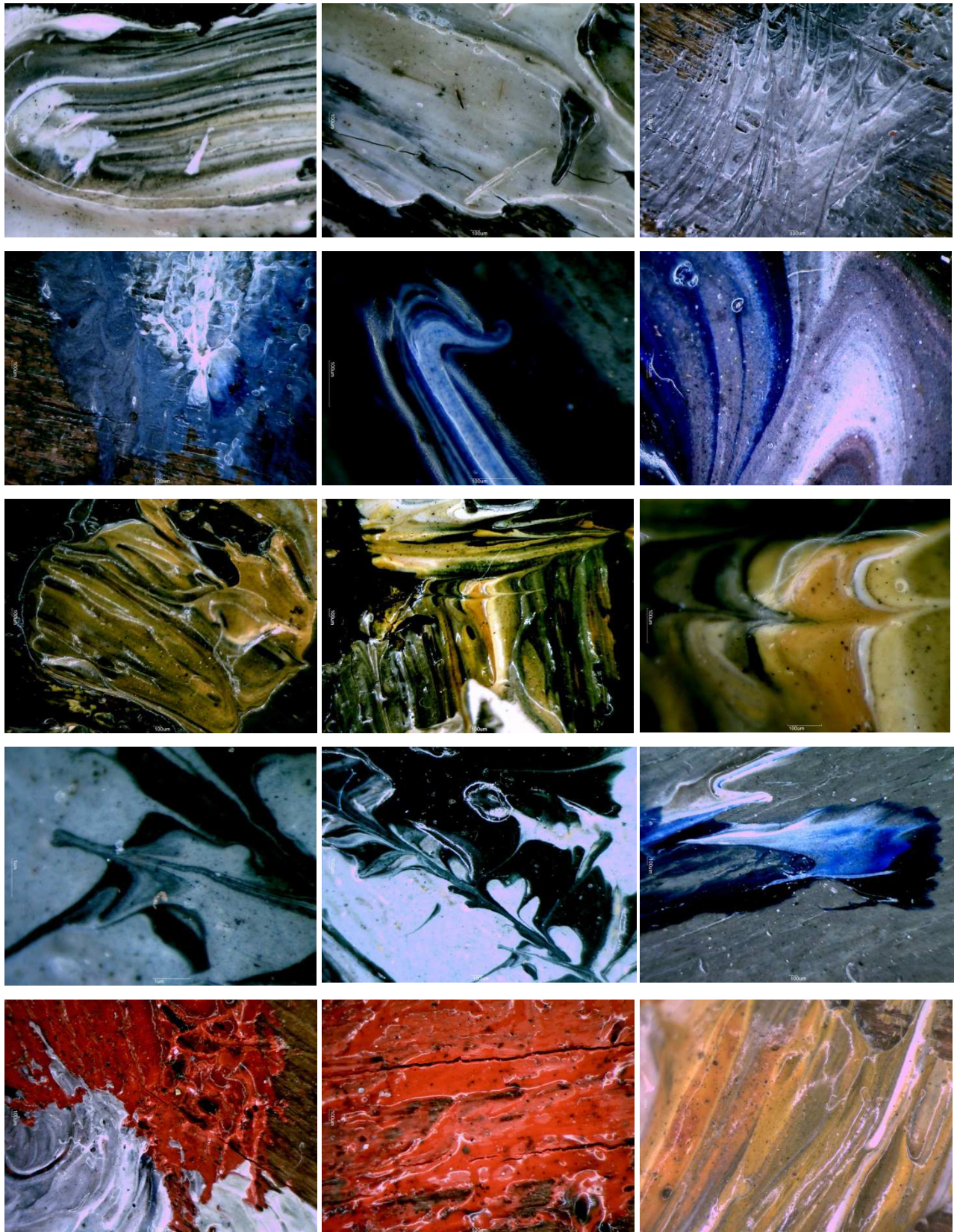


FIG. 150 Morphological ArtFingerprints: microphotograph of “Flowers” under stereomicroscope (different magnification).

As concern, instead, conservative conditions, the investigation of surface at microscopic level revealed that, in addition to those craquelures that are also naked eye visible, there is a networks made by very thin μ -craquelures, wide about from 5-10 μm to 20 μm (FIG.). Even if the artworks was subjected to a cleaning restoration action, it was possible to recognize the black soot particles, homogeneously spread under the pictorial layer in a random way (FIG.).

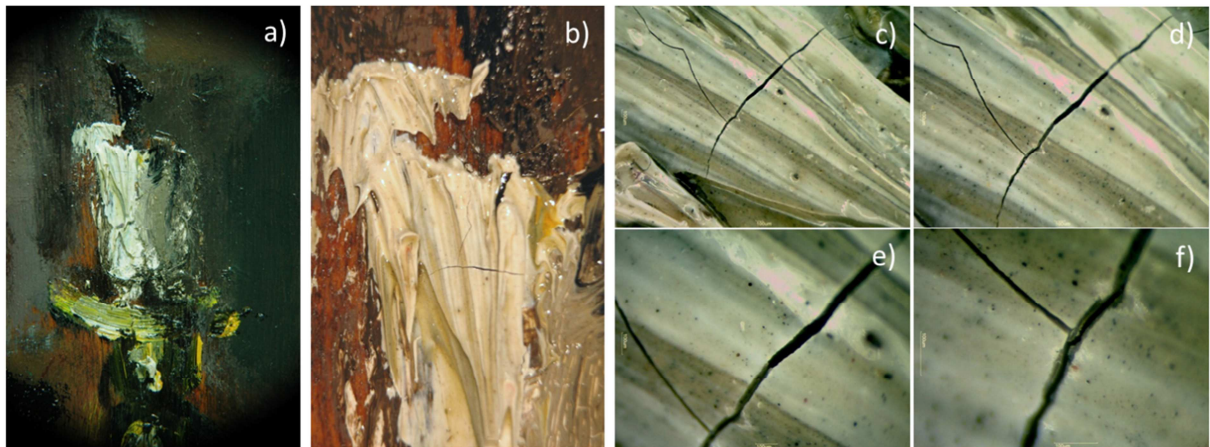


FIG. 151 Detail of craquelures in the wax candle painted in “Flowers” by F. De Pisis: a) b) VIS photograph; c) μ photograph by stereomicroscope (VIS, 13.4 x); d) μ photograph by stereomicroscope (VIS, 20 x); e) f) μ photograph by stereomicroscope (VIS, 80 x), craquelures 15-30 μm (w).

In addition to be considered art-fingerprints, all these features were also useful in support to a good image processing (choice of predominant colors, etc.) and to select the main interesting regions that were subsequently deepened by XRF analysis on painting and by analysis on samples (FIG.152).

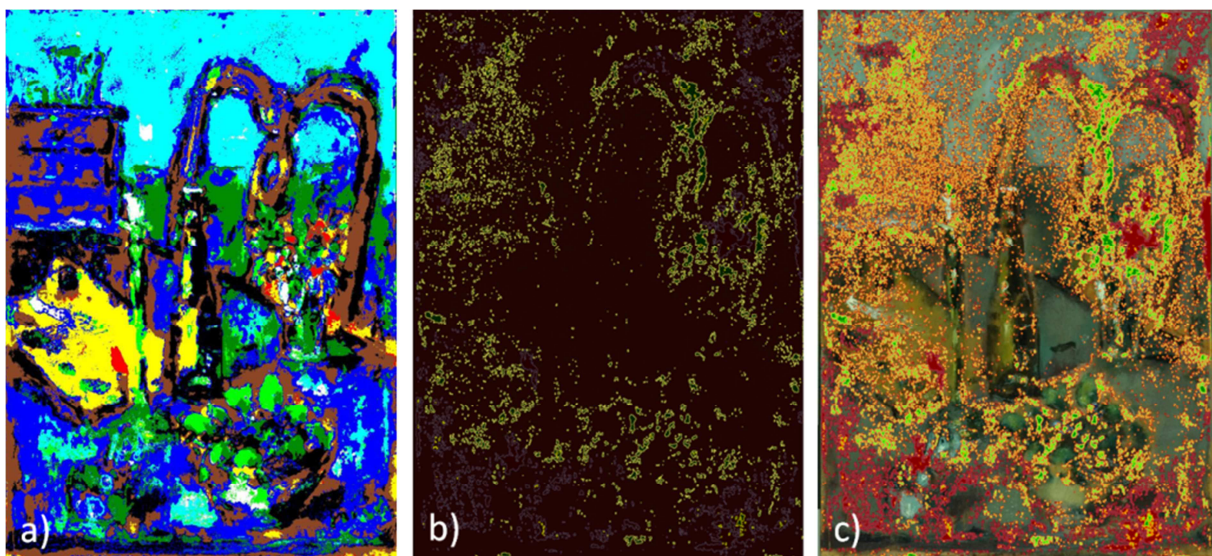


FIG. 152 Image Processing on “Flowers” by F. De Pisis: a) ROIs’ color class; b) profile of pictorial region enriched in matter; c) ROIs’ thickness brushstrokes overlapping VIS image (from green to red: from point enriched in matter to point with few pictorial matter).

5.5.4.2 Pigment analysis

The preliminary investigation, performed with EDXRF on the whole painting, examined both area enrich in matter and area where the pictorial layer was accurate spread (sampling point 12-14) to know what it could be the possible chemical contribution of the support (TABLE 8).

TABLE 11 EDXRF analysis on painting “Flowers”: average of Net Area values, gathered for color. Experimental set up: voltage 50 KeV, current 700 μ A, Live time: 120 s, no filter, Air, Anode Molybdenum, collimator 0.650. In italic, average value greater than σ .

	Zn	Ca	Ba	Pb	Sr	Fe	Cd	Se	Cr
White	<i>1628972</i>	<i>5703</i>	<i>3439</i>	<i>768</i>	<i>3643</i>	<i>743</i>	<i>73</i>	<i>79</i>	-
Red	<i>93825</i>	<i>1817</i>	<i>4636</i>	<i>2774</i>	<i>5851</i>	<i>2696</i>	<i>858</i>	<i>3166</i>	107
Green	<i>579983</i>	<i>4666</i>	<i>7974</i>	<i>39415</i>	<i>10328</i>	<i>17313</i>	<i>277</i>	<i>280</i>	<i>7237</i>
Yellow	<i>56082</i>	<i>2792</i>	<i>125</i>	<i>457806</i>	-	<i>5754</i>	<i>524</i>	<i>6946</i>	<i>54</i>
Blue	<i>577308</i>	<i>2349</i>	<i>468</i>	<i>43979</i>	<i>3219</i>	<i>12707</i>	<i>521</i>	<i>633</i>	-
Violet	<i>1408773</i>	<i>2493</i>	<i>1656</i>	<i>11667</i>	<i>1122</i>	<i>3783</i>	<i>621</i>	<i>484</i>	-
Brown	<i>14730</i>	<i>3893</i>	<i>79</i>	<i>34316</i>	<i>797</i>	<i>2395</i>	<i>146</i>	<i>453</i>	-
Support	<i>16281</i>	<i>1743</i>	<i>18.5</i>	<i>3354</i>	<i>155</i>	<i>5540</i>	-	-	<i>0.5</i>

	Sn	Hg	Cu	Mn	Co	K	Ti	Al	Si	Cl
White	<i>139</i>	-	-	-	-	-	<i>219</i>	-	-	-
Red	<i>240</i>	<i>501</i>	-	-	-	-	-	-	-	-
Green	<i>68</i>	<i>3824</i>	<i>617</i>	-	-	-	-	-	-	-
Yellow	<i>416</i>	-	-	<i>14</i>	-	-	-	-	-	-
Blue	-	<i>190</i>	-	<i>280</i>	<i>1049</i>	<i>11</i>	-	-	-	-
Violet	-	<i>884</i>	-	-	-	-	-	-	-	-
Brown	-	-	<i>308</i>	-	-	-	-	-	-	-
Support	-	-	<i>147</i>	<i>48</i>	-	<i>198</i>	-	<i>3</i>	<i>0.7</i>	<i>47</i>

Even if some chemical elements, such as zinc, calcium, barium, lead, iron and strontium were found on the whole painting (also in support), the detected difference between the colors’ chemical composition allowed to suppose the following proposal pigments (Montagna G., 1999; Secaroni C. *et al.*, 2002; Eastaugh N. *et al.*, 2008):

- White pigment: white zinc oxide mixed with barium sulphate (mixture: probably lithopone), calcium carbonate (Ca), tin white (Sn) and maybe white titanium dioxide (Ti);
- Red pigment: vermilion (Hs, S), minio (Pb), Cadmium red (S, Se, Cd) or Chrome red (Cr, Pb);
- Green pigment: Zinc green (Fe, Zn), Chromium Green (Cr), Lamoriniere Green (Cr), Guinet Green (Cr, Zn), Cadmium Green (Cd, Cr) or Cinnaber Green (Fe, Pb, Cr) or Green lac (Fe);

- Yellow: Lead-tin yellow (Pb, Sn), Lead oxide yellow (Pb), Raw Sienna Earth (Fe, Mn), Barium yellow (Ba, Cr) or Chrome yellow (Pb, Cr);
- Blue: Cobalt Blue (Co), Paris Blue or Prussian Blue (Fe), Brunswick Blue (Fe, Zn);
- Violet: probable mixture among red and blue pigments;
- Brown: Iron brown (Fe), Mars brown (Fe), Cassel earth (Fe), Sienna burnt (Fe) or Earth burnt (Fe, K, Mn).

The group of above listed pigments can be implemented by other possible pigments that are difficult to detect through EDXRF, such as organic pigment or pigments mainly constituted by light elements (i.e., Ultramarine Blue, Ultramarine Red, etc.). Considering, then, the complexity of the pictorial layer in which overlapping brushstrokes mix colored pigment particles and the lack of a pure one shade colored area, the list of the possible pigments employed by the artist could increase further.

Therefore, for a better pigment analysis, μ samples were collected from the pictorial surface and the chemical-mineralogical analysis allowed to better characterize and identify pigment particles.

White pigment

The analysis on white color was carried out on samples taken from the white area on the painting (FIG.4) and in the inner part of some colored specimens, that, under microscope, show different layers and a white inner core (FIG. 6).

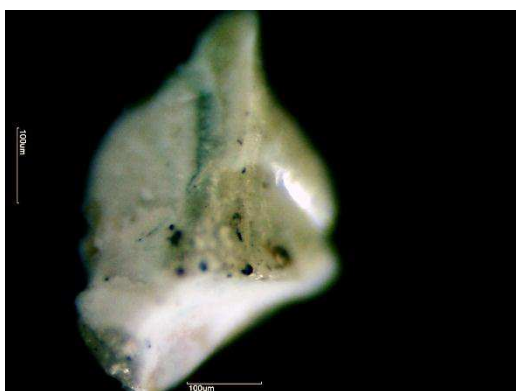


FIG. 153 Sample DeP_C06: OM photograph (90x).



FIG. 154 Sample DeP_C07: image taken by 3D Microscope HIROX KH-7700.

EDXRF measurements previously carried out on the background (carbon tape – aluminum stub) allowed to better interpret the chemical composition of white pigments: analysis on samples confirms the presence of titanium and zinc, supposing a white pigment made by white titanium ox-

ide and zinc oxide (FIG.) (Montagna G., 1999; Seccaroni C. *et al.*, 2002; Eastaugh N. *et al.*, 2008).

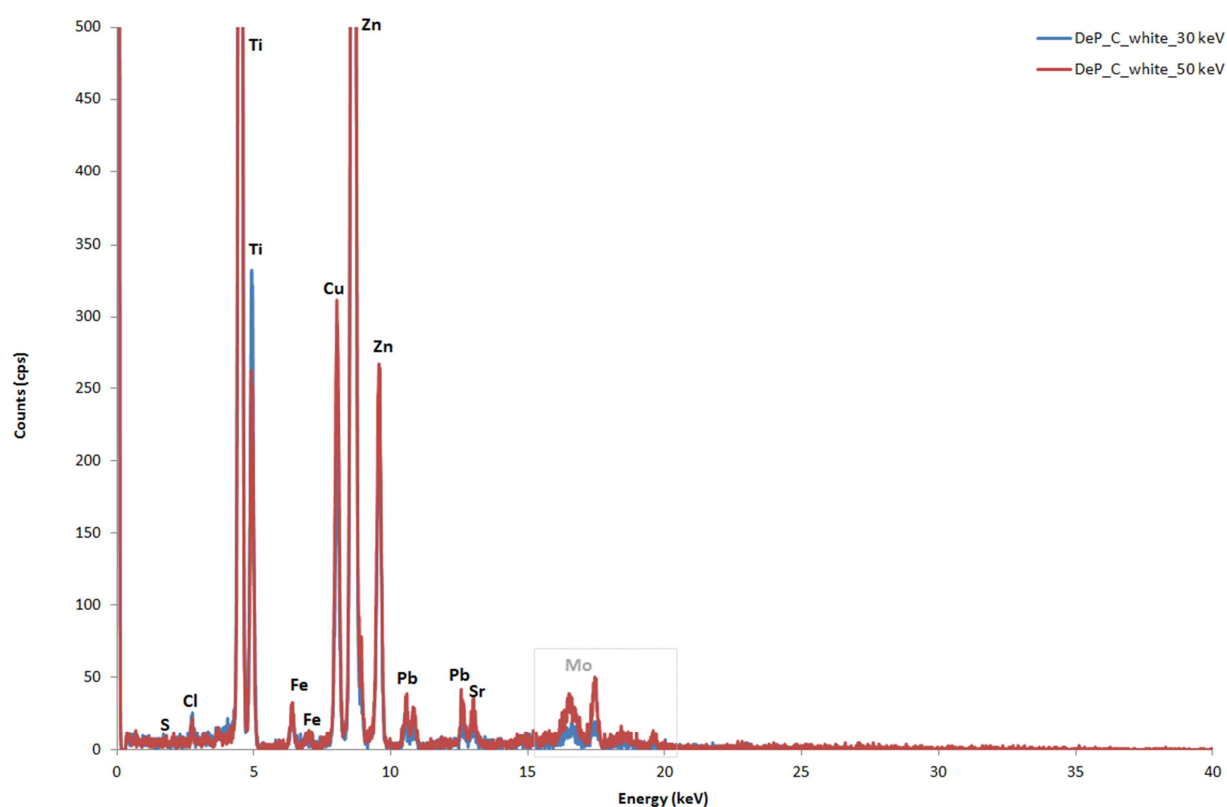


FIG. 155 XRF spectra on White pigment: total spectra from different set-up, not subtracting background. Experimental set up: voltage 50 KeV and current 700 μ A, voltage 30 KeV and current 1300 μ A. Live time: 60 s, no filter, Helium flow, Anode Molybdenum, collimator 0.200.

The chemical composition, suggested for the white color, is also verified by PIXE analysis that revealed titanium and zinc. The detection of element such as chlorine and sulfur allowed to suppose a White Titanium production methods linked to chlorine process; but the complexity of the pictorial matrix did not permit to exclude other hypothesis, in which sulfur could be linked to other pigment or contamination and chlorine due, for example, to salts on surface. Even that, PIXE analysis revealed further chemical elements, not detected with previous analysis on white samples (such as Ba, Cr, Fe, Mn) that, being linked to the analyzed surface and pigments, they can be considered art-fingerprints of the entire system pictorial layer-support.

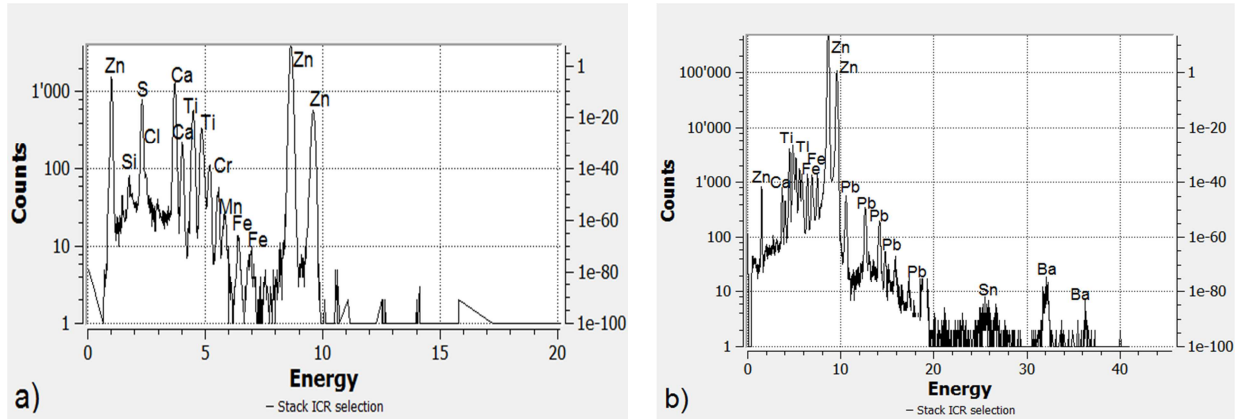


FIG. 156 PIXE spectra of white pigment: a) low energy detector; b) high energy detector. Experimental set up: particle/energy 3 MeV, current p+, Dose/s 200, Helium flow.

SEM/EDS analysis revealed small and rounded pigment's particles, which dimensions are less than $1\ \mu\text{m}$ (FIG. 157); this particular morphology suggests artificial origin of the used pigments (Montagna G., 1999) and it confirms anatase morphology (Eastaugh N. et al., 2004^B; Kampfer W.A. 1973). The chemical analysis confirms that pigment particles of white color are mainly constituted by titanium and zinc meanwhile calcium and sulfur peaks are probably due to calcium sulfate, that is usually contained in pigments based on this compound (FIG.158). Considering that, it is possible to suggest the use of mixture of artificial pigments White titanium dioxide and White Zinc Oxide (Eastaugh N. et al., 2008; Montagna G., 1999; West Fitzhugh E.,1997).

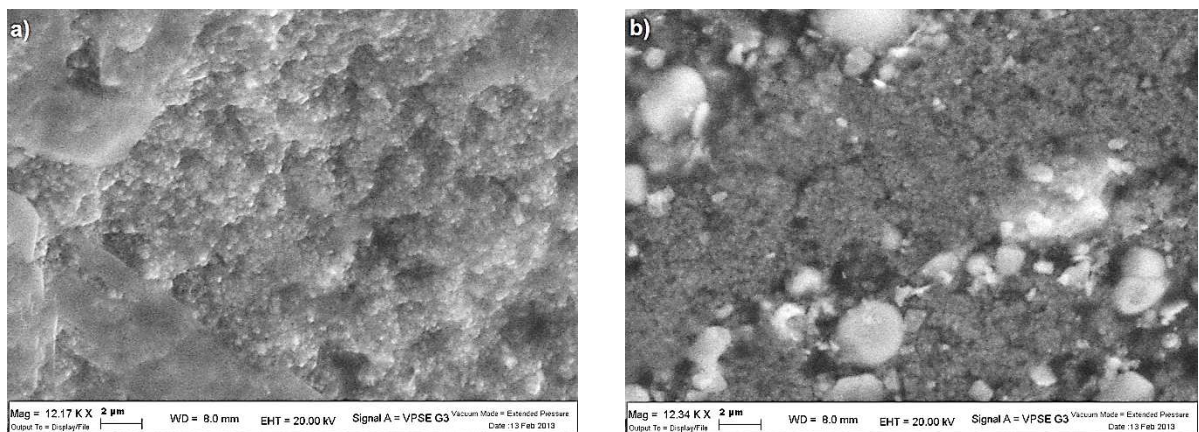


FIG. 157 SEM microphotograph of White samples: a) white pigment particles (magnification 12.17 KX); b) inter-layer between white pigment particle and organic covering varnish (magnification 12.34 KX).

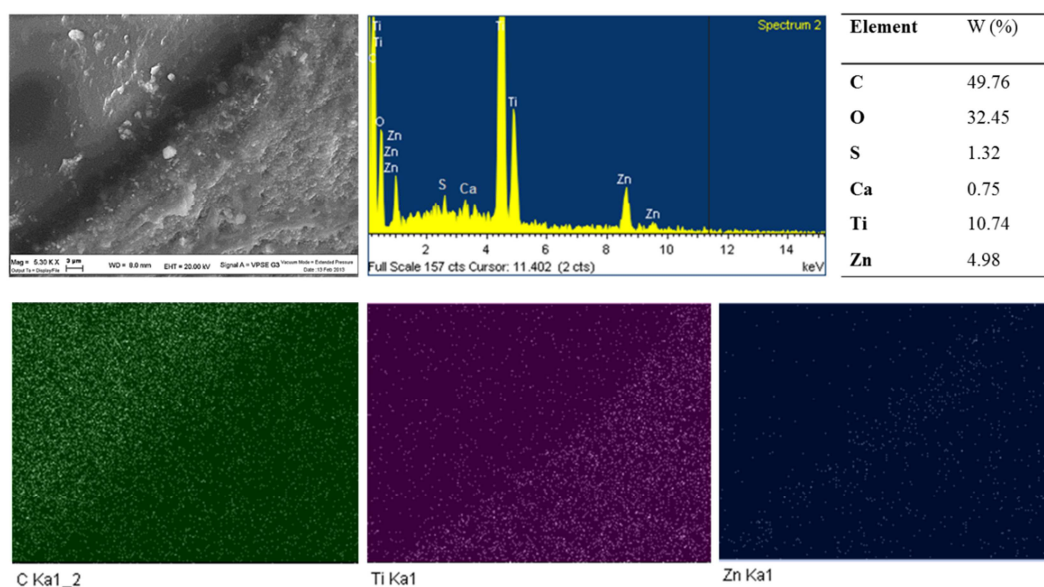


FIG. 158 EDS spectra and EDS mapping analysis on the investigated area of white samples, as presented in FIG.157.

Finally, Raman spectroscopy confirm the presence of White titanium dioxide, in particular Raman bands of Anatase phase at 395 cm^{-1} (w), at 514 cm^{-1} (w) and at 638 cm^{-1} (m) (Clark R.J.H. *et al.*, 2007; Ohsaka T. *et al.* 1978; Griffith, W.P., 1987; Schroeder P.A. *et al.*, 2003) and White Zinc Oxide, which Raman bands are at 329 cm^{-1} (m), 385 cm^{-1} (m), 437 cm^{-1} (vs) (Ghimbeu C.M. *et al.*, 2007) (FIG.159). Moreover Raman spectra of other white point revealed the presence of barite and calcite: Raman bands at 454 cm^{-1} (s) and at 981 (vs) are due to barite [28-30] meanwhile, for calcite identification, the strong band due to symmetric stretching of CO_3 is located at 1081 cm^{-1} (weak peak) and other characteristic band of calcite at 281 cm^{-1} is also recognized (Jehlička J. *et al.*, 2009 ; Lécuyer C. *et al.*, 2012 ; Park K., 1967; Vagenas N.V. *et al.*, 2003) (FIG.160). Like for calcium sulfate, barium sulfate could be contained in pigments based on White titanium dioxide.

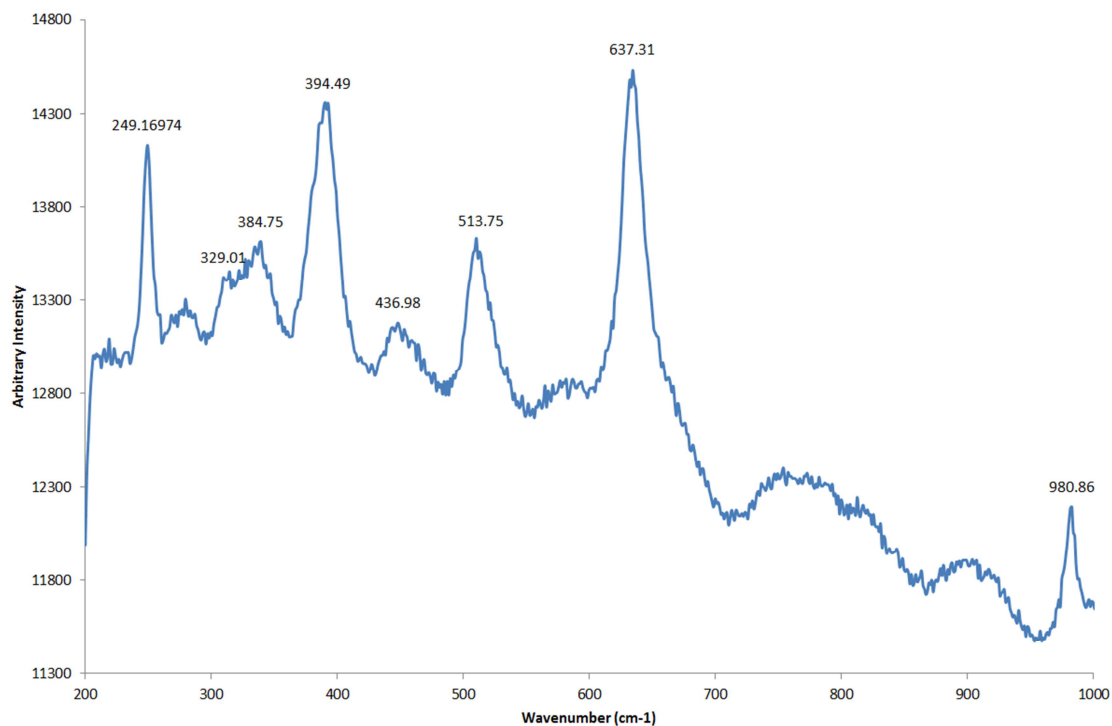


FIG. 159 Raman spectra on white samples (632,81 nm excitation, 50 x magnification): Anatase phase and Zinc Oxide.

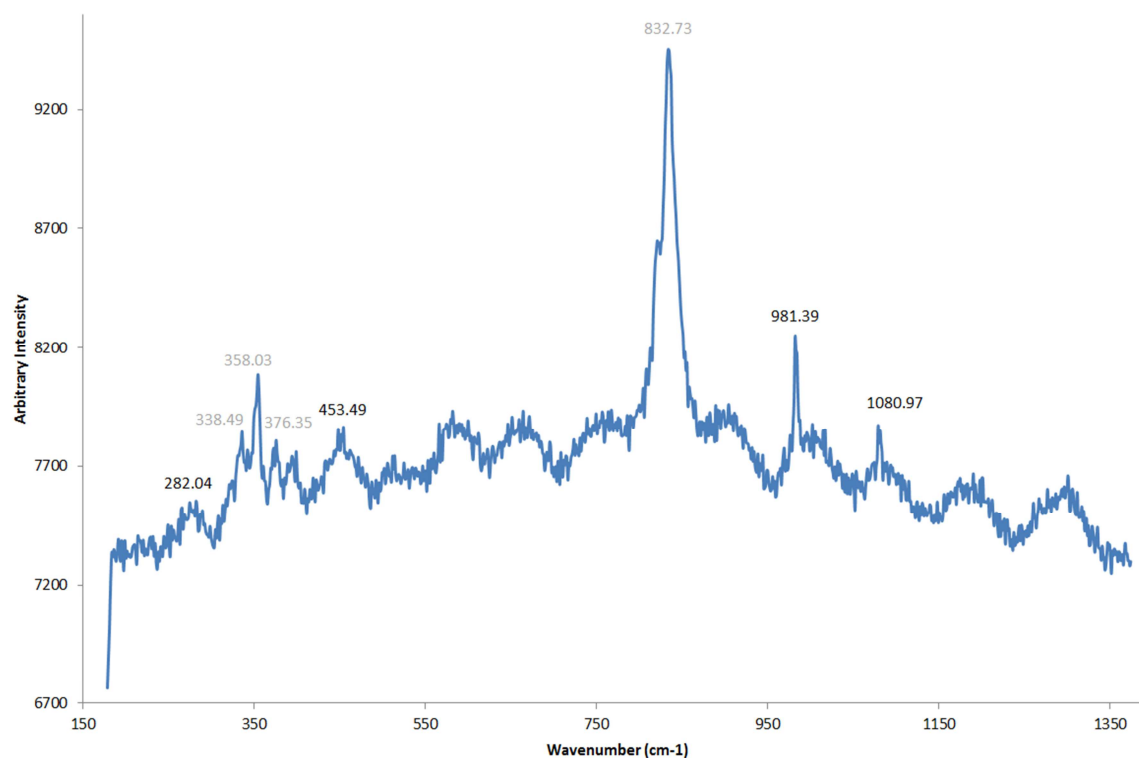


FIG. 160 Raman spectra on white-yellow samples (632,81 nm excitation, 50 x magnification): Calcite; Raman bands in grey color are due to crocoite phase of yellow compounds.

In conclusion, pigment analysis suggest that for white color, the artist mainly used White titanium dioxide (Anatase phase) mixed with Zinc Oxide compost (White Zinc Oxide or Lithopone, mixture of White Zinc Oxide and White Barium Sulphate). Furthermore, considering that chemical analysis revealed average low value for Calcium and for Barium, the presence of these elements could be linked to White titanium dioxide and White Zinc Oxide blends rather White Calcium pigment (i.e., calcium carbonate, calcium sulfate) and White Barium Sulfate pure pigments.

Blue pigment

Due to difficulty to find one shade blue colored painting's area, for the identification of Blue pigments, analysis were carried out on samples in which blue pigment are mixed with white and red particles. For this reasons, all the analysis, except for Raman spectroscopy, revealed also the interference of these two colored compounds.

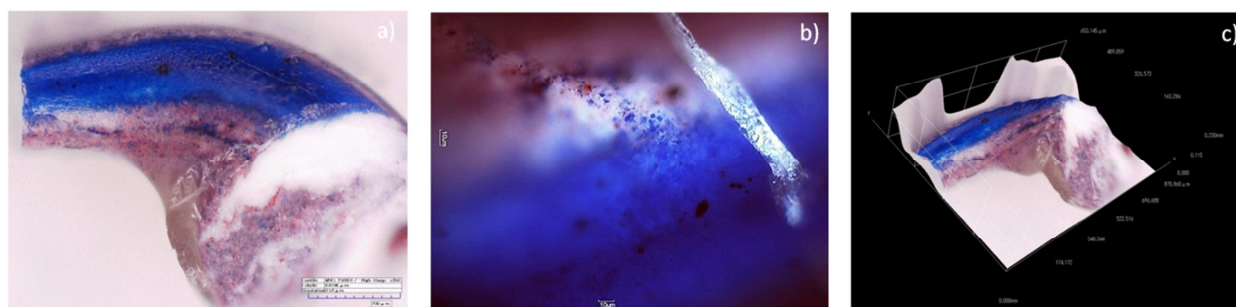


FIG. 161 Sample DeP_C02: a) c) image and 3D model taken by 3D Microscope HIROX KH-7700 (magnification 10x) ; b) OM photograph (magnification 100x).

Considering the contribution of the background (carbon tape – aluminum stub) to chemical composition detected by EDXRF on these samples, chemical analysis did not reveal characteristic chemical elements that are usually used to identify pigments trough EDXRF (Montagna G., 1999; Seccaroni C. *et al.*, 2002). In fact, the signals of copper or iron, that are usually searched for EDXRF blue pigment identification, were well detected also for the background (FIG.162); thereby, EDXRF analysis did not allow to consider these elements as representative for pigments identification and the blue color could be obtained using organic compounds or some kind of pigments that contains light element.

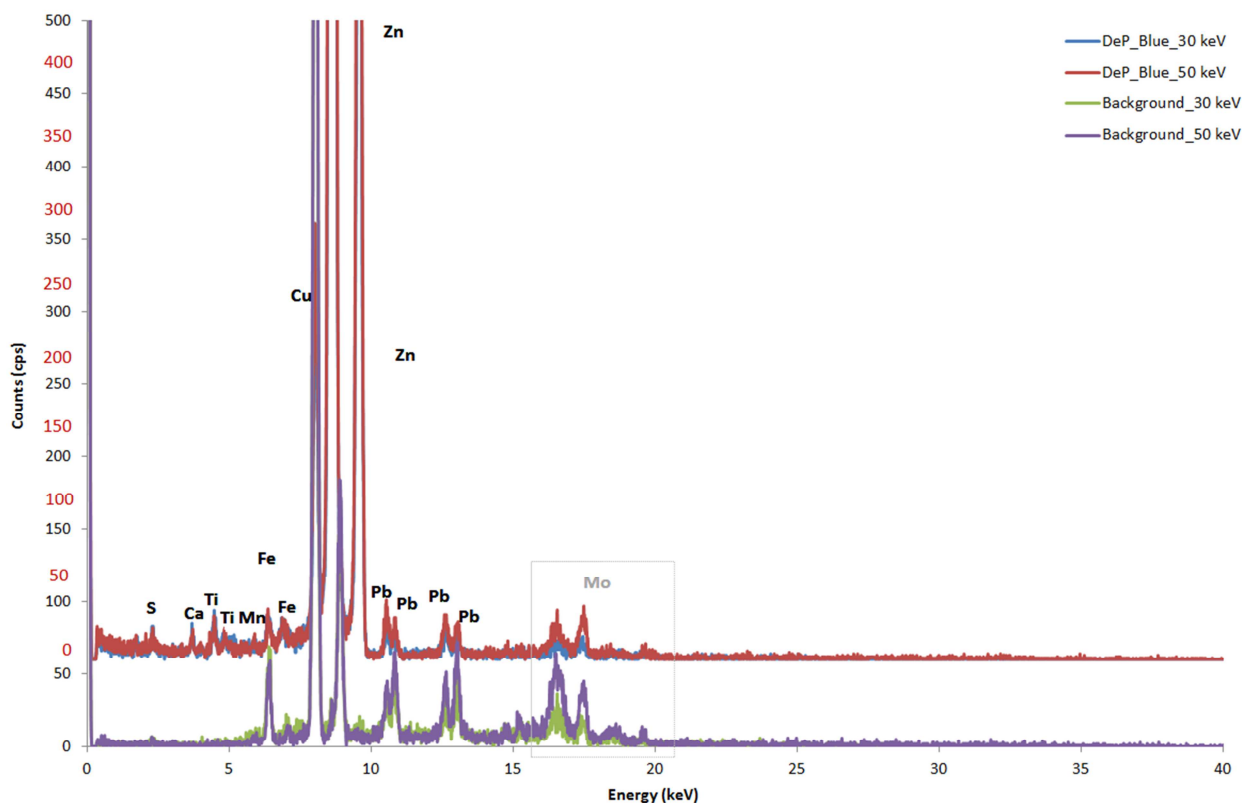


FIG. 162 XRF spectra on Blue/white/red pigment: total spectra from different set-up, not subtracting background. Experimental set up: voltage 50 KeV and current 700 μ A, voltage 30 KeV and current 1300 μ A. Live time: 60 s, no filter, Helium flow, Anode Molybdenum, collimator 0.200.

Results from PIXE analysis allowed to suppose that, from chemical point of view, Ultramarine Blue (natural or artificial) could be considered among the possible Blue pigments, being characterized for the presence of Na, Al, Si and S Oxide (Eastaugh N. et al., 2008), meanwhile Titanium, zinc and barium are due to white components.

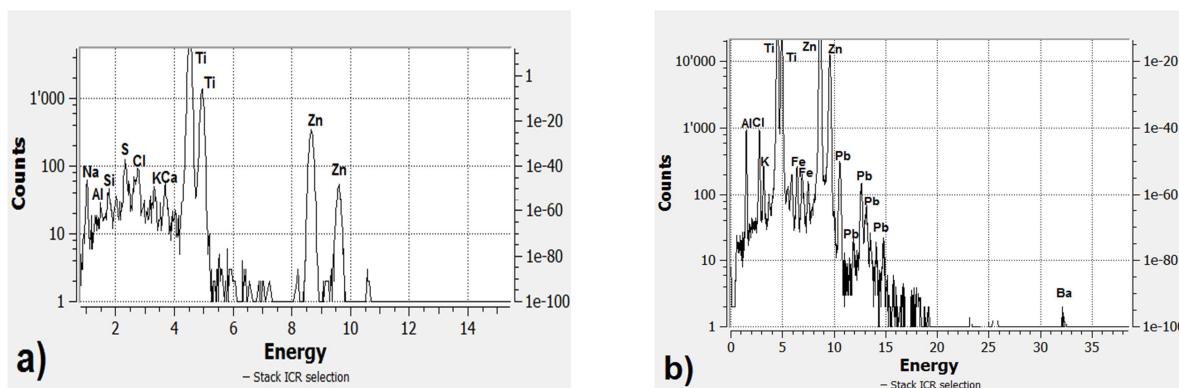


FIG. 163 PIXE spectra of blue/white pigment: a) low energy detector; b) high energy detector. Experimental set up: particle/energy 3 MeV, current p+, Dose/s 200, Helium flow.

Through SEM analysis, it is possible to detect fine-grained pigment and narrow particle size range less than 1 μm . Moreover, SEM images revealed also some particles present in crumb-like aggregates. Considering that Ultramarine (synthetic analogue of the mineral lazurite) is distinguished from the natural analogue by the finer grain size and absence of impurity and that previous studies reported ultramarine particle size of ultramarine pigment in 1950s in the range 0.5-5.0 μm (Eastaugh N. *et al.*, 2004^B), it is possible consider this pigment that Blue color was obtained using this pigment. Furthermore, other chemical elements detected by PIXE, such as Ca, Cl, K, Pb and also Fe, could be attributed to other color or to production process used by company and not to impurity that in natural Ultramarine Blue are present (Ca, Fe, etc.).

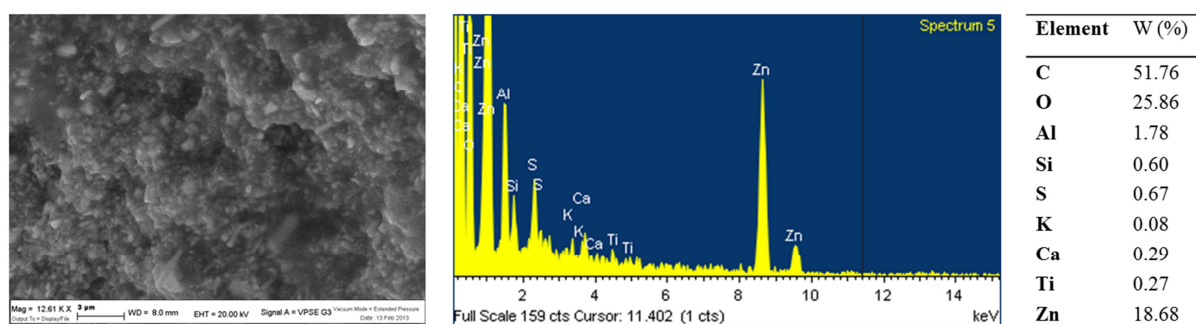


FIG. 164 SEM/EDS on Blue/White samples: SEM photograph of blue-white (magnification 12.61 KX); EDS spectra of the investigated area. Source: Ferrara University.

Micro-Raman analysis carried out on individual blue crystals from the white-blue pigment samples confirmed the presence of Artificial Ultramarine Blue: the characteristics Raman bands of lazurite were detected at 258 cm^{-1} (s), 548 cm^{-1} (vs), 581 cm^{-1} (sh), 802 cm^{-1} (v) and 1096 cm^{-1} (w) (Barsan M.M. *et al.*, 2012; Clark R.J.H. *et al.*, 1997; Osticioli I. *et al.*, 2009) [28-30].

The absence of calcite, a mineral that is commonly present in natural lapis lazuli, which Raman bands are usually at 283 cm^{-1} (w), 713 cm^{-1} (w) and 1086 cm^{-1} (vs), confirms the hypothesis of the artificial origin of the Ultramarine Blue (Osticioli I. *et al.*, 2009) [28-30], that is typically low in impurity such as calcite, pyrite, etc. (Eastaugh N. *et al.*, 2004^B).

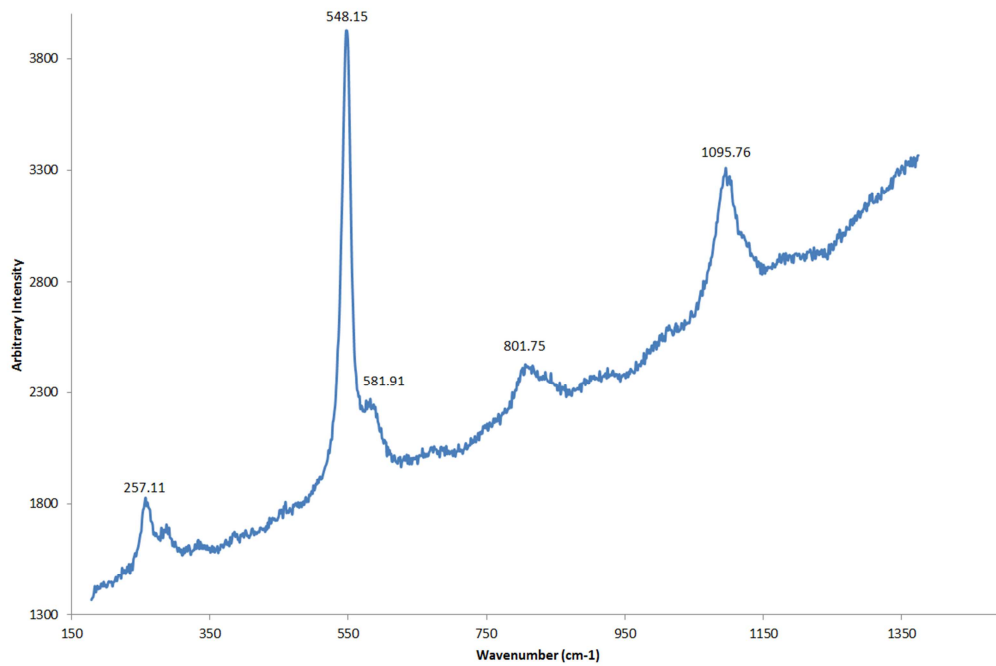


FIG. 165 Raman spectra on blue particles (632,81 nm excitation, 50 x magnification): Artificial Ultramarine Blue.

In conclusion, for the blue pigment, analysis suggest Artificial Ultramarine Blue, which discover dated around 1827 ([Eastaugh N. et al., 2008](#); [Montagna G., 1999](#)).

Red pigment

Previously investigation under stereomicroscope of the whole paintings revealed the presence of two different nuance of red color: red and red-violet. The sampling interested both the color shade but, if for the red nuance the sample is pure without other color mixed together, the red-violet color analysis was carried out on samples in which red-violet, white and blue colors are gathered together.

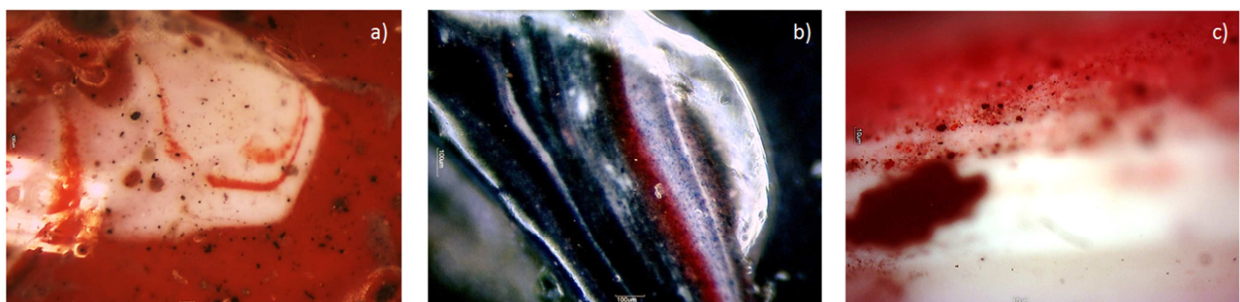


FIG. 166 Red color: a) b) microphotograph of painting, respectively spot area C04 and C02 (magnification 60x); c) OM photograph of sample in which red color and red-violet particles are visible (magnification 100x).

As revealed by EDXRF analysis and better by PIXE, the two red colors show different chemical compositions: for red one, characteristic elements are selenium, cadmium, lead, sulfur and mercury meanwhile calcium for red-violet. Also in this case, iron, that is one of the useful elements for EDXRF pigment identification, is also well detected in the background; in this way it was possible not to exclude a red pigment characterized by iron (red ochre, etc.) or assure its presence. Therefore, for the red color, EDXRF analysis carried out on the sample confirms results from EDXRF on painting: vermilion (Hg, S), minio (Pb), Cadmium red (S, Se, Cd) or Chrome red (Cr, Pb) (Eastaugh N. *et al.*, 2008; Montagna G., 1999; Seccaroni C. *et al.*, 2002). As concerns, instead, the red-violet nuance, the completely different composition allowed us to think that it was not obtained by mixing red color with blue color but that it is another pigment compound.

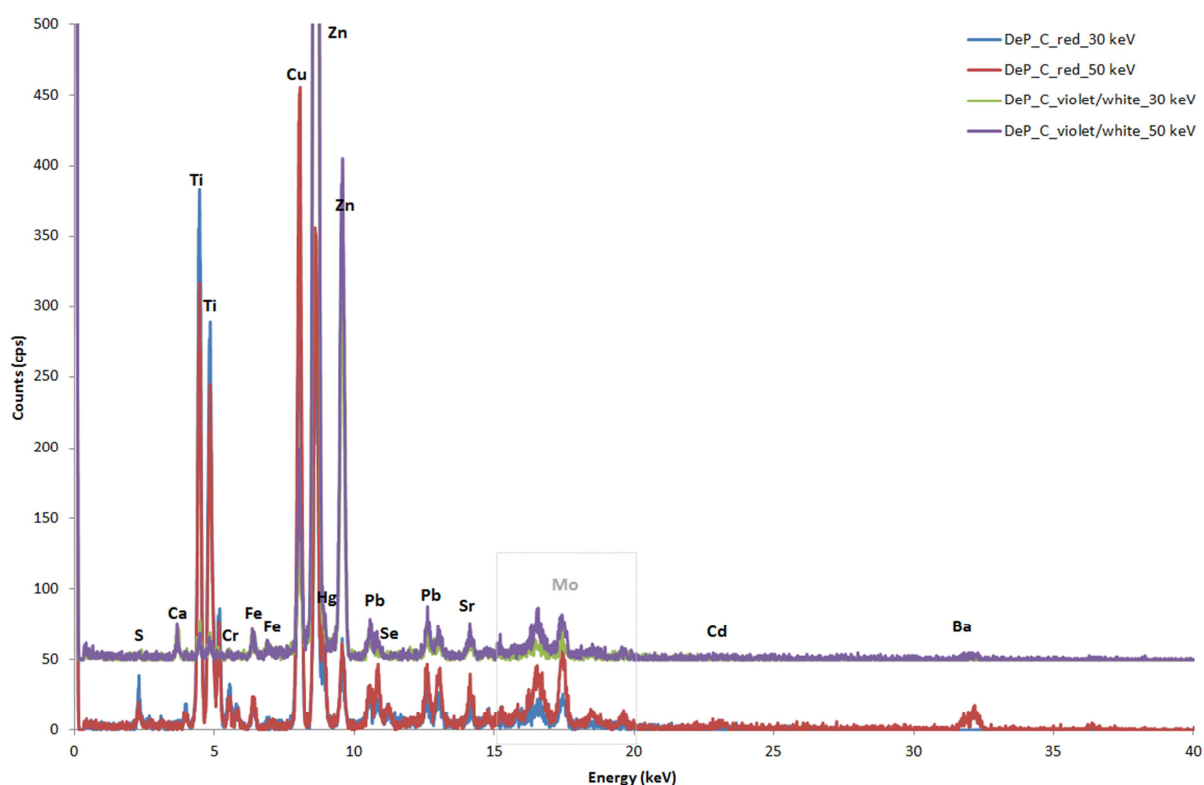


FIG. 167 XRF spectra on red and red/violet/white/blue blend: total spectra from different set-up, not subtracting background. Experimental set up: voltage 50 KeV and current 700 μ A, voltage 30 KeV and current 1300 μ A. Live time: 60 s, no filter, Helium flow, Anode Molybdenum, collimator 0.200.

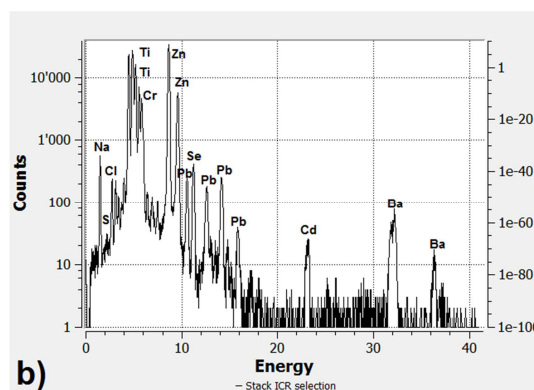
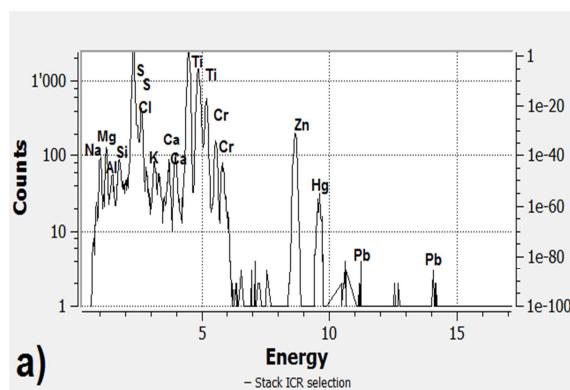


FIG. 168 PIXE spectra of red pigment: a) low energy detector; b) high energy detector. Experimental set up: particle/energy 3 MeV, current p+, Dose/s 200, Helium flow.

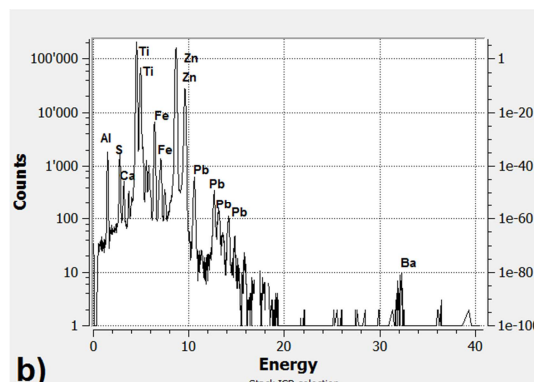
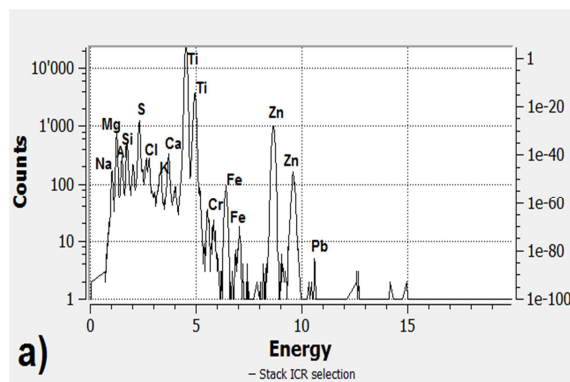


FIG. 169 PIXE spectra of red-violet pigment: a) low energy detector; b) high energy detector. Experimental set up: particle/energy 3 MeV, current p+, Dose/s 200, Helium flow.

According to red or red-violet area, SEM photographs show different morphologies of pigment grain: for red-violet, particles have irregular and angular shape with fine and very fine grain size (different from the surrounding homogeneous and rounded particle smaller than 1 μm of White titanium dioxide) meanwhile, in the red samples, particles appear spherical with grain size less than 1 μm (FIG.170). It is confirmed, also for these two pigment, the artificial origin (Eastaugh N. *et al.*, 2004^B; Eastaugh N. *et al.*, 2008; Montagna G., 1999). After that, other chemical elements detected by PIXE, such as Ca, Cl, K, Pb and also Fe, could be attributed to production process, being Red Ultramarine obtained by further calcination of Ultramarine Blue.

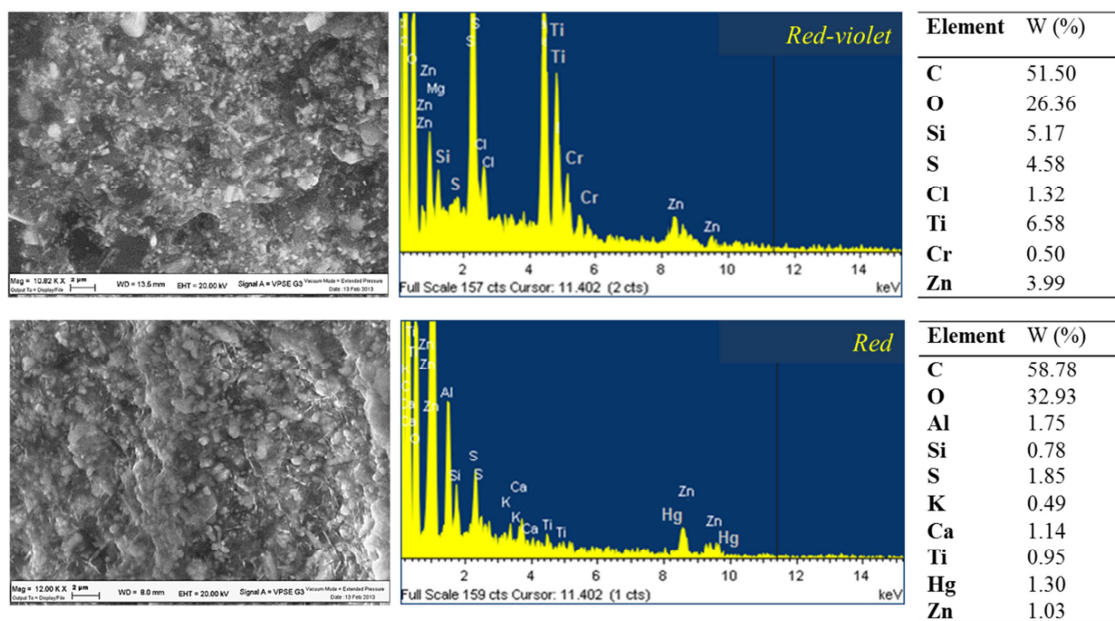


FIG. 170 SEM/EDS on red-violet/white and red samples: SEM photograph of red-violet (magnification 10.82 KX) and of red (magnification 12.00 KX); EDS spectra of the investigated area.

Raman spectra of the red-violet particle match closely that Red-Violet Ultramarine Pigment, showing in particular characteristic band at 547 cm^{-1} (vs), 582 cm^{-1} (sh), 1299 cm^{-1} (w) [29; LabSpec 5 Raman Spectroscopy Library]. The likelihood with Raman spectra of Ultramarine Blue is probably linked to the production of the Violet shade from Ultramarine Blue (Eastaugh N. et al., 2008; Montagna G., 1999).

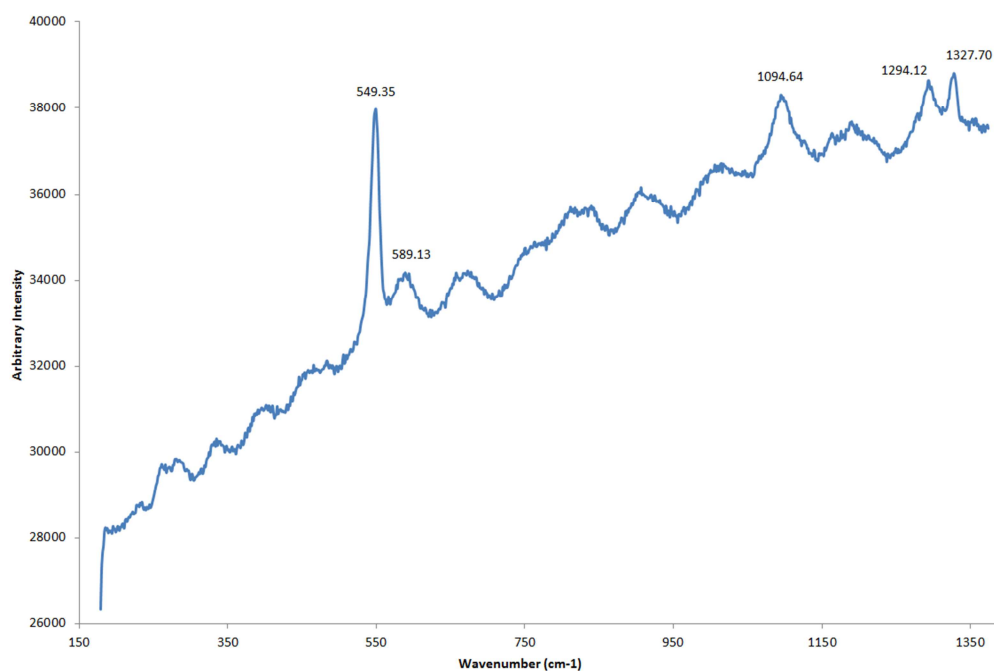


FIG. 171 Raman spectra on red-violet particles (632,81 nm excitation, 50 x magnification): Artificial Violet-Red Ultramarine.

Otherwise, red pigment particles show characteristic Raman bands of Vermilion, the artificial compound of Cinnabar, at 250 cm^{-1} (vs), 283 cm^{-1} (w-sh), 343 cm^{-1} (m) (Bell I.M. *et al.*, 1997) [29]. In this sample three characteristic Raman peaks of Anatase are also recognizable at 395 cm^{-1} (w), at 514 cm^{-1} (w) and at 638 cm^{-1} (m) (Clark R.J.H.*et al.*, 2007; Ohsaka T. *et al.* 1978; Griffith, W.P., 1987; Schroeder P.A. *et al.*, 2003)

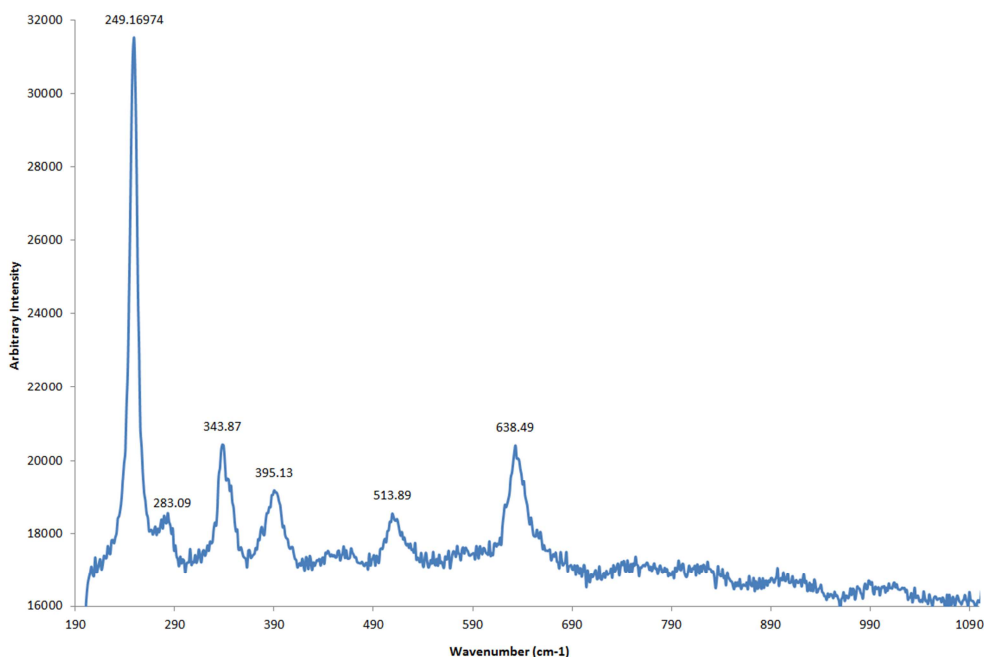


FIG. 172 Raman spectra on red-white particles (632,81 nm excitation, 50 x magnification): Vermilion and White titanium dioxide (Anatase phase).

Finally, considering all the analysis carried out on red samples, it is possible to suppose the use of different red color shade: Vermilion and Violet-Red artificial Ultramarine but it is not possible to exclude Cadmium Red, Lead Red and Chrome red.

Yellow pigment

Sampling of yellow spot on painting allowed to take specimens in which yellow color is mixed with green area and yellow.

The complexity mixture of painting is also confirmed by investigation under microscope of yellow samples: green or white blend are found mixed with the yellow color but different colored pigment particles follow brushstrokes' direction, easing the identification of the several colored zones. Moreover, as shown in FIG. 173, a varnish layer, about 20 μm thick, is placed on pictorial surface; differently to Specular reflection investigation, organic covering layer, on the external

surface of all the colored samples, suggest that the artist could apply protective layer only in correspondence of spot enrich in matter or that this thick covering layer is due a reaction/deposition of pigment particles in medium blends.

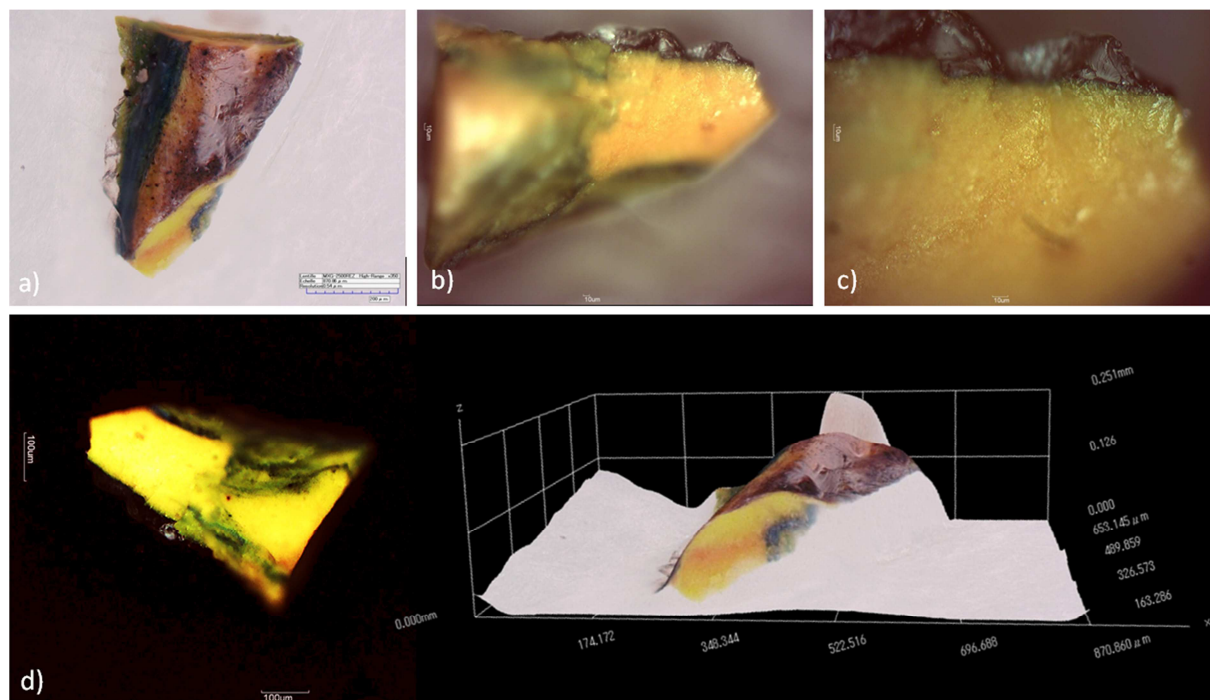


FIG. 173 Microphotograph of yellow sample DeP_C09: a) d₂) image taken by 3D Microscope HIROX KH-7700 (magnification 25x); b) c) d₁) OM microphotographs respectively at 35 x, 50 x, 30 x.

Chemical analysis carried out on yellow-white and yellow-green specimens suggested that yellow color could be obtained using Chrome yellow (cochroite or phoenicochroite: Cr, Pb) (Eastaugh N. et al., 2008; Montagna G., 1999; Seccaroni C. et al., 2002): EDXRF spectra and PIXE analysis confirmed the presence of lead and chromium in both samples. Even if Chrome yellow is more plausible than other yellow pigment, according to chemical composition of the samples, other pigments could be also hypothesized. If we excluding the contribution of background and recognized white pigment (white titanium dioxide and white zinc), for the yellow colors the artist could use yellow ochre (limonite, Fe) or Lead oxide yellow (Litharge, Pb) (Eastaugh N. et al., 2008; Montagna G., 1999; Seccaroni C. et al., 2002).

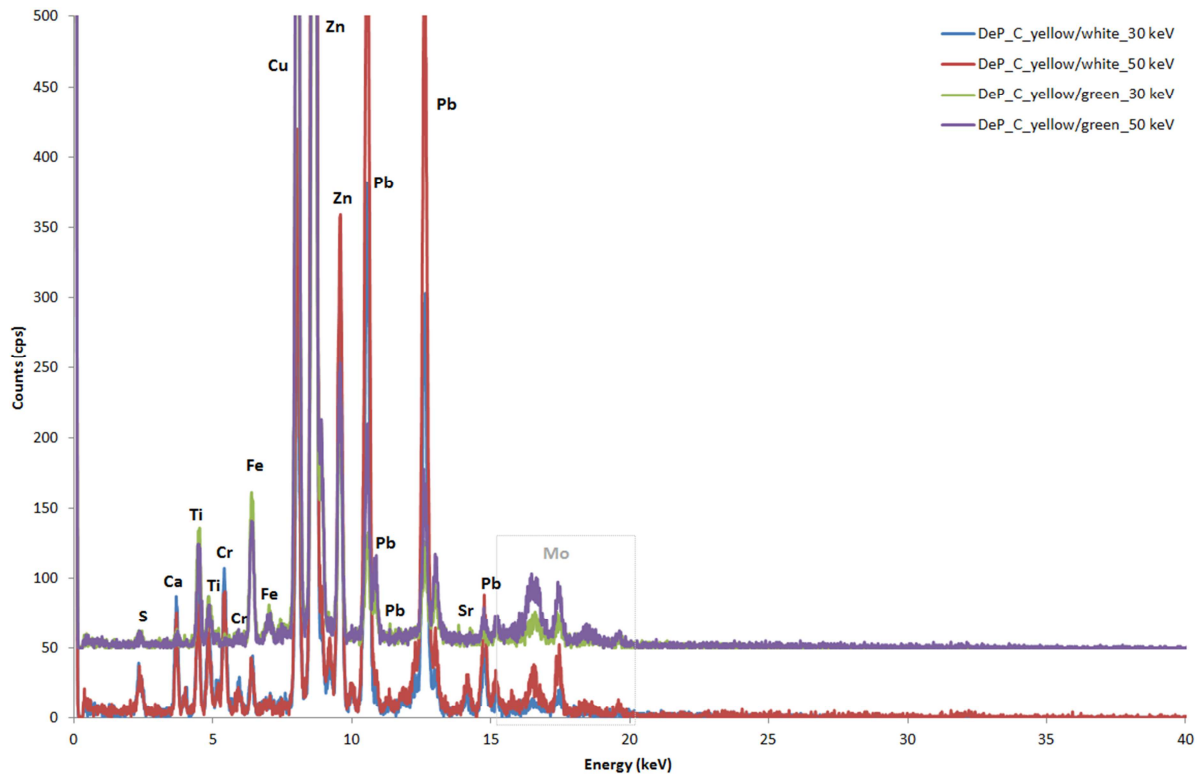


FIG. 174 EDXRF spectra on yellow/white and yellow/green blend: total spectra from different set-up, not subtracting background. Experimental set up: voltage 50 KeV and current 700 μ A, voltage 30 KeV and current 1300 μ A. Live time: 60 s, no filter, Helium flow, Anode Molybdenum, collimator 0.200.

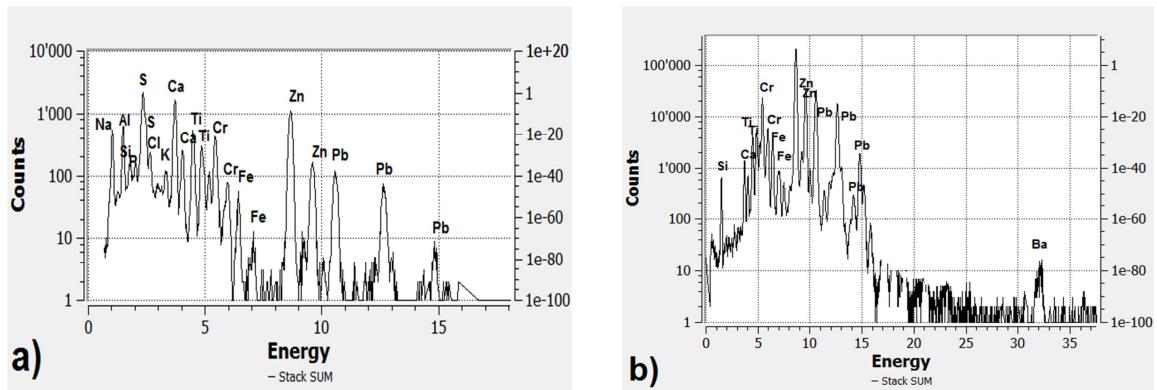


FIG. 175 PIXE spectra of yellow/white: a) low energy detector; b) high energy detector. Experimental set up: particle/energy 3 MeV, current p+, Dose/s 200, Helium flow. Source: AGLAE facility, C2RMF Laboratory (Louvre, Paris – France).

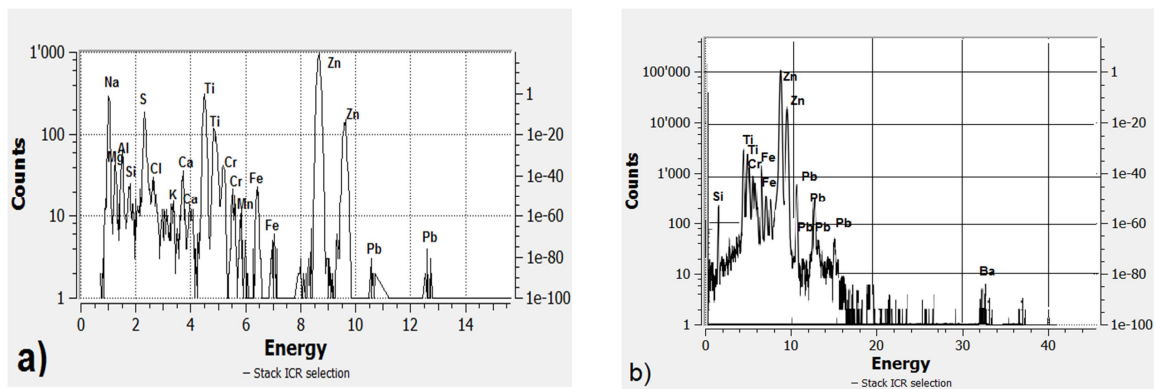


FIG. 176 PIXE spectra of yellow/green pigment: a) low energy detector; b) high energy detector. Experimental set up: particle/energy 3 MeV, current p+, Dose/s 200, Helium flow. Source: AGLAE facility, C2RMF Laboratory (Louvre, Paris – France).

Results from SEM/EDS analysis confirmed the hypotheses of Chrome yellow for yellow pigments: delimited area, which chemical composition is characterized by chrome and lead, show small particles similar to bladed laths, about $1\mu\text{m}$ wide and $2\mu\text{m}$ long, that are attributable to lead chromate - crocoite or phoenicochroite phase (Eastaugh N. *et al.*, 2004^B; McCrone *et al.*, 1979). FIG. 177 shows different particle pigments in correspondence of yellow-white color area: characteristic bladed laths are mixed with very small particle with rounded shape and size less than $1\mu\text{m}$ due to Anatase of White titanium dioxide components (Eastaugh N. *et al.*, 2004^B; Kampfer W.A., 1973).

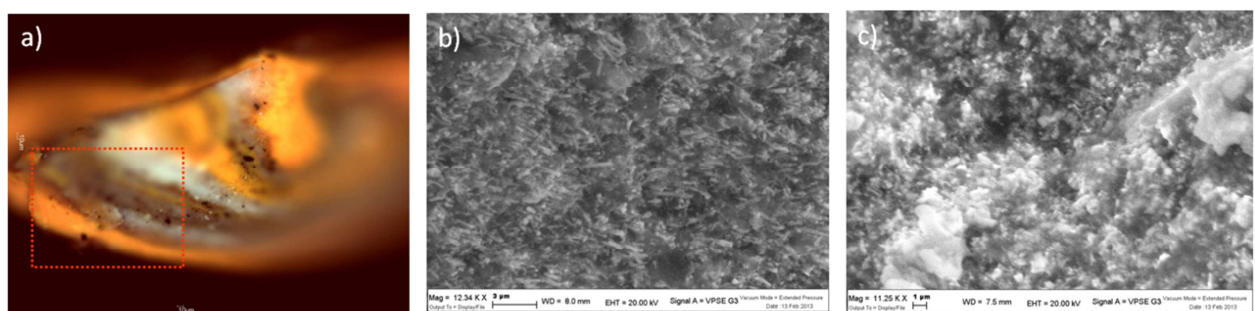


FIG. 177 SEM/EDS analysis on yellow/white sample: a) μ photograph (OM, 52x); b) SEM photograph of yellow pigment particles (magnification 12.34 KX); c) SEM photograph of yellow/white pigment particles interlayer (magnification 11.25 KX). Source: Ferrara University.

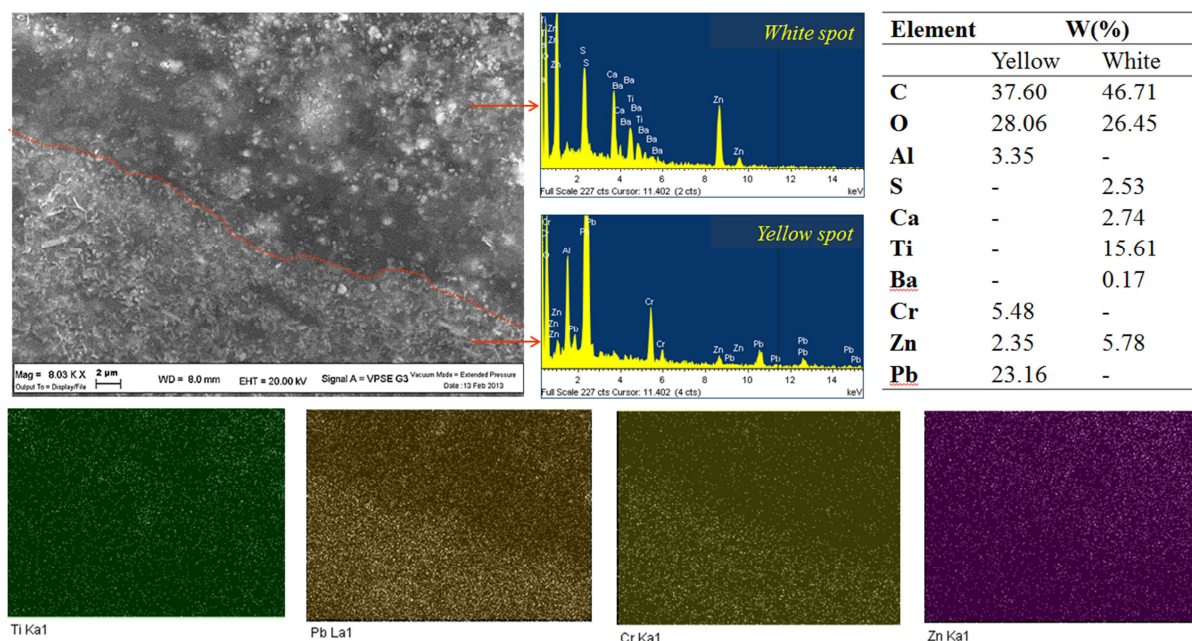


FIG. 178 EDS spectra and EDS mapping analysis on the investigated area of yellow/white samples, as presented in FIG.177

The Raman spectra recorded on several yellow particles confirmed the presence of lead chromate, in particular crocoite phase with characteristics Raman bands at 336 cm^{-1} (m), 358 cm^{-1} (s), 374 cm^{-1} (m), 401 cm^{-1} (w) and 838 cm^{-1} (vs) [28; 30; 31; LabSpec 5 Raman Spectroscopy Library].

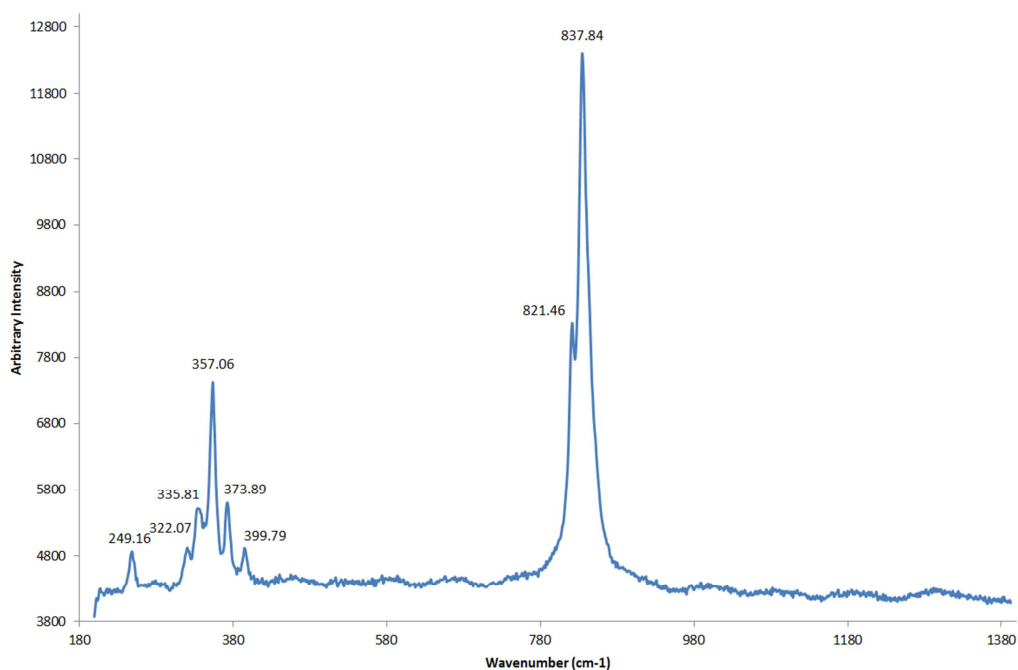


FIG. 179 Raman spectra on yellow particles (632,81 nm excitation, 50 x magnification): Lead chromate, crocoite type.

As concern, instead, green particles found in the yellow-green sample, considered that μ Raman carried out on individual green crystal revealed high signal of organic medium and varnish that cover characteristic Raman peaks, chemical analysis carried out allowed to exclude only Cadmium Green but not green pigment based on iron (Zinc green, Green lac), chrome (Chromium Green, Lamoniere Green, Guinet Green).

In conclusion, pigment analysis revealed that the most probable pigment used for the yellow is the Chrome yellow (crocoite).

TABLE 12 PIXE analysis on “Flowers” samples. Average value: region of interest were extracted using PyMCA software, data expressed in counts. Experimental set up: particle/energy 3 MeV, current p+, Dose/s 200, Helium flow.

Low Energy										
	Mg	Al	Si	P	S	Cl	K	Ca	Ti	Cr
White	-	2957	9001	140	36237	766	241	48311	4273	-
Yellow	1743	61638	3837	3768	39995	1898	514	57341	3939	59581
Red	77306	13447	19462	2695	32480	5494	2122	5235	307999	-
Blue	5113	33865	19529	1128	26284	5576	2255	21688	3718	392
High Energy										
	Mg	Al	Si	P	S	Cl	K	Ca	Ti	Cr
White	-	-	-	-	-	-	22526	55694	880	266
Yellow	-	-	-	-	1710000000	-	19506	86460	7216	85917
Red	-	-	-	-	2620000000	-	15257	9336	34694	131
Blue	-	-	-	-	-	-	16622	29947	4656	386
Low Energy										
	Mn	Fe	Co	Ni	Cu	Zn	Sr	Ba # LA	Hg # LA	Pb # LA*
White	115	1292	-	30	-	560757	-	89950	-	5047
Yellow	-	5723	225	-	153	136369	-	79725	3195	264299
Red	226	8443	218	85	-	78061	-	66008	484	2769
Blue	159	932	-	118	-	594910	-	18525	1851	6585
High Energy										
	Mn	Fe	Co	Ni	Cu	Zn	Sr	Ba # LB	Hg # LA	Pb # LA
White	-	1559	8	669	93	560757	1568	90517	112	2576
Yellow	-	5437	230	338	138	136369	958	90429	4478	267856
Red	-	6670	71	680	215	497206	158	172815	-	17672
Blue	279	2160	94	621	78	594910	183	25724	1292	9486

5.5.5 Conclusion

The study carried out allowed to evaluate the conservative condition of the painting (i.e. μ -craquelures network), artistic techniques (oil on plywood, covering layer, etc.) and material employed by the artist. All these information demonstrated to be important and useful as artfingprints and in support of dating studies, actually in progress, and for further restoration project. The complete analytical procedure suggested for the identification of artfingprints bring to identification of more plausible pigments and new software application allowed a more precise analysis and data interpretation. For example, even if analysis suggest numerous pigment, according to Pigment analysis, the most plausible pigment are the following:

- White color: White titanium dioxide (Anatase phase) mixed with White Zinc Oxide or Lithopone (White Zinc Oxide and Barium sulfate); considering their concentration, the presence of barium sulfate and calcium sulfate are probably linked to White titanium dioxide;
- Blue color: Ultramarine;
- Red color: Red-Violet Ultramarine and Vermilion;
- Yellow: Chrome yellow (crocite phase).

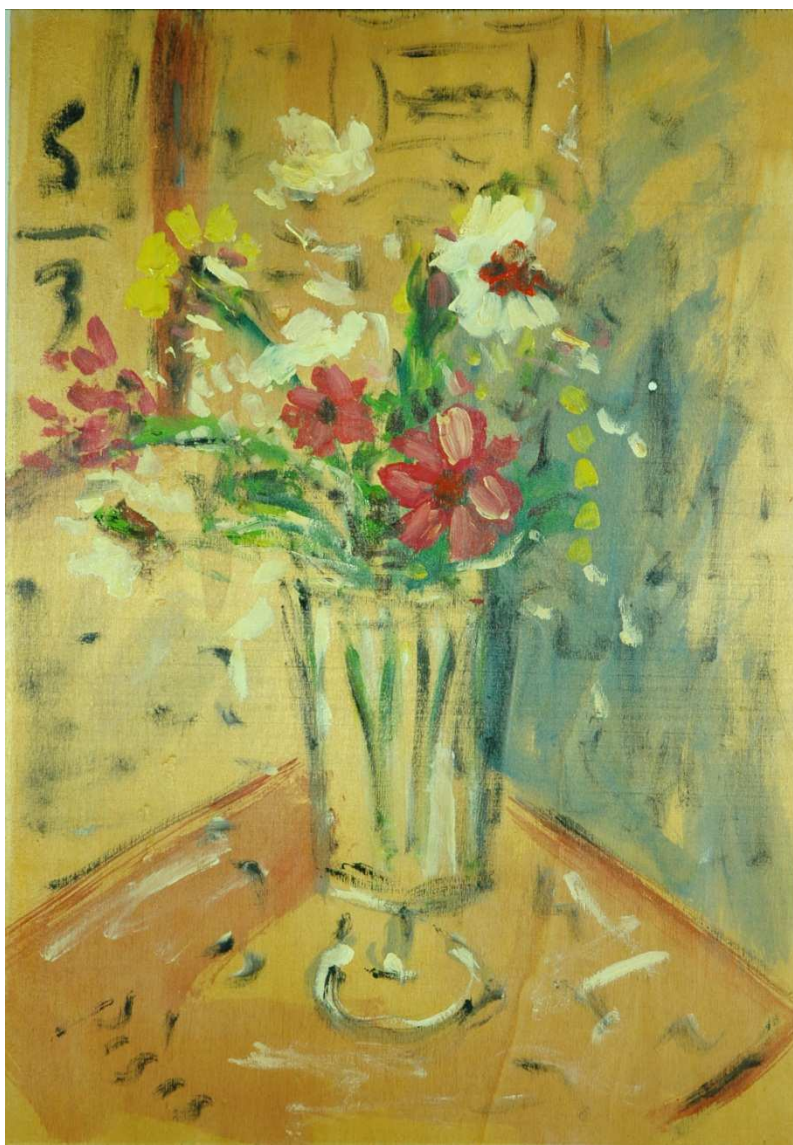
In addition to be useful for the restoration project, the pigment-artfingprints can support dating studies, despite for all the listed pigment, the patents and the consecutive commercial diffusion started in 19th and the painting, the mineralogical in-depth analysis on White titanium dioxide allows to attest “Flowers” compatibility with the period in which the painting, if attributed to Filippo De Pisis, should be made (1896-1956). In fact, if we consider that:

- the introduction on commerce of pigments based on Anatase/ BaSO_4 or Anatase/ CaSO_4 happened respectively in 1923 and 1925 ([McCrone W., 1994](#); [Leonardi R., 2005](#); [Lewis P.A., 1987](#));
- numerous studies sustain that artist were not inclined to use White titanium dioxide pure, especially at the beginning, and that they tested this new products mixing with other more admitted white pigment such as White Zinc Oxide ([Eastaugh N. et al., 2008](#));
- since 1939, the industrial process began to introduce Rutile phase, more easy to produce, and the first pigment based on pure Rutile appeared on 1957;

the detection of this mineralogical phase can be used in support to dating purpose, recommending a painting’s achievement not before than 1923 and after 1957.

Finally, from scientific point of view, it is possible to attest “Flowers” compatibility with the period of artistic production of Filippo De Pisis and that it could be created by a painter in the last thirty years of life of the painter in question.

ARTWORK PLATE VI



Author: *Filippo De Pisis (Italian artist, 1896-1956)*

Title: *Fiori nel bicchiere (Flowers in glass vase)*

Object: *Painting (oil on wood)*

Date: *1945*

Overall: *50 cm (height) * 35cm (width)*

Location: *Private Collection*

Note: *sealed handwritten text with information about artist and date (painting verso); study of Artist attribution and dating in progress.*

5.6 “Flowers in glass vase” by Filippo De Pisis (oil on plywood, 1945)

Size: 50.01 cm (height) x 35.02 cm (width)

The painting belongs to private collection since the end of 20th century, when it was acquired in art merchant and thenceforth, it has not been subjected to restoration intervention. On the verso of the painting, a handwritten text, signed by Giovanni Commisso, names the painting as “*Fiori nel bicchiere*” (“*Flowers in glass vase*”) and declares that the artwork was made by Filippo De Pisis in 1945. Two seals, in which “GC” letters are impressed on a piece of wax, were used to fix the text as a mark of authentication.

Having doubts about the originality of the painting and, especially, of the “expertize” signed by Commisso on the verso of the artwork, the owner decided to verify if, from chemical point of view, the pigment and artistic technique could be the same or very similar to that used in the painting Artwork plate n.V, in support to artist authentication and dating presently in progress. Moreover, considering the owner’s interest for the painting, Art-fingerprints were collected and gathered together in the art-fingerprints database, allowing to test also for this artwork the analytical proposal procedure to detect these microscopic peculiarities.

As for the previous artworks, the precise spatial coordinates of all points analysis collected for this painting are not reported, for previous agreement with owners about the confidential data.

5.6.1 The artist: 1943-1956

In 1943, Filippo De Pisis moved away from Milan (bombarded since August, 1943) to Venice, where he bought house, beginning to paint venetian glimpse and landscape. His artworks were so appreciated by literary and artistic world, that several Art Galleries, among that Biennale of Venice, organized art exhibition of his masterpieces in national and international cities. The recognized artistic award were numerous, even if his homosexuality created several problems. He travelled a lot in Italy and to Paris until 1948, when his illness (Alzheimer pathology) constrained him to reduce his travel. In the last period of his life, he often sojourned in the mental institution *Villa Fiorita* (Brugherio, Milan – Italy), where, even if he was free to walk and paint in the village, he was in a huff, losing his hope to cure himself of the his disease. He dead on April 2nd, 1956 in Milan (Italy) (Ferrari C.G., 2000).

5.6.2 The painting: subject

In this painting, the artist depicted some of the characteristic elements that it is possible to find in De Pisis' artworks of this period: floral composition is placed on the table and it captures the attention from the background, where a picture was sketched. The letters "S/B" refer to the De Pisis' atelier in Campo San Barnaba (Venice, Italy) (Commisso G., 1954). and they are easy to find in De Pisis artwork of this period (Brigante G.,1991). On the right bottom there is the signature "PISIS".



FIG. 180 "Flowers in glass vase": signature Pisis.

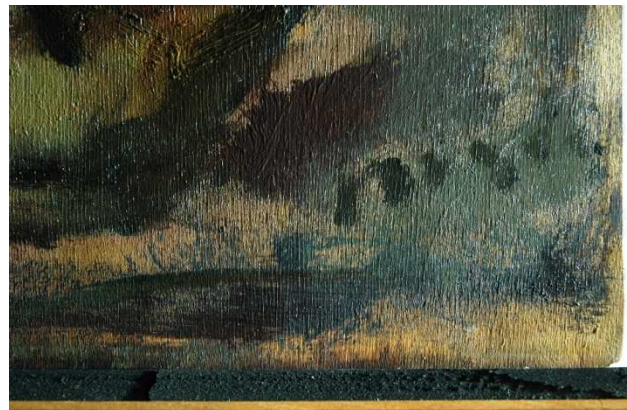


FIG. 181 "Flowers" (artwork plate V): signature Pisis.

5.6.3 Experimental methods

After a preliminary investigation of artistic technique and conservative condition through multispectral imaging analysis (VIS, UV, IR), stereomicroscope investigation and image processing, pigment analysis was carried out by EDXRF analysis on the whole painting (FIG.182).

Considered EDXRF results and that the principle aims of this study is to compare data with those obtained from other painting (artwork V), the sampling interested area with the same color: five micro-samples amount of painted materials (maximum size: 1,5-2 mm²) were taken from convenient red, white, yellow and green areas with a sterilized lance and under microscope (FIG.182).

Initially, the specimens, not embedded in resin, were observed with optical microscope both to known their

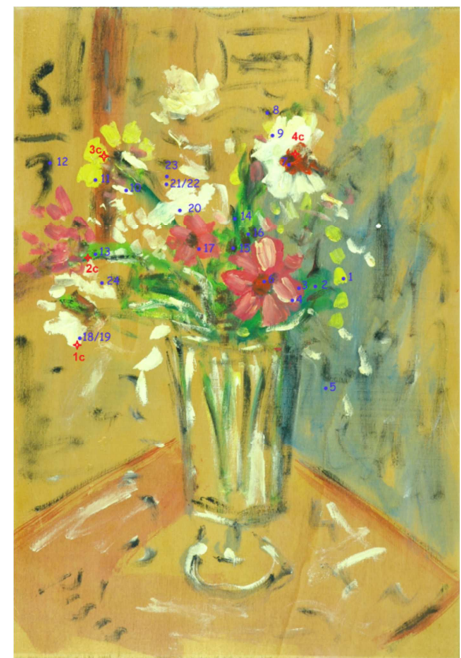


FIG. 182 *Flowers in glass vase*: EDXRF point analysis (in blue color) and sampling point (in red color).

nature for a good data interpretation and to select the most representatives for further deepened analysis. For their morphology, some samples were cut and placed in order to obtain a cross section.

μ -EDXRF, PIXE and SEM/EDS analysis were performed on untreated specimens to detect chemical composition of pigments and μ -Raman spectroscopy were carried out for a better pigment identification.

5.5.4 Results and discussion

5.5.4.1 Artistic technique and conservative conditions

The artistic technique is quite different from that used in previous artwork (Artwork plate V), even if, also in this case, it is oil (or resin medium) on commercially plywood. The wooden plank were not previously treated and there are not brushstroke enricher in matter than in “Flowers”. The color was usually spread onto the support and, probably, a final varnish covering was applied onto the whole painting (FIG. 183).



FIG. 183 GL photograph (detail): a) b) “Flowers in glass vase”(detail); c) “Flowers” (Artwork plate V).

The comparison between VIS and GL images is particularly useful to study the conservative state of the painting and artistic technique. Under GL investigation, the wood panel shows several abrasions that do not interest the pictorial layer; this damage can probably dates before the painting, as suggested by the presence of pigment compound within the tracks. In FIG.184 , the white spot, in the blue colored area, highlight a hole, 3.01 mm large, likely due to a metallic nail.

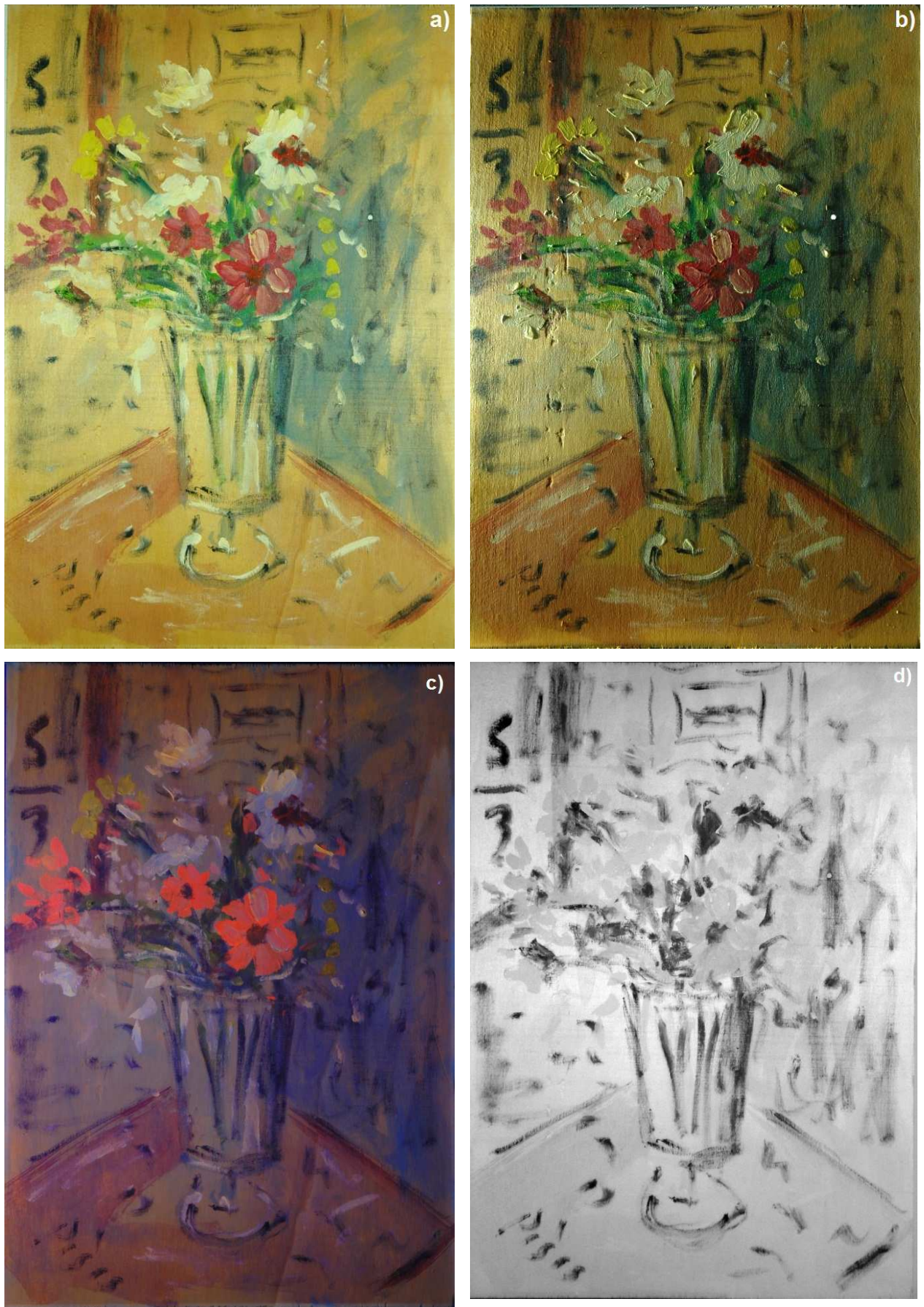


FIG. 184 “Flowers in glass vase”: a) VIS photograph; b) GL photograph; c) UV-VIS photograph; d) IR photograph.

Moreover, lower and higher border panel show an initial loss of wood fibers and, consequently, decrease of strength (FIG.185).



FIG. 185 GL photographs of the some damaged area of the painting: a) b) abrasions that do not interest the pictorial layer; c) lower border of wood panel with losing of wood fibers.

As concern, instead, the artistic technique, pictorial layer were spread not creating brushstrokes so enriched in matter, as in the previous artwork (“Flowers”, Artwork plate V). In fact, most of pictorial surface shows the wooden support, colored by diluted blend. Among the zone enriched in matter, those characterized by one color shade are numerous (as suggested by image processing, FIG.188), even if there are some pictorial area, especially in correspondence of floral subjects, in which color are mixed together to create that particular pictorial thickness characterizing De Pisis’ artworks. In spite of the arching of wooden panel in the middle part, wide *craquelures* network was not detected, probably linked both to plasticity of employed matter and to the thin pictorial layer. Instead, the investigation of surface at microscopic level revealed that, in addition to pictorial depression linked to drying medium process, there is a networks made by very thin μ -*craquelures*, about from 5 μm to 15 μm wide.



FIG. 186 “Flowers in glass vase”: microphotographs of brushstroke differently enriched in matter (magnification 13.4 x): a) pigment particles are collected within wood panel fibers; b) pictorial layer spread on wooden support; c) brushstroke rich in pictorial matter.

The comparison between VIS image and UV image shows the fluorescence of some pictorial blend, in particular the orange fluorescence of pink color and the light violet for some white area

(FIG. 184c). UV investigation allowed also to confirm the presence of covering varnish that was applied on the whole artwork, with the exception of narrow stripe on the painting border. The absence of retouches suggests that the entire composition, included signature, was made in the same period.

Finally, IR survey did not detect underpainting or some guide-line, supporting the idea that the two artworks were not made by the same artist.

In addition to confirms the artistic techniques previously observed by multispectral imaging and to study conservative condition, stereomicroscope allowed to capture further art-fingerprints that were collected in the database.

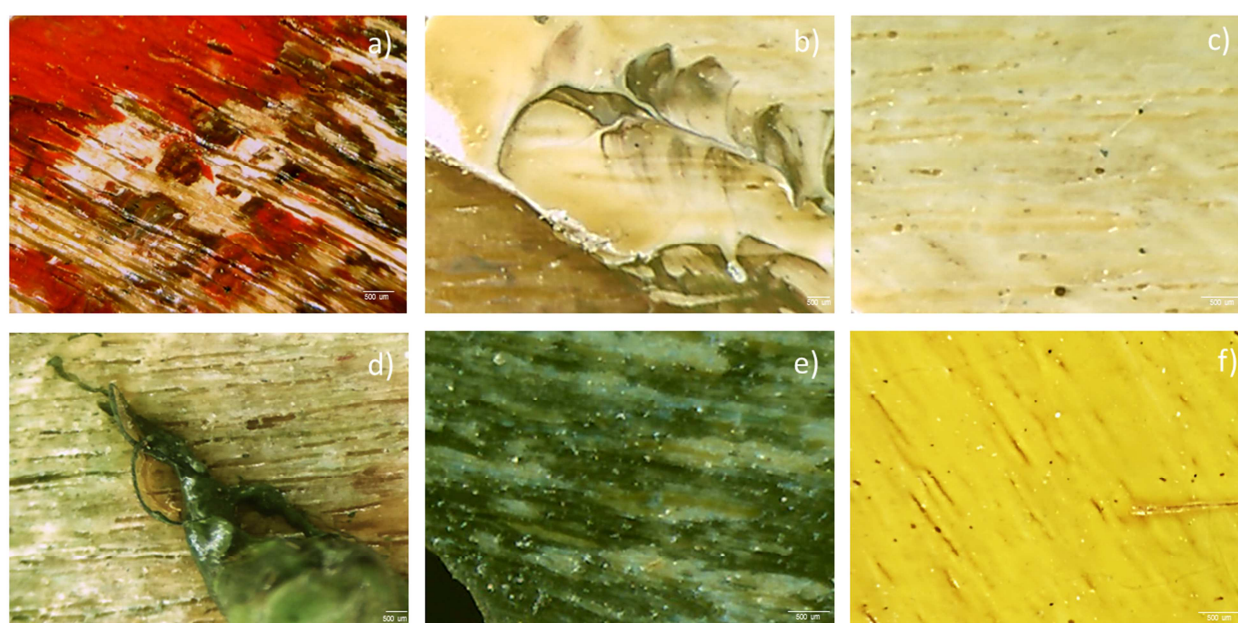


FIG. 187 “Flowers in glass vase”, observation under stereomicroscope at different magnification: a) microphotographs of color painting and wooden panel (magnification 40 x); b) d) brushstroked enriched in matter; c) e) microphotographs of color painting (magnification 45 x); f) microphotographs of color painting and μ -craquelures (magnification 60 x).

5.5.4.2 Pigment analysis

Considering results obtained by Image processing on the photograph of the previous diagnostic investigation (FIG.188), a preliminary EDXRF analysis was carried out on several points both on the painting recto (one color shade pictorial layer, support, support with varnish) and painting verso (wooden panel, wooden panel-varnish) for a better data analysis.

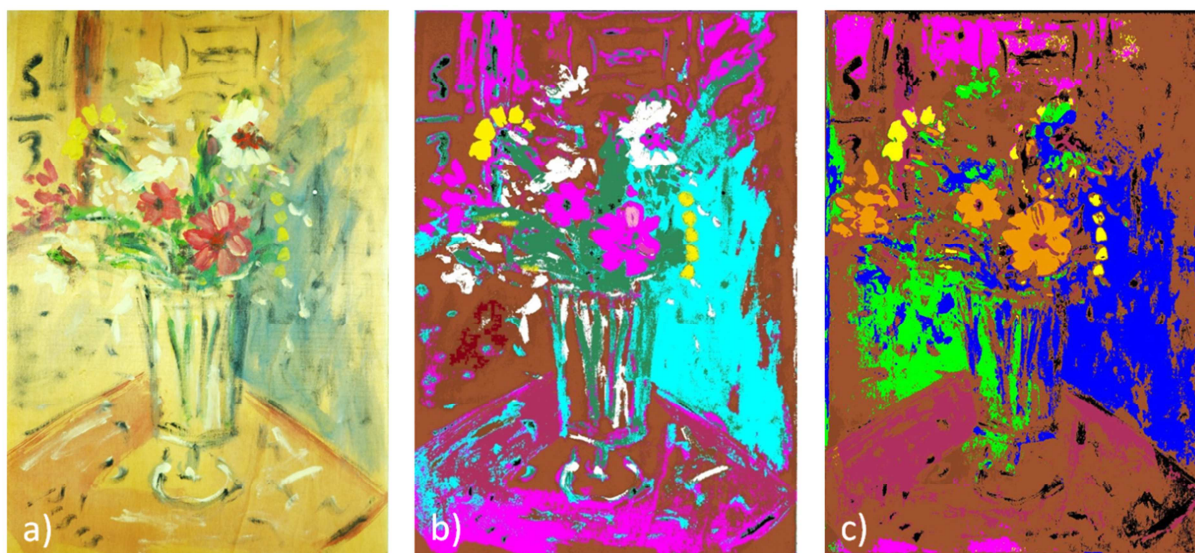


FIG. 188 Image Processing on “Flowers on glass vase” by F. De Pisis: a) VIS photograph; b) main ROIs’ color class; c) main ROIs’ UV fluorescence class (orange for intense orange fluorescence, etc.). Source: Ferrara University – ENEA.

The results of EDXRF analysis performed on the whole painting are shown in the following table.

TABLE 13 EDXRF analysis on painting “Flowers in glass vase”: average of Net Area values, gathered for color. Experimental set up: voltage 50 KeV, current 700 μ A (analysis on wooden panel: voltage 15 KeV and current 1500 μ A), Live time: 120 s, no filter, Air, Anode Molybdenum, collimator 0.650. In italic, average value greater than σ .

	Ba	Pb	Fe	Ca	Sr	Zn	Cr	Ti
White	78857	-	780	<i>1560.75</i>	6120.25	232.25	-	252345
Red	<i>39118.5</i>	<i>363799</i>	10565.5	531	3812.5	1762	33663	1857
Green	<i>30373.2</i>	<i>143874</i>	15488.8	1744	6991.4	1294.8	7469.4	-
Yellow	<i>69498.3</i>	<i>163414</i>	<i>417.333</i>	203	<i>24157.3</i>	-	<i>7297.67</i>	101915.7
Pink	<i>41821</i>	<i>28591.7</i>	<i>3272.667</i>	<i>32359</i>	<i>7584.33</i>	<i>165083</i>	<i>1731</i>	<i>97624.33</i>
Blue	<i>19349</i>	-	1778	2080	-	-	-	28569
Black	<i>31178.5</i>	<i>4426</i>	1736	<i>4435</i>	<i>5032.5</i>	7751.5	-	-
Wood panel	-	-	3912	<i>3168.33</i>	<i>2192.33</i>	-	-	-
Wood panel-varnish	688.5	-	<i>1984.25</i>	<i>1911</i>	<i>1847</i>	858.25	-	-

	Mg	Cu	K	Mn	Sn	Al	Si	Cl
White	-	-	<i>1160.5</i>	-	-	-	530	-
Red	-	<i>1439</i>	-	432	-	-	-	-
Green	-	<i>1671.8</i>	228.8	283.2	120.8	-	-	-
Yellow	-	-	<i>101.3333</i>	-	-	-	-	-
Pink	-	<i>700.667</i>	136	-	-	-	-	-
Blue	-	-	<i>1148</i>	-	-	6	10	-
Black	-	-	<i>515</i>	-	-	-	-	-
Wood panel	206	-	<i>1206</i>	-	-	8	17	39
Wood panel-varnish	<i>198</i>	-	<i>932</i>	-	-	3	5	40

The comparison between the untreated wood panel and the wood support with varnish suggest that the covering layer can contain barium and zinc, that are usually used as accelerator drying medium process. As concern, instead, pigments composition, EDXRF analysis revealed a blend less complex than in “Flowers”, suggesting the following pigments (Montagna G., 1999; Seccaroni C. *et al.*, 2002; Eastaugh N. *et al.*, 2008):

- White: barium sulphate, calcium carbonate and white titanium dioxide;
- Red pigment: Chrome red (Pb, Cr);
- Green pigment: Chromium Green Opaque or Viridian (Cr), Lamoriniere Green (Cr), Cinnabar Green (Fe, Pb, Cr) or Green lac (Fe);
- Yellow: Barium yellow (Ba, Cr), Chrome yellow (Pb, Cr) Strontium yellow (Sr, Cr) or maybe lead yellow (massicot or litharge);
- Pink: not a probable mixture among red and blue pigments but a compound based on zinc oxide (white base pigment) and red-pink organic pigment;
- Blue: Paris Blue or Prussian Blue (Fe);
- Black: Mars black (Fe), Black Iron Oxide (Fe), Prussian Black (Fe).

The list of pigments can be implemented by other possible pigments that are difficult to detect through EDXRF, such as organic pigment. Even if the proposal pigments are less than in “Flowers”, further deepened analysis were performed in order to exclude or confirm some of them, characterizing and identifying pigments particles through chemical-mineralogical analysis on μ -samples.

White pigment

The analysis on white color were carried out on samples taken from white colored area on the painting. In spite of the thick covering varnish, specific analysis on white particle pigments were achievable thank to the possibility to cut one of the white μ -sample and to placed it onto a stub in vertically, obtaining a cross section without embedding it into resin (FIG. 189). Investigation on the cross section allowed to measure the thickness of pictorial layer: covering varnish is about 14.2 μm ($\sigma=0.30$) meanwhile the white layer thickness has average value of 24.7 μm ($\sigma=0.31$).



FIG. 189 OM photograph of Sample DeP_L04 at different magnification: a) 10x, GL; b) 20x; c) 50x, GL.

Considering the previous measurements carried out on the background (carbon tape – aluminum stub) to avoid error interpretation, EDXRF analysis on samples suggested a white pigment made by white titanium dioxide, barium sulfate (FIG.) (Montagna G., 1999; Seccaroni C. *et al.*, 2002; Eastaugh N. *et al.*, 2008). There are, instead, some doubts White Lead Oxide contribution: EDXRF analysis, in fact, detect lead peaks but these signals are also well identifiable for the background.

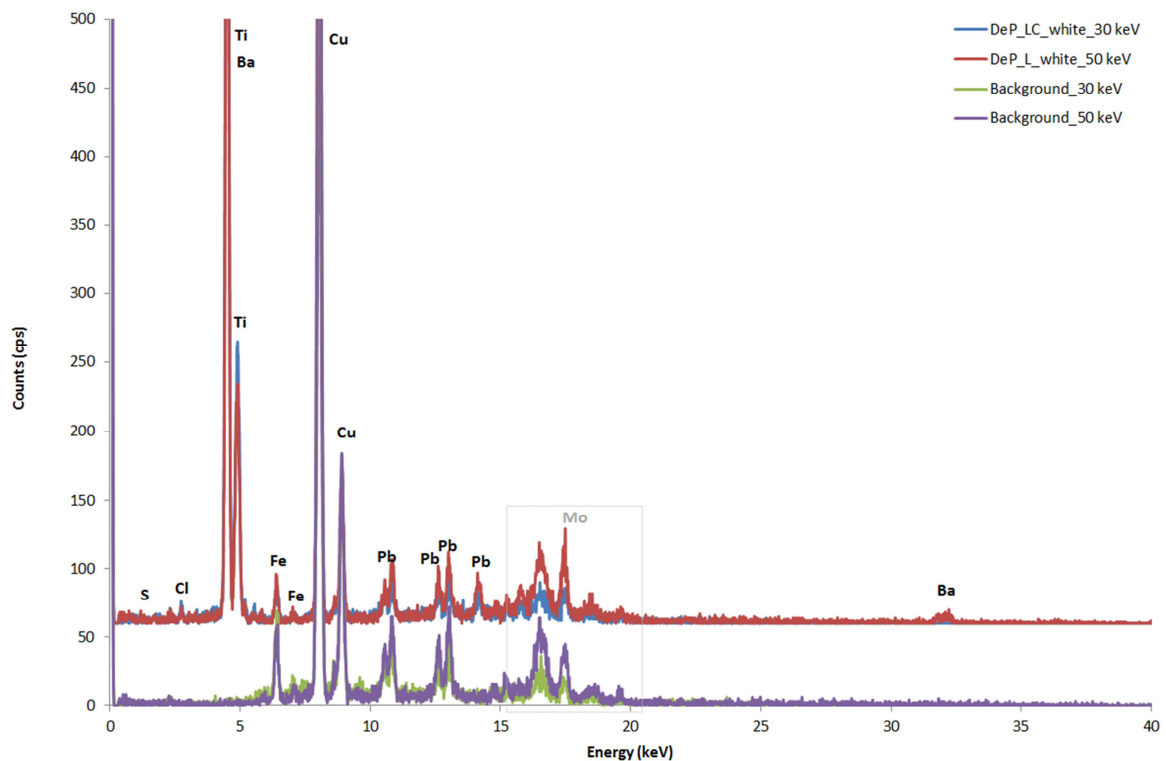


FIG. 190 XRF spectra on White pigment: total spectra from different set-up, not subtracting background. Experimental set up: voltage 50 KeV and current 700 μ A, voltage 30 KeV and current 1300 μ A. Live time: 60 s, no filter, Helium flow, Anode Molybdenum, collimator 0.200.

PIXE analysis performed on free samples confirmed the presence of white titanium dioxide and barium sulfate, instead, zinc detected by analysis could be due to the use in the pictorial medium

as auxiliary driers, being known for its properties as drier accelerator for paints and coatings (Anderson J., 2006). Moreover, it is possible, instead, to exclude White Lead Carbonate as component for white color. In addition to further chemical elements detected also by EDXRF, PIXE analysis revealed some particular element such as strontium, chromium and light element as phosphor, potassium and chlorine that could belong to pre-available pigment compounds.

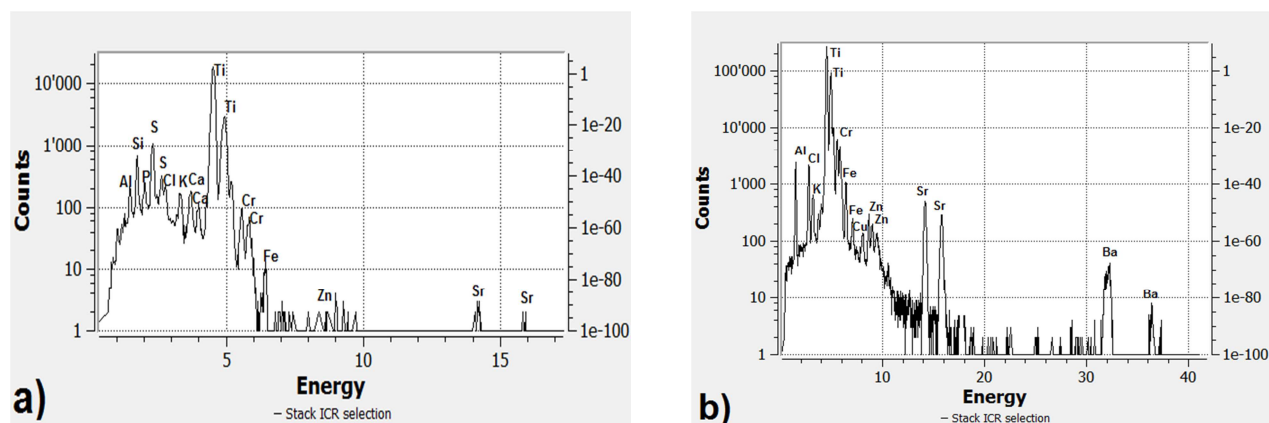


FIG. 191 PIXE spectra of white pigment: a) low energy detector; b) high energy detector. Experimental set up: particle/energy 3 MeV, current p+, Dose/s 200, Helium flow. Source: AGLAE facility, C2RMF Laboratory (Louvre, Paris – France).

SEM photographs show two kind of fine rounded particles immersed in an organic compound (pigment medium). It is possible to detect some grains with a diameter of 1.0 μm and other which particle size lies in the region of 0.3 μm .

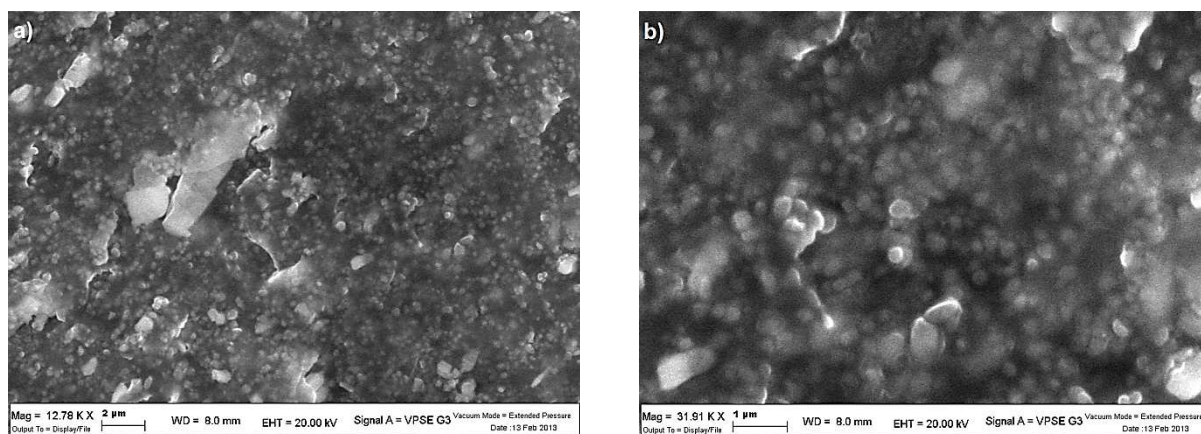


FIG. 192 SEM microphotograph of White samples: a) fine-grained aggregates and particles with rounded shape (magnification 12.78 KX); b) White titanium dioxide and Barium sulfate fine grains (magnification 31.91 KX). Source: Ferrara University.

EDS analysis revealed that the smallest particles are mainly made by titanium and oxygen, meanwhile sulfur and barium are detectable for bigger grains, allowing positive feedback with reference research on this pigment (Eastaugh N. et al., 2004^B).

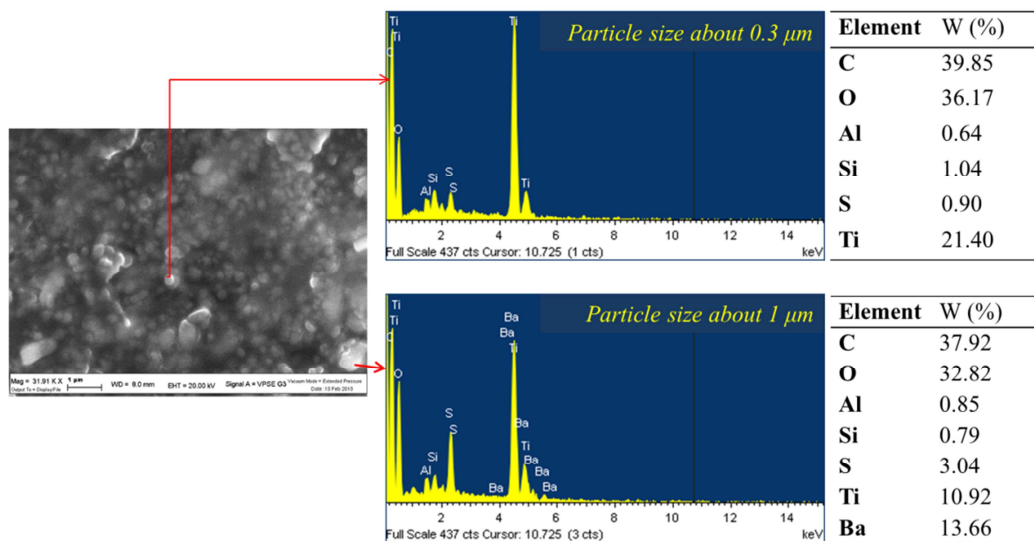


FIG. 193 EDS spectra on the investigated area of white samples, as presented in Fig.192.b.

Investigation, on white compound-varnish interlayer, highlights the organic nature of covering layer, enriched also in silicon and aluminum, probably linked to their drying properties for oil painting, recognized also in the past (Lutzenberger K. et al., 2010).

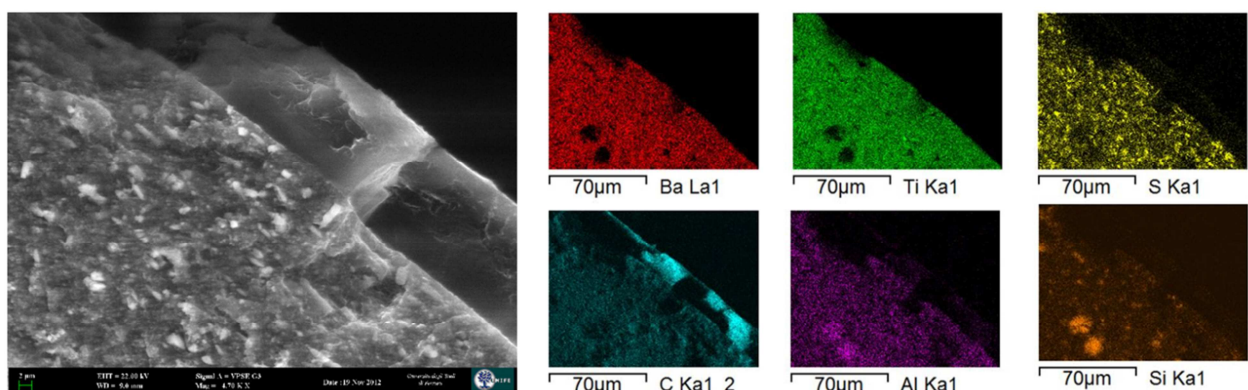


FIG. 194 EDS mapping analysis on the white pigment-varnish interlayer. Source: Ferrara University.

Moreover, results from Raman spectroscopy, on white particles, confirm the use of White titanium dioxide, detecting characteristic Raman bands of Rutile phase at 446 cm^{-1} (s) and at 609 cm^{-1}

(s) (Burgio L. *et al.*, 2001; Chen G. *et al.*, 2012; Ropret P. *et al.*, 2008) and Raman bands of Barium Sulfate at 990 cm^{-1} (s) (Halac E.B. *et al.*, 2012) (FIG.195).

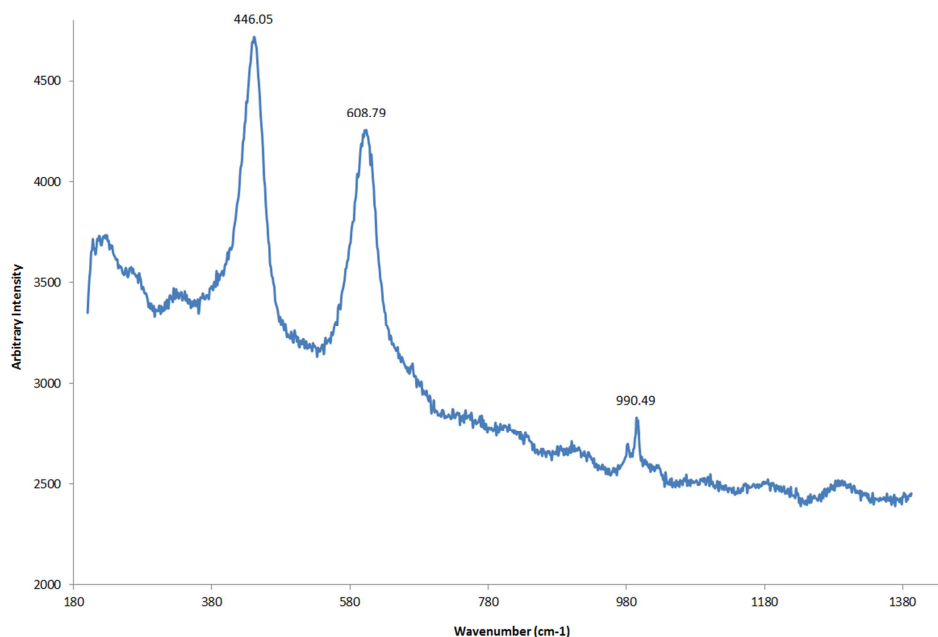


FIG. 195 Raman spectra on white samples (632,81 nm excitation, 50 x magnification): Rutile phase and Barium Sulfate. Source: Ferrara University.

Finally, pigment analysis suggest that the painter used White titanium dioxide (Rutile phase) for the white area and the presence of White Barium Sulfate is detected because pigments based on this compound (White titanium dioxide) can additionally contain other chemical composts such as barium sulfate or calcium sulfate.

Yellow pigment

Specimens, taken from a yellow colored area, show a reflective covering surface, behind that it is possible to see only red-orange particles in a white and homogeneous layer. Even if the presence of this varnish cause several difficulties to carry out some kind of analysis, its observation under microscope pointed out a network constituted by μ -*craquelures prématurée*, wide less than $10\ \mu\text{m}$, that mainly interested the upper layern (FIG.196)

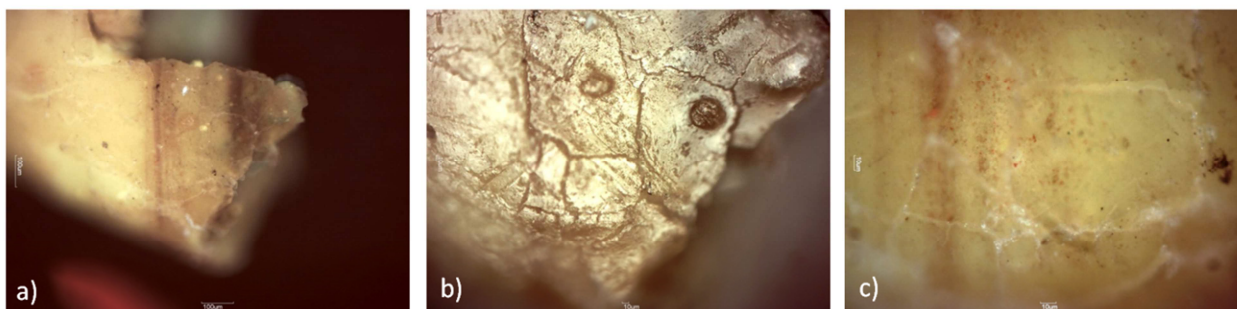


FIG. 196 OM photograph of Sample DeP_L05 at different magnification: a) 10x; b) 20x; c) 50x.

Considering the results from previous EDXRF analysis carried out on the whole painting, that suggested to exclude pigment only based on barium, and chemical composition of the background (carbon tape – aluminum stub), EDXRF analysis on samples did not give additional information about possible yellow pigment employed by the artist. The measurements on specimens, in fact, allowed to hypothesize Strontium Yellow (CrO_4Sr) or Chrome Yellow (PbCrO_4), being the spectra characterized by lead, strontium and chrome. Yellow Lead Oxide (PbO , litharge or massicot phase) were excluded, considering that lead is also present in the background spectra and the peak intensity is not higher (same analytical working conditions) (Montagna G., 1999; Seccaroni C. *et al.*, 2002; Eastaugh N. *et al.*, 2008).

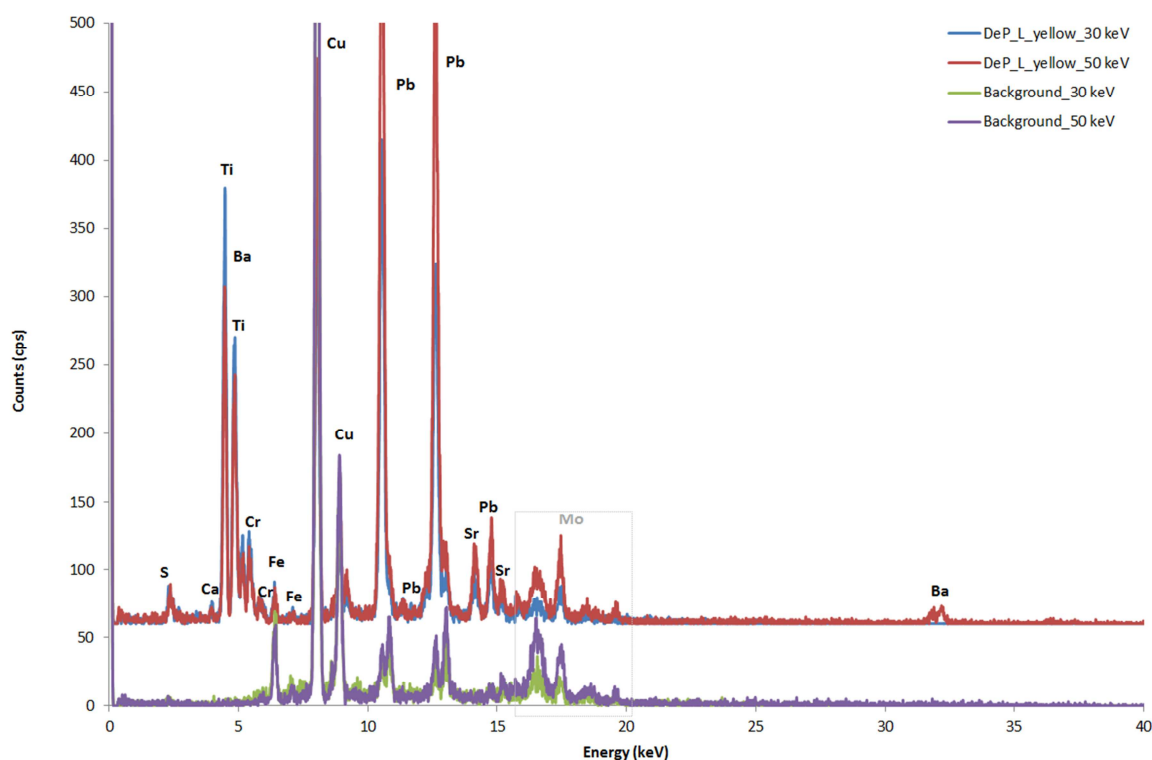


FIG. 197 EDXRF spectra on Yellow pigment: total spectra from different set-up, not subtracting background. Experimental set up: voltage 50 KeV and current 700 μA , voltage 30 KeV and current 1300 μA . Live time: 60 s, no filter, Helium flow, Anode Molybdenum, collimator 0.200.

Considering that microscope investigation showed that the yellow color is applied onto white layer, from the comparison between PIXE spectra of this two color, it is possible to consider that lead is typical chemical element for the yellow shade. Furthermore PIXE analysis on yellow confirm element (P, K, Cl, Fe, Cr, etc.), previously detected on white sample, suggesting their belonging to pre-available pigment-medium material. In this way, it is not possible to exclude litharge or massicot.

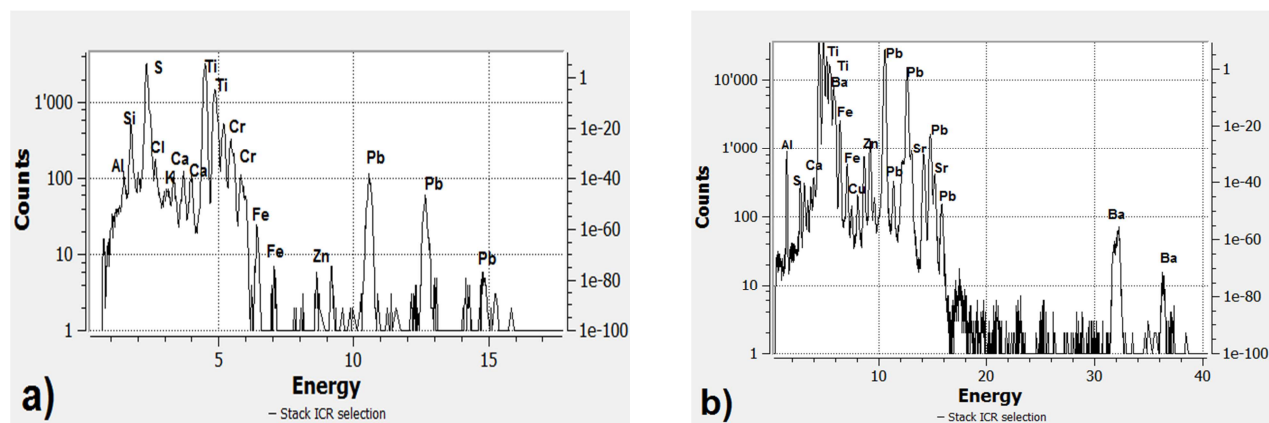


FIG. 198 PIXE spectra of yellow pigment: a) low energy detector; b) high energy detector. Experimental set up: particle/energy 3 MeV, current p+, Dose/s 200, Helium flow. Source: AGLAE facility, C2RMF Laboratory (Louvre, Paris – France).

Unfortunately, through SEM/EDS analysis and μ Raman it was not possible to find pure particle to carry out more precious analysis on pigment crystal.

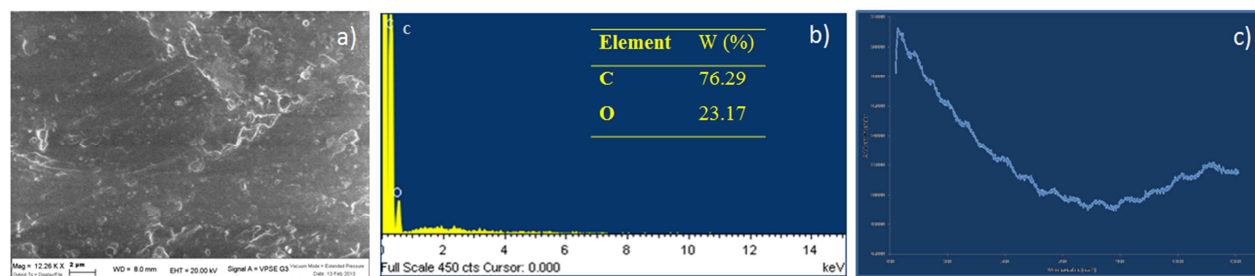


FIG. 199 Analysis on yellow samples: a) SEM microphotograph of yellow upper layer and fine-grained aggregates shape (magnification 12.26 KX) and b) EDS spectra on the corresponding investigated area; c) Raman spectra shows high reflectance value (before 300 cm^{-1}) that hid possible yellow pigment particles. Source: Ferrara University.

In conclusion, considering the results of all the analysis, it is possible hypothesize different proposals for yellow pigment such as Strontium Yellow (CrO_4Sr), Chrome Yellow (PbCrO_4) or Yellow Lead Oxide (PbO , litharge or massicot phase), even if there are some doubts for the latter, especially if we consider the morphology of yellow pictorial layer under microscope.

Red pigment

The analysis on red color were carried out on samples taken from painted red flowers. Under microscope, specimens highlight craquelures network spread on the surface of covering varnish, but that not interested completely pictorial layer (FIG. 200).



FIG. 200 OM photograph of red sample DeP_L09: red pictorial layer behind cracked covering varnish (magnification 20x); b) GL photograph of investigate area in a) highlight craquelures network (magnification 20x); c) red pictorial particles (magnification 50x). Source: Ferrara University.

EDXRF measurements previously carried out on the carbon tape – aluminum stub (background) allowed to better interpret the chemical composition of red pigments: analysis on samples confirms the presence of lead and chromium, supposing red pigment mainly made by Chrome Red (FIG.201) (Montagna G., 1999; Seccaroni C. *et al.*, 2002; Eastaugh N. *et al.*, 2008).

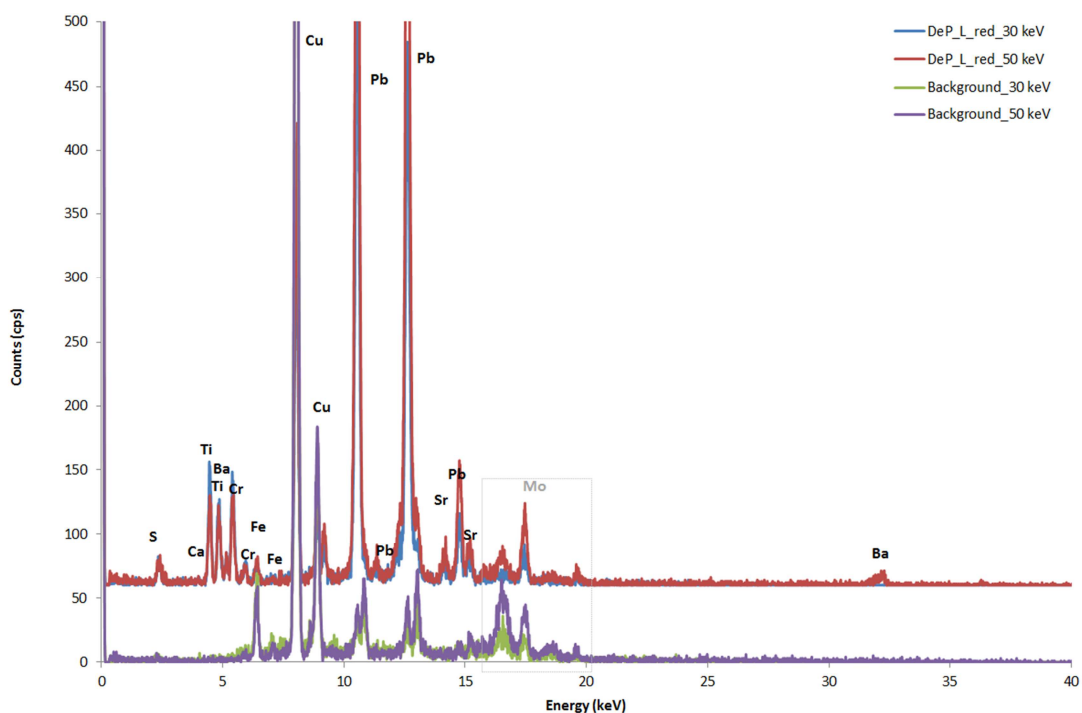


FIG. 201 XRF spectra on red pigment: total spectra from different set-up, not subtracting background. Experimental set up: voltage 50 KeV and current 700 μ A, voltage 30 KeV and current 1300 μ A. Live time: 60 s, no filter, Helium flow, Anode Molybdenum, collimator 0.200.

The chemical composition, suggested for the red color, is also verified by PIXE analysis that revealed high peaks of lead and chrome. Even if the detection of cadmium can suppose the presence of Cadmium red, the absence of Selenium on red specimens exclude this pigment, being Cadmium selenide sulfide or Cadmium selenide. Even that, PIXE analysis revealed further light chemical elements, not detected with previous analysis on red samples (such as Al, Si, Cl, K), probably due to covering varnish or to deposition onto covering surface (salt, particulate, etc.); however, being linked to the analyzed surface and pigments, they can be considered art-fingerprints of the entire system pictorial layer-support.

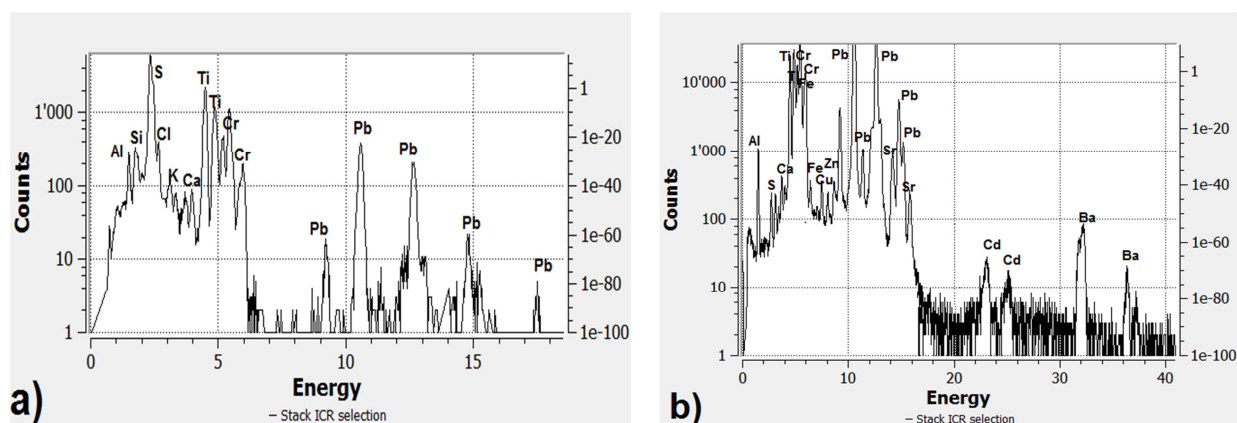


FIG. 202 PIXE spectra of red pigment: a) low energy detector; b) high energy detector. Experimental set up: particle/energy 3 MeV, current p+, Dose/s 200, Helium flow. Source: AGLAE facility, C2RMF Laboratory (Louvre, Paris – France).

SEM/EDS analysis revealed very fine-grained particles of 0.5 μm or less, with spherical shape, immersed in an organic compound; the chemical composition of these fine grains is characterized by chrome and lead, supporting the hypothesis of Red Chrome pigment (Eastaugh N. et al., 2004^B; Montagna G., 1999). Moreover, some crystals with different shape and size, mainly composed by sulfur, barium and lead, were detected on the same samples: particle shape is typically of crushed angular and the size ranges from fine to bigger (less than 2 μm), with broad size distribution. Considering this particular morphology and the chemical composition, the latter grains could be attributable to baryte crystals, a mineral that can be contained as adulterants in less pure Red Chrome products (Eastaugh N. et al., 2008).

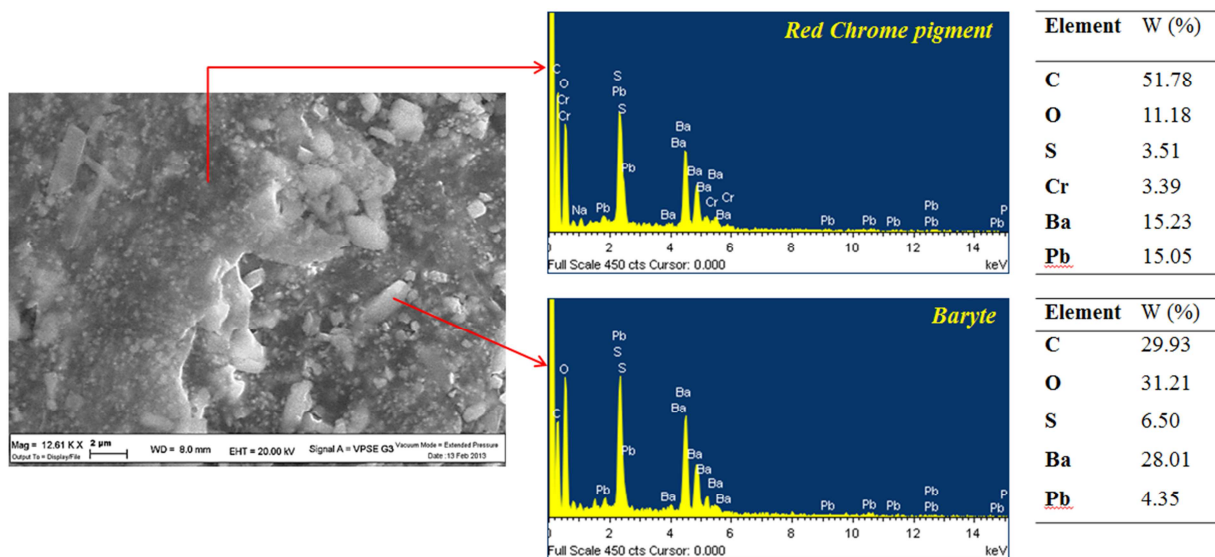


FIG. 203 SEM/EDS analysis on red sample: SEM photograph (magnification 12.61 KX) and EDS spectra on the investigated area. Source: Ferrara University

Raman spectroscopy confirm the presence of Red Chrome, with characteristics Raman bands at 323 cm^{-1} (m), 341 cm^{-1} (s), 355 cm^{-1} (m), 824 cm^{-1} (vs), 987 cm^{-1} (w) [28]; the peak at 987 cm^{-1} can be also attributable to 988 cm^{-1} (vs) of baryte (Bell I.M. *et al.*, 1997; [28; 30]).

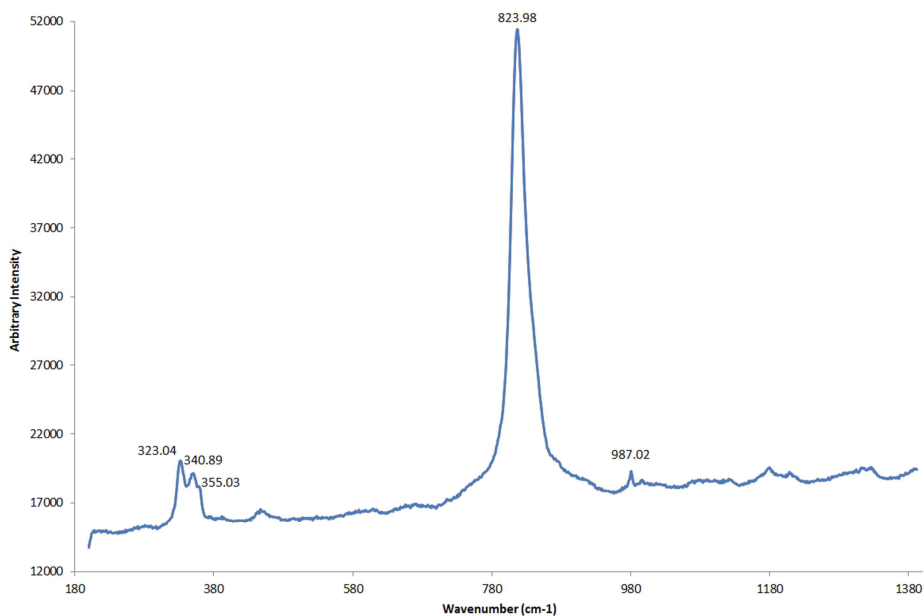


FIG. 204 Raman spectra on red samples (632,81 nm excitation, 50 x magnification): Chrome Red and Barium Sulfate. Source: Ferrara University.

Finally, pigment analysis confirmed the use of Red Chrome for red pictorial layer; the presence of baryte allowed to suppose that the pigment is less pure.

Green pigment

Samples, collected in correspondence of light green leads, show the overlapping of three different layers (FIG. 205b): green pictorial layer, about 1.662 mm ($\sigma=0.58$) thick (FIG. 205b,1), inter-layer green-varnish, thick about 22.9 μm ($\sigma=0.70$) (FIG. 205b,2) and the varnish covering is about 16.5 μm ($\sigma=0.27$) (FIG. 205b,3).

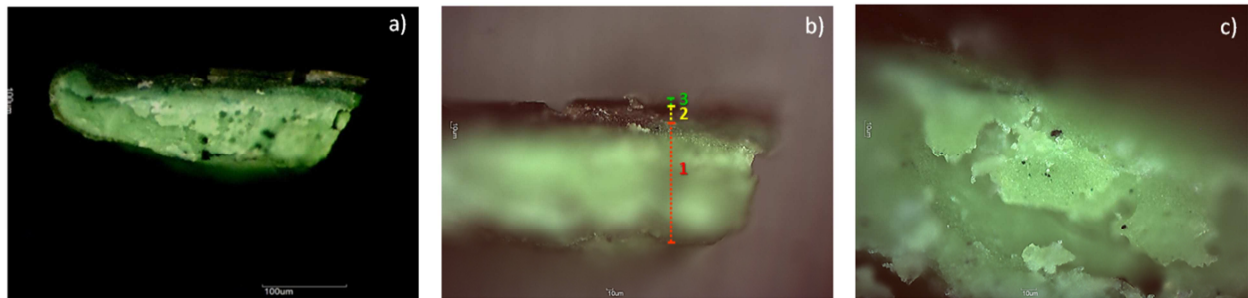


FIG. 205 OM photograph of sample DeP_L09 at different magnification: a) 10x; b) 20x; c) 50x.

Both EDXRF analysis carried out on the pure green colored area in the cross section and on the green/brown samples (green samples covered by varnish) revealed the same chemical composition but with a reduction of signal peaks for spectra of green/brown varnish specimens; in this way, it is possible to hypothesize the organic nature of varnish. Therefore, excluding the elements which signals are also linked to background, EDXRF spectra suggest the use of Chromium Green (opaque: Cr_2O_3 ; transparent: $\text{Cr}_2\text{O}_3 \cdot 2\text{H}_2\text{O}$) for the green color (Montagna G., 1999; Seccaroni C. et al., 2002; Eastaugh N. et al., 2008). Peaks of barium, titanium and sulfur are probably due to white color interference.

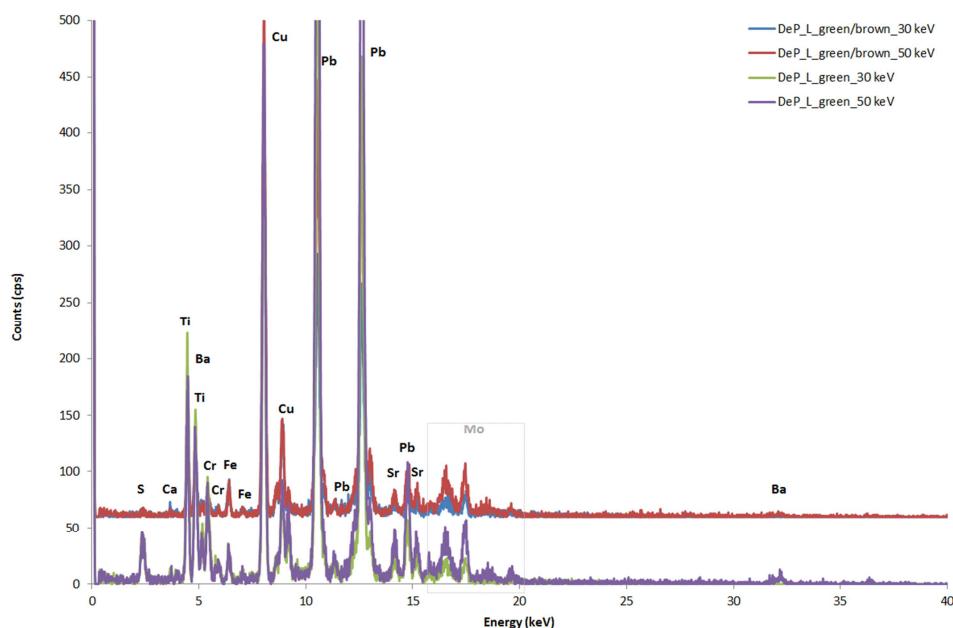


FIG. 206 XRF spectra on Green pigment: total spectra from different set-up, not subtracting background. Experimental set up: voltage 50 KeV and current 700 μA , voltage 30 KeV and current 1300 μA . Live time: 60 s, no filter, Helium flow, Anode Molybdenum, collimator 0.200.

Furthermore, in addition to confirm proposed Chromium Green, the detection of other chemical elements by PIXE analysis allow to consider also the presence of Green Earth, being characterized by Na, K, Mg, Fe, Al and Si. Barium, titanium and sulfur could be attributed to other color contamination (i.e., White pigment), meanwhile lead as dryer in medium pigment or due to the contamination of green samples by red particles (Montagna G., 1999; Eastaugh N. *et al.*, 2008).

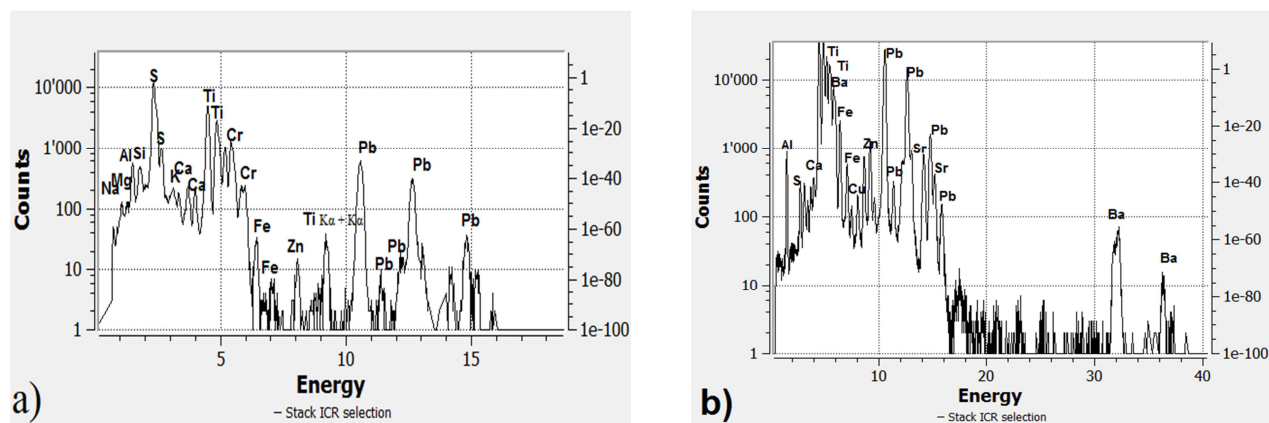


FIG. 207 PIXE spectra of green pigment: a) low energy detector; b) high energy detector. Experimental set up: particle/energy 3 MeV, current p+, Dose/s 200, Helium flow. Source: AGLAE facility, C2RMF Laboratory (Louvre, Paris – France).

SEM/EDS analysis revealed not homogeneous compost made by small particles with variable shape and size: it is possible, in fact, to observe aggregates of very fine particles with irregular and angular shape and grain size less than with 1 μm and other, which dimension are about 2 fine μm . This particular morphology can support the hypothesis of Green Earth towards to Chromium Green, because the latter is usually characterized by very particles with round shapes (Eastaugh N. *et al.*, 2004^B; Montagna G., 1999).

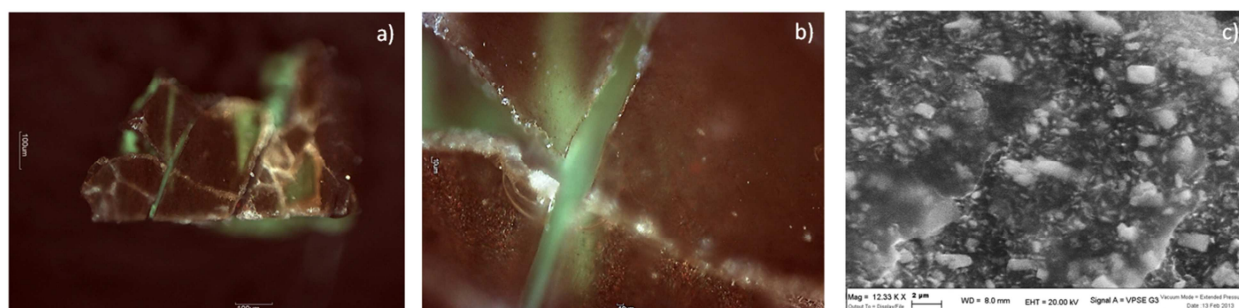


FIG. 208 Microphotograph of green/brown samples DeP_L11: a) OM photograph (magnification 10 X); b) OM photograph (magnification 50 X); c) SEM image of area behind the varnish layer (through cracks) shows fine-grained aggregates and particles with irregular shape (magnification 12.33 KX). Source: Ferrara University.

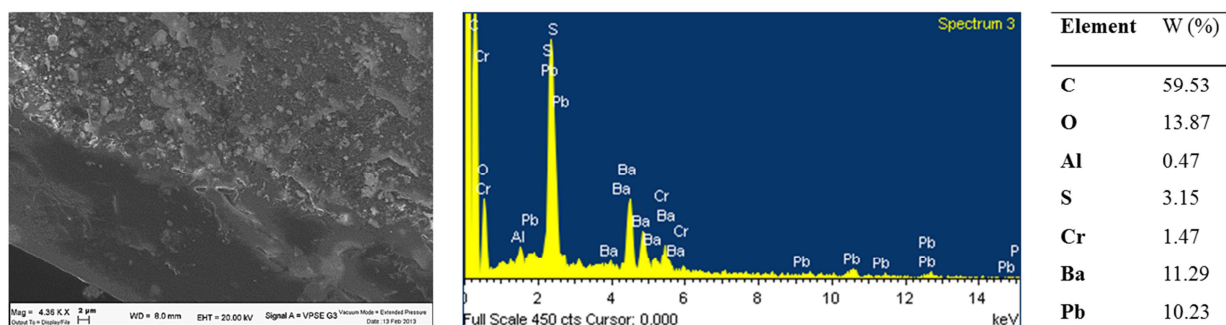


FIG. 209 SEM/EDS on cross section sample DeP_L09: SEM photograph of interlayer green-varnish (magnification 4.36 KX) and EDS spectra of the investigated green area. Source: Ferrara University.

Finally, Raman spectra of green samples confirm the presence of Green Earth, that is characterized by the following Raman bands at: 1532 cm^{-1} (w), 1033 cm^{-1} (w), 1393 cm^{-1} (w), 1293 cm^{-1} (w), 1280 cm^{-1} (w), 1216 cm^{-1} (w), 1083 cm^{-1} (w), 815 cm^{-1} (w), 774 cm^{-1} (w), 740 cm^{-1} (w), 687 cm^{-1} (m), 645 cm^{-1} (w), 508 cm^{-1} (w) [28; 29; 31; LabSpec 5 Raman Spectroscopy Library].

In pigment analysis, the term *Green Earth* indicates geological deposits characterized by mixtures of minerals, among that, green minerals are predominant; thereby, the mineralogical composition can be different, especially for artificial compounds linked to secret patents and commercial companies (Eastaugh N. et al., 2008). Considered that, the identification of the pigment's mineralogical composition could be particularly interesting to detect more detailed art-fingerprints.

The study allowed to identify the following mineralogical phases among the detected Raman bands of green specimens (Green Earth pigment):

- Celadonite : 701 cm^{-1} , 1081 cm^{-1} , 544 cm^{-1} , 392 cm^{-1} (Aliatis I. et al., 2009; 28; 30);
- Calcite: 1083 cm^{-1} (w) (Aliatis I. et al., 2009; Jehlička J. et al., 2009 ; Lécuyer C. et al., 2012 ; Park K.,1967; Vagenas N.V. et al., 2003);
- Baryte: 647 cm^{-1} (w), 981 cm^{-1} (vs) (Jehlička J. et al., 2009; 28; 30);
- Graphite: 1330 cm^{-1} , 1532 cm^{-1} (Smith G.D. et al., 2004; Van der Weerd J. et al., 2004; 28; 30).

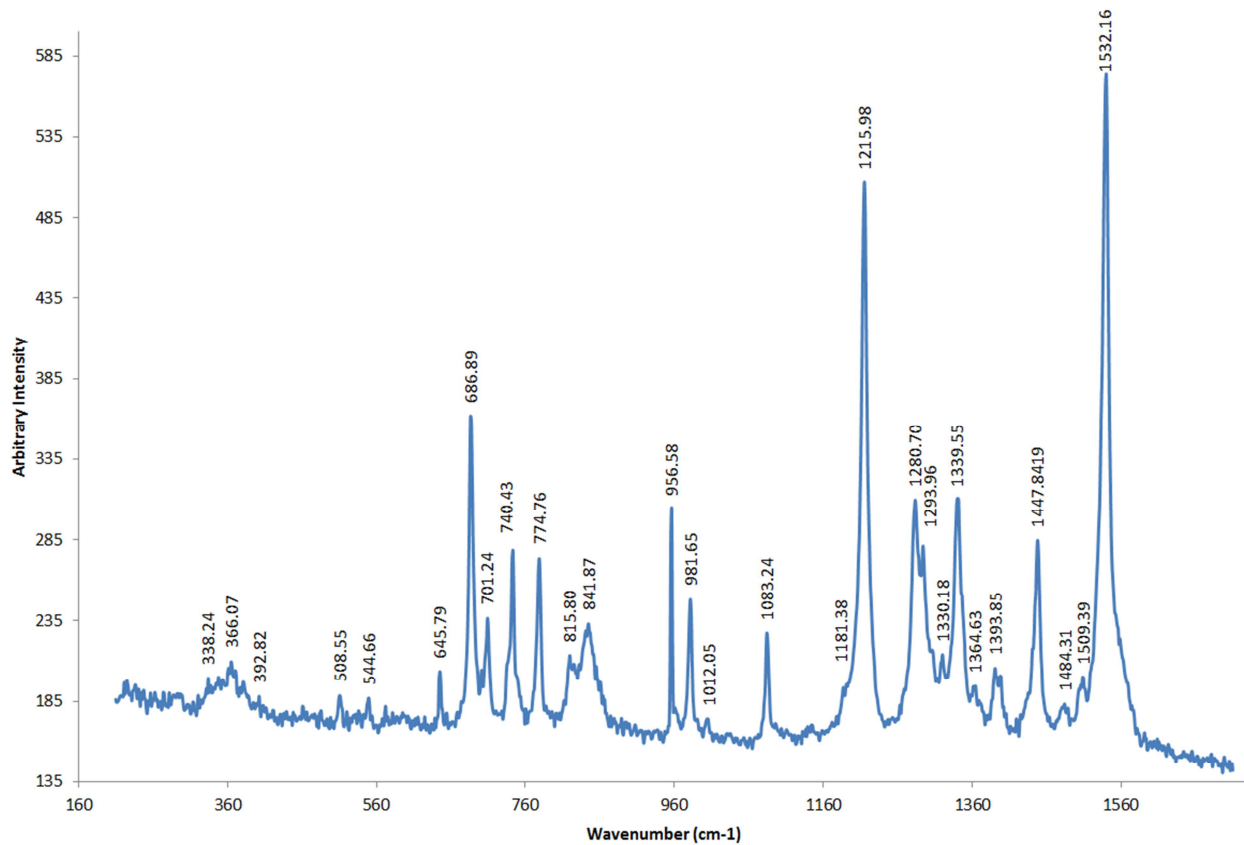


FIG. 210 Raman spectra on green samples (632,81 nm excitation, 50 x magnification): Green Earth. Source: Ferrara University.

In conclusion, pigment analysis suggest that the artist used Green Earth as pigment for green color and that chromium, found in chemical analysis, is attributable to a contamination by red particles rather than a green blend made by Green Earth and Chromium Green.

TABLE 14 PIXE analysis on “Flowers in glass vase” samples. Average value: region of interest were extracted using PyMCA software, data expressed in counts. Experimental set up: particle/energy 3 MeV, current p+, Dose/s 200, Helium flow.

Low Energy										
	Na	Mg	Al	Si	P	S	Cl	K	Ca	Ti
White	5772	864	13405	28766	8057	32716	2211	3620	1830	346146
Yellow	3004	984	6398	17823	3975	22018	5709	2374	2620	377637
Green	2918	1144	9204	3966	936	87176	11744	1811	2037	6299
Red	1913	0	9214	6348	1892	66115	6674	1435	905	4499

High Energy										
	Na	Mg	Al	Si	P	S	Cl	K	Ca	Ti
White	-	-	-	-	-	202418480	0	11275	2634	346146
Yellow	-	-	-	-	-	974840640	0	16252	3968	377637
Green	-	-	-	-	-	0	0	15393	3200	6804
Red	-	-	-	-	-	0	0	13359	1423	3950

Low Energy										
	Cr	Fe	Cu	Zn	Sr	Ba # LA	Hg # LA	Pb # LA*	Pb # MA	Ni
White	-	488	38	87	-	188341	0	0	4490	-
Yellow	-	1029	116	298	-	209527	0	0	0	-
Green	37240	848	875	0	-	354939	0	274944	244834	-
Red	64444	141	0	176	-	310713	824	301842	306806	-

High Energy										
	Cr	Fe	Cu	Zn	Sr	Ba # LB	Hg # LA	Pb # LA	Pb # M1	Ni
White	-	365	9	45	1284	173399	8	18	483948	55
Yellow	-	706	46	133	1271	205020	13	20	254340	11
Green	37240	831	739	102	2573	370629	101	176258	-	114
Red	64444	137	75	116	2057	315624	72	188652	-	134

5.6.5 Conclusion

In addition to identify useful microscopic features for the art-fingerprints database, the study carried out allowed to evaluate the conservative condition of the painting, artistic techniques (oil on plywood, covering varnish, etc.) and material employed by the artist.

All these information were compared with those obtained by the study on artwork “Flowers”, which authentication and dating research are currently in progress.

The analysis show a different artistic technique characterized by brushstrokes spread on the wooden panel in a rapid way and with few pictorial blend. The support and the painting were treated with a varnish enrich in barium and zinc, likely as drying accelerator medium process. Even if the pictorial layer is poor in matter, the painting film shows the beginning of a *craquelures* network with *μ-craquelures*, around 10 μm wide. Pigment analysis allowed to better characterize the pictorial compounds, decreasing the list of pigments proposed by EDXRF. The analysis on samples, in fact, suggest the following pigment (identifying – when possible – the mineralogical phases):

- White: White titanium dioxide (Rutile phase), in which the presence of barium sulfate can be attributed to an additional contents in White Titanium pigment rather than to White Barium Sulfate pigment. It is usually, in fact, that compounds based on this pigment can additionally contain other chemical composts such as barium sulfate or calcium sulfate.
- Yellow: the particularly morphology of specimens (thick varnish layer) does not allowed to exclude any pigment proposed by EDXRF analysis on painting (even if there are some doubts for litharge and massicot phase);
- Red: Red Chrome, in which the presence of baryte crystals allowed to suppose that the pigment is not pure;
- Green: Green Earth pigment, characterized by minerals celadonite as main coloring agents and by other minerals such as calcite, baryte and graphite.

In addition to see out the research of new and more specific art-fingerprints, a deepened pigment analysis, based on chemical-mineralogical pigment identification, can support also the dating studies of the artwork. For instance, considering the history of use of Titanium White pigment, we can suggest two possible post-quem date for this painting:

- Artwork made after 1939 because it is known that Rutile/BaSO₄ came into use in 1939 (McCrone W., 1994; Leonardi R., 2005; Lewis P.A., 1987);

- Artwork made after 1957, if we consider that the particle size of analyzed pigment lies in the region of 0.3 μm (production of high quality) and that pure rutile of this quality was introduced on commerce in 1957 (McCrone W., 1994; Leonardi R., 2005; Lewis P.A., 1987).

If we consider valid the second hypothesis about post-quem date (1957), even if the pigment is mixed with barium sulfate (probably added intentionally by the artist), it is possible to suggest that the analyzed artwork could be a counterfeit painting, being made after the death date of F. De Pisis (1956). For this reason, it is suggested a more in-depth analysis and artistic-historical research.

In conclusion, all this information demonstrated to be important and useful not only as art-fingerprints but also in support of authentication and dating studies, in progress, and for future restoration projects.

6. CONCLUSION

It is known that one of the most important problem of artwork's uniqueness is related to the handling of the works for art exhibitions around the world and the risks linked to this aspect, likely the replacement of original paintings with counterfeit artworks. For these reasons, the knowledge of some artworks' characteristics, difficult to reproduce and punctual placed, allows to identify "elements of uniqueness" belonging to paintings, that, as *art-fingerprints*, are helpful to control the paintings' identity during transportation phase.

Taking advantage from methodologies usually used in Earth Science disciplines, this research focused its attention both to art-fingerprints based on pictorial surface, its morphology and on in-depth pigment analysis. The scientific contribution of these techniques demonstrated to be particularly useful for the study of painting structure-texture and, especially, for the chemical-mineralogical identification of inorganic pigments. In-depth pigment analysis based on to the identification of the mineralogical phases, contained in pigment compounds, allowed to detect some characteristic features that, sometimes, are not detected with routine pigment analysis. For instance, the traditional pigment namely *Green Earth*, being mixtures of minerals, in the majority green minerals, can be characterized by several mineralogical compositions, especially for artificial compounds linked to secret patents and commercial companies (Eastaugh N. et al., 2008). In this way, the identification of the pigment's mineralogical composition can be considered as an *art-fingerprints*. In sample taken from *Flowers in glass vase* (artwork plate VI), in-depth pigment analysis allowed to suggest the use of Green Earth pigment composed by several minerals such as celadonite, calcite, baryte and graphite. The study carried out on white samples brought interesting results, especially for the pigment White titanium dioxide. This pigment, used in artistic pigment compound since earlier 20th century, is usually considered dating pigment for ancient and modern artworks. Its effectiveness, as dating pigment, encounters difficulties for dating studies of Modern and Contemporary artworks, in which White titanium dioxide pigment can be one of the material employed to create the paintings. For these reasons, the identification of which mineralogical phase (rutile or anatase) constitutes the analyzed White Titanium pigment can be useful both as art-fingerprints and in support of dating studies. Pigment analysis carried out on White titanium dioxide samples revealed the presence of rutile phase in all the analyzed artworks, except for *Flowers* (artwork plate V), in which anatase phase was found. Considering the history of use of Titanium White Pigment, it is possible to suggest different post-quem achievement date according to the purity and morphology of pigment based on rutile. The production, in fact, of $\text{TiO}_2/\text{BaSO}_4$ (rutile form), of $\text{TiO}_2/\text{CaSO}_4$ (rutile form) or of high

quality pigment (pure rutile pigment with particle size around 0.3 μm) suggest respectively three following post-quem date: 1939, 1941, 1957 (Eastaugh N. *et al.*, 2008; McCrone W., 1994; Leonardi R., 2005; Lewis P.A., 1987; West Fitzhugh E., 1997). Therefore, in addition to the identification of art-fingerprints, the detection of the mineralogical phase can help art investigations on dating purpose. For instance, pigment analysis on samples taken from Flowers in glass vase revealed the presence of White titanium dioxide – Rutile/BaSO₄ or high quality rutile form (particle size lies in the region of 0.3 μm), suggesting respectively 1939 and 1957 as post-quem achievement data. In this case, if the detected barium sulfate is linked not to a component of White titanium dioxide (Rutile/BaSO₄ process) but to a mixture of White titanium dioxide and White barium sulfate, studied painting could be made after 1957. The above mentioned post-quem date is later than 1945 (date proposed for this painting according to handwritten text signed G. Commisso) and later than death date of the artist Filippo De Pisis (1956). For these reason, considering that materials employed could be not compatible with an attribution to De Pisis period, it is important to examine further in-depth the artwork, the artistic techniques, its material and their history to assist better the historical-artistic investigation for dating and attribution purpose.

Multi-analytical approach, employed in this study, was tested both on paintings and on specimens, taken in not-repainted area and where the conservative condition of the painting allowed the sampling. For the investigation of art-fingerprints concerning the morphology and pictorial layer, microscope investigation demonstrated to be very useful for the detection of μ -features characterizing brushstrokes, conservative condition (*craquelures d'âgé* and *craquelures prématurée*), etc. Image processing, carried out taking advantage of a software that is usually used in Earth Science, allowed a good elaboration of data obtained by multispectral imaging, in particular useful for the choice of point analysis. Analysis of pictorial film, that began with in-depth study of chemical composition, employing several techniques (EDXRF, PIXE, SEM/EDS), was supported by other analytical techniques to obtain more precise information about the identification of pigment and mineralogical phases (μ -Raman, XRD). Even if it was not always possible to apply the above mentioned multi-analytical suite to whole artworks, the study carried out on few μ -samples allowed to detecting art-fingerprints, without damaging (or modifying) specimens, in order to preserve them for further analysis (e.g., μ -XRD, XRD-XRF on the same samples).

Art-fingerprints database (traditional and AIAD) has been successfully tested in the collection of different art-fingerprints detected on studied artworks. Even if, at the moment, it is not possible to consult AIAD as the traditional database (query, report, etc.), the displaying of results on image allows to obtain an intuitive and complete overall view of the analyzed painting.

In conclusion, this research belongs to this cognitive path in which Earth Science *know-how* can be transferred to Cultural Heritage domain. The art-fingerprints set, identified for each studied artwork (TABLE 12) through methodologies used in Earth Science discipline, and AIAD could be useful for assurance policy, creating a more detailed and interactive condition report, to assist art-historical studies and art investigations on attribution decision and for future restoration and maintenance actions.

After all, “... il falso caratterizza una funzione essenzialmente spettacolare, necessaria al dominio del semblante. Offre l’illusione che dà, in superficie, l’apparenza dell’originale ma senza possedere la capacità di ricreare l’autenticità, che appartiene solo al suo modello. Non essendo ne autenticità ne originalità, il falso riproduce con esattezza ciò che copia, ma senza quelle due dimensioni che distinguono precisamente l’opera imitata. In fondo, il falso è definito da ciò che gli manca...” (Ribettes J.M., 1991).

(“...the forgery characterizes essentially a spectacular function, that is necessary to the dominion of the semblance. It offers the illusion that the appearance of the original gives on the surface, but without possessing the ability to recreate the authenticity, that belongs only to its model. Not being neither authenticity nor originality, the forgery exactly reproduces what it copies, but without those two dimensions that precisely distinguish the imitated artwork. After all, the forgery is defined by what it misses it.”, Ribettes J.M., 1991).

TABLE 15 Main results of art-fingerprints' research in nineteenth-twenties century paintings by optical microscopy, SEM/EDS, EDXRF, PIXE, μ -Raman and XRD.

Painting, title and date	Art-fingerprints		
	Pictorial layer	Description of sample	Pigment analysis
John Singer Sargent, <i>Caffè orientale sulla Riva degli Schiavoni</i> (Artwork plate I), probably post c.1880-1882	unknown	White samples and white/brown samples with red and black particle in a brown layer.	SEM: rounded grains, particle size < 1 μ m; agglomerated particles with size from 4/5 μ m to 10 μ m SEM/EDS,EDXRF,PIXE: Ti, Ca, Mg μ -Raman: rutile, hematite, burnt green earth XRD: rutile, calcite, dolomite, hematite
Pablo Picasso, <i>Cubist figure</i> (Artwork plate II), probably c. 1909	unknown	White sample, white/red sample, white/blue sample. Pictorial film is around 70 μ m thick	SEM: particles with rounded shape (particle size < 1 μ m) and grains with angular shape grains, particle size < 2 μ m SEM/EDS,EDXRF, PIXE: Ti, Ca, Ba, S, Fe (red), Cu (blue) μ -Raman: rutile, barium sulfate, Lead white, calcite, hematite, Blue Phthalocyanine XRD: rutile, calcite and hematite
Amedeo Modigliani, <i>Schoolboy with picture book</i> (Artwork plate III), c. 1905	unknown	White samples with red and blue particles and covered by rganic varnish. Pictorial film is around 248 μ m thick. Support made by linen fibers.	SEM: rounded and very fine particles SEM/EDS,EDXRF, PIXE: Pb, S, Cr, Ca, Cd, Zn μ -Raman: hematite, ultramarine blue XRD: cerussite, lazurite, hematite

<p>Attributed to Giovanni Boldini, <i>Reader woman on bed and old man</i> (Artwork plate IV), probably post c. 1914</p> <p>Note: study of Artist attribution and dating in progress</p>	<p>Numerous <i>craquelures prématurées</i> and <i>craquelures d'age</i> that caused lack of pictorial layer, discovering support fibers.</p>	White sample (recto), painting border	<p>SEM: fine grained particles of 1 μm or less, with irregular shape SEM/EDS,EDXRF, PIXE: Zn, Pb μ-Raman: barium sulfate, high fluorescence peak due to varnish</p>
	<p>Support: canvas made by cotton fibers.</p>	White sample (verso), painting border	<p>SEM: aggregate particle with particle size less than 1.5 μm SEM/EDS,EDXRF, PIXE: Si, Al, Mn, Fe μ-Raman: high fluorescence peak due to medium</p>
		Dark red sample was taken in correspondence of under-painting in a damage area on the border of painting.	<p>SEM: fine-grained particles with spherical appearance and particle size < 1 μm SEM/EDS,EDXRF, PIXE: Hg, Pb, Cr, Cd, Fe μ-Raman: litharge, vermilion</p>
<p>Attributed to Filippo De Pisis, <i>Flowers</i> (Artwork plate V), unknown</p> <p>Note: study of Artist attribution and dating in progress</p>	<p>Brushstrokes enriched in matter and other part in which the pigment was accurately spread onto the support. Under-drawing line and not UV color fluorescence. Support: plywood.</p>	White sample	<p>SEM: rounded fine particles, particle size < 1 μm SEM/EDS,EDXRF, PIXE: Ti, Zn, Cl, S μ-Raman: anatase, zinc oxide, barite and calcite</p>
		Blue sample	<p>SEM: rounded fine particles, particle size < 1 μm SEM/EDS,EDXRF, PIXE: Na, Si, Al, S μ-Raman: Ultramarine Blue</p>

<p>Attributed to Filippo De Pisis, <i>Flowers</i> (Artwork plate V), unknown</p> <p>Note: study of Artist attribution and dating in progress</p>		<p>Dark red sample and violet-red sample</p>	<p>SEM: particle with irregular angular shape SEM/EDS,EDXRF, PIXE: Hg, Pb, S, Cd, Cr, Ca μ-Raman: Red/violet Ultramarine, Vermillion</p>
		<p>Yellow sample</p>	<p>SEM: particle pigment similar to bladed laths, 1μm wide and 2μm long SEM/EDS,EDXRF, PIXE: Cr, Pb, Fe μ-Raman: Lead chromate (crocoite)</p>
<p>Attributed to Filippo De Pisis, <i>Flowers in glass vase</i> (Artwork plate VI), 1945</p> <p>Note: study of Artist attribution and dating in progress</p>	<p>Pigment spread accurately on the support, probably treated with varnish. UV fluorescence of pink and white color. Network of μ-<i>craquelures</i>, about from 5 μm to 15 μm wide. Support: plywood.</p>	<p>White sample with covering organic varnish: white layer thickness has average value of 24.7 μm, covering varnish is about 14.2 μm thick.</p>	<p>SEM: rounded particles, particle size from 0.3 μm to 1 μm SEM/EDS,EDXRF, PIXE: Ti, Ba μ-Raman: Rutile</p>
		<p>Green sample shows three different layer: green colored layer 1.662 mm thick, inter-layer green-varnish 22.9 μm thick and covering varnish is about 16.5 μm thick.</p>	<p>SEM: particles with angular shape, particle size from 1 μm to 2 μm. SEM/EDS, EDXRF, PIXE: Cr, Na, Mg, Mg, Si, Fe μ-Raman: Green Earth (celadonite, calcite, baryte, graphite, etc.)</p>
		<p>Red samples with covering varnish show μ-<i>craquelures</i> that interest the upper layer of varnish.</p>	<p>SEM: particles with spherical shape, particle size about 0.5 μm SEM/EDS, EDXRF, PIXE: Cr, Cd, Pb μ-Raman: Red Chrome, baryte</p>

<p>Attributed to Filippo De Pisis, <i>Flowers in glass vase</i> (Artwork plate VI), 1945</p> <p>Note: study of Artist attribution and dating in progress</p>		<p>Yellow samples show a spread network of μ-<i>craquelures prématurée</i>, wide less than 10 μm, that mainly interested the upper layer.</p>	<p>SEM, SEM/EDS, μ-Raman: thick varnish layer does not allow to obtain reliable data. EDXRF, PIXE: Pb, Sr, Cr, Fe, P, K; suggested pigment: Strontium Yellow (CrO_4Sr) or Chrome Yellow (PbCrO_4)</p>
--	--	---	---

The following figure shows an example of a sample condition report format [7].

CONDITION REPORT

Purpose (check one): Traveling Exhibition Photography Acquisition Loan Other

EXHIBITION TITLE: _____
 EXHIBITION SPONSOR: _____
 EXHIBITION LOCATION: _____
 ITEM NUMBER: *(start with # 1 if you are sending more than one artwork to the exhibition.)* _____

ARTIST: _____ **RETAIL PRICE:** _____
Title: _____ **Year:** _____
Media: _____
Dimensions: _____
Piece Number: _____
Collection of: _____
Address: _____
Phone: _____

Artists should check Artwork before it leaves the studio describing pre-existing wear or imperfections, Be as specific as possible using the words listed below, as necessary.

Outgoing SHIPPING Method: _____
Preferred Return SHIPPING Method: _____
Insurance valuation for shipping: _____

*****Exhibition Staff Only - Artists do not fill out the section below*****

Condition In:	Excellent	Good	Fair	Poor	
Dirt/grime		Tarnish		Powering	Bulges
Abrasions		Warping		Holes	Cracking
Stained		Shrinkage		Tears	Mold/mildew
Corrosion		Flaking		Scratches	Moisture damage

Type of Shipping Container: Crate Box Tube Other _____

Packing materials: Paper Plastic Tupperware® Foam Bubble Wrap Peanuts
 Other _____

Instructions included for: Packing Assembly Mounting Installation

If there are no packing instructions take notes on the reverse side of this paper while unpacking the work.

Conditioned by: _____ Date: _____
 Condition out: _____ Date: _____
 RETURN SHIPPING METHOD: _____ Date: _____

LOAN RETURN at the end of the exhibition **DATE:** _____

The Artist hereby releases the Exhibition Sponsor from all liability or obligation for the above Artwork and any Artworks listed in the LIST OF ARTWORK TO EXHIBITION SPONSOR.

ARTIST'S SIGNATURE: _____ DATE: _____

Continue information on the back of this page as necessary.

Ion Beam Analysis (IBA)

Ion Beam Analysis (IBA) are analytical techniques that, exploiting the interaction between accelerated charged particle beam (usually protons) and material, detect different signals (X-rays, γ -rays, visible photon, etc.). The suite of this techniques probes chemical-physical nature and state of atoms constituent the material. Any material surface, in fact, when it is bombarded by particles or radiation, interacting with incident beam, emits scattered particle and/or X or γ radiation with distinctive energy for each chemical element (Artioli G., 2010; Breese M. *et al.*, 1996; Hellborg R., 2005; Jeynes C. *et al.*, 2012).

In cultural heritage field, the most used IBA techniques are:

- PIXE (Particle Induced X-rays Emission) that, using MeV protons beam, detects X-ray emitted by surface specimen allowing the determination of trace and minor element (Caligaro T. *et al.*, 2003; Colombo E. *et al.*, 2008; Dran J.C. *et al.*, 2004; Guerra M.F., 2000; Johansson S.A.E. *et al.*, 1995);
- PIGE (Particle Induced γ -rays Emission) to study light element, catching γ -rays Emission of material using MeV protons beam (Climent-Font A. *et al.*, 2008; Grassi N. *et al.*, 2007; Jembrih-Simbuerger D. *et al.*, 2004; Kos M. *et al.*, 2011; Quarta G. *et al.*, 2011);
- RBS (Rutherford Backscattering Spectrometry) that is mostly used for analysis of heavy elements in light matrix, exploiting interaction between He⁺ ions with MeV energy (Chêne G. *et al.*, 2012; Ioannidou E. *et al.*, 2000; Mahnke H.E. *et al.*, 2009; Morella M., 2005; Pascual-Izarra C. *et al.*, 2007; Sokaras D. *et al.*, 2011);
- SIMS (Secondary Ions Mass Spectrometry) to give information about elemental, isotopic and molecular composition of superficial layer and depth profiling, catching secondary ions emanated after sample's bombardment by primary negative (e.g. O⁻) or positive (e.g. O₂⁺, Ar⁺) ions (Adriaens A., 2000; Adriaens A., 2005; Adriaens A. *et al.*, 2006; Dowsett M. *et al.*, 2004; MCPheil D.S., 2006);
- IL (Ionoluminescence) or IBIL (Ion Beam Induced Luminescence) that detects photon emission in the IR/VIS/UV range coming from a material excited by MeV ion beam, providing in this way to obtain data on material structure and impurity content; IL is also useful for the identification of chemical phases and of certain trace elements (Calusi S. *et al.*, 2008; Colombo E. *et al.*, 2008; Re A. *et al.*, 2011).

Using X-rays or electron probes it was possible to obtain most of these information, but, thanks to the different interaction between electrons/X-rays and matter or protons and matter, IBA methods are not limited such as other analysis could be. It is easy to understand the potentiality of these techniques, if we consider for example the difference of behavior between electron probe and ion probe in the same matter (FIG. 211-212). In FIG. 212 it is better showed the different lateral displacement scales along the x-axis in the two case (20 KeV electrons beam and 2MeV protons beam) in PMMA layer (Watt F. *et al.*, 2007), material that is often used in contemporary artworks (Ohama Y. *et al.*, 1997) and in restoration field (Scicolone G.C., 2004).

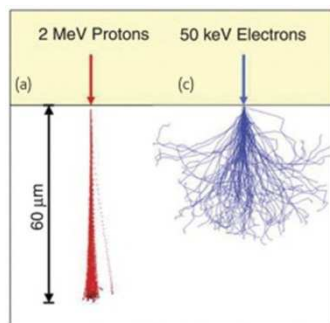


FIG. 211 Comparison between p-beam (a) and e-beam (c) writing. The images were simulated using SRIM and CASINO software packages, respectively (Watt F. *et al.*, 2007).

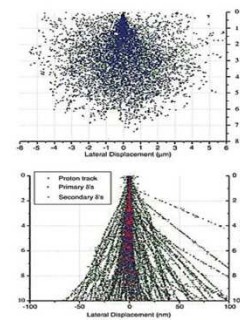


FIG. 212 Simulator profiles of one thousand 20 keV electrons penetrating a 10 μ m thick PMMA layer (a) and simulator profiles of one thousand 2 MeV protons penetrating a 10 μ m thick PMMA layer (b) (Watt F. *et al.*, 2007).

In addition, the possibility to use different IBA techniques simultaneously allows to obtain other complementary information that could better characterize investigated materials, gathering several complementary information combining, for instance, PIXE/RBS (Morella M. *et al.*, 2005), PIXE/PIGE (Grassi N. *et al.*, 2007), etc.

REFERENCES

- Abry P., Wendt H., Jaffard S. (2013).** “When Van Gogh meets Mandelbrot: Multifractal classification of painting’s texture”. *Signal Processing*, 93, 3, pp. 554-572
- Accame V. (1995).** “La pratica del falso. Vecchi e nuovi misfatti in nome della cultura: dai falsari dell’arte ai falsari delle comunicazioni di massa”. Spirali editore, collana L’alingua (*).
- Adriaens A. (2000).** “The role of SIMS in understanding ancient materials” in “Radiation in Art and Archeometry” edited by Creagh D.C. and Bradley D.A. Elsevier editor, pp. 180-201
- Adriaens A. (2005).** “Non-destructive analysis and testing of museum objects: an overview of 5 years of research”. *Spectrochimica Acta Part B: Atomic Spectroscopy*, 60, pp. 1503-1516
- Adriaens A., Dowsett M. (2006).** “Applications of SIMS to cultural heritage studies”. *Applied Surface Science*, 252, pp. 7096-7101
- Aliatis I., Bersani D., Campani E., Casoli A., Lottici P.P., Mantoan S., Marino I.G., Ospitali F. (2009). “Green pigments of the Pompeian artists’ palette”. *Spectrochimica Acta A*, 73, 3, pp. 532-538
- Ambraseys N.N. (2006).** “Earthquakes and archaeology”. *Journal of Archaeological Science*, 33, 7, pp. 1008-1016
- Anderson J. (2006).** “Drier accelerator for paints and coatings”. *Pitture e vernici. European coatings*, pp.37-35 <http://www.rtvanderbilt.com/additivi.pdf>
- Appoloni C.R., Blonski M.S., Parreira P.S., Souza L.A.C. (2007).** “Study of the pigments elementary chemical composition of a painting in process of attribution to Gainsborough employing a portable X-rays fluorescence system”. *Nuclear Instruments and Methods in Physics Research A*, 580, pp. 710-713
- Arbizzani R., Casellato U., Fiorin E., Nodari L., Russo U., Vigato P.A. (2004).** “Decay markers for the preventative conservation and maintenance of paintings”. *Journal of Cultural Heritage*, 5, pp. 167-182
- Artioli G. (2010).** “Scientific Methods and Cultural Heritage. An introduction to the application of materials science to archaeometry and conservation science”. Oxford University Press, pp. 18-20, 24, 94-97
- Ayres L. (1986).** “Sargent in Venice.” In “John Singer Sargent” edited by Hills P. et al., Exh. cat. Whitney Museum of American Art, New York, pp. 49-73
- Bacci M., Casini A., Cucci C., Picollo M., Radicati B., Vervat M. (2003).** “Non-invasive spectroscopic measurements on the Il ritratto delle figliastra by Giovanni Fattori: identification of pigments and colourimetric analysis”. *Journal of Cultural Heritage*, 4, pp. 329-336

- Battarbee R.W. (1988).** “The use of diatom analysis in archaeology: a review”. *Journal of Archaeological Science*, 15, 6, 621-644
- Barsan M.M., Butler I.S., Gilson D.F.R. (2012).** “High-pressure resonance Raman spectroscopic study of ultramarine blue pigment”. *Spectrochimica Acta A*, 98, pp. 457-459
- Bell I.M., Clark R.J.H, Gibbs P.J. (1997).** “Raman spectroscopic library of natural and synthetic pigments (pre- ~ 1850 AD)”. *Spectrochimica Acta Part A*, 53, pp. 2159-2179
- Bikiaris D., Daniilia S., Sotiropoulou S., Katsimbiri O., Pavlidou E., Moutsatsou A.P., Chrysoulakis Y. (2000).** “Ochre-differentiation through micro-Raman and micro-FTIR spectroscopies: application on wall paintings at Meteora and Mount Athos, Greece”. *Spectrochimica Acta A*, 56,1, pp. 3-18
- Blaugrund A. (1986).** "Sunshine Captured: the development and dispersment of Sargent's Watercolors" In “John Singer Sargent” edited by Hills P. et al., Exh. cat. Whitney Museum of American Art, New York, pp. 209-242, 244-249
- Bollanti S., Bonfigli F., Di Lazzaro P., Flora F., Mezi L., Montereali R.M., Murra D., Torre A., Vincenti M.A. (2012).** “Is this artwork original or is it a copy? The answer by a new Anti-Counterfeiting Tag”. *ENEA Review EAI Energia, Ambiente e Innovazione*, II-2012 Knowledge, Diagnostic and Preservation of Cultural Heritage, pp. 162-168
- Bonifazzi C., Ferriani S., Maino G., Tartari A. (2003)^A.** “Multispectral examination of paintings and works of art: A principal component analysis approach” in *Proceedings of CLADAG 2003 Meeting of the Classification and Data Analysis Group of the Italian Statistical Society*, Bologna (Italy), September 22nd -24th, 2003, CLUEB Bologna, pp. 67-70.
- Bonifazzi C., Ferriani S., Maino G., Tartari A. (2003)^B.** “Three-way data analysis of γ -ray spectra. Material composition study and density imaging” in *Proceedings of CLADAG 2003 Meeting of the Classification and Data Analysis Group of the Italian Statistical Society*, Bologna (Italy), September 22nd -24th, 2003, CLUEB Bologna, pp. 63-66.
- Bonneau A., Pearce D.G., Pollard A.M. (2012).** “A multi-technique characterization and provenance study of the pigments used in San rock art, South Africa”. *Journal of Archaeological Science*, 39, 2, pp. 287-294
- Brachert T. (1988).** “Seit wann gibt es Titanweiss?”, *Restauro* 94, n.4, 252 (*)
- Breese M.B.H., Jamieson D.J., King P.J.C. (1996).** “Materials Analysis using a nuclear microprobe”. John Wiley & Sons, New York (*)

- Brigante G. (1991).** “De Pisis. Catalogo generale. Tomo II: opere 1939-1953”. Electa editore, pp. 471, 493-494, 503-504, 506, 515-516, 518-550, 523, 525-526, 534, 549, 551-552, 557, 563-564, 585-584, 594-596, 601, 615, 624, 628, 642, 682-670³³, 701, 736-739
- Broz'ek-Pluska B., Szymczyk I., Abramczyk H. (2005).** “Raman spectroscopy of phthalocyanines and their sulfonated derivatives”. *Journal of Molecular Structure*, 744-747, pp. 481-485
- Bruni S., Maino G., Vaccaro C., Volpe L. (2012).** “Investigation and characterization of artistic techniques in works of modern and contemporary art”. *ENEA Review EAI Energia, Ambiente e Innovazione*, II-2012 Knowledge, Diagnostic and Preservation of Cultural Heritage, pp. 129-134.
- Burgio L., Clark R.J.H. (2001).** “Library of FT-Raman spectra of pigments, minerals, pigment media and varnishes, and supplement to existing library of Raman spectra of pigments with visible excitation”. *Spectrochimica Acta A*, 57, 7, pp. 1491-1521
- Calusi S., Colombo E., Giuntini L., Lo Giudice A., Manfredotti C., Massi M., Pratesi G., Vittone E. (2008).** “The ionoluminescence apparatus at the LABEC external microbeam facility”. *Nuclear Instruments and Methods in Physics Research B*, 266, pp. 2306-2310
- Calligaro T., Dran J.C., Poirot J.P., Querré G., Salomon J., Zwaan J.C. (2000).** “PIXE/PIGE characterization of emeralds using an external micro-beam”. *Nuclear Instruments and Methods in Physics Research B*, 161-163, pp. 769-774
- Calligaro T., Dran J.C., Klein M. (2003).** “Application of photo-detection to art and archaeology at C2RMF”. *Nuclear Instruments and Methods in Physics Research A*, 504, Issue 1-3, pp. 213-221
- Calligaro T., Dran J.C., Salomon J., Walter Ph. (2004).** “Review of accelerator gadgets for art and archaeology”. *Nuclear Instruments and Methods in Physics Research B*, 226, pp. 29-37
- Calligaro T., Coquinot Y., Pichon L., Moignard B. (2011).** “Advances in elemental imaging of rocks using the AGLAE external microbeam”. *Nuclear Instruments and Methods in Physics Research B*, 269, pp. 2364-2372
- Camesasca E. (1970).** “L'opera completa di Boldini”. *Classici dell'arte*, Rizzoli editore, vol.37, p. 86, 129
- Castellano A., Quarta s., Donativi M. (2007).** “Tecniche radiografiche per l'archeometria” in “Elementi di archeometria. Metodi fisici per i beni culturali” by Martini M., Castellano A., Sibilia E., Egea editore, pp. 177-201

³³ Artistic production:1946-1947.

Cetica M., Marras L., Materazzi M., Poggi P. (2007). “Tecniche di imaging multispettrale” in “Elementi di archeometria. Metodi fisici per i beni culturali” by Martini M., Castellano A., Sibilia E., Egea editore, pp. 231-252

Chen G., Chen J., Srinivasakannan C., Peng J. (2012). “Application of response surface methodology for optimization of the synthesis of synthetic rutile from titania slag”. *Applied Surface Science*, 258, pp. 3068-3073

Chêne G., Bols S., Dupuis T., Marchal A., Mathis F., Garnir H.P., Strivay D. (2012). “New external beam and particle detection set-up of Liège cyclotron – First applications of high energy beams to cultural heritage”. *Nuclear Instruments and Methods in Physics Research B*, 273, pp. 208-212

Chinoglia I., Bertelli P. (2004). “Giovanni Boldini (Ferrara, 1842-Parigi, 1931)” in “De nittis: a léontine”. Silvana Milano editore, pp. 215-216

Claire J., Michel O. (1998). “Picasso. 1917-1924”. Bompiani editore, pp. 334-354

Clark R.J.H., Curri M.L., Laganara C., (1997). “Raman microscopy: the identification of lapis lazuli on medieval pottery fragments from the south of Italy”. *Spectrochimica Acta A*, 53, pp. 597-603

Clark R.J.H., Quanyu W., Correia A. (2007). “Can the Raman spectrum of anatase in artwork and archaeology be used for dating purposes? Identification by Raman microscopy of anatase in decorative coatings on Neolithic (Yangshao) pottery from Henan, China”. *Journal of Archaeological Science* 34, pp. 1787-1793

Climent-Font A., Muñoz-Martin A., Ynsa M.D., Zucchiatti A. (2008). “Quantification of sodium in ancient Roman glasses with ion beam analysis”. *Nuclear Instruments and Methods in Physics Research B*, 266, pp. 640-648

Colombo E., Calusi S., Cossio R., Giuntini L., Lo Giudice A., Mandò P.A., Manfredotti C., Massi M., Mirto F.A., Vittone E. (2008). “Recent developments of ion beam induced luminescence at the external scanning microbeam facility of the LABEC laboratory in Florence”. *Nuclear Instruments and Methods in Physics Research B*, 266, Issue 8, pp. 1527-1532

Commisso G. (1954). “Mio sodalizio con De Pisis”, edited by Neri Pozza (2010), pp. 118-119

Cucci C., Picollo M., Vervat M. (2012). “Trans-illumination and trans-irradiation with digital cameras: potentials and limits of two imaging techniques used for the diagnostic investigation of paintings”. *Journal of Cultural Heritage* 13, 83-88

Dini P., Dini F. (2002). “Boldini. Catalogo ragionato”. Umberto Allemandi & C. editore, Vol. III, 2, pp. 655-689

- De Faria D.L.A., Lopes F.N. (2007).** “Heated goethite and natural hematite : can Raman spectroscopy be used to differentiate them ? ”. *Vibrational Spectroscopy*, 45, pp. 117-121
- De Rossi L. (2009).** “John Singer Sargent. Caffè Orientale sulla Riva degli Schiavoni a Venezia” in “Arte documento, 23. Ceramica attica e magnogreca” directed by Giuseppe Maria Pilo (section: Da Tiziano al contemporaneo). Edizioni della laguna, pp. 236-239
- Doria B. (1998).** “Boldini amico mio”. Rizzoli editore
- Dowsett M., Adriaens A. (2004). “The role of SIMS in cultural heritage studies”. *Nuclear Instruments and Methods in Physics Research B*, 226, pp. 38-52
- Dran J.C., Salomon J., Calligaro T., Walter P. (2004).** “Ion beam analysis of art works: 14 years of use in the Louvre”. *Nuclear Instruments and Methods in Physics Research B*, 219-220, pp. 7-15
- Eastaugh N., Walsh V., Chaplin T., Siddall R. (2004)^A.** “Pigment compendium. A dictionary of historical pigments”. Elsevier Ltd
- Eastaugh N., Walsh V. (2004)^B.** “Pigment compendium. Optical Microscopy of Historic Pigments”. Elsevier Ltd
- Eastaugh N., Walsh V., Chaplin T., Siddall R. (2008).** “Pigment compendium. A dictionary of historical pigments”. Elsevier Ltd
- Edwards H.G.M. (1999).** “Art works studied using IR and Raman Spectroscopy”, *Encyclopedia of Spectroscopy and Spectrometry*, pp. 2-17
- Feller R.L. (1985).** “Artists’ Pigments. A handbook of their history and characteristics”. National Gallery of Art, pp. 47-65, 169-187
- Ferrari C.G. (2000).** “DE PISIS. La poesia nei fiori e nelle cose”. Art exhibition catalogue of Art exposition on 2000, in Acqui Terme (Alessandria, Italy)
- Frausto-Reyes C., Ortiz-Morales M., Bujdud-Pérez J.M., Magaña-Cota G.E., Mejía-Falcón R. (2007).** “Raman spectroscopy for the identification of pigments and color measurement in Dugès watercolors”. *Spectrochimica Acta Part A: Molecular and Biomolecular Spectroscopy*, 74, pp. 1272-1279
- Giardino M.J. (2011).** “A history of NASA remote sensing contributions to archaeology”. *Journal of Archaeological Science*, 38, pp. 2003-2009
- Ghimbeu C.M., Schoonman J., Lumbreras M., Siadat M. (2007).** “Electrostatic spray deposited zinc oxide films for gas sensor applications”. *Applied Surface Science*, 253, pp. 7483-7489
- Grassi N., Giuntini L., Mandò P.A., Massi M. (2007).** “Advantages of scanning-mode ion beam analysis for the study of Cultural Heritage”. *Nuclear Instruments and Methods in Physics Research B*, 256, pp. 712-718

- Grifa C., Cultrone G., Langella A., Mercurio M., De Bonis A., Secastián E., Morra V. (2009).** “Ceramic replicas of archaeological artefacts in Benevento area (Italy): petrophysical changes induced by different proportions of clays and temper”. *Applied Clay Science*, 46, 3, pp. 231-240
- Griffith, W.P. (1987).** “Advances in the Raman and infrared spectroscopy of minerals”. In: Clark, R.J.H., Hester, R.E. (Eds.), *Spectroscopy of Inorganic based Materials*. Wiley, Chichester. pp. 119-186 (*)
- Gordon B.M., Kraner H.W. (1972).** *J. Radional. Chem.* 12 (1), 181 (*)
- Guerra M.F. (2000).** “The study of the characterization and provenance of coins and other metalwork using XRF, PIXE and Activation Analysis” in “Radiation in Art and Archeometry” edited by Creagh D.C. and Bradley D.A. Elsevier editor, pp. 378-416
- Halac E.B., Reinoso M., Marcelo L., Marte F. (2012).** “Raman mapping analysis of pigments from Proas Iluminadas by Quinquela Martín”, *Journal of Cultural Heritage*, 13, pp. 469-473
- Hamilton G.H. (1976).** “Picasso, Pablo Ruiz Y”. in Halsey W.D. “*Collier’s Encyclopedia*, 19. Macmillan Educational Corporation New York, pp. 25-26 (*)
- Harley R.D. (1982).** “Artists’ Pigments. c.1600-1835”. National Gallery of Art-Oxford University, Butterworth scientific
- Hellborg R. (2005).** “Electrostatic Accelerators. Fundamentals and Applications”. Springer editor, pp. 530-559
- Hellbusch E. (1921).** “Titanweiss” in *Chemische-Technische Wochenschrift* 5 , n. 22, pp. 165-166 (*)
- Hilton T. (1988).** “Picasso”. *Rusconi Arte*, pp. 95-100, 107, 273
- Homburg J.A. (2005).** “Archeology in relation to soils”. *Encyclopedia of Soils in the Environment*, pp. 95-102
- IAEA, International Atomic Energy Agency (2003).** “Intercomparison of PIXE spectrometry software packages”. IAEA-TECDOC-1342, pp.1- 11, 17-18
http://www-pub.iaea.org/MTCD/publications/PDF/te_1342_web.pdf
- Ioannidou E., bourgarit D., Calligaro T., Dran J.C., Dubus M., Salomon J., Walter P. (2000).** “RBS and NRA with external beams for archaeometric applications”. *Nuclear Instruments and Methods in Physics Research B*, 161-163, pp. 730-736
- Jagut P. (1988).** “Etude du reseau de craquelures des tableaux”. Stage report kept in Bibliothèque du Laboratoire de Musées de France, site Carrousel.

- Jehlička J., Víték P., Edwards H.G.M., Heagraves M., Čapoun T. (2009).** “Application of portable Raman instruments for fast and non-destructive detection of minerals on outcrops”. *Spectrochimica Acta A: Molecular and Biomolecular Spectroscopy*, 73, pp. 410-419
- Jembrih-Simburger D., Neelmeijer C., Maeder M., Schreiner M. (2004).** “Iridescent Art Nouveau Tiffany Glass – Simultaneous PIGE, PIXE and RBS for Non-destructive determination of the glass composition”. Act of 10th International Conference on Particle Induced X-ray emission and its analytical applications, June 4-8, 2004 Portorož – Slovenia, pp. 845.1-845.4
- Jeynes C., Bailey M.J., Bright N.J., Christopher M.E., Grime G.W., Jones B.N., Palitsin V.V., Webb R.P. (2012). “Total IBA-Where are we?”. *Nuclear Instruments and Methods in Physics Research B*, 271, pp. 107-118
- Johansson S.A.E., Campbell J.L., Malmqvist K.G. (1995).** “Particle-Induced X-ray Emission Spectrometry (PIXE)”. John Wiley & Sons, pp. 153-156
- Jusuf S.K., Wong N.H.m Hagen E., Anggoro R., Hong Y. (2007).** “The influence of land use on the urban heat island in Singapore”. *Habitat International*, 31, pp. 232-242
- Kampfer W.A. (1973).** “Titanium Dioxide’ Pigment Handbook“, 1, Patton, T.C. (ed.) John Wiley, New York, pp. 1–36 (*)
- Kellner R., Mermet J.-M., Otto M., Widmer H. M. (1998).** “Analytical Chemistry”. Willy-VCH, Weinheim (Germany), pp. 641-657,662-675
- Kellner R., Mermet J.-M., Otto M., Widmer H. M. (2003).** “Chimica Analitica”. Casa Editrice Edises, pp. 187-200, 362
- Kilmurray E., Ormond R., eds. (1998).** “John Singer Sargent”. Exhibition catalogue. London: Tate Gallery, pp. 34, 209-240 (*)
- Kilmurray E., Ormond R. (1999).** “John Singer Sargent”. Tate Gallery publishing, pp. 75-79, 209-218
- Kooistra M.J., Kooistra L.I. (2003).** “Integrated research in archaeology using soil micromorphology and palynology”. *CATENA, achievements in Micromorphology*, 54, 3, pp.603-617
- Kos M., Šmit Ž. (2011).** “PIXE-PIGE analysis of 18th and 19th century creamware from Slovenia and Northern Italy”. *Journal of Cultural Heritage*, 12, pp. 236-242
- Krystof D. (2000).** “Modigliani”. Benedict tashen ed, pp. 94-95
- Kumar Dr. S. (2005).** “Basics of Remote Sensing and GIS”. Laxmi Publications, pp.1
- Lécuyer C., Hutzler A., Amiot R., Daux V., Grosheny D., Otero O., Martineau F., Fourel F., Balter V., Reynard B. (2012).** “Carbon and oxygen isotope fractionations between aragonite and calcite of shells from modern mollusks”. *Chemical Geology* 332-333, pp. 92-101
- Lega C. (1963).** “Ricordo del pittore Boldini”. Ferrara: SATE editore (*)

- Lega C., De Grada R. (1994).** “Giovanni Boldini: l’uomo, il pittore e i rapporti con i familiari”, Ferrara G. Corbo
- Leonardi R. (2005).** “Nuclear physics and painting: sub-topic of the wide and fascinating field of Science and Art”. Nuclear Physics A, 752, pp. 659c-674c
- Less S. (2009).** “Giovanni Boldini nella Parigi degli impressionisti”, Cassa di Risparmio di Ferrara, Ferrara, pp. 21-23
- Lewis P.A. (1987).** “Pigment handbook. Vol 1, Properties and economics”. Wiley-interscience publication, II edition, pp.1-42
- Lottman H. (2007).** “Amedeo Modigliani. Principe di Montparnasse”. Jaca book editor, pp.17-31
- Lutzenberger K., Stege H., Tilenschi C. (2010).** “A note on glass and silica in oil paintings from 15th tot he 17th century”. Journal of Cultural Heritage, 11, 4, 365-372
- Mahnke H.E., Denker A., Salomon J. (2009).** “Accelerator and x-rays in cultural heritage investigations”. Comptes Rendus Physique, 10, pp. 660-675
- Mahon D., Centeno S. (2005).** “A technical study of John Singer Sargent’s portrait of Madame Pierre Gautreau”. Metropolitan Museum Journal, 40, pp. 14-15, 121-129
- Macphall R.I. (2008).** “Soils and archaeology”. Encycolpedia of Archaeology, pp. 2064-2072
- Maggio M., [9].** “La protezione di una mostra d’arte”, educational material kindly give by Dr. Massimo Maggio, president of Progress FineArt – a division of Progress Insurance Broker. Talk took place during Master in “Management dell’arte e dei Beni Culturali”, organized by Sole24ore business school.
- Malinverni E.S., Fangi G. (2009).** “Comparative cluster analysis to localize emergencies in archaeology”. Journal of Cultural Heritage, 10S, pp. e10-e19
- Mamoli Zorzi R. (2007).** “James, Sargent e Venezia” in “Sagent and Venice”, exh. Cat. Art exhibition in Venice 2007, 24th March-22nd July, p.105
- Marinelli N., Palomba G. (2011).** “A model for pricing Italian Contemporary Art paintings at auction”. The Quarterly Review of Economics and Finance, 51, pp. 212-224
- Martin J. W. (2003).** “The Local Chemical Analysis Of Materials”. Pergamon Materials Series, edited by Cahn R.W. Elsevier Editor, pp. 50-57, 97-100
- Marsiglia L., Valli L. (1996).** “De Pisis a Villa Fiorita. Tra arte e follia. Quasi un romanzo”. Mazzotta editore
- McCrone W., McCrone, L., Delly, J.G. (1979).** “Polarised Light Microscopy Ann Arbor Science Publishers, Ann Arbor, Michigan (*)

- McCrone W. (1987).** “Microscopy in the Gallery/Museum”. *The International Journal of Museum Management and Curatorship*, 6, pp. 75-82
- McCrone W. (1994).** “Polarized Light Microscopy in Conservation: a personal perspective”. *Journal of the American Institute for Conservation*, 33, no.2, pp. 101-114
- Montagna G. (1999).** “I pigmenti. Prontuario per l’arte e il restauro”. Nardini Editore, pp. 52-53, 60-63
- Moravia A., Lecaldano P. (1979).** “L’opera completa di Picasso. Blu e Rosa”. Rizzoli editore, I classici dell’Arte, pp. 83-86
- Morella M., El Masri Y., Heits Ch., Prieels R., Van Mol J., Dran J.C., Salomon J., Calligaro T., Dubus M. (2005).** “PIXE and RBS applied to cultural heritage objects: complementary and limitations”. *Nuclear Instruments and Methods in Physics Research B*, 240, pp. 600-605
- MCPhail D.S. (2006).** “Some applications of SIMS in conservation science, archaeometry and cosmochemistry”. *Applied Surface Science*, 252, pp. 7107-7112
- Nadim C.S., Zumbuehl S., Delavy F., Fritsch A., Kuehnen R. (2009).** “Synthetic organic pigments of the 20th and 21st century relevant to artist’s paints: Raman spectra reference collection”. *Spectrochimica Acta A*, 73, pp. 505-524
- Ohama Y., Kawakami M., Fukuzawa K. (1997).** “Polymers in concrete”. E&FN SPON editor, pp 54-56
- Ohsaka T., Izumi F., Fujiki Y. (1978).** “Raman spectrum of anatase, TiO₂”. *Journal of Raman Spectroscopy* 7, pp. 321-324 (*)
- Ormond R. (2007).** “Lungo il Canal Grande, 1900-1913” in “Sargent and Venice”. Musei Civici Veneziani, Mondadori Electa ed., pp. 51-94
- Osticioli I., Mendes N.F.C., Nevin A., Gil F.P.S.C., Becucci M., Castellucci E. (2009).** “Analysis of natural and artificial ultramarine blue pigments using laser induced breakdown and pulsed Raman spectroscopy, statistical analysis and light microscopy”. *Spectrochimica Acta A*, 73, pp. 525-531
- Pallot-Frossard I., Loisel C., Marie-Victoire E., Textier A., Detalle V. (2007).** “From the monument to the microsample” In “Small samples – Big objects. Proc. EU-Artech Seminar, May 2007. Bayerisches Landesamt fuer Denkmalpflege, Munchen, pp 80-95. (*)
- Paolini C., Faldi M. (2000).** “Glossario delle tecniche artistiche e del restauro”. Istituto per l’Arte e il Restauro Palazzo Spinelli, p. 110-111, 238-239
- Panconi T. (1998).** “Giovanni Boldini, l’uomo e la pittura”, *Enciclopedia Boldiniana*, Pacini editore, pp. 20 - 21
- Papini G. (1951).** “Picasso Confesses” in “Il libro nero”. Vallecchi, Firenze (*)

- Park K. (1967).** “Thermal variation of a Raman line width in calcite”. *Physics Letters A*, 25, Issue 7, pp. 490-491 (*)
- Pascual-Izarra C., Barradas N.P., Reis M.A., Jeynes C., Menu M., Lavedrine B., Ezrati J.J., Röhrs S. (2007).** “Towards truly simultaneous PIXE and RBS analysis of layered objects in cultural heritage”. *Nuclear Instruments and Methods in Physics Research B*, 261, pp. 426-429
- Penny N., Spring M. (1995).** “Veronese's Paintings in the National Gallery, Technique and Materials: Part I”. *National Gallery Technical Bulletin*, Vol 16, pp. 4–29. http://www.nationalgallery.org.uk/technical-bulletin/penny_spring199
- Perusini G. (2004).** “Il restauro dei dipinti e delle sculture lignee, storia, teoria e tecniche”. Del Bianco editore, p. 235
- Piccioni L., Ceroni A. (1981).** “I dipinti di Amedeo Modigliani”. Rizzoli editore Milano, pp. 83-86
- Pichon L., Beck L., Walter Ph., Moignard B., Guillou T. (2010).** “A new mapping acquisition and processing system for simultaneous PIXE-RBS analysis with external beam”. *Nuclear Instruments and Methods in Physics Research B*, 268, pp. 2028-2033
- Preatoni F., Rossi A., Scicolone G.C. (2008).** “Un condition report pret a porter. La strutturazione del Condition Report nell’arte Contemporanea”. *Proceedings of the VI National Conference IGIIC “Lo Stato Dell’arte”, Spoleto (Italy), October 2nd - 4th, 2008* [6]
- Quarta G., Maruccio L., Calcagnile L. (2011).** “Provenance studies of obsidians from Neolithic contexts in Southern Italy by IBA (Ion Beam Analysis) methods”. *Nuclear Instruments and Methods in Physics Research B*, 269, Issue 24, pp. 3102-3105
- Querré G., Bouquillon A., Calligaro T., Dubus M., Salomon J. (1996).** “PIXE analysis of jewels from an Achaemenid tomb (IVth century BC)”. *Nuclear Instruments and Methods in Physics Research B*, 109-110, pp. 686-689
- Ratcliff C. (2001).** “Sargent”. *Abbeville Press Publishers, New York London*, pp. 29, 243-245
- Re A., Lo Giudice A., Angelici D., Calusi S., Giuntini L., Massi M., Pratesi G. (2011).** “Lapis lazuli provenance study by means of micro-PIXE”. *Nuclear Instruments and Methods in Physics Research B*, 269, pp. 2373-2377
- Reis D., Vian B., Bajon C. (2006).** “Le monde des fibres”. *Belin editor*, pp.56-60, 64, 67-85, 103, 107, 112-115, 128, 174
- Ribettes J.M. (1991).** “Sotto il regno della falsificazione generalizzata” in *Aa.Vv. “Veramente falso”, Mondadori Arte*, p. 13
- Richards J.A., Jia X. (1999).** “Remote sensing digital image analysis: an introduction”. Edited by Springer, p. 240 (*)

- Richardson J. (1991).** “Picasso.1881-1906”. Leonardo edizioni, pp. 26, 38-45
- Roi A. (1986).** “Artists’ Pigments. A handbook of their history and characteristics”. National Gallery of Art-Oxford University, Vol. II, pp. 69-79, 203-244
- Roi A. (1999).** “The National Gallery Van Dycks: Technique and Development”. National Gallery Technical Bulletin, Vol 20, pp. 50-83. <http://www.nationalgallery.org.uk/technical-bulletin/roy1999a>
- Romanelli G. (2007).** “John Singer Sargent. Una Venezia moderna” in “Sargent and Venice”. Musei Civici Veneziani, Mondadori Electa ed., pp. 35
- Ropret P., Centeno S.A., Bukovec P. (2008).** “Raman identification of yellow synthetic organic pigments in modern and contemporary paintings: Reference spectra and case studies”. Spectrochimica Acta A, 69, pp. 486-497
- Salomon J., Dran J.C., Guillou T., Moignard B., Pichon L., Walter P., Mathis F. (2008).** “Present and future role of ion beam analysis in the study of cultural heritage materials: the example of AGLAE facility”. Nuclear Instruments and Methods in Physics Research B, 266, pp. 2273-2278
- Salvagnini S. (2006).** “De Pisis”, Art dossier, Giunti editore
- Scicolone G.C. (2004).** “Il restauro dei dipinti contemporanei. Dalle tecniche di intervento tradizionali alle metodologie innovative”. Nardini Editore, pp. 135-140, 178-179, 185-200
- Schroeder P.A., Melear N.D., Pruett R.J. (2003).** “Quantitative analysis of anatase in Georgia kaolins using Raman spectroscopy”. Applied Clay Science 23, pp. 299-308
- Seccaroni C., Moiola P. (2002).** “Fluorescenza X. Prontuario per l’analisi XRF portatile applicata a superfici policrome”. Nardini editore
- Smith G.D., Clark R.J.H. (2004).** “Raman microscopy in archaeological science”. Journal of archeological science, 31, 8, pp. 1137-1160
- Sokaras D., Bistekos E., Georgiou L., salomon J., Bogovac M., Aloupi-Siotis E., Paschalis V., Aslani I., Karabagia S., Lagoyannis A., Harissopoulos S., Kantarelou V., Karydas A.G. (2011). “The new external ion beam analysis setup at the Demokritos Tandem accelerator and first applications in cultural heritage”. Nuclear Instruments and Methods in Physics Research B, 269, pp. 523-527
- Solé V.A., Papillon E., Cotte M., Walter Ph., Susini J. (2007).** “A multiplatform code for the analysis of energy-dispersive X-ray fluorescence spectra”. Spectrochimica Acta B, 62, pp. 63-68
- Taylor R.P., Guzman R., Martin T.P., Hall G.D.R., Micolich A.P., Joans D. (2007).** “Authenticating Pollock paintings using fractal geometry”. Pattern Recognition Letters 28, pp. 695-702

- Tanese S., Bouwman E., Reedijk J. (2004).** “Role of additives in cobalt-mediated oxidative crosslinking of alkyd resins”. *Applied Catalysis A*, 259, 1, pp. 101-107
- Tassini G. (1964).** “Curiosità Veneziane”. Filippi Editore, Venezia, p. 608 (*)
- Thompson A., Attwood D., Gullikson E., Howells M., Kim K.J., Kirs J., Kortright J., Lindau I., Liu Y., Pianetta P., Robinson A., Scofield J., Underwood J., Williams G. (2009). “X-ray data booklet”. Center for X-Ray Optics and Advanced Light Source, LBNL/PUB-490 Rev.3, <http://cxro.lbl.gov/PDF/X-Ray-Data-Booklet.pdf>
- Torboli M. (2000).** “Biografia di Giovanni Boldini, 1842-1931”.
- Vagenas N.V., Kontoyannis C.G. (2003).** “A methodology for quantitative determination of minor components in minerals based on FT-Raman spectroscopy. The case of calcite in dolomitic marble”. *Vibrational Spectroscopy*, 32, pp. 261-264
- Van Den Berg K.J., Daudin M., Joosten I. (2008).** “A comparison of light microscopy techniques with scanning electron microscopy for imaging the surface cleaning of paintings”. Act of 9th International Conference on NDT of Art, May 25-30, 2008 Jerusalem - Israel, pp. 2-9. <http://www.ndt.net/article/art2008/papers/033VandenBerg.pdf>
- Van der Weerd J., Smith G.D., Firth S., Clark R.J.H. (2004).** “Identification of black pigments on prehistoric Southwest American potsherds by infrared and Raman microscopy”. *Journal of Archeological Science*, 31, 10, pp. 1429-1437
- Verma H. R. (2007).** “Atomic and Nuclear Analytical Methods”. Springer editor
- Vila A., Ferrer N., García J.F. (2007).** “Colored inks analysis and differentiation: a first step in artistic contemporary prints discrimination”. *Analytica Chimica Acta*, 588, pp. 96-107
- Walter I.F. (1990).** “Pablo Picasso”. Benedikt Taschen, pp. 33-34, 90-95
- Walter I.F. (1991).** “Pablo Picasso. 1881-1973”. Benedikt Taschen editor, Vol. II, 683-725
- Wang Y.Y., Gan F.X., Zhao H.X. (2013).** “Inclusions of black-green serpentine jade determined by Raman spectroscopy”. *Vibrational Spectroscopy*, 66, pp. 19-23
- Warren A. (2006).** “Sargent’s Venice”. Yale University, pp. 17, 26-29, 72-139
- Warren A. (2007).** “La vita di Sargent: rotta verso Venezia” in “Sargent and Venice”. Musei Civici Veneziani, Mondadori Electa ed., pp. 11-32
- Watt F., Breese M.B.H., Bettiol A.A., Van Kan J.A. (2007).** “Proton beam writing”. *Materialstoday*, 10, Issue 6, pp. 20-29
- Werner A. (1990).** “Modigliani”. Garzanti editore, pp. 9-45; 47
- West Fitzhugh E. (1997).** “Artists’ Pigments. A handbook of their history and characteristics”. National Gallery of Art-Oxford University, Vol. III, pp. 295-355

Williams R.S. (1981). Unpublished analytical report available from Canadian Conservation Institute, Ottawa – Canada (*)

Note: (*) indicates a reference taken from other reference work but not available to me.

WEB REFERENCES

- [1] BBC October 16, 2012. <http://www.bbc.co.uk/news/entertainment-arts-19959224> - 06/11/2012 – 19.07
- [2] FOXNews November 16, 2012. <http://www.foxnews.com/us/2012/11/16/priceless-works-art-worth-little-if-anything-on-black-market-authorities-say/> - 20/11/2012 – 18.30
- [3] <http://mattinopadova.gelocal.it/cronaca/2011/12/06/news/e-un-de-chirico-no-e-falso-1.2835787> - 07/10/2012 – 18.45
- [4] <http://www.patrimoniosos.it/rsol.php?op=getarticle&id=36183> - 07/10/2012 – 19.11
- [5] <http://www.scienceomega.com/article/652/cataloguing-the-fingerprints-of-our-cultural-heritage> - 07/11/2012 – 18.06
- [6] <http://giovannascicolone.com/articoli.html> - 04/10/2012 – 18.06
- [7] <http://www.sfartscommission.org/gallery/2012/packaging-art/> - 04/10/2012 – 18.16
- [8] http://www.lloyds.com/news-and-insight/news-and-features/market-news/specialist-2010/art_in_motion_moving_great_masters - 04/10/2012 – 21.16
- [9] <http://www.formazione.ilsole24ore.com/business-school/LA5458-master-economia-management-dell.php> - 16/02/2013 – 20.24
- [10] <http://www.futur-ism.it/polizza.htm> - 17/11/2012 – 12:06
- [11] http://www.vittoriaassicurazioni.com/Allegati/Professionisti/PDF_arte_PROF/Musei/scheda-MUSEI_0510.pdf - 17/11/2012 – 12:24
- [12] http://www.vittoriaassicurazioni.com/Allegati/Privati/PDF_arte_priv/arte/scheda-serv-ESPRTI-ARTE_0510.pdf - 17/11/2012 – 12:34
- [13] http://www.nsa-srl.it/assicurazione_opere_darte/assicurazioni_opere_arte.html - 17/11/2012 – 12:15
- [14] <http://www.assicurarte.it/achi2.php> - 17/11/2012 – 12:21
- [15] <http://www.vittoriaassicurazioni.com/pages/DettSempl.aspx?idArea=2&IdCat=20&iddet=75> - 17/11/2012 – 12:32
- [16] http://www.carabinieri.it/Internet/Cittadino/Consigli/Tematici/Beni+interesse+culturale/02_Beni_culturali_DECALOGO.htm - 17/11/2012 – 15:45
- [17] <http://www.carabinieri.it/Internet/Cittadino/Consigli/Tematici/Beni+interesse+culturale> - 17/11/2012 – 15:55
- [18] http://www.fbi.gov/news/stories/2008/march/artscam_032108 - 17/02/2013 – 19:51
- [19] <http://www.fbi.gov/news/stories/2006/july/protecting-your-treasures-advice-from-our-art-theft-expert> - 17/02/2013 – 19:55

- [20] CBS News October 07, 2012 http://www.cbsnews.com/8301-202_162-57534558/in-art-heists-reality-rarely-matches-imagination/ -17/11/2012 –23:32
- [21] <http://www.elettra.trieste.it/comunicazione/events/sincrotrone-trieste-and-civic-museums-of-udine-the-new-invisible-technology-to-protect-artistic-heritage.html> - 18/11/2012 – 21:08
- [22]http://www.enea.it/it/enea_informa/events/techitaly2012/07M.PeloiSINCROTRONETRIES TE.pdf - 18/11/2012 – 21:15
- [23] <http://ncartmuseum.org/pdf/conservation-primer.pdf> - 19/11/2012 – 19.45
- [24] <http://www.sanders-studios.com/instruction/tutorials/historyanddefinitions/grounds.html> - 19/11/2012 – 19.50
- [25] <http://www.webexhibits.org/pigments/intro/visible.html> - 07/12/2012 – 22.50
- [26] <http://www.exelisvis.com/language/en-us/productsservices/envi.aspx> - 11/14/2012 – 18:38
- [27] http://www.realarte.it/artisti_dettaglio.php?id=65 - 11/02/2012 – 08:03
- [28] <http://www.ehu.es/udps/database/database.html> - 09/11/2012 – 18:25
- [29] http://oldweb.ct.infn.it/~archo/ColoRaman%20site/spectra_monitorFrameSet.htm - 05/03/2012 – 19:07
- [30] <http://rruff.info/> - 09/11/2012 – 18:45
- [31] <http://www.chem.ucl.ac.uk/resources/raman/index.html> - 29/11/2012 – 19:59
- [32] <https://picasso.shsu.edu/> - 14/06/2012 – 18.45
- [33] http://www.princeton.edu/~achaney/tmve/wiki100k/docs/Pablo_Picasso.html -14/06/2012 – 17.25
- [34] http://quote.robertgenn.com/auth_search.php?name=Pablo%20Picasso - 24/11/2012 - 07.45
- [35] <http://www.nga.gov/cgi-bin/tbio?tperson=1858&type=a> - 17/11/2012 - 19:43
- [36] http://it.wikipedia.org/wiki/John_Singer_Sargent -11/11/2012 - 00:15
- [37] http://it.wikipedia.org/wiki/Biblioteca_Nazionale_Marciana - 12/11/2012 - 21:45
- [38] <http://www.nationalgallery.org.uk/paintings/research/the-restoration-of-margaret-the-artists-wife/margarets-red-dress> - 24/11/2012 – 15.48
- [39] http://www.artisticomunari.it/dispense/home08_file/schede/13%20fibre%20tessili.htm – 20/11/2012 - 18:48

Table

TABLE 1 History of use of Titanium White pigment in art field.....	20
TABLE 2 Summary of the main pigments identified in samples belonging to studied paintings: Modern and Contemporary Art, 1882-1956.....	21
TABLE 3. Some of the most employed non-invasive and non-destructive analytical techniques used for Cultural Heritage studies are explained. The techniques used in this research are highlighted in bold type.....	25
TABLE 4. Comparison between remote sensing principles and its application on Cultural Heritage domain.	31
TABLE 5. SEM–EDS analytical data of pigment: results of average of measure carried out in different point on white pigment and on dark-brown specimens (σ from 1.2 to 1.9).....	60
TABLE 6 XRF data of pigments: results of average measure carried out in different point on white pigment and on dark-brown specimens.....	62
TABLE 7 PIXE analysis on Sargent sample: data are referred to area that cover white zone (sarg_1 e sarg_2) and dark-brown/white zone pigment (sarg_3). Average value: region of interest were extracted using PyMCA software, data expressed in counts. Experimental set up: particle/energy 3 MeV, current p+, Dose/s 200, Helium flow.....	63
TABLE 8 PIXE analysis on Picasso samples: data are referred to area with white pigment and red-white, blue-white pigment. Average value: region of interest were extracted using PyMCA software, data expressed in counts. Experimental set up: particle/energy 3 MeV, current p+, Dose/s 200, Helium flow.....	81
TABLE 9 EDXRF analysis on painting “Reader woman on bed and old man”: average of Net Area values, gathered for color. Experimental set up: voltage 30 keV, current 1300 μ A, Live time: 120 s, no filter, Helium flow, Anode Molybdenum, collimator 0.650. In italic, average value greater than σ	109
TABLE 10 PIXE analysis on Boldini samples. Average value: region of interest were extracted using PyMCA software, data expressed in counts. Experimental set up: particle/energy 3 MeV, current p+, Dose/s 200, Helium flow.	114
TABLE 11 EDXRF analysis on painting “Flowers”: average of Net Area values, gathered for color. Experimental set up: voltage 50 KeV, current 700 μ A, Live time: 120 s, no filter, Air, Anode Molybdenum, collimator 0.650. In italic, average value greater than σ	132
TABLE 12 PIXE analysis on “Flowers” samples. Average value: region of interest were extracted using PyMCA software, data expressed in counts. Experimental set up: particle/energy 3 MeV, current p+, Dose/s 200, Helium flow.	151

TABLE 13 EDXRF analysis on painting “Flowers in glass vase”: average of Net Area values, gathered for color. Experimental set up: voltage 50 KeV, current 700 μ A (analysis on wooden panel: voltage 15 KeV and current 1500 μ A), Live time: 120 s, no filter, Air, Anode Molybdenum, collimator 0.650. In italic, average value greater than σ	161
TABLE 14 PIXE analysis on “Flowers in glass vase” samples. Average value: region of interest were extracted using PyMCA software, data expressed in counts. Experimental set up: particle/energy 3 MeV, current p+, Dose/s 200, Helium flow.....	176
TABLE 15 Main results of art-fingerprints’ research in nineteenth-twenties century paintings by optical microscopy, SEM/EDS, EDXRF, PIXE, μ -Raman and XRD.	182

ACKNOWLEDGEMENTS

I would like to thank all those people that have allowed me to undertake this path and helped me in the preparation of this Thesis.

I am grateful to my tutor Prof. Carmela Vaccaro, Dr. Stefania Bruni and Prof. Giuseppe Maino for their availability and for involving me in this research, giving permission to study these samples and artworks.

Particular thanks to the owners of the studied paintings for their great willingness and to whom cordially kept in contact with them.

Financial support by the Transnational Access to Research Infrastructures activity in the 7th Framework Programme of the EU (CHARISMA Grant Agreement n. 228330) is gratefully acknowledged for PIXE analysis performed at AGLAE facility (Centre de Recherche et de Restauration des Musées de France, CNRS UMR171, Palais du Louvre, Paris, France).

A special thanks to all AGLAE team and in particular to Prof. Claire Pacheco, Eng. Laurent Pichon and Dr. Quentin Lemasson for their precious advices, their availability and great patience.

I am grateful to Prof. Clodoaldo Roldán (Universidad de Valencia, Spain) and Prof. Giuseppe Cultrone (Universidad de Granada, Spain) for their competence and great willingness.

I would like to thank Prof. Giuseppe Cruciani (Ferrara University, Italy) for his kind collaboration in performing XRD measurements and interpretation XRD data and Prof. Francesco Immordino and Archt. Elena Candigliota (ENEA, Italy) for their availability to accomplish interesting results by Image processing.

Special thanks go to Prof. Ferruccio Carlo Petrucci and his staff (Ferrara University, Italy), in particular Dr. Fauzia Albertin, Dr. Eva Peccenini, Dr. Virginia Pellicori, and Dr. Flavia Tisato for their kind collaboration in performing Multispectral Imaging and X-ray measurements on paintings.

I gratefully acknowledge Dr. Massimo Maggio, president of Progress FineArt (Italy), for the precious information about assurance policy and for his availability.

I wish thank Andrea B., Chiara S., Salvatore C., Parviz H. for the great willingness and patience.

A special big thanks to whom accompanied me in this path, offering me own friendship and warm moral support in this adventure: Elena C., Virginia P., Sabrina R., Salvo P., Chiara S., Giulia G. ... thanks for all, especially for being excellent patient listeners.

... ed anche se quest'ultima intera pagina non è in grado di contenere tutta la mia più sentita gratitudine, desidero rivolgere un ringraziamento speciale a mio padre, a mia madre ed a mia sorella Angela, che mi sono sempre stati vicini e mi hanno sostenuto in qualsiasi momento della mia vita, dandomi la forza di continuare ad affrontare le difficoltà e gioendo insieme a me dei momenti di felicità.

Un particolare grande grazie anche a nonna Agnese, che mi ha sempre sostenuta in tutto, a Manuel, Maria Teresa, Giuseppe e Valeria per il grande supporto ed incoraggiamento.

Infine, ringrazio tutti, anche chi non ho citato in modo esplicito, ma che mi ha sempre aiutato a crescere e a divenire ciò che sono.

Un Grazie sincero e di Cuore a tutti.

-Lisa-